Northern Development Corridor, Haiti

Urban Development and Climate Change Study

November 2014

Environmental Resources Management
1776 I Street N.W.
Washington D.C.
20006

www.erm.com

EMERGING and SUSTAINABLE CITIES Initiative

IDB

ERM

TABLE OF CONTENTS

LIST OF FIGURES

LIST OF TABLES

LIST OF APPENDICES

ACRONYMS

ACKNOWLEDGEMENTS

This report has been prepared by Environmental Resources Management on behalf of the Inter-American Development Bank (the Bank)'s Emerging and Sustainable Cities Initiative (ESCI). The contributions and support of the following are acknowledged:

- Ellis Juan and Horacio Terraza
- Gines Suarez, Maricarmen Esquivel, Martin Kerres, Gisela Campillo, David Maleki
- The team leader for the city as well as the colleagues who support him/her
- Local counterparts who contributed (if individual names would make the list too long or if it proves difficult for other reasons, you can also thank institutions rather than individuals)

1. INTRODUCTION

1.1 Background and ESCI

Cities and urban areas play a key role in the economy of Latin America and the Caribbean (LAC), both through opportunities generated (such as diffusion of expertize and innovation, concentration of specialized labor, and provision of educational, cultural, and recreational services), and the associated challenges such as poverty created by in-migration and the increasing and often unsatisfied demands for urban and social services, decent housing conditions, employment and opportunities to generate income. Overcoming these challenges means that cities and urban areas require a comprehensive approach that enables them to develop sustainably and simultaneously improve their citizens' quality of life.

As a response to this situation and in light of continuing urbanization process in the LAC region, the Inter-American Development Bank (the Bank) launched its Emerging and Sustainable Cities Initiative (ESCI). The purpose of this Initiative is to contribute to the improvement of the quality of life in LAC's cities in terms of environmental, urban, and fiscal sustainability. Through the ESCI, the Bank combines the expertise of its different sector departments in the formulation of comprehensive action plans designed to facilitate sustainable city planning. It leverages its capacities as the leading source of development financing for the region and applies its long experience in supporting the countries of LAC.

The ESCI methodology aims to provide decision makers with the tools, data and initial frameworks for managing urban growth and territorial expansion. Formal and informal growth often leads to negative environmental, social, and economic impacts. Municipal policy makers usually lack adequate data and analysis to inform the design of policies that help promote growth in a sustainable way. In many cases, the implications for the municipal budget in terms of financing infrastructure development and operation costs have not been clarified in newly urbanized areas. Additionally, the environmental impacts of city growth are often not fully considered. Areas for conservation and aquifer recharge need to be protected or established and vulnerability to natural disaster and the effects of climate change reduced. Anticipatory planning can also help reduce greenhouse gas emissions (GHG) as a major factor affecting climate change.

1.2 ESCI in Haiti

Haiti's Northern Development Corridor (NDC) (see *Figure 1*) presents a special case for the ESCI that requires flexibility in the implementation of the

Figure 1 - Area of study in Haiti's geographic context

initiative's methodology. In mid-2013, ESCI launched the implementation of an adapted version of its methodology in Haiti's Northern Corridor, currently home to approximately 500,000 people in the country's Nord and Nord-Est departments. The NDC includes the communes closest to the Caracol Industrial Park (PIC), a flagship economic development project that may bring up to 25,000 new jobs to the region in the next few years, unlocking rapid demographic and urban growth and putting pressure on the region's services and resources.

In partnership with strategic actors in Haiti, such as the Interministerial Committee for Territorial Planning (CIAT) and the Ministry of Economy and Finance, ESCI is working to help mitigate urban development impacts and catalyze interdisciplinary planning processes in Northern Haiti. ESCI's ultimate goal for the NDC is: ***to deliver site- and city-specific plans for urban and infrastructure development in the municipalities closest to the PIC, namely Limonade, Trou-du-Nord, Terrier Rouge and Caracol***. To achieve this goal, ESCI's tailored approach in Haiti involves the implementation of four baseline studies:


Bor de Mer de Limonade, Northern Haiti

1. *Vulnerability and Risk Assessment of Natural Hazards*. The assessment focuses on four risk categories – flooding (inland and coastal); seismicity; hurricanes; and drought – and using newly developed digital terrain models, includes a probabilistic modeling of their impact on the region's natural and urban landscapes and an estimation of impacts on existing infrastructure.

2. *Urban Growth Study*. This study presents multi-horizon projections of urban and demographic growth with two basic scenarios (rapid versus slow) and their respective spatial distribution and impact on existing ecological and urban assets. The growth models include the potential spatial and growth impacts of new developments (e.g., port upgrades in Cap Haïtien) on the four communes' area of influence.

3. *Sustainable Mobility Plan*. The plan will engage in unprecedented data collection exercises in Northern Haiti, including an origin and destination survey and counts. Based on this data, the Plan will include demand projections and draw recommendations for priority mobility projects, such as transport hub infrastructure, multimodal options, and improved services for PIC workers. The geographic focus is threefold: the PIC, the surrounding communes, and Route National 6.

4. *Living Conditions Survey*. There are considerable gaps in social and economic information, especially with regard to wages and labor, health and education levels, access to services, disaster preparedness, etc. In order

to develop planning strategies and instruments based on up-to-date and reliable information, ESCI will implement a complete household survey in the urban and rural areas of Limonade, Terrier Rouge, Trou-du-Nord, and Caracol, and gather basic social and demographic information as well as select information on public opinion. The ultimate goal is to develop a baseline of information about the households adjacent to the PIC.

Building on the results, community feedback, and recommendations from each of these studies, ESCI will provide and socialize four site- and city-specific urban development plans for Limonade, Terrier Rouge, Trou-du-Nord and Caracol. The plans will also build on previous planning exercises by local partners such as the CIAT, which have sketched a regional vision for the NDC but require local specificity and detail and a more thorough consideration of future development alternatives. This dual approach – to develop a foundation for planning based on detailed studies, as well as to build on relevant, past efforts – will ensure that the four urban plans help guide Haitian stakeholders and their domestic and international partners in key urban development areas for the NDC. ESCI's work will include proposed interventions at a pre-investment level, so as to facilitate swift action according to local priorities.

These proposals touch on areas such as mixed-use development strategies, design-driven conservation of landscape and resources, more resilient siting proposals for topics such as housing, and recommendations for transportation infrastructure at both the commune and regional levels, including mobility options to connect the PIC and its surrounding communes with new regional hubs such as an upgraded port in Cap-Haïtien.

1.3 This Report

Environmental Resources Management, Inc (ERM) was engaged by ESCI to undertake the first two studies for the NDC: the Vulnerability and Risk Assessment of Natural Hazards (Risk Study) and Urban Growth Study (Urban Study). These two studies build upon the work and methodologies ERM has used and developed in conjunction with the ESCI team for similar studies in Cochabamba, Bolivia and Managua, Nicaragua. This report presents the consolidated findings of the study, and further details and information are contained in both the referenced appendices and supporting deliverables such as a GIS database.

This report presents the results of the two studies (collectively referred to as the ESCI Growth Study) undertaken and importantly, the analysis, findings and recommendations have been combined to seek to address the complex question of where and how should urban development occur in the NDC given the different dynamics and forces that will shape population growth and migration in the area. This report is intended to provide planning tools and insights, and a building block upon which more prescriptive plans and planning policies can be developed, as well as to help guide decisions about accommodating and influencing future growth.


Caracol Industrial Park

2. METHODOLOGY AND APPROACH

2.1 Methodology for the Risk and Urban Studies

The two studies presented in this report (Risk and Urban Studies), while having clear and defined objectives individually, also have significant overlaps and connections to each other. The methodology used illustrates the combined approach taken that captures the key elements of the individual studies and also the respective connections:

i. Development and understanding of current **baseline conditions** of current and known conditions in the study area using:
   - readily available information from key stakeholders, covering physical, biological, hydrological and urban systems;
   - Supplementing this information with defined studies and assessments comprising current and historical land cover assessments;

   Section 3 of this report presents the results of the baseline assessments.

ii. The baseline is further supplemented by the ***hazard and risk assessment studies***, and these are detailed in *Section 4*.

iii. Identifying and defining **future growth and development considerations** including future population growth projections, future hazard and risk considerations when accounting for climate change projections and future development projects. This is presented in *Section 5*.

iv. **Geospatial land suitability modelling** using the baseline conditions and future projections to identify land potentially suitable for development, which is presented in *Section 6*, and also includes stakeholder feedback as part of an engagement workshop held for the project.

v. **Development of a sustainable growth scenario** for the study area, considering both slow and fast growth, presented in *Section 7.*

vi. Presentation of key **conclusions and recommendations**, contained in *Section 8*.

2.2 Study Area

The study area, which is shown in *Figure 2*, covers an area of 49,391 hectares and it is located along the Atlantic Ocean, in close proximity to the cities of Cap Haïtien to the West, and Fort Liberté to the East, partially covering the North and Northeast Departments. Geographically, the area of study is located at the heart of the territory known by Haitians as the Plains du Nord, the coastal plateau where the Massif du Nord mountainous chain meets the Atlantic Ocean.

The delineation of the study area was defined by

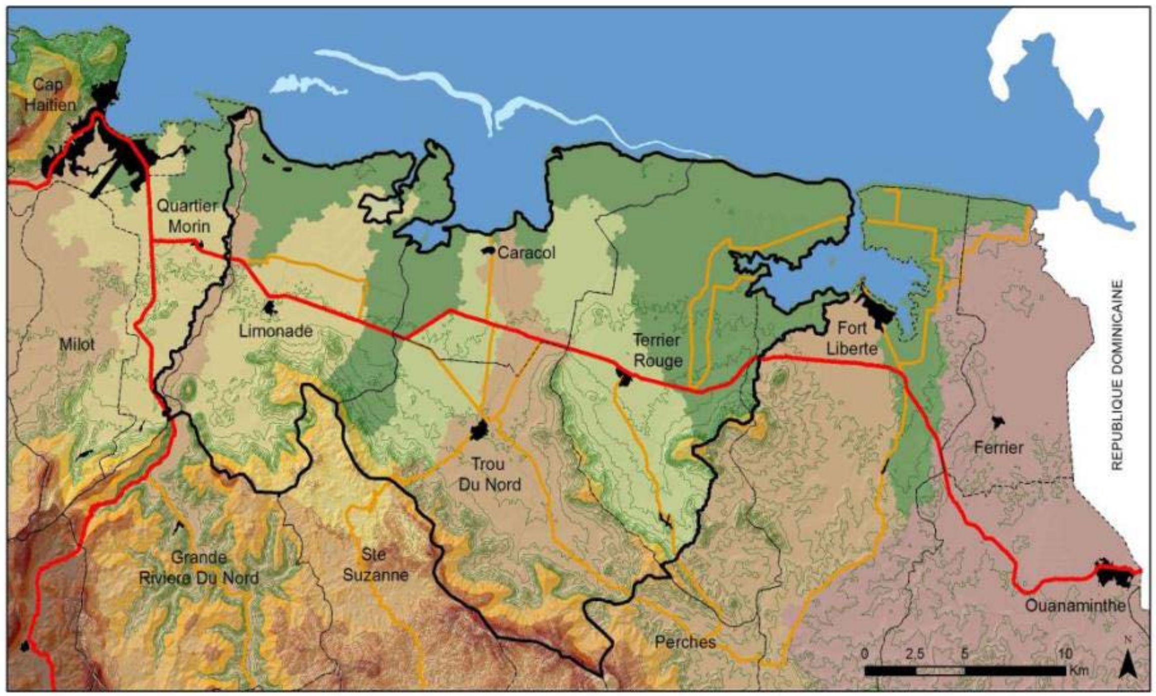

Figure 2 – Area of Study

consideration of the following factors:

- The presence of the Route National (RN6), the Park Industriel du Caracol (PIC) and their areas of influence;
- The proposed development projects being planned in the NDC;
- The proposed upgrade and expansion of the Cap Haïtien seaport;
- Watersheds, catchment areas and natural features; and
- Municipal Boundaries.

The study area comprises the key towns of Limonade, Trou-du-Nord, Caracol and Terrier Rouge. The study area boundaries have been defined based upon the following:

- The main core of the study area is to be NDC and the PIC along RN6 given the socio-economic development and growth being promoted as a result of the construction of this corridor;
- The southern and eastern boundaries are defined by the water catchment zoning;
- The west is defined by both the water catchment area of the Grande Rivière du Nord and the municipality of Limonade; and
- The proposed Three Bays Marine Park will be taken as part of the study area and the Three Bays Marine Park will define the northern boundary, albeit the study has been limited to the coastline.

In delineating the study area, it is acknowledged that the urban areas of Cap Haïtien, Fort Liberté and Ouanaminthe are important influencers throughout the NDC, and these factors have been considered during the study.

2.3 Building on Key Planning Efforts

The NDC has been the subject of a number of important planning efforts conducted recently. This ESCI Growth Study does not seek to replace or supersede these other studies, but rather to build upon and contribute to them. The two key planning studies of interest are:

- ***The Cap Haïtien-Ouanaminthe Development Corridor Regional Comprehensive Plan, AIA Legacy (referred to hereinafter as the AIA Study)***. This was published in December 2012, following a year of work carried out by the American Institute of Architects nonprofit foundation, AIA Legacy, with funds from the IDB and the United States Agency for International Development. The study was carried out in close interaction with the CIAT and the Technical Execution Unit of Economy and Finance.

- ***The Plan d'Aménagement du Nord / Nord-Est: Couloir Cap – Ouanaminthe, CIAT (the CIAT Strategic Plan)***. This strategic plan produced by the CIAT is aimed at developing the Haitian territory, and in this case the north, with greater regard for its natural resources, the risks and vulnerabilities it faces, and the opportunities it offers. It comprises two documents, the first of which is titled Haïti Demain (Haiti Tomorrow) and offers a country-wide framework; the second, titled La Boucle Artibonite (The Artibonite Loop), defines the space and functionality that ought to be developed in this area with some of the lowest natural risks of the country and numerous conditions that could turn it into a major economic pole.

There are a number of areas in which the ESCI Growth Study can contribute to the AIA Study and the CIAT Strategic Plan, and further commentary on this is provided below.

2.3.1 AIA Study

The AIA Study is divided in three volumes, comprising in the first volume a regional comprehensive plan; in the second urban growth plans for the different municipalities; and in the third are detailed analyses by sectors (or 'focus areas' as it refers to them), which add up to a cumulative impact assessment report that is the basis of both the regional comprehensive plan, and the urban growth area plans. Key aspects of this work include:

- It presents a framework for how future development of the region should occur, including (i) the principles that should guide development in terms of natural resources, economic growth, infrastructure support and human development; (ii) the levels of plan implementation, that is, the regional, municipal and community levels, with clear indications regarding the roles and responsibilities of each; (iii) the mechanisms for implementation, including administrative measures such as zoning, and (iv) what the plan calls 'supplemental' measures, such as community compacts, anchor investments, and others.

- Based on the diagnoses and analyses carried out at the regional and municipal levels, the plan reiterates or defines new, significant development projects at those scales, which should catalyze development around

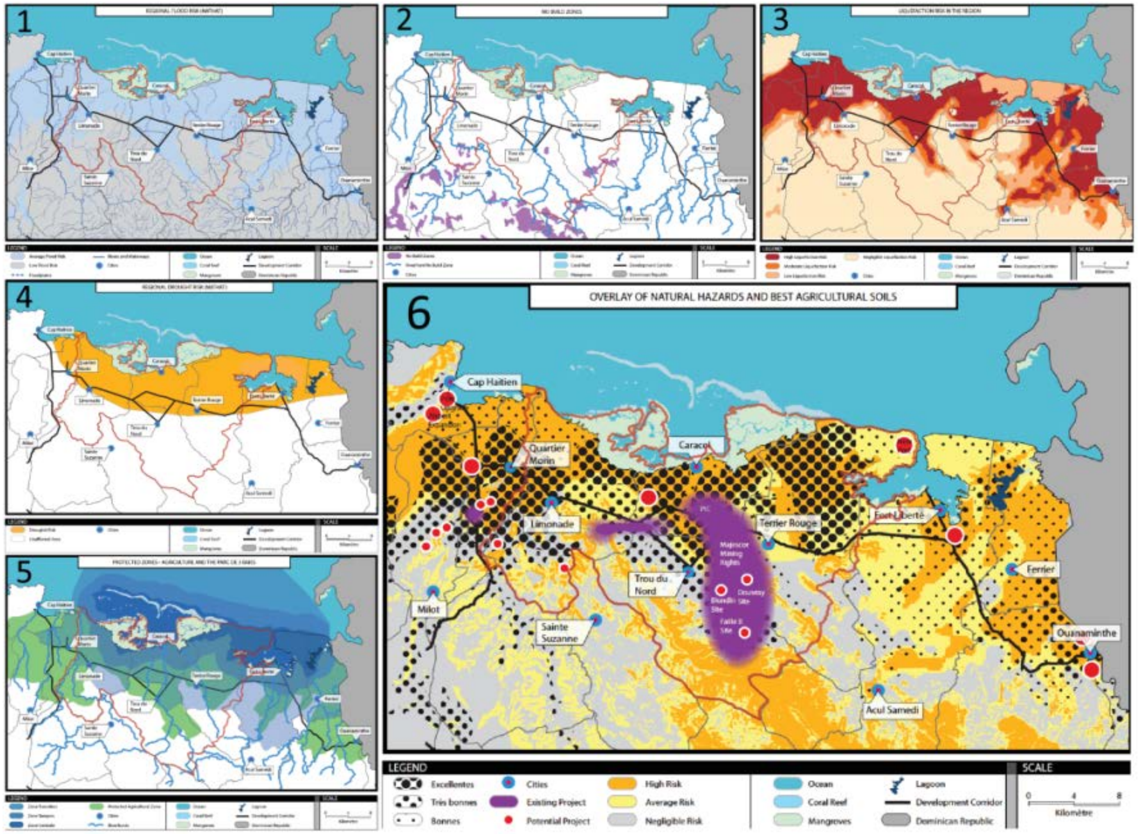

Figure 3 - Composite of some of the mapping developed by the AIA Study (Illustrative Only)

themselves and regionally as a result of their aggregation.

- In terms of spatial form and land transformation, the plan suggests an area of urban development the south side of RN6. The plan seems to indicate that this area would in reality be formed of two separate areas: one to the south east of Limonade, with limited or non-developed areas east and west; the other, between Trou-du-Nord, the PIC area and Terrier Rouge.

- The plan then shifts to the local level, by means of offering local development plans for the eight municipalities that comprise their area of study (the whole North and Northeast Region). These local plans focus on their urban and immediate areas of influence, providing clear guidance on green and grey infrastructure, social services, road and transport, housing and other land uses. The plans include key data with regards to urban growth, based on population projections and housing and land demand.

- The plan includes a proposal for a new development for 6,000 people, Caracol Nouvelle, that is shown as a model of a planned, mixed use and environmentally sound settlement. The plan suggests that this could serve as seed for additional settlement.

Figure 3 provides a composite that illustrates some of the elements and plans considered by the AIA Study's regional comprehensive plan and the results of aggregating them There are four specific contributions that this ESCI Growth Study work will bring in relation to the AIA Study. First, because the regional comprehensive plan is a high-level, multi-sectorial, multi-institutional and multi-leveled instrument, it is not intended to provide detail on the spatial configuration of the region as a whole, other than that which would result from the process of settlement along RN6, and the local development processes of each municipality. The AIA Study represents the process of settlement along RN6 as occurring mostly along the south side of the corridor and the local plans are focused on the urban areas only. This does not acknowledge development north of RN6 or the rural and intermediate areas where settlement may and is likely to happen. This ESCI study will be contributing in this regard by including information from recent surveys and aerial imagery from the area, analyzing what would the actual and projected growth patterns at the regional level be, and comparing them with the results of the AIA regional comprehensive plan. This will include not only the main townships but also smaller villages or hamlets.

Secondly, the ESCI Growth Study will enhance the AIA analysis of potential settlement areas by:

- Introducing a larger number of restriction variables (15-20 layers versus the AIA's 7 layers) as well as a larger number of attraction variables (5-10 versus 2).
- Introduce greater resolution to the geography of some these restrictions and attractions.
- Application of a geo-spatial model to identify the areas suitable for human settlement.

This enhancement will enable recommendations to be provided that will either confirm, or suggest re-orienting, of the results of the AIA regional comprehensive plan in terms of where should development occur.

Third, the AIA Study implies that the core of the urbanization of the entire region is to occur within the NDC area, with measures to prevent spatial growth of Quartier Morin and Limonade in the west, and the implication that the stronger economic links between Ouanamithe and Fort Liberté in the east will reduce the pressure for urbanization beyond Terrier Rouge. It can however be expected that RN6 will continue to attract settlement along its edges, which could turn the area into a long, semi-urbanized strip, and better understanding the attraction factors for development, which this ESCI Growth Study seeks to do, will enable a better understanding of existing, trending and more 'intelligent' urbanization patterns that the region should exhibit as a whole.

Lastly, each of the local development plans produced by the AIA Study offers a series of elements associated to the growth process. Of particular significance are the delineation of the existing urban boundary, an approximation to the extent of each municipality's population growth, and the areas where this should be accommodated. With the results from the ESCI Growth Study modeling, an assessment of the location of these areas will be offered.

2.3.2 CIAT Strategic Plan

The CIAT Strategic Plan comprises three elements, under a 2012 – 2030 time horizon: a regional diagnostic; a Plan d'Amenagement (layout plan), and a series of implementation measures. The regional diagnostic focuses on seven challenges as being the ones that have to be addressed, namely:

1. Accompany the growth in population
2. Structure the towns
3. Transform the economic structure
4. Modernize the agriculture
5. Enhance the heritage
6. Reduce the vulnerabilities
7. Ensure good, collective management

The Plan d'Aménagement contains five components: an urban program; an economic program around major projects; a management strategy; a transport plan and forms of habitat and access to public services. The third part of the Strategic Plan focused on implementation, and provides three main elements, comprising a discussion on the governance and operational structure that ought to be set; a series of orientations or guidelines for elaborating urban development plans at the local level; and an investment plan.

Important considerations from the CIAT Strategic Plan for the ESCI Growth Study include:

- The plan reads as being supported and supportive on the results and the process of the AIA Study, and reiterates numerous elements of the diagnosis.
- It offers a series of guidelines on the areas that ought to be developed at the local level and the criteria or principles that should be followed in each municipality. Because of its scope, it does not provide detailed approximations to the geography or the land use patterns to which many of its propositions should translate.
- The plan does not appear to endorse the consolidation of an urban continuum along RN6; rather it highlights the need to urbanize the triangle within the Champin area as the fundamental intervention (in the NDC) that will ensure the balanced distribution of population in the region.
- The plan is very clear in the pursuit to consolidate four polarities in the region, one of which would be the area covered by the present study (the Champin pole – see *Figure 4*). It also offers key elements that would identify it as such, like the new planned development, but also the proposed 'urban' corridor between Sainte Suzanne, Trou-du-Nord, Champin and Caracol. This is a fundamental element not visible in the AIA Study, for it represents the only direct link between the mountain areas of the Massif du

Nord, the plateau and the coast, between Cap Haïtien and Ouanaminthe.

There are four specific contributions that ESCI Growth Study brings to this CIAT plan. First, an updated demographic analysis has been performed that yields more detailed and disaggregated information useful to offer a better approximation of where would human settlement likely grow, and the extent of this. Secondly more refined approximations will be offered to the geography of the elements that are fundamental to the economy: agricultural milieus, economic development projects, protected areas, etc.

Third, the CIAT Strategic Plan's vision will be embraced, such as a network of services that complement each other, as opposed to compete against each other; and acknowledging the geographical areas that should be protected for their potential economic value.

Finally, alternative locations for new planned settlements will be identified should the suitability analysis yield areas more attractive as a result of the modeling.

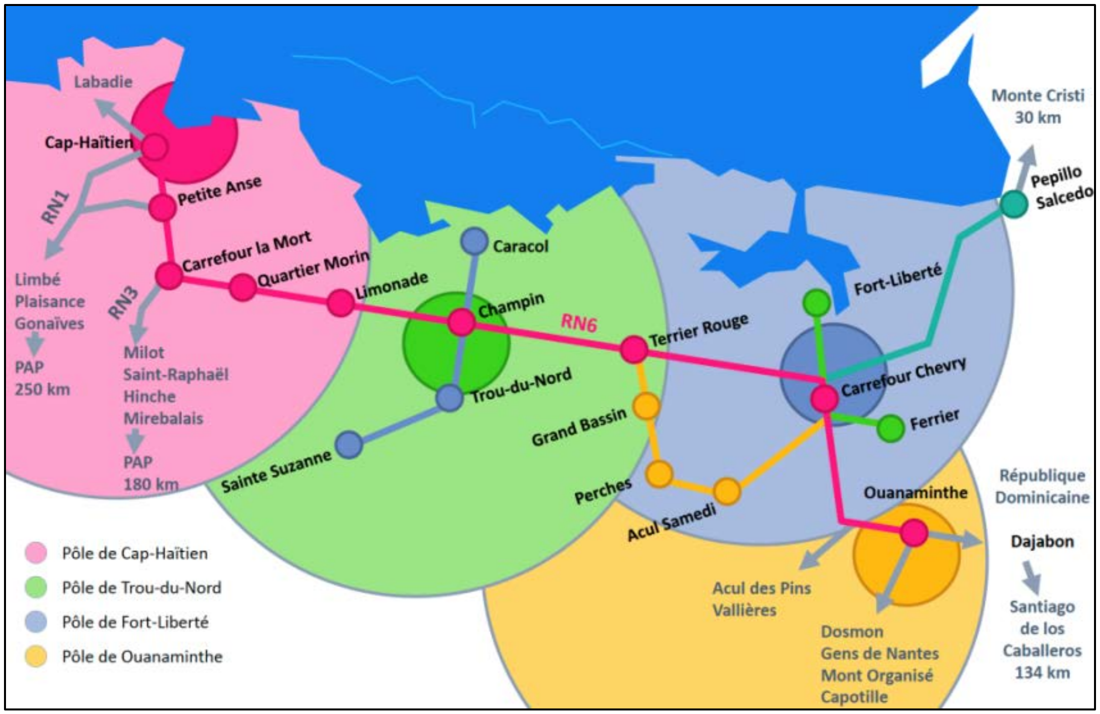

Figure 4 - Extract of the CIAT Strategic Plan showing four poles of economic attraction that would result from the implementation of two new urban centres (Champin and Carrefour Chevry)

3. BASELINE CONDITIONS

3.1 Current Study Area

The proposed study area presented in *Figure 2* is defined as follows:

- The main core of the study area comprises the west-east corridor along RN6;
- The Trou-du-Nord catchment boundary defines the southern extent of the study area, and the coastline and associated bays along the northern coast naturally define the northern extent of the study area;
- The easterly boundary is partly defined by the Trou-du-Nord watershed and in the north-east by the Terrier Rouge and Fort Liberté municipal boundary; and
- To the west, the study is defined by the Limonade and Quartier Morin municipal boundary.

In defining the study area, the urban areas of Cap Haïtien, Forte Liberté and Ouanaminthe are recognized as important influencers and have been fully considered.

The overall NDC area can be characterized as rural because of the traditional land use patterns that it exhibits, including large plantations of sisal and plantain, and traditional small to medium scale farming for production of fruits, plantain, livestock, cassava, vegetables and others. The agglomeration patterns that have emerged are townships, hamlets, farms, 'linear' settlements along roads, and planned settlements, which are presented in *Figure 5*.

Figure 5 – Human settlements in the NDC

Map source: From geographic information layers by AIA (2012), CIAT (2012), CNGIS (c.2012), IADB (c.2013), NATHAT (2010), USAID-OFDA (c.2012), OSM (2013), OCHA (c.2010), PDNA (2010) and DTM (2013). Georeferencing, digitizing and remote sensing analysis from satellite imagery 1986, 2010 and 2013.

3.1.1 Townships

In the NDC, there are three main townships: Limonade, Trou-du-Nord and Terrier Rouge, representing a first tier of settlements. They are founded at regional crossroads, and their urban structure is largely formed by a town center with the main administrative and religious buildings, followed by an 'organic' grid of roads that configure blocks of irregular shape and dimensions. These tend to be between a quarter and a third of a hectare in area. Inside these blocks there is a parcel structure that in general terms is half built, with the remaining area being used as solarium and orchard. Consequently, the idea of a town in the NDC is largely that of an agglomeration of single-family dwellings with a yard.

The township is surrounded by countryside of medium sized farms, whose produce is generally sold or ex-changed at the township's market. In terms of land use, the townships are almost entirely configured as mixed use, with buildings serving as home as well as office, store, training center, phone booth, restaurant, etc. An example is shown in *Figure 7*, which shows Terrier Rouge.

3.1.2 Hamlets

Hamlets are the second tier settlements present in the NDC, and include places such as Caracol, Bor de Mer de Limonade, Phaeton, Paulette and Jacquezy. These are normally located along secondary or tertiary roads, and they exhibit a much simpler structure, where the main road widens and becomes the main center, in which the churches, playfields, administrative posts and other service-related buildings are located. This leads into a network of a few streets or paths that reach the surrounding areas, some of which are used for agriculture. An example is shown in *Figure 6*, which shows the hamlet of Paulette.

In Paulette and in other cases, hamlets are also places were international relief organizations have developed housing programs. In this case, a difference is clearly visible between the 'organic' grid of the 'natural' town and the orthogonal grid of the planned settlement.

3.1.3 Farms

In the NDC there are numerous types of farming operations, from the small one beside the road that houses two to three generations of a family, and is exploited for family subsistence and market exchanges of the surplus; to large or very large estates exploited for sisal, plantain, citrus, cane and other crops. The presence of small farmers along the internal roads in the NDC is partly as a result of the fact that they used (or continue) to be employed in the large plantations, whose owners have given them small parcels to settle. Other, medium parcels and farms are the result of subdivision of the large plantations over the years.

3.1.4 Settlement along roads

As a consequence of population growth and the subdivision of the original farms along the road, linear areas of agglomeration begin to form, also visible in *Figure 8*. In some cases because of their

Figure 7 - Typical township in the NDC area (Terrier Rouge)

Figure 6 - Typical hamlet in the NDC area. (Paulette)

population size, they become recognized as 'urban' by the IHSI.

3.1.5 Planned settlements

The NDC has also been the subject of numerous efforts by international relief and cooperation organizations to provide Haitians with shelter and sanitation, including Food For the Poor, the Red Cross, CARE, OXFAM, CHF and others. USAID has been intensely involved, having pledged after the 2010 disaster to build 3,000 homes as part of the coordinated efforts that brought about the PIC, the completion of RN6, the upgrading or reconstruction of several water and sanitation facilities and other projects of similar nature.

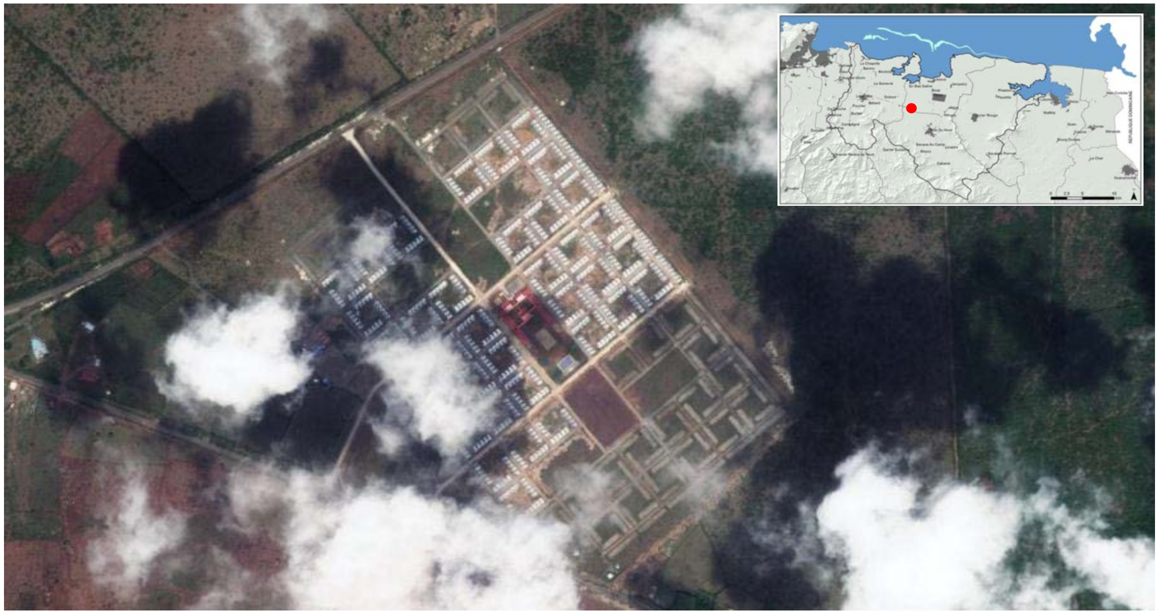

Figure 9 - EKAM neighborhood development developed by USAID

The EKAM project is the largest residential development in the study area and was developed by USAID (see *Figure 9*). The project is located equidistant to the PIC, the University of Limonade and the township of Trou-du-Nord. It includes 750 homes, a community center, shopping areas and recreational spaces, to be placed on a 47 hectare site approximately.

Figure 8 - Typical road-side settlements

Another project for approximately 135 homes is to be built on an 8.5 hectare site that is located just east of the PIC and the crossing known as Jesús. This project is immediately flanked to the west by a customs facility, and to the east by a farm of approximately twice the size that is being exploited with sisal that is then sent to a factory located inside the CIP. This sisal exploitation is expected to grow to a 5,000 hectare operation that is described later in this document.

3.1.6 Growth of settlements

Using remote sensing analysis of two LANDSAT satellite images (1986 and 2010), and through the use of a 2013 high resolution image collected and used by the IDB to create a digital terrain model for the NDC (see *Section 3.2* for more details on the methodology), it has been possible to assess the changes and growth of the urban footprints in the study area. As illustrated in *Figure 10*, in the year 1985 the main settlements in the NDC were Limonade, Trou-du-Nord, Terrier Rouge, Caracol, Paulette and Phaeton. At the crossing of the road that connects RN6 with Bord de Mer de Limonade was also a small settlement. Twenty five years later, in 2010, the coastal towns of Bord de Mer de

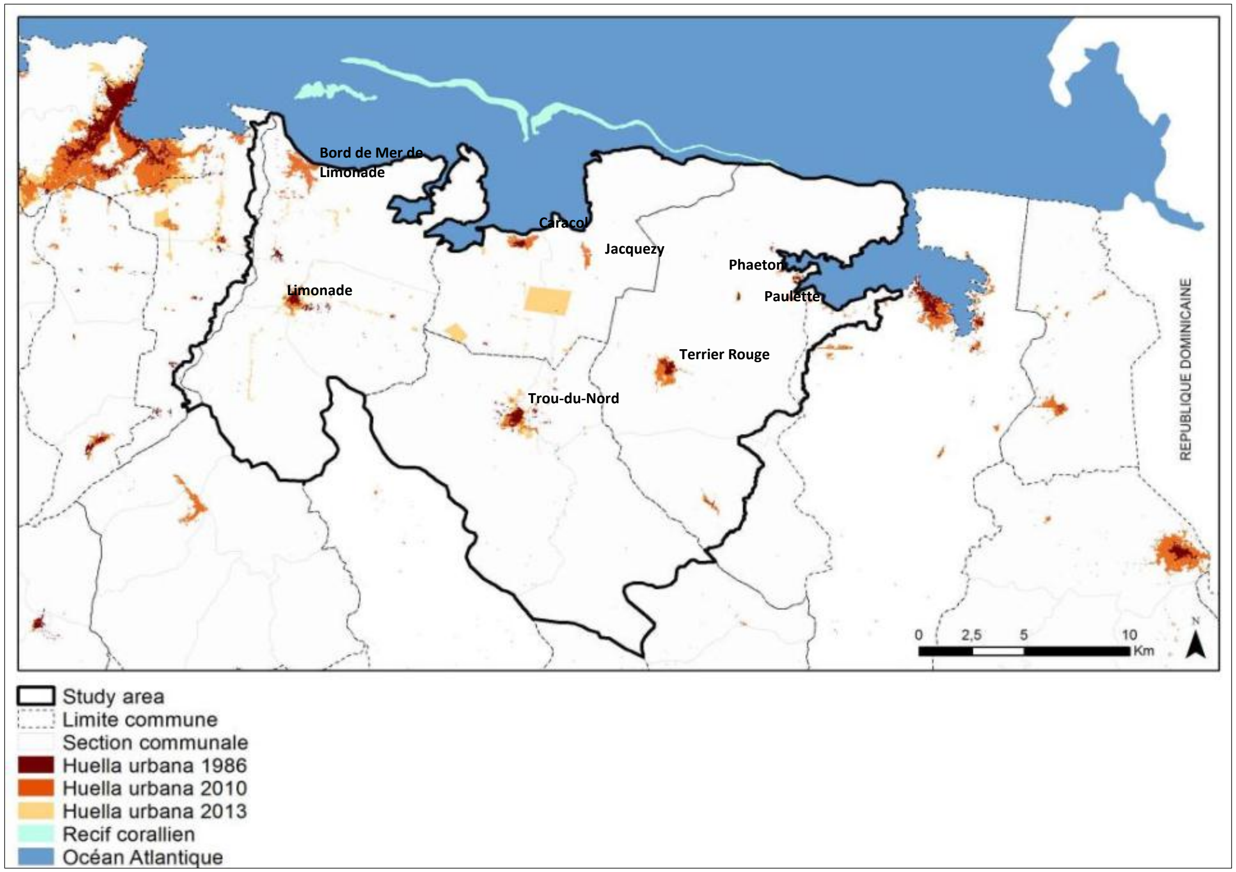

Figure 10 - Footprint growth of urban settlements in the NDC

Map source: From geographic information layers by AIA (2012), CIAT (2012), CNGIS (c.2012), IADB (c.2013), NATHAT (2010), USAID-OFDA (c.2012), OSM (2013), OCHA (c.2010), PDNA (2010) and DTM (2013). Georeferencing, digitizing and remote sensing analysis from satellite imagery 1986, 2010 and 2013.

Limonade, Caracol and Jacquezy had seen the had seen the largest growth. Bord de Mer de Limonade passed from an almost invisible concentrated area at the regional scale, to an area with the largest footprint of all three. Caracol saw its area almost tripled, and Jacquezy had also grown dramatically.

The inland townships, however, saw a more normal expansion, in which Terrier Rouge exhibited the largest expansion with 2.5 times the area of 1985, followed by Trou-du-Nord with an expansion of double the size of 1985, and Limonade, with a slightly lower expansion. By 2013, what clearly appeared in the map as agglomerations were the series of linear settlements along RN6 and some of the secondary roads connecting the different townships. The settlements along the roads connecting RN6 to Bord de Mer de Limonade as well as the road connecting Limonade with the township of Campegne to its South appear to be the more defined ones.

Presently, this linear pattern seems to be the one acquiring more speed. *Figure 11* exhibits a series of images from the area along RN6, in the vicinities of the intersection of this thoroughfare with the road that connects to Caracol and serves as one of two access points to the PIC. The series begins in 2007 and ends in 2013, passing by images from 2009 and 2010. The area bound by a continuous yellow line is where a piecemeal process of settlement has occurred, likely with the support of an international organization. The settlement is currently comprised of a total 37 homes and what appears to be a small communal or commercial facility. The area was rural up until 2007 and during 2008-2009 settlement appeared, which is also when the construction of RN6 took place. According to the images, the settlement began with approximately

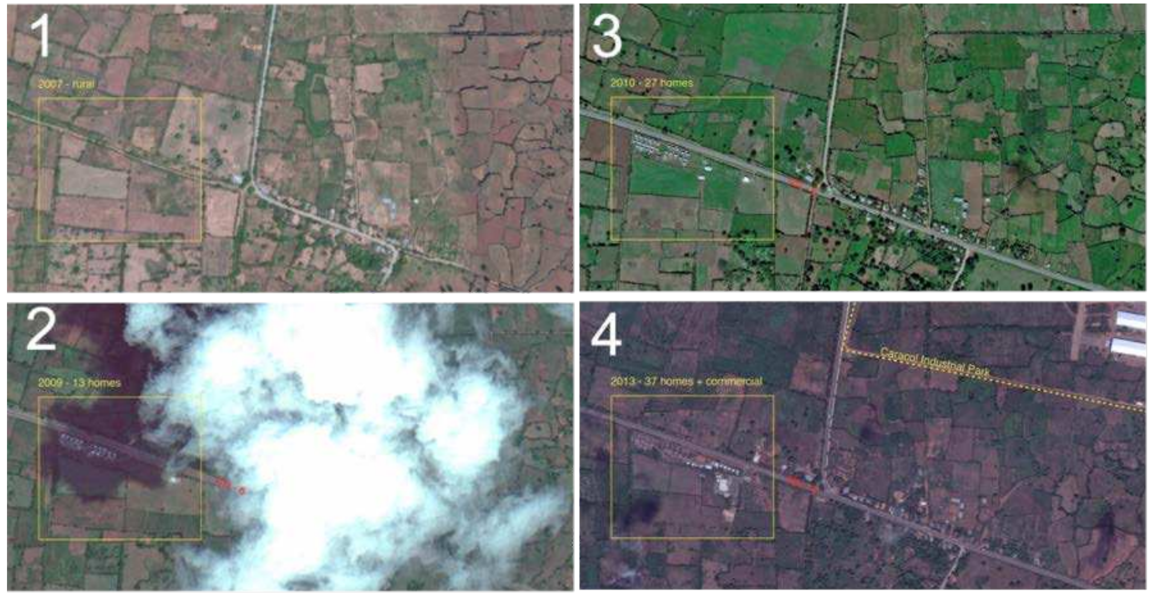

Figure 11 - Evolution of a housing development in the PIC area

13 homes in 2009, jumping to 27 homes in 2010 and 37 in 2013. The settlement is likely to continue growing, and if a measure of the intensity with which it has grown from its inception was applied, the result in 20 years would be a settlement of anywhere between 70 housing units if it grew conservatively to 160 dwellings if it grew with intensity.

3.2 Current and Historical Land Cover

A remote sensing analysis of two LANDSAT satellite images (1986 and 2010) covering a span of 24 years was performed to analyze eleven land cover classes for urban, rural and natural areas over time.

Final land cover classification was checked for quality assurance and quality control issues (QA/QC) through a site survey of the area of study, a process known as ground-truthing. Data collected in the field was used to calibrate the training regions in the most recent supervised classification and inform the execution of all other supervised classifications on the historical imagery. The results provide an understanding of the evolution of land cover in the northern development corridor from 1986-2010.

As *Figure 12* demonstrates, the urban areas and corridors have grown noticeably. In 1986, the urban footprint of the NDC only occupied 0.4 percent of the total area of study expanding to 7.7 percent of the total area in 2013. In addition, the non-urban lands appear to illustrate a significant deterioration, with a reduction in natural and agricultural lands.

In terms of green infrastructure, the NDC experienced its significant deforestation before the period of analysis and a slow, but sustained deterioration of its hydric system. The area has lost 5.030 hectares of cultivated areas despite having vast extensions agrological classified soils and in 2010 only half of the area suited for agriculture (6,315 hectares) was utilized.

As shown in *Table 1*, the most important land use changes occurred in rangeland increasing by 6,647 hectares, cultivated areas decreasing by 5,030 hectares and barren land decreasing by 2,158 hectares. Besides rangeland, urban areas have increased significantly: medium intensity 55 hectares, low intensity 363 hectares and open space 530 hectares associated to road development. In contrast, the hydric system lost 49 hectares of water bodies and 257 hectares of forested wetlands associated to deforestation, erosion, flooding and pollution or the rivers, wetlands, mangroves and riparian forests.

Table 1 – Land use change observed between 1986 and 2010 in the study area

Land Cover	1986	2010	% Change
Urban			
High density	0	0	0
Medium density	67	123	83.6%
Low Density	109	472	333.0%
Open space	0	0	0
Vegetation			
Agriculture/cultivated	17,661	12,630	-28.5%
Rangeland	9,609	16,257	69.2%
Scrub	9,010	8,923	-1.0%
Forest	0	0	0
Water Features			
Water body	951	902	-5.2%
Forested wetland	4,318	4,061	-6.0%
Emergent wetland	1	2	100.0%

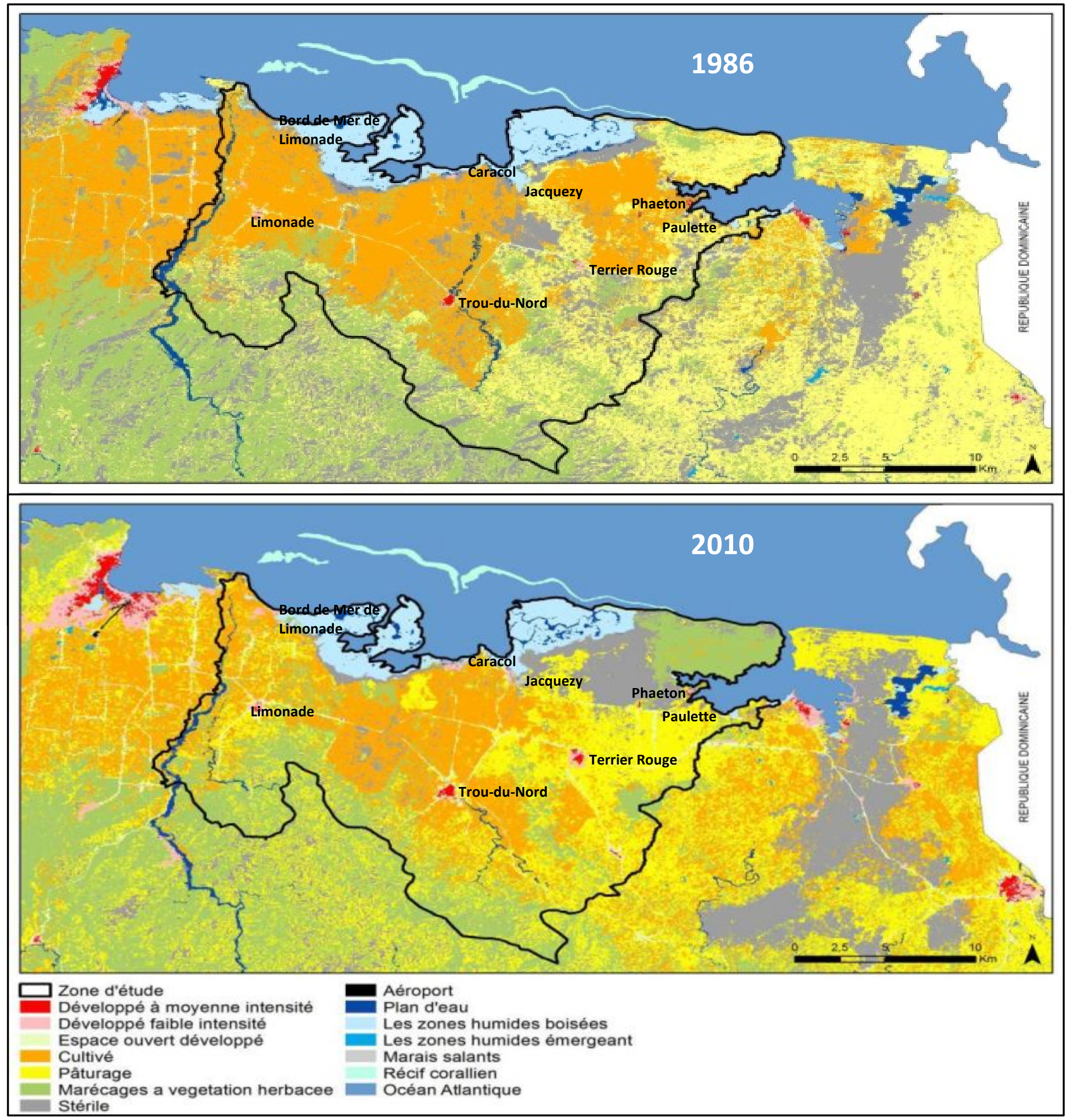

Figure 12 - Land Use for 1986 and 2010 for the NDC

Source: Remote sensing analysis from satellite imagery 1986 and 2010

3.2.1 Urban Areas

Urban land use was assessed from the 1986 and 2010 LANDSAT analyses described above, and a third reference point was also obtained from a high resolution image collected and used by the IDB to create a digital terrain model for the area. Urban land use was classified in four categories, based on imperviousness levels (the area that ceases to be permeable due to construction non-absorbing surfaces such as buildings and roads): developed high intensity, developed medium intensity, developed low intensity and developed open space. The first three are occupied by buildings and the fourth one is composed by parks, roads, cemeteries and infrastructure inside the urban footprint or connecting discontinuous urban areas, such as the RN6.

An average urban density of 78.09 inhabitants per hectare was reached in 2012 and surpassed the 100 Inhabitants per hectare in Caracol and Limonade, however this analysis of imperviousness levels did not show areas classified as developed high intensity. Developed areas of medium and low intensity increased significantly during the 24 years of the analysis and the urban footprint of the NDC grew more than three times its size between 1986 and 2010, while open space, basically road infrastructure, doubled during the same period.

Comparing the 1986 and 2010 urban footprints shows that the NDC is mainly developed with lower levels of density, predominantly compact built environment concentrated around traditional settlements and more recently along roads.

In addition, after the 2010 earthquake and the construction of the PIC, the urban footprint of the NDC grew significantly reaching a total of 934 hectares in October 2013. Between 1986 and 2010 the urban footprint grew 419 Hectares at 17 hectares per year) in contrast with a 340 Ha between January 2010 and October 2013, at a rate of 113 Has per year. *Figure 12* illustrates the urban growth between 1986 and 2013, and *Figure 14* focuses in on key areas of the NDC. *Figure 15* provides the urban intensities (in terms of density of development) as assessed in 2010.

One fourth of the 2010-2013 growth is the area of the PIC (246 Ha), the other three thirds are housing projects such as EKAM, the UNH-RHC in Limonade and organic urbanization processes associated with these development projects, along the RN6, around the existing towns and in the region between Limonade and Quartier Morin, as seen in *Figure 14*.

This development has started the urbanization process of a vast rural area that started as 0.4

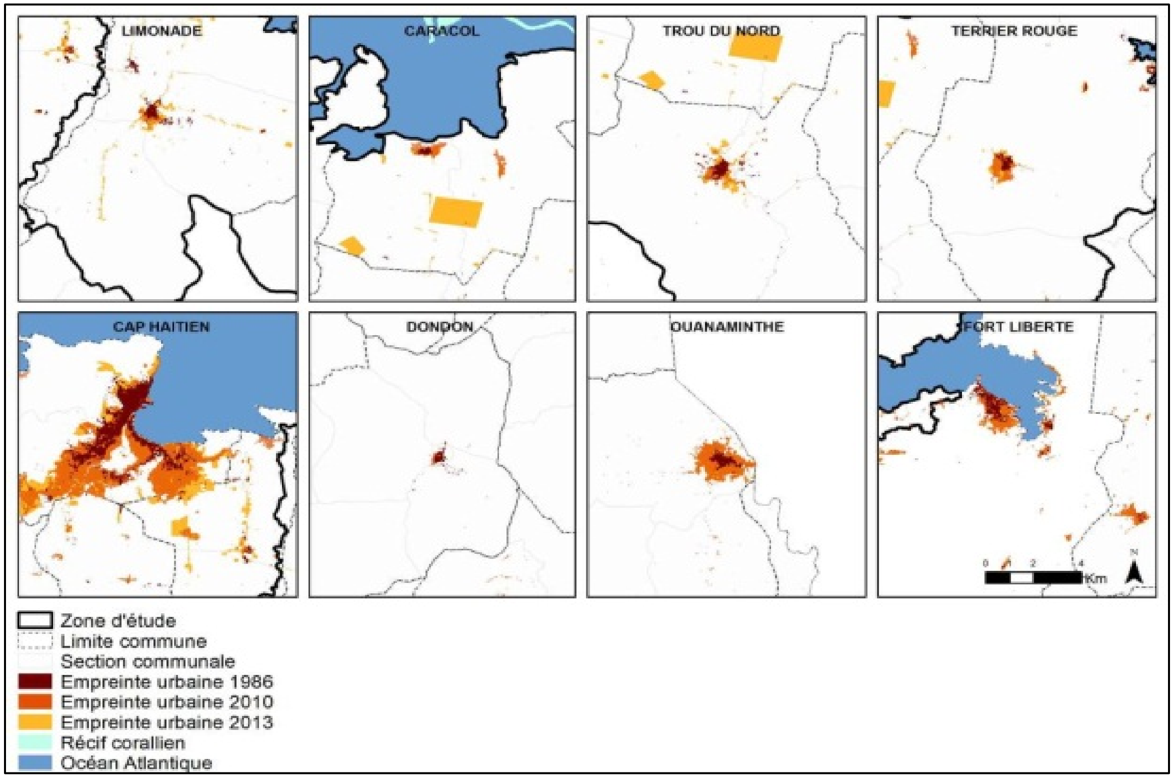

Figure 14 - Urban footprint growth 1986-2010-2013 for key urban areas

Source: Remote sensing analysis from satellite imagery 1986, 2010 and 2013 percent urban to 1.2 percent at the beginning of 2010 and 1.9 urban in 2013. These growth trends, in combination with the development and infrastructure projects expected for the area, will attract more population and are likely to continue the urbanization process.

3.2.2 Vegetation and Agriculture

The findings demonstrate a lack of forested areas. Like most part of Haiti, the mountains of the northern coast have been deforested pushed by demands for agricultural land, charcoal and construction materials. There was also a sharp decrease of cultivated areas, despite the rich quality of soils present in the area of study, in contrast with a steep increase in grasslands, while scrub decreased slowly. Vast plantations of sisal like the Dauphine Plantation halted production due to market conditions, other areas might have been displaced by urbanization and charcoal production, and areas around Terrier Rouge have faced irrigation problems.

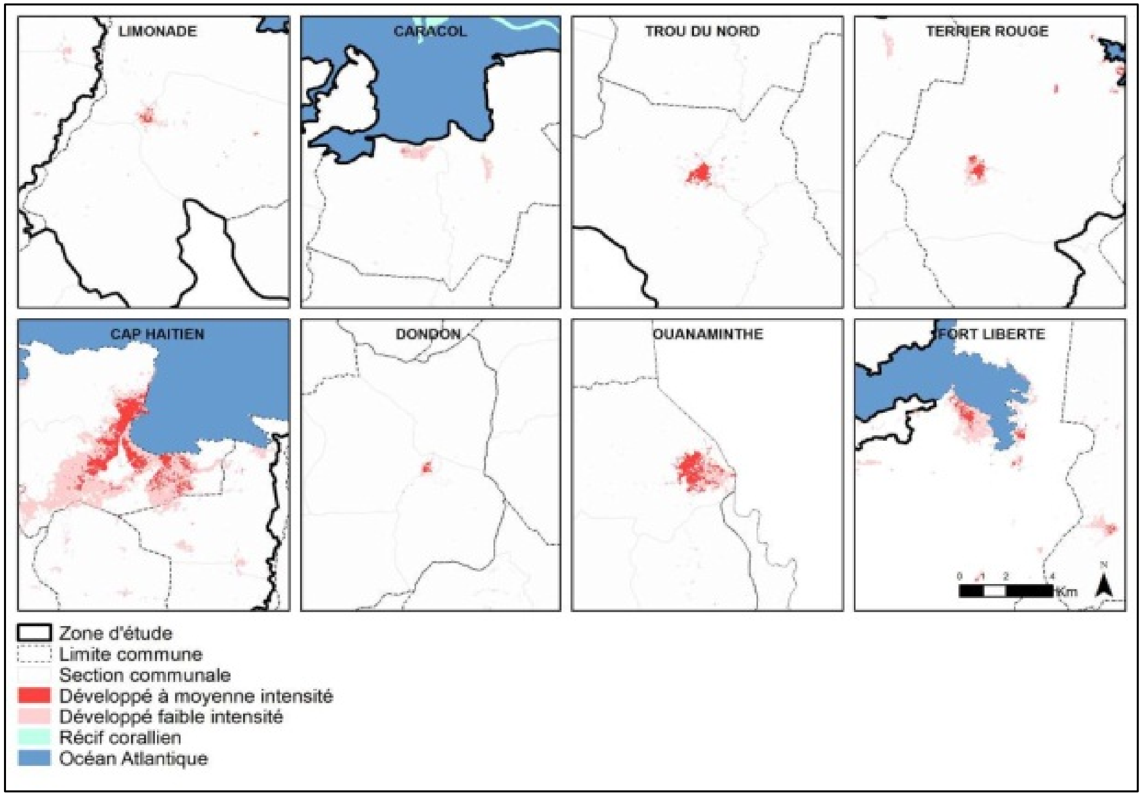

Figure 15 - Urban intensities in 2010

Source: Remote sensing analysis from satellite imagery 2010

3.2.3 The Hydric System

Four land use categories were evaluated to analyze the hydric system: water bodies, forested wetland, scrub wetland and emergent wetlands. However the forested wetlands and scrub wetlands were consolidated because they belong to the mangrove ecosystem in the area of study. The area of water bodies has not changed significant with a reduction of 49 hectares (0. 5 percent) between 1986 and 2010.

The relative isolation of the northern coastline of Caracol and Limonade has protected its hydric system and ecosystems; however, the environmental impacts of deforestation, erosion and flooding have slowly deteriorated the riparian forests of tributary rivers, reducing the area of forested wetlands from 4,318 to 4,061 hectares (0.6 per cent). Finally, it is important to clarify that the areas subject to emergent wetlands were difficult to identify because the study was performed on satellite images without cloud cover and they correspond to the dry season.

3.3 Physical, Biological and Hydrological Baselines

Regional baseline information has been obtained from a variety of sources. A GIS database has been assembled from the various information sources including:

- ***Topography***, which shows that more than half of the study area is relatively flat and its southern border is part of the Grand Massif du Nord, a mountainous formation that elevates from the southern border of RN6 towards the center of Hispaniola island.

- The ***hydric system*** composed by superficial water, underground water, riparian forests and flood plains, as well as all bodies of water, wetlands, reservoirs and protection buffers around them, aquifer recharge and discharge areas and the coastal and inland flooding areas defined by the Risk Study (see *Section 4*).

- ***Strategic ecosystems and protected areas***, comprising the region's two main strategic ecosystems: marine-coastal and highlands. The Three Bays Marine Park was created the in December 2013. This covers an area of approximately 90,000 hectares that includes the bays of Limonade, Caracol and Fort Liberté, as well as the Lagon aux Boeufs, east of Fort Liberté. The newly established Three Bays Marine Park will help protect the mangroves, eel grass beds, reefs and habitats housing important fisheries that are crucial for providing livelihoods to nearby communities. It will also help protect the area from storm surges and provide local communities with ecosystem services such as carbon sequestration, tourism value and more. The MPA is also home to numerous threatened species, including sea turtles, whales, manatees and migratory birds. The highlands ecosystem is composed by areas adequate for reforestation and riparian habitats, crucial for the improvement of the hydric systems, from the head of the rivers and their watersheds. Like most parts of Haiti, the mountains of the northern coast have been deforested pushed by demands for agricultural land, charcoal and construction materials. In between the two main ecosystems, the plains have smaller ecosystems composed of disperse woods and riparian forests.

- The ***normalized difference vegetation index*** (NDVI), an indicator of vegetation health, used to monitor degradation processes. NDVI is the result of a remote sensing process in which vegetation health is evaluated according to the reflection intensity in different color bands captured by the satellite, in particular infrared. In general, vegetation in the NDC is healthier than in most of Haiti, however, it is important to highlight that the healthier vegetation in the NDC corresponds to agricultural areas. In contrast, the highlands ecosystems are less healthy, which explains why the remote sensing process classified most vegetated areas in the mountains as scrub.

- ***Agrological quality of soils classification***, where the NDC area is rich in land classes I through IV, while limited in classes V through VIII. It is also noted that ecologically-valuable lands belonging to classes VI, VII and VIII are located closer to the coastline or in the mountain areas, and coincide with marine-coastal and highlands ecosystems in the region as discussed above.

These information sources have been used to create individual GIS layers and maps of the area specific to the technical topic, and *Appendix 1* contains all of the individual maps. *Figure 16* provides a composite map showing the collective main ecological system (comprising physical, hydric and biological aspects) for the NDC. Slightly less than half of the surface area of the main ecological structure corresponds to three main groups: areas with potential for forest protection (22%), areas crucial for the protection of water (14%) and key ecosystems (12%), mainly mangroves, disperse forests and dunes and beaches.


Agricultural land with Grand Massif du Nord in the distance

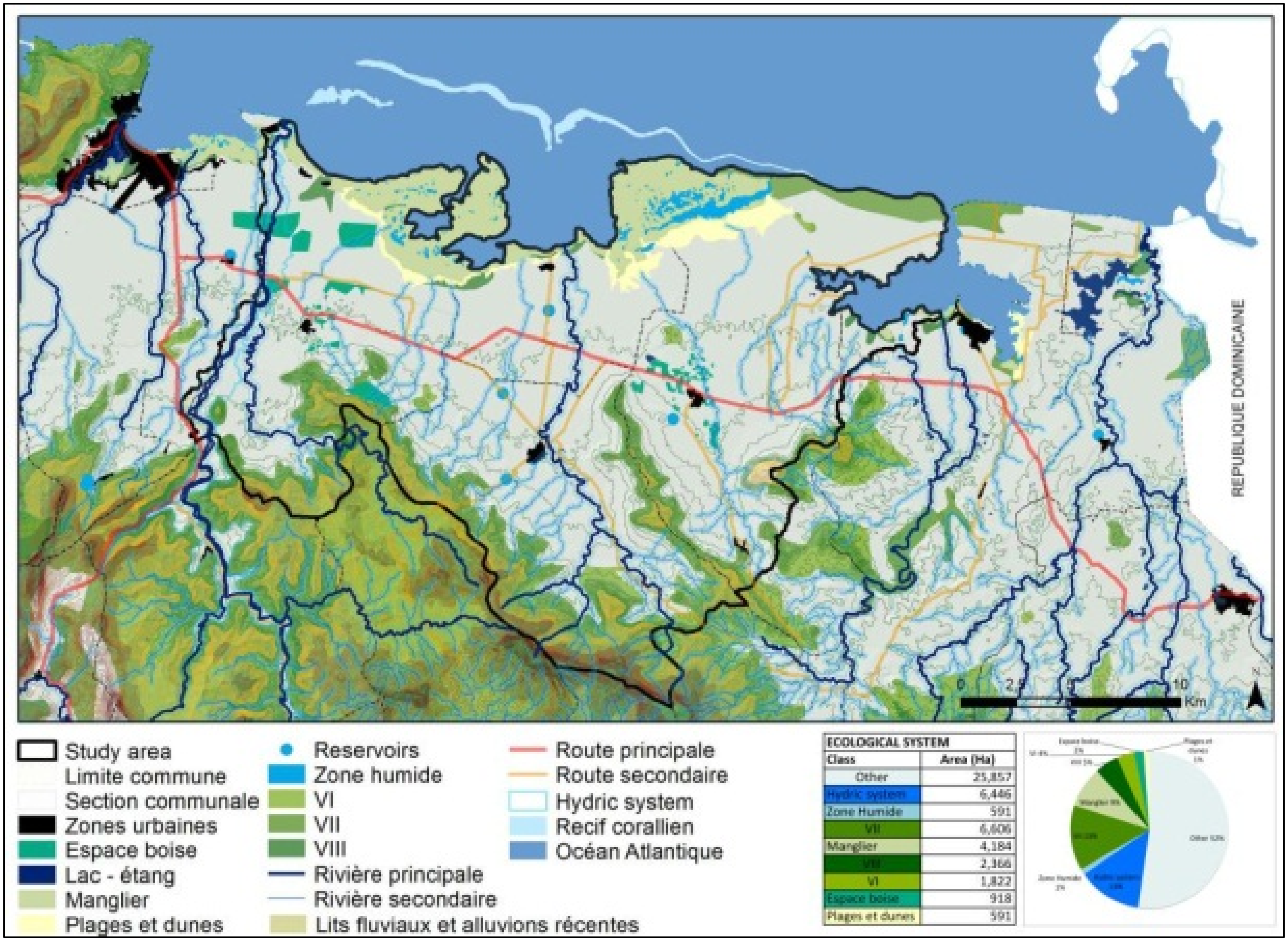

ECOLOGICAL SYSTEM	
Class	Area (Ha)
Other	25,857
Hydric system	6,446
Zone Humide	591
VII	6,606
Manglier	4,184
VIII	2,366
VI	1,822
Espace boise	918
Plages et dunes	591

Figure 16 - Main ecological system on the Northern Development Corridor

Map source: From geographic information layers by AIA (2012), CIAT (2012), CNGIS (c.2012), IADB (c.2013), NATHAT (2010), USAID-OFDA (c.2012), OSM (2013), OCHA (c.2010), PDNA (2010) and DTM (2013). Georeferencing, digitizing and remote sensing analysis from satellite imagery 1986, 2010 and 2013.

3.4 Cultural Heritage

Northern Haiti has a vast and valuable cultural heritage, documented through field surveys and historical research, as illustrated in *Figure 17*. The region possibly has the earliest Pre-Columbian Amerindian sites in the Caribbean, and the earliest documented in Haiti (early lithic, possibly 4,000 B.C.), as well as sites associated with the Arawak and Taino cultures. La Navidad, the first known European settlement in the Americas, is located in the shoreline between Limonade and Caracol, and in front, with its traces lost in the Ocean, is the potential site of the wreckage of Christopher Columbus' Santa Maria ship, the best known of several underwater archaeology, traditional shipbuilding, fishing traditions, and the historical implications of maritime trade throughout the Caribbean Basin.

Spanish and French colonial heritage left forts, fortifications and military buildings, and later, independence, with the earliest and most significant slave re-volts, ended in the first free Black Republic of the Americas and their heritage. The eighteen, nineteen and twentieth century contributed with sugar, indigo and sisal plantations and the remains of their facilities, including some investments from United States.

Such history also left a rich architectural heritage and construction techniques: traditional wattle-and-daub vernacular architecture, Caribbean wood, rubble and ashlar and stone masonry colonial structures and early modern reinforced concrete typologies. Urban fabric and settlement patterns mostly display European colonial array in contrast with disperse Caribbean configurations.

Figure 17 - Cultural heritage

Map source: From geographic information layers by AIA (2012), CIAT (2012), CNGIS (c.2012), IADB (c.2013), NATHAT (2010), USAID-OFDA (c.2012), OSM (2013), OCHA (c.2010), PDNA (2010) and DTM (2013). Georeferencing, digitizing and remote sensing analysis from satellite imagery 1986, 2010 and 2013.

3.5 Urban, Commercial and Infrastructure

The urban and infrastructure development has also been mapped, and has comprised the following:

- Industrial uses such as the PIC and mining concessions;
- Roads acknowledging the hierarchy of roads including national routes, urban roads, secondary roads and tertiary roads.

- Public utilities, acknowledging that the NDC is significantly undeserved and the 98% of the study area that is currently rural lacks basic utilities, such as water supply, wastewater collection, storm water drainage, solid waste management and electricity; and

- Employment and key economic activities such as commercial (transnational, regional and local markets), industrial (the PIC), services (hotels, financial institutions and fuel stations), institutional (health facilities, universities, police stations, wastewater and solid waste treatment areas) and mining activities.

- Social services and infrastructure including health and education facilities.

These information sources have been used to create individual GIS layers and maps of the area specific to the technical topic, and *Appendix 2*.

4. HAZARD AND RISK ASSESSMENT STUDIES

This section presents the work undertaken for building a baseline risk assessment and vulnerability analysis for the NDC. It outlines the results of a probabilistic risk assessment, impact analysis and mapping of prioritized hydro-meteorological and geophysical hazards. It utilizes the common risk framework, where risk is a function of hazard, exposure and vulnerability. The results from this aspect of the study will assist decision makers in:

- Better understanding hydro-meteorological and geophysical hazards;
- Identify which assets are most exposed to the natural hazards; and
- Understand the most serious potential consequences of climate change such as physical damage, economic loss and loss of human life.

4.1 Prioritized Hazards

Based upon a review of available hazard records and information, discussions with the IDB specialists and Haitian stakeholders (see *Table 2*), the following five hazards were prioritized and studied:

- ***Seismicity***: Haiti shares the island of Hispaniola with the Dominican Republic. This portion of the Greater Antilles is located at the northern edge of the Caribbean tectonic plate, at its boundary with the North-American plate. The limit between the two tectonic plates is defined by a strike-slip left-lateral motion, since the Caribbean plate moves relatively to the east-northeast and the North-America plate moves relatively to the west. This kind of interaction induces a strong liberation of mechanical energy, typically and frequently materialized as earthquakes, and can trigger tsunamis. The boundary between the two plates is not defined by a single border line, but instead by a zone where several tectonic fault systems which run across the island and show evidence of historic and/or pre-historic activity. Within the system, there have been historic evidence of several destructive earthquakes, the most recent being the earthquake of January 12th, 2010. The northern coast has been struck repeatedly by earthquakes and tsunamis.

- ***Hurricanes***: The World Bank's Climate Risk and Adaptation Country Profile states that over the past 30 years, Haiti has been hit by six hurricanes, where the impacts of these storms can be expected in all areas, including northern regions, where impacts of include flooding, loss of life, livestock, destruction of agricultural lands, erosion, river siltation, increased incidence of water-borne diseases, and famine.

- ***Inland Flooding***: Flooding is by far the most destructive hazard in Haiti. The country's most populated cities are all nestled in flat coastal valleys. Widespread deforestation in the upper reaches of these valleys, coupled with the lack of storm water drainage infrastructure in urban areas, creates an environment conducive to inland flooding.

- ***Coastal Flooding***: Settlements along the coast and in low lying areas, along with damage to

Flooding in Limonade

and dwindling mangrove assets and deterioration of littoral environments, result in exposure of populations and communities along the northern coast to coastal flooding.

- ***Drought***: The north of Haiti has frequently experienced repeated droughts, brought about by a combination of erratic rainfall patterns coupled with a limited water management infrastructure. In Haiti, droughts have destroyed crops, reduced agricultural production, and decreased food security. Missing or poorly managed water infrastructure makes the agricultural regions and hence, the livelihoods that depend on them, particularly vulnerable to a changing climate.

Table 2 – Haitian stakeholders

Stakeholders engaged
• Comité Interministériel d'Aménagement du Territoire (CIAT) • Direction Nationale de l'Eau Potable et de l'Assainissement (DINEPA) • Ministère de l'Agriculture • Ministère des Travaux Publics, Transport et Communication (MTPTC) • Ministère de l'Economie et des Finances (MEF) • Centre National de l'Information Géo-Spatiale (CNIGS) • Direction de la protection Civile (DPC) • Institut Haïtien de Statistique et d'Informatique (IHSI) • Bureau Des Mines Et Energies

4.2 Methodology

The process for the risk and hazard assessment comprised the following steps:

i. Climate change assessment;
ii. Development of hazard profiles;
iii. Vulnerability assessment; and
iv. Loss estimation.

Section 7.12 then presents risk reduction recommendations, where hazard losses are compared and a series of sustainability recommendations are presented for each hazard, as well as a cost-benefit analysis for five mitigation strategies.

4.3 Climate Change Projections

4.3.1 Approach

The available information and studies on climate change scenarios relevant to the study area in northern Haiti were researched and summarized. The key findings were then inputted into the risk assessment work in order to enable the natural hazards of flooding (both inland and coastal), hurricanes and drought to be assessed when taking into consideration future climate change predictions.

The Climate Studies Group (at Mona, Jamaica), part of the University of West Indies, was commissioned to undertake an assessment of climate change parameters and projections applicable to northern Haiti. This work is presented in *Appendix 3*, and comprises the following:

- Projected Changes in 5 Atmospheric Variables for selected grid boxes over Haiti from the PRECIS RCM, February 2014; and
- Evaluation of trends in sea levels and tropical storm intensities, February 2014.

The climate change parameter projections were obtained through the running of PRECIS (Providing REgional Climates for Impacts Studies), which is a Regional Climate Model (RCM) and was developed by the Hadley Centre (UK) in order to help generate high-resolution climate change information for as many regions of the world as possible. PRECIS is made freely available to groups of developing countries in order that they may develop climate change scenarios at national centres of excellence, simultaneously building capacity and drawing on local climatological expertise.

For this project, the PRECIS projections assumed an A1B emissions scenario. Under this scenario, as defined in the Inter-governmental Panel on Climate Change's (IPCC) Special Report on Emission Scenarios (SRES), it relates to a future world of very rapid economic growth, global population that peaks in mid-century and declines thereafter, and the rapid introduction of new and more efficient technologies. A1B assumes a balance across all energy sources (where balanced is defined as not relying too heavily on one particular energy source, on the assumption that similar improvement rates apply to all energy supply and end-use technologies). No projections were available for other emissions scenarios or the new Representative Concentration Pathways (IPCC 2013).

4.3.2 Temperature and Precipitation

Future change data are provided for five variables when considering an A1B emissions scenario. For four of the five variables the data was provided as absolute change. These variables are: minimum temperature (^{o}C), maximum temperature (^{o}C), mean temperature (^{o}C) and 10 m wind speed (m/s). Percentage change is provided for precipitation. The change for each variable and for each period is calculated for the 2040s consistent with the time horizons of the overall ESCI study. *Table 3* summarizes the future change data ranges.

4.3.3 Sea Level Rise and Tropical Cyclones

An assessment of current literature on current and projected trends in sea level rise and storm intensities with particularly emphasis (where possible) on future values for the Caribbean region was also undertaken.

Table 3 – Summary of Climate Change Projections for the 2040s for Northern Haiti

Months	Mean Temp (°C)	Min Temp (°C)	Max Temp (°C)	Precip (%)
NDJ	1.37 to 1.74	1.62 to 1.85	1.41 to 1.76-	-11.03 to - 3.01
FMA	1.36 to 1.60	1.63 to 1.94	1.45 to 1.78	-0.83 to 9.98
MJJ	1.30 to 1.77	1.73 to 2.06	1.54 to 2.11	-10.14 to - 4.4.3
ASO	1.48 to 1.91	1.72 to 2.02	1.51 to 2.07	-15.72 to - 7.14
Annual	1.38 to 1.74	1.67 to 1.97	1.48 to 1.93	-9.50 to - 3.69

Data is averaged for over three month seasons: November-January (NDJ), February-April (FMA), May-July (MJJ) and August–October (ASO), roughly consistent with the Caribbean dry season and wet season.

For sea level rise, projected increases in global mean sea levels were taken from IPCC (2013), relative to 1986-2005 as a baseline; suggest a likely range of 0.17-0.38m increase in the 2046-2065 timeframe.

For storm intensities, simulations are consistently finding that greenhouse warming causes tropical

Tsunami warning in Cap Hatien

cyclone intensity to shift towards stronger storms by the end of the 21st century (2 to 11% increase in mean maximum wind globally). When simulating 21st century warming under A1B, the present models and downscaling techniques suggest increases in intensity and fraction increases in the number of most intense storms.

The IPCC Fifth Assessment Report (IPCC 2013) indicates that the frequency of the most intense storms is more likely than not to increase by more than +10%, while the annual frequency of tropical cyclones are projected to decrease or remain relatively unchanged for the North Atlantic.

This suggests no major change in the frequency of hurricanes in North Atlantic region comprising Haiti. The SRES scenario A1B for study area of Haiti suggests that the wind speeds are projected to decrease by very small magnitude of 0.25 m/s (0.559 mph) over the projected for the 2040s relative to the 1960-1990 baseline. These projected changes have applied to model wind speed over the return period to develop wind hazard maps for Haiti that reflect projected climate change scenarios. The resultant maximum wind speed with projected climate change scenario are compared to modeled wind speeds for Haiti and are outlined in Table 4.8.

4.4 Hazard Profiles

For the five prioritized hazards, profiles were developed by investigating the various natural hazard occurrences within the study area. The hazard identification process included consultations with key Governmental, NGO and community stakeholders, as well as observations during field missions. Information on past hazard events were also downloaded from the Disaster Information Management System (http://www.desinventar.net/). The profiling of hazards includes determining the spatial extent of hazards, where possible (i.e. maps), understanding the frequency or probability of future events, their magnitude, and climate variability factors that may affect their severity. Each identified hazard has unique characteristics that can impact northern Haiti. *Appendix 4* provides the detailed hazard profiles, and these are summarized below.

4.4.1 Seismic

An earthquake is caused by a sudden motion or trembling of the earth due to an abrupt release of stored energy in the rocks beneath the earth's surface. When stresses due to underground tectonic forces exceed the strength of the rocks, they will abruptly break apart or shift along existing faults. The energy released from this process results in vibrations known as seismic waves that are responsible for the trembling and shaking of the ground during an earthquake.

The seismic hazard in Haiti has its origin in the interaction of the North American and Caribbean plates, which have a relative eastward movement of 2 cm/year (20 mm/yr). The island of Hispaniola is considered a complex area of deformation which presents both subduction zones off the northern and southeastern coast and strike-slip fault zones that transect the northern and southern portion.

While there is a verifiable record of earthquake occurrences dating back more than 500 years in the Caribbean, in general, the occurrence of seismic events in Haiti has been poorly recorded. A review of the information available has indicated that since 1750 approximately 19 major earthquake events have been recorded, culminating in the tragic event in January 2010 which claimed the lives of over 200,000 people.

Appendix 4 provides full details of the methodology applied to determine the seismic hazard for the study area, which has involved assembling relevant seismic data and information for Haiti, geo-referencing the information to the study area, and overlaying against local geological characteristics and slope indices in order to generate earthquake hazard maps, expressed in terms of peak ground acceleration (PGA) soil values at 10 m horizontal resolution. The PGA is a measure of how hard the earth shakes in a given geographic location, in other words the intensity of an event. A series of maps has been developed for different return periods, and *Figure 18* provides an example hazard map

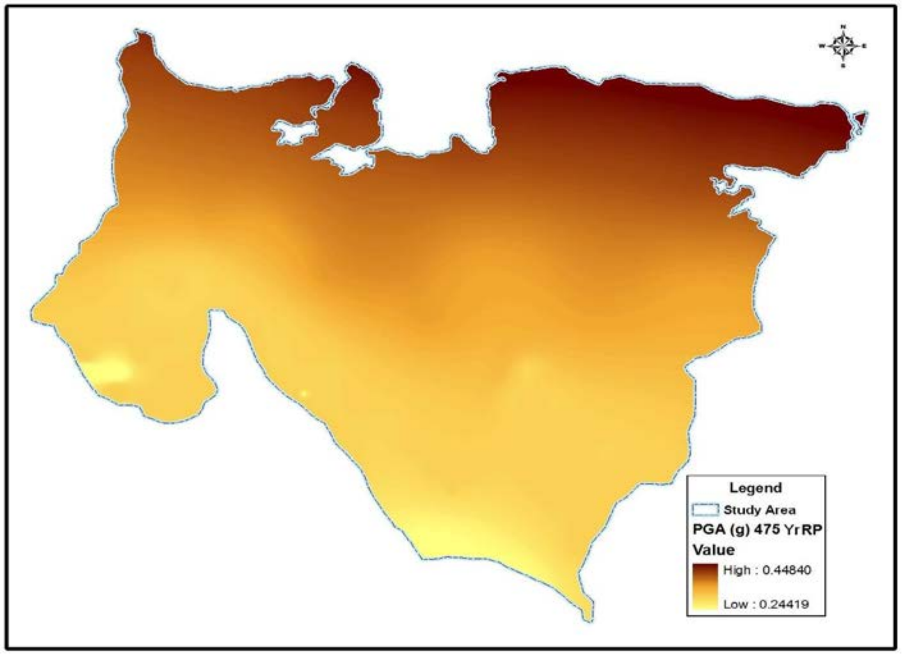

Figure 18 - PGA probabilistic seismic hazard map for 10% probability in 50 years, i.e. 475-year return period

developed for the study area.

The assessment indicates that areas at higher seismic risk (as indicated by the darker areas in *Figure 18* which correspond to higher PGA values), principally due to the underlying soil conditions, are those areas closer to the coastline where softer and deeper soils exist.

4.4.2 Hurricanes

Hurricanes and tropical storms are large-scale systems of severe thunderstorms that develop over tropical or subtropical waters and have a defined, organized circulation. Hurricanes have a maximum sustained (meaning 1-minute average) surface wind speed of at least 74 mph; tropical storms have wind speeds of 39 mph to 74 mph.

Hurricanes get their energy from warm waters and typically lose strength as the system moves inland. Hurricanes and tropical storms can bring severe winds, inland flooding, storm surges, coastal erosion, extreme rainfall, thunderstorms, lightning, and tornadoes. Hurricanes and tropical storms typically have enough moisture to cause extensive flooding.

Haiti is among the most hurricane-prone locations in the world. In 2004, the Food and Agriculture Organization (FAO) reported that during a period from 1909 - 2004, forty-seven (47) tropical storms and hurricanes hit Haiti. From 2004 to 2012, twelve (12) wind storms have made landfall in Haiti. Data from the Prevention Web , which provides information on human and economic losses from disasters, indicates that between 1980 and 2010, over four million (4,171,407) persons have been affected by hurricanes in Haiti, with 4,990 deaths caused and economic impacts for the same period of US$ 822 million.

One of the most serious components of hurricanes is high winds. Because of the extensive size of a catastrophic hurricane, a storm need not pass directly over Haiti to cause severe damage. A hurricane passing within close proximity to the island of Hispaniola can also cause major damage to property and even loss of life. Essentially there are no areas of Haiti that are free from hurricane force winds. The coastal and low lying areas, such as those of the study area, experience the first effects of damaging winds. The rains that accompany hurricanes are intense and last for several days. Intense and prolonged rainfall, winds and pressure can cause both coastal flooding (see *Section 4.4.3*) and inland flooding (see *Section 4.4.4*).

The methodology developed for the identification of wind hazards for this study was based on numerical modeling of hurricane motion using existing models and verifying and calibrating this work against the local study area parameters, as well as building in the projections for future climate change implications. *Appendix 4* provides full details of the methodology applied to determine the hurricane hazard for the study area.

These results model wind speed over various return periods in order to develop wind hazard maps for Haiti that reflect projected climate change scenarios. Hurricane risk, associated with wind speed, is a relatively homogeneous factor across the study area, and therefore no discernible geographical variation was noted for the study area.

4.4.3 Coastal Flooding

High waves associated with tropical storms and hurricanes are potentially very dangerous and damaging to the coastal settlements due to the storm surges which can cause extreme flooding in coastal areas, particularly when storm surge coincides with normal high tide.

The storm surge is produced by water being pushed toward the shore by the force of the winds moving cyclonically around the storm. The impact on surge of the low pressure associated with intense storms is minimal in comparison to the water being forced toward the shore by the wind. The intensity of the storm surge is affected by the width and slope of the continental shelf. A shallow slope will potentially produce a greater storm surge than a steep shelf. The north of Haiti is prone to storm surge.

Towns such as Bor de Mer de Limonade, Caracol and Phaeton are susceptible to coastal flooding caused by storm surge. The American Association of Architects, indicate that these settlements are in a precarious location to shoreline (American Institute of Architects, 2012). There is, however, limited documented history concerning storm surges in Haiti, let alone well documented instances of coastal flooding within the NDC.

To assess coastal flooding, a regional model was utilized and adopted to understand wave and surge heights in the study area. The information utilized for this study effort was derived from the Atlas of Probable Storm Effects in the Caribbean Sea, which was developed under the Caribbean Disaster Mitigation Project (CDMP), a joint effort of the Organization of American States (OAS) and the US Agency for International Development (USAID).

Wave and storm surge heights for four return periods (10, 20, 50, and 100 years), which were reported for specific points along the Haitian coast. For this study, wave height and surge heights that were reported for Cap Haitian were adopted for the entire study area. These water levels were then projected onto the coastal land using a GIS to demarcate the horizontal extent of inundation. The effects of projected climate change were also integrated into the assessments, including minor changes in sea level rise as per *Section 4.3.3*, are represented on the extent of flooding. *Appendix 4* provides full details of the methodology applied to determine the coastal flooding hazard for the study area, and *Table 4* presents the projected results of coastal flooding.

Figure 19 shows the 50-year return flood map for the study area showing the potential for inundation, and illustrating the vulnerabilities of coastal settlements such as Caracol, Jaquezy, Borde de Mer de Limonade, and Phaéton to flooding.

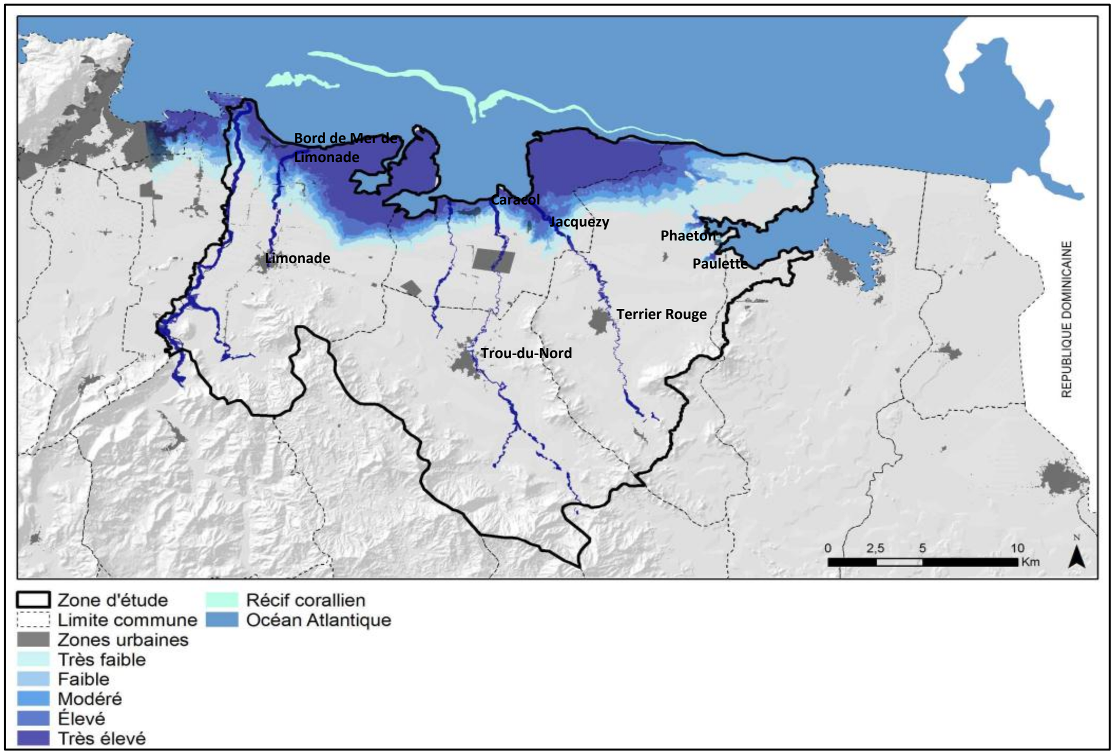

Figure 19 – Coastal flooding with climate change projections for a 50-year return period

Table 4 - Coastal flooding projections (including for climate change to 2040)

Return Period	Predicted Flood Level (m)	Predicted Area of Flooding Inundation (km^2)
10 Year	3.55	101
25 Year	4.65	115
50 Year	5.35	128
100 Year	6.15	141

4.4.4 Inland Flooding

Floods can arise from a variety of causes. The most commonly understood floods occur when water levels in rivers rise and the waters overtops their banks, and adjacent floodplains and lowlands are subject to recurring floods. This type of flooding usually occurs after intense or prolonged rainfall. A second type of flooding can also occur due to heavy rains where infiltration of rainfall is impeded (through either impermeable soils or increase in impervious surfaces due to development).

Floods in Haiti, as in other Caribbean islands, follow tropical weather patterns. Haiti has two distinct rainy seasons, one from April to June and another from October to November. There have been a number of large-scale devastating flooding events in Haiti over time and most of the flooding events have been linked to large-scale climatic events (i.e. tropical cyclones), as well as more recently smaller low pressure systems which have impacted Haiti on a yearly basis.

Haiti's rugged and mountainous terrain coupled with environmental degradation and poor watershed management has created optimal conditions for flooding problems.

ERM Flooding Study

As part of this ESCI study, a flooding study was performed on the two principal watersheds in the study area, the Trou-du-Nord and the Grande Rivière du Nord (see *Figure 20*). ERM's study only assessed river-related flooding.

The Trou-du-Nord watershed measures 110 km². The Rivière Franiche, Rivière Pilette and Rivière Cabaret are the main tributaries to this river and are intermittent streams and are dry part of the year. The Petite Rivière, an intermittent river, is also located in this basin and drains into the Trou-du-Nord plain. The Grande Rivière du Nord watershed measures 680 Km². The Rivière Caracol and Rivière Cartache are main tributaries to this river. The Rivière Caracol is a permanent river with a constant source of water, while the Rivière Cartache is an intermittent stream and is dry part of the year.

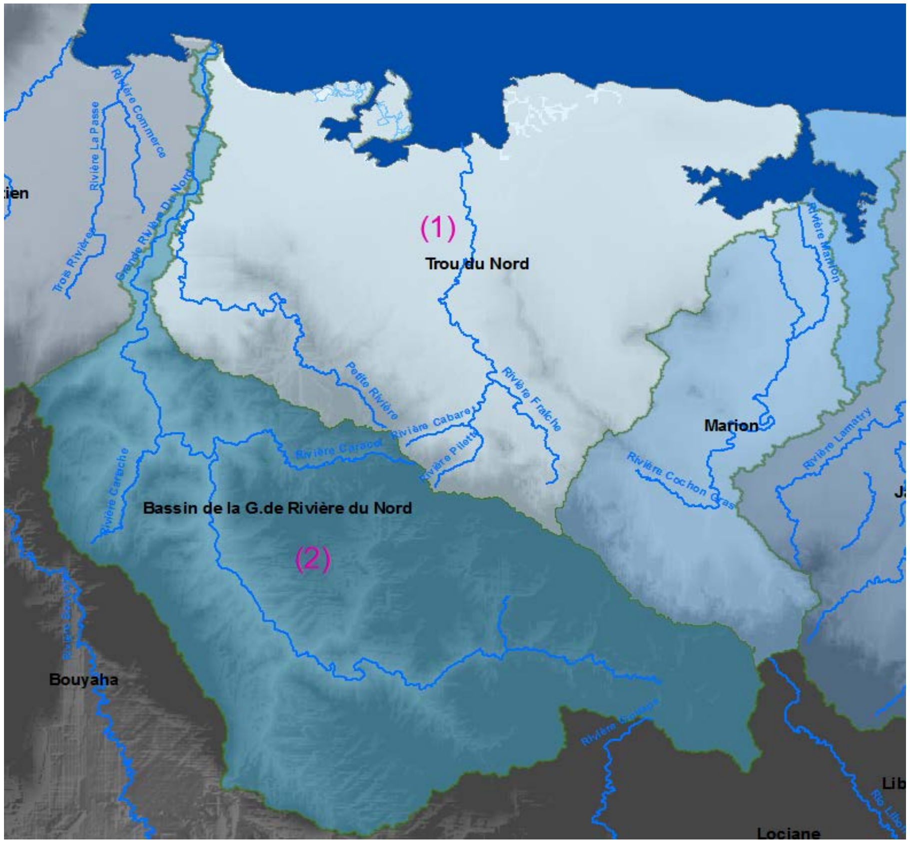

Figure 20 – Key watersheds in the study area

Source: CNGIS

The vulnerability of these two watersheds is significant, with widespread deforestation, clearing of land for agriculture and increased urbanization all contributing to the flooding problems in the region.

The commune of Quarter Morin, which is situated in a moist, low lying alluvial plan and bordered on the east by the Grand Rivière du Nord, is prone to flooding. Several factors have worked to increase the susceptibility of flooding, including more intense climatic events, increased run-off, and the accumulation of debris downstream. Limonade is bordered by the Grand Rivière du Nord on the west. While the Barrage de Tannerie previously helped to contain flood waters and provide irrigation during the dry season, the dam failed in the 1960s and has not been repaired. Intense rainfall causes flooding and the accumulation of water in low-lying areas which are slow to drain following flooding events due to limited or inadequate storm water drainage infrastructure. Limonade receives an average of 1200-1400 mm rainfall annually.

In Trou-du-Nord, the terrain, rainfall and soil types, in both the mountains and plains, give rise to a fairly dense network of rivers. The Trou-du-Nord river is the most important river system. In low-lying portions of commune, there are a series of smaller tributaries and torrential gullies. Large areas of the plain are subject to frequent flooding caused by torrential downpours. The heavy clay content of the soil causes erosion and results in frequent sediment build up in streams. Urban areas are adjacent to the main river with development occurring in riparian zones. Historically, the city has been flooded severely.

Flood risks are also present in the northeast portion of the Terrier Rouge commune, sometimes impacting the city on its northern edge. To the south, settlements experience higher annual rainfall amounts, and as a result, experience flash floods. The urban development of the city is constrained by low lying topography, which is prone to flooding.

A detailed flood hazard assessment methodology was undertaken which included a meteorological analysis and a probabilistic simulation of rainfall which has considered climate change. Hydrologic modeling was undertaken to simulate the precipitation-runoff processes, and hydraulic modeling of the main rivers identified above was also undertaken to develop probabilistic flood forecast maps for six return periods (2-, 5-,10-, 25-, 50-, 100-return periods) for the portions of the basin that intersect the study area, and including climate change projections. *Appendix 4* provides full details of the methodology applied to determine the inland river flooding hazard for the study area, including some of the challenges encountered.

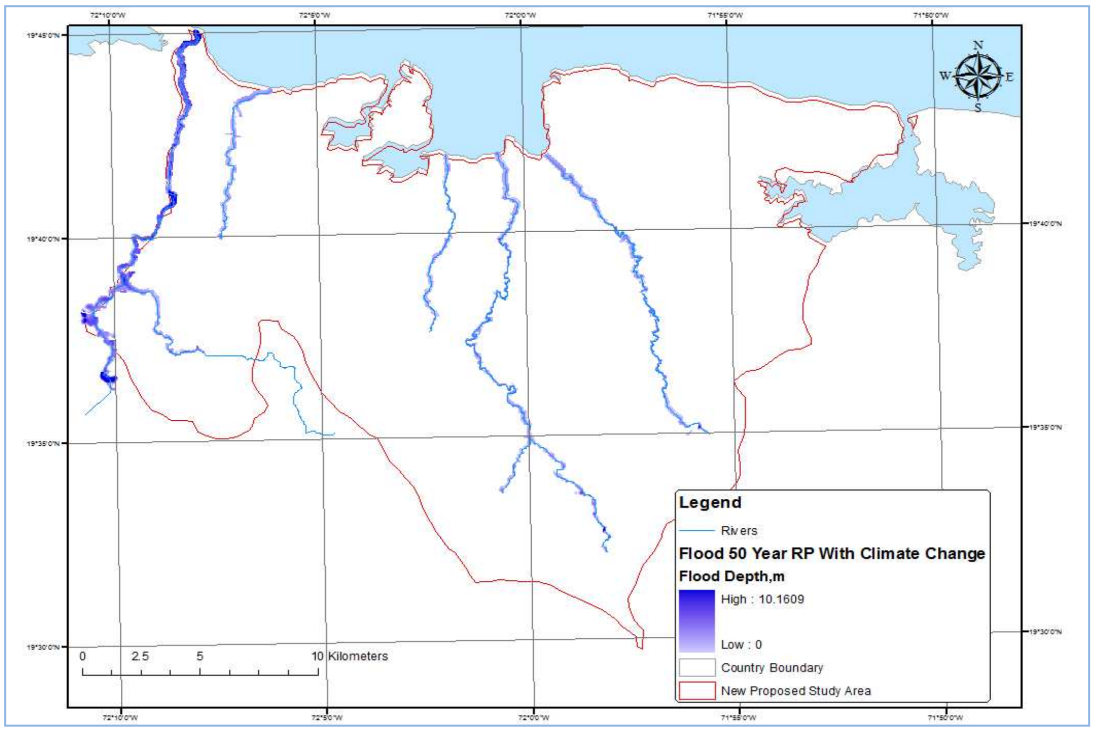

Figure 21 - Inland flood hazard map with climate change 50 year return period

Table 5 presents the projected results of inland river flooding across the study area, and *Figure 21* shows the 50-year return flood map for the study area showing the potential for flooding. The results shows that with climate change on an average flood depth will increase by about 0.23 m (23 cm) across all return periods.

Table 5 – Inland river flooding projections (including for climate change to 2040)

Return Period	Predicted Flood Level (m)	Predicted Area of Flooding Inundation (km^2)
2 Year	8.89	8.2
5 Year	9.36	10.3
10 Year	9.81	11.4
25 Year	9.91	12.4
50 Year	10.16	13.0
100 Year	10.36	13.6

IDB Flooding Study

Commentary and key results to be inserted

4.4.5 Drought

Drought manifests itself in many forms. The drought hazard in Haiti results from a combination of erratic rainfall patterns during the two distinct rainy seasons: April–June and October–November. According to the World Bank, El Niño/ ENSO episodes have tended to delay the arrival of the rainy season(s) and create drought conditions in the country. NATHAT (2012), in a national level hazard assessment, indicated that farmers are reporting longer dry seasons and wetter and shorter rainy seasons. The NATHAT study has also categorized most of the northern coast as being susceptible to drought hazard (see *Figure 22*). The cumulative effects of longer dry periods are crop losses and that more families are becoming reliant on food assistance during the "hunger season", which is the three-month period between rainy seasons, in which there is little harvesting and employment opportunities.

The Famine Early Warning System Network (FEWS Net) reported in August 2011 that the north and northeast were affected by drought and estimated that major crop yields would be diminished by 20 percent. The FEWS Net furthered detailed what is a recurring phenomenon in the northern coastal plains and reported that "*rainfall in wet mountain areas [of the Northeast] has helped spur crop growth and development, while crops in Ferrié, Fort Liberté (except on the Maribaroux plains), Terrier Rouge, Caracol, and Trou-du-Nord have failed due to the drought conditions in these areas, prolonging the lean season, which generally "ends in June... [and that]... virtually the entire northern region has been affected by the drought which delayed the start of the spring planting season, which eventually got underway in June with the onset of the rains...*" (FEWS 2012).

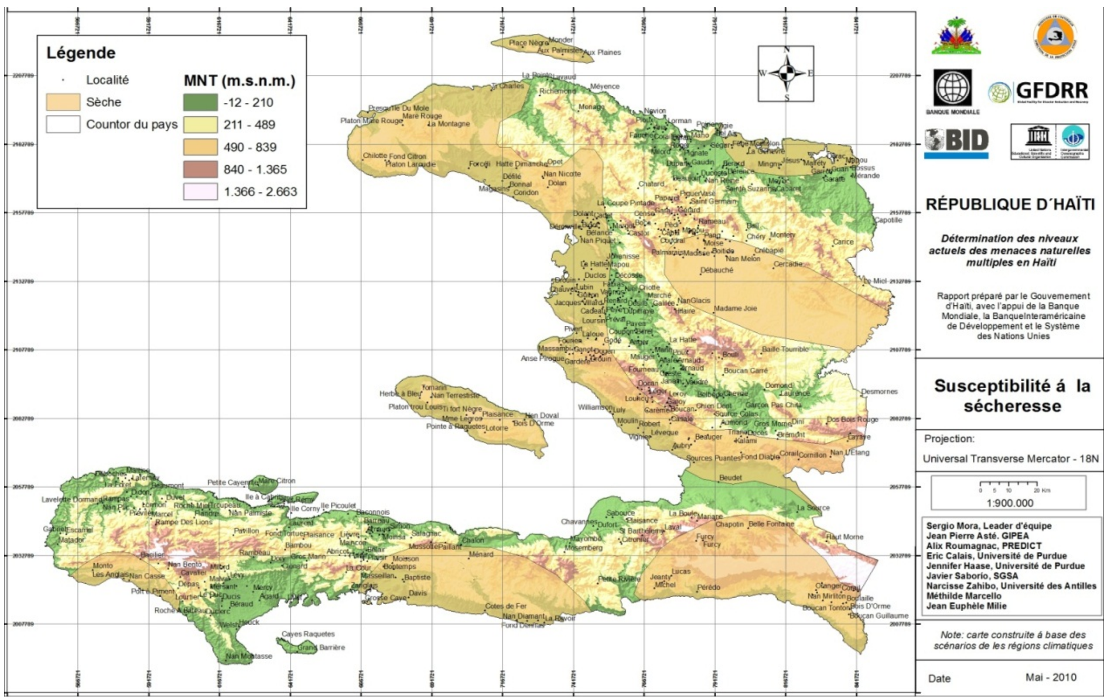

Figure 22 – Drought susceptible areas in Haiti as presented by NATHAT, 2012

Of greater concern to stakeholders is the impact that these short term fluctuations in precipitation will have on the surface and subsurface water supply or the hydrological regime of watersheds that intersect the NDC. It takes longer to recognize the effects of hydrological drought on soil moisture levels, stream flows, as well as in groundwater and reservoir levels. The frequency of hydrological drought is typically measured over the longer term and predicates a need for understanding of both the supply and demand for water. Hydrological drought concerned with the problems associated with deficiencies in precipitation (the supply) and that of competing interests for water access and utilization (the demand).

An assessment of drought has been performed focusing on the influence of precipitation, and how this is coupled with the anticipated effects of development and climate variability, will impact the current and future water supply. Current and future water balance was estimated for the two main watersheds that intersect the study region. This study does not seek to address the broader environmental, political and socio-economic factors that also play a role in water access issues.

The hydrological drought assessment has been performed by estimating components of the classical hydrological cycle. The movement of water through the hydrological cycle varies significantly in both time and space. The hydrological cycle emphasizes the four factors of interest to hydrologists:

- Precipitation;
- Evapotranspiration;
- Surface runoff; and
- Groundwater.

For this analysis, the hydrological models that were developed for the flood hazard assessment, along with other conventional methods of hydrological assessment, have been used to assess potential water availability for the watersheds of Grand River Du Nord and Trou-du-Nord. The climate change projections have also been integrated into the assessment.

Appendix 4 provides full details of the methodology applied to determine the drought hazard for the study area. Based on the estimates of water availability potential and demands, overall summary of water balance is shown in *Table 6*.

The current water availability potential is considerably more than the demands. But in future projections, the water availability potential is merely sufficient to meet the projected demands.

The monthly variations in the availability and demand potentials are shown in *Figure 23* for present day, while *Figure 24* shows the monthly variation for future growth (2040, using growth projections and development growth presented in Section 5) that takes into consideration climate change.

Table 6 – Summary of water balance for the study area

	Current	Future Projections, 2040
Water Demand, Mm^3		
Urban Population, Mm^3	5.2	5.4
Rural Population, Mm^3	2.4	6.0
Industrial Demand, Mm^3	2.4	8.4
Water Use and Demand , Mm^3	1.5	5.9
Agricultural Demand, Mm^3	101.0	163.2
Total Demand, Mm^3	112.6	188.8
Water Availability Potential, Mm^3		
Surface Water Potential (Runoff), Mm^3	87.6	75.0
Ground Water Potential (Recharge), Mm^3	103.7	152.9
Total Water Potential, Mm^3	191.3	228.0
Surplus/Deficit, Mm^3		
Water Surplus, Mm^3	78.7	39.1

Monthly variation shows that during the dry season of the year, the gap between demand and availability increases as compared to the wet season. There is however a significant gap between the demand and availability potential particularly during the dry season (June to October) as compared to the wet season.

This water deficit during the dry period indicates prolonged periods of hydrological drought, and climate change and projected growth will further reduce the available water stock and make the impacts of prolonged periods of water deficit more significant. Such impacts will become more pronounced during years with below average rainfall.

Figure 23 – Monthly variation in water demand and availability (current conditions)

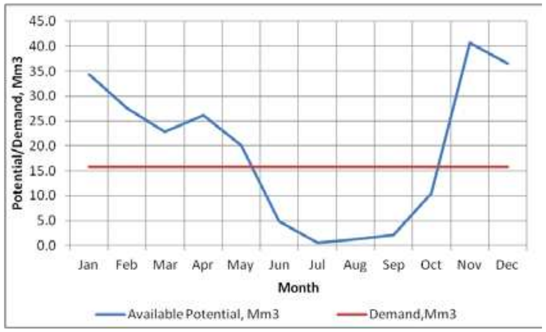

Figure 24 – Monthly variation in water demand and availability (projection for 2040 including climate change)

4.5 Vulnerability Assessment

The vulnerability assessment considers the study area's social vulnerability as well as the more traditional assessment of the potential impacts to the built environment. The social assessment seeks to identify a variety of indicators to inform of the underlying causes of vulnerability in the region, while the more traditional vulnerability assessment identifies assets, characterizes structures and infrastructure so as to determine the built environment's potential performance to different levels of hazard intensity (i.e. acceleration, flood depth, etc.). A vulnerability assessment is performed to assess the specific damage and loss characteristics of each asset identified.

4.5.1 Social Vulnerability

This section informs the underlying causes of vulnerability in the region and the potential impacts of the identified hazards to demographic groupings in the study area. Vulnerability considers the social and environmental aspects that increase and accentuate impacts of hazard events. Social vulnerability focuses on the economic, educational and financial factors that impact the ability of people or communities to adapt to hazards. The vulnerability of the study area is exacerbated by the many factors that define the NDC including:

- Extreme poverty;
- Demographics with more children present (and therefore vulnerable);
- A reliance on self-employment;
- Limited education opportunities;
- Gender inequalities;
- Land access challenges;
- Food shortages and reliance on subsistence farming;
- Limited access to basic needs such as clean water; and
- Environmental degradation such as deforestation.

4.5.2 Characteristics of Assets Exposed

The inventory of exposed assets involves understanding the distribution of people, buildings and infrastructure that may be affected by natural phenomena. Remote sensing along with a rapid field assessment method was used to estimate the number and distribution of assets in the study area. This included understanding the building density and types for each land use category within defined administrative boundaries. Administrative boundaries (i.e. section communal) were then subdivided based on density of building footprints so as to allow for the definition of an appropriate scale from which to capture inventory elements. *Appendix 5* provides a more detailed description of the methodology applied to characterize the assets exposed, and a brief summary is applied below.

This mapping process provided the basis for classifying buildings and for using a suitable classification hierarchy for the capture of a wide range of structures and densities. Such an approach is consistent with standard methodologies used to develop exposure models and supports the required inputs for undertaking a probabilistic risk assessment by providing an approximate spatial location of exposed elements for each block subdivision within the section communal (see *Figure 25*).

Figure 25 - Distribution of block boundaries in the study area

Building occupancy mapping and distribution was then undertaken and structure classification of structures applied. Structural information is an important factor in determining the vulnerability or how likely structures are to fail when they are subjected to hazards, such as wind pressure that exceeds their design. The models of the different types of infrastructure were determined based on experience with the typical construction of Haiti. The basic structural systems were grouped according to the following general construction: reinforced concrete, masonry structure, unreinforced masonry, and earthen.

Replacement values for buildings are then estimated through a review with local construction practitioners, and were then aggregated to create economic values for assets in the different blocks, such as the example shown in *Figure 26*. Similar maps have been produced for commercial and industrial buildings.

A similar process is also followed for facilities and infrastructure, including hospitals, schools, roads, and bridges, utilities such as water, electricity and wastewater.

4.6 Loss Estimation

Probabilistic loss estimates were then determined for seismic, hurricane, coastal and inland flood hazards using standard risk assessment methodologies that take into consideration hazard parameters, in conjunction with damage ratios, to determine the economic loss potential for each hazard (with the exception of drought). *Appendix 6* provides a more detailed description of the methodology applied for loss estimation, and the associated results, and a brief summary is presented below.

These estimates should be used to understand relative risk from hazards and potential losses and are not intended to be predictive of precise results. Uncertainties are inherent in any loss estimation methodology arising in part from incomplete scientific knowledge concerning natural hazards and their effects on the built environment. Uncertainties also result from approximations and simplifications used in the development of hazard maps or the inability to perform a more detailed inventory assessment.

Vulnerability can be assessed by considering the potential and performance of the built environment at different levels of hazard intensity (i.e. acceleration, flood depth, peak gust, etc.). Vulnerability functions were therefore developed for seismic hazards such as earthquake, hydro-meteorological hazards such as flood (both inland and coastal floods) and hurricanes.

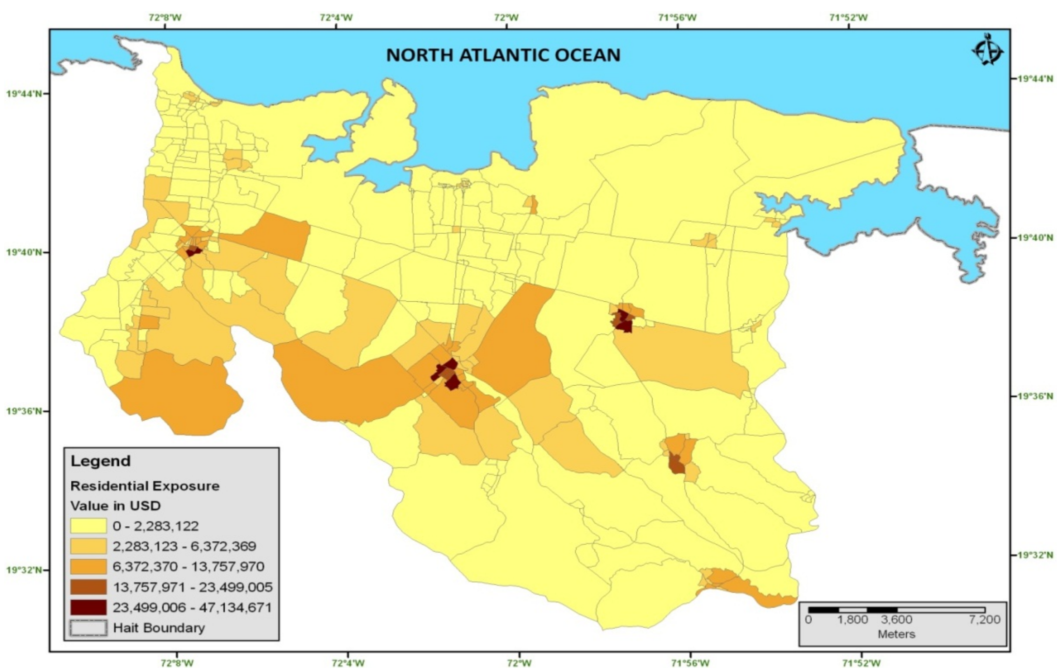

Figure 26 - Distribution and Exposure Values of Residential Buildings in the study area

Vulnerability functions relate the damage or loss magnitude to a specific intensity of a hazard. Vulnerability functions are specific to the particular structure type and must be assigned to each asset according to their characteristics. *Figure 27* presents an example vulnerability function created for coastal flooding for a low rise masonry structure. *Appendix 6* presents the range of vulnerability functions generated as part of this study.

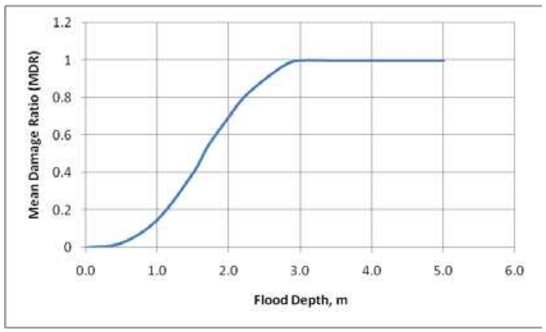

Figure 27 - Example of vulnerability function for Coastal Flood Hazard for low rise masonry structure

Based upon these results, estimates of the losses attributable to each hazard can then be made, and the findings can be used to support local and regional decision makers in their understanding of the potential impacts of each hazard and allow a comparison of hazards by quantifying potential impacts. These estimates can be used to understand relative risk from hazards and potential losses.

The economic loss results are presented here using three risk indicators:

- *Probable Maximum Loss (PML)* - an estimate of losses that are likely to occur, considering existing mitigation features, due to a single hazard event;
- *Loss Exceedance Curve* - plots consequences (losses) against the probability for different events with different return periods; and
- *Average Annualized Loss (AAL)* - estimated long-term value of losses to assets in any single year within the study area.

The risk metrics described above, particularly, the AAL, can be used to provide an understanding of the spatial extent of losses and help to identify and prioritize the urban areas or localities that are under risk. A street light indicator methodology, where the colors on the map coincide with the level of risk, has been used to map risk.

By mapping risk at the block level (see *Figure 28* as an example) stakeholders have a better understanding of where potential losses will be the highest and where monies should be allocated for risk reduction. All the areas and exposure categories that have a high and very high risk are automatic choices for risk reduction measures. *Appendix 6* presents the full set of results from the loss estimates based upon the above risk metrics, and *Table 7* provides stakeholders with an overview of impacts expected for each hazard and a summary of aggregate loses (maximum probable losses), which include economic losses for general occupancy classes and infrastructure.

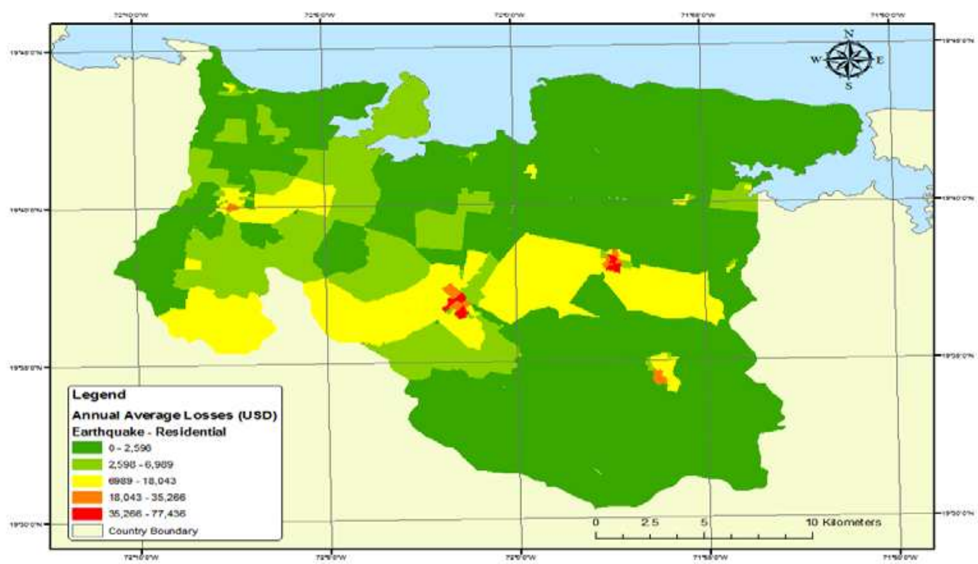

Figure 28 - Risk Map: Average Annualized Loss for Earthquake Hazard, Residential

Table 7 - Summary of Impacts and Loss Estimates by Hazard

Hazard	MRP (Years)	Potential Impacts	Aggregate Economic Losses (USD 10^6)
Earthquake	2,500	• Damage to all structures (residential, commercial and industrial), reconstruction costs can be substantial (heavy walls poor reinforcement); • Loss of Life; • Loss of business and industrial production; • Loss of business production; • Disruption of transport, failure to bridges; • Disruption to electrical network, substation damage; • Extensive damage to lifelines (i.e. water pipe networks, pumping stations, sewage treatment); • Social displacement and unrest;	1694.47
Hurricane	1,700	• Extensive residential and commercial property damage, roof failures, water damages • Moderate damages to industrial property, short term loss of industrial production • Loss of life, • Emergency evacuation needs; • Commercial - Extensive property damage, roof failures, water damages • Property damage to critical facilities, transportation infrastructure (associated flooding biggest threat to transportation infrastructure), substantial damage to electric distribution network, utility disruption	815.81
Flooding	100	• Loss of housing, particularly on areas where there are rapid flows; • Undercutting of rural residential buildings or failure along river banks, where the water may erode soil under foundations • Damage to houses, commercial buildings and critical facilities due to inadequate drainage infrastructure due to prolonged flooding; • Damages to transportation infrastructure, especially in areas of confluence of rivers (i.e. bridges, culverts), restricts transportation throughout study area. • Water and Waste Water Infrastructure - Inadequate drainage prone to blockage by silt, earthen debris, and many cases, garbage; damages to culverts; increase in contamination and secondary threats such as waterborne and vector-borne diseases	10.78
Coastal Flooding	100	• Extensive damage to coastal settlements, and supporting infrastructure. • Health and education facilities located within inundation areas prone to extensive damages • Damages to transportation infrastructure, restricts transportation. • Damages to water lines below ground level and well above ground level • Increase in contamination and secondary threats such as waterborne and vector-borne diseases	93.47

5. FUTURE GROWTH PROJECTIONS

Sections 3 and *4* have presented baseline information that helps define the current interaction of natural and urban activities and which can be used as a basis for determining potential suitability for land use. The projection of future land use needs based on economic development and growth, as well as population increases are also needed to be inputted into the modelling process, and this section presents this information.

5.1 Future Development Projects

The future development projects include on-going and planned development projects, and GIS layers were developed for the following, which are also shown in *Figure 29*:

Committed Projects:

- The Caracol industrial park (PIC);
- The National University of Haiti Roi Henri Christophe Campus in Limonade (UHN-RHC);
- Housing developments (EKAM in Caracol: 750 Housing units and 535 plots, Feed the Poor projects along RN6 and fishing villages); and
- An existing quarry.

Planned Development Projects:

- Sea Port expansion in Cap Haïtien;
- Mining concessions and infrastructure projects (thermic plants, water networks, solid waste treatment plants and wastewater treatment plants); and
- Projected housing (PIC resettlement called Calles or Faias: 572 housing units and Food for the Poor in Terrier rouge: 242 housing plots).

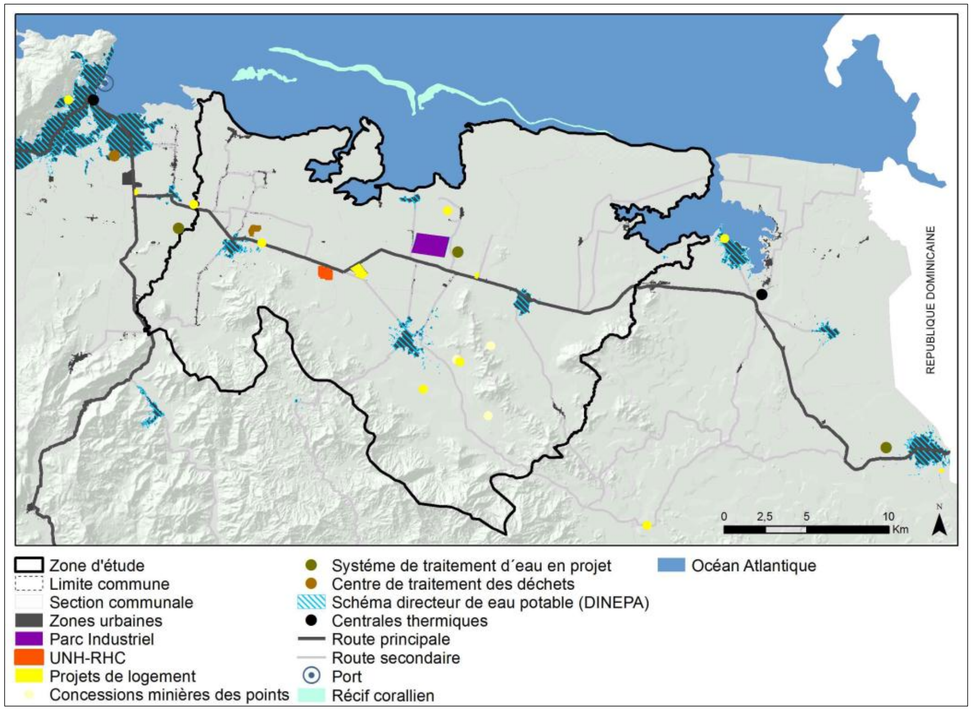

Figure 29 - Development projects

Map source: Variables built from geographic information layers by AIA (2012), CIAT (2012), CNGIS (c.2012), IADB (c.2013), NATHAT (2010), USAID-OFDA (c.2012), OSM (2013), OCHA (c.2010), PDNA (2010) and DTM (2013).

5.2 Population and Demographics

5.2.1 Overview

A detailed analysis of the population of the area of study was performed to understand the dynamics in place and better predict the impact of development projects and investments and the future needs. This analysis focused on two population projections to be calculated for the year 2040:

- ***Slow Growth***: based on the assumption of non-fulfillment of identified development projects (this assumes only the committed projects as described in *Section 5.1*are delivered, and the planned projects do not progress); and

- ***Fast Growth***: based on the assumption that all projects get implemented as described above.

The population assessment has been undertaken, utilizing, and where appropriate supplementing, the AIA Study and the CIAT Strategic Plan. The Institut Haïtien de Statistique et d'Informatique (IHSI) was used as the primary data source (IHSI 2004, 2009a, 2009b, 2009c and 2012; IHSI and CELADE / ECLAC 2008), although it is also acknowledged that IHSI has made only two censuses during the period 1980 to 2003, and while a census is being planned for 2014, data presented for recent years represents projections made by IHSI.

5.2.2 AIA Population Projections

According to the AIA Study, and as illustrated in *Table 8*, a total of 387,339 people were living in the northern area of Haiti in 2009, and specifically in the NDC area, the population is 51,607 (shown as the PIC node, comprising Limonade, Caracol, Terrier Rouge and Trou-du-Nord).

The AIA Study also projects that if the same growth rates of the recent past are extrapolated out to 2020, the region would reach a population of 505,743, representing a growth rate of 1.3% over the period. Of these projections, the NDC area would be characterized by a higher growth rate and represent a total of 67,381 of the total projected population for 2020. A growth rate of 1.2% was then applied to the 2020 to 2030 period resulting in a total population of 598,587 in 2030, of which the NDC would account for 79,753 of this total. The AIA Study therefore projects a that between 2009 to 2030, based on historical growth rates the northern region would grow by 1.54 times.

The AIA Study also includes projections for what it calls a 'high growth', which is assumes that the proposed investments in the area progress. This projection assumes a 2.15 growth rate reaching a population of 832,000 by 2030. Most of the growth was anticipated around the PIC and in Limonade, Trou-du-Nord, Terrier Rouge and Fort-Liberté, and the NDC would contribute 136,172 of this total.

This ESCI study seeks to verify the extent to which the existing projections remain valid, and where appropriate update them based upon best available data including from IHSI, which is the only source of reasonably accurate information and projections in Haiti.

Table 8 – Northern Region Population and Growth Projections (source AIA Study)

POPULATION	2009	2020		2030	
		Baseline	High Growth	Baseline	High Growth
Ville de Cap-Haïtien	155,505	203,041	224,797	240,315	317,061
Quartier de Petite Anse	89,155	116,408	128,882	137,779	181,779
Ville de Quartier Morin	3,500	4,570	5,060	5,409	7,136
Subtotal for the Cap-Haïtien Urban Node	248,160	324,019	358,739	383,503	505,976
Ville de Limonade	14,886	19,436	24,125	23,005	39,279
Ville de Caracol	2,690	3,512	4,359	4,157	7,098
Ville de Trou-du-Nord	21,805	28,470	35,338	33,697	57,535
Ville de Terrier Rouge	12,226	15,963	19,814	18,894	32,260
Subtotal for PIC Node	51,607	67,381	83,636	79,753	136,172
Ville de Sainte Suzanne	1,488	1,943	2,151	2,300	3,034
Ville de Fort-Liberté	18,417	24,047	29,847	28,461	48,596
Ville Industrielle de Derac	2,046	2,671	2,958	3,162	4,172
Ville de Ferrier	7,371	9,624	10,655	11,391	15,029
Ville de Ouanaminte	58,250	76,056	84,206	90,018	118,767
TOTAL	387,339	505,743	572,191	598,587	831,745

5.2.3 Demographic Trends

Existing demographic trends and baseline data exists for Haiti through a number of studies and assessments as follows:

(i) National Demographic Trends (1950-2050). Data for national demographic trends comes from IHSI and CELADE / ECLAC 2008. In this paper, projections are calculated using a methodology and a model developed by IHSI with the help of the CELADE and the United Nations Fund for Population Activities (UNFPA). The methodology is based on data from the General Census of Population and Housing conducted in Haiti in 2003 and recent economic and demographic surveys, and provides national population projections (1950 to 2050) and average growth rates for both the urban and rural populations. The key trends from this work predicts strong growth in both urban and rural areas, although rates of urbanization are much higher than rural, and a gradual lowering of the growth rate. These national trends are reflected at the local level and in the study by urban growth and the slow decline of the rural population area.

(ii) Demographic trends at the municipal level (2000-2015). The data from IHSI analyses (IHSI 2009b) presents projections of the total, urban and rural population at the departmental and municipality level and the trends for key towns in the north are shown in *Figure 30* and *Figure 31*. This data at the municipal level does not extend beyond 2015.

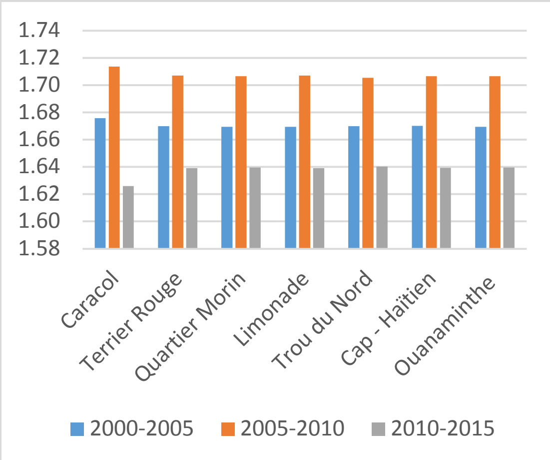

Figure 30 - Average annual growth of total population

Source: IHSI 2009b

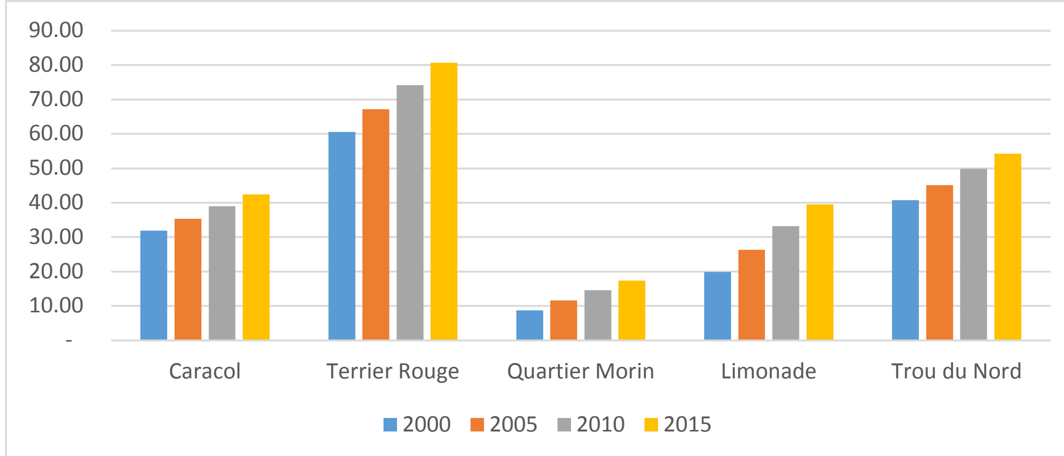

Figure 31 - Urbanization rate in the municipalities of the study area

Source: IHSI 2009b

(iii) Increasing urbanization - the data above can be used to calculate the rate of urbanization for key municipalities in the north, which reinforces the trend of towards concentration of the population in urban centers.

5.2.4 Migration Trends

Understanding migration patterns to urban centers and rural areas allows a better prediction of future population trends and projections. Migrants are considered those persons whose place of birth is not the place of current residence, and the number and percentage of migrants is an important indicator of the attractiveness of a given locality.

Long-Term or Permanent Migrations

The General Census of Population and Housing 2003 (IHSI 2003) contains useful information on migration including place of birth and length of residence, as well as an analysis of migration flows. Migration trends over time play an important role in demographic change. The data indicates that on average, 10.76% of the population of the municipalities in the north are migrants, and specific to the study area, migration rates of 6.8%, 9.25% and 16.8% applied for Trou-du-Nord, Terrier Rouge and Caracol respectively. The results also show that the average percentage of migrants is higher in urban than in rural areas, and that most migrants in the north are from local adjacent departments (6.86%) compared to departments from other regions of Haiti (2.61%) and abroad (0.81%).

Daily Commuting

To better understand migration flows associated with project implementation, IDB collected data for the PIC workers was also analyzed (IDB 2012). This data details the residency of employees, and can be consider as a sample of the working population in terms of daily commuting for employment. The data is summarized in *Table 9* and shows that 19.4% of PIC workers live in Caracol and EKAM, and the remaining 82.6% live in other towns of the Departments of the North and Northeast.

Table 9 - Place of residence of PIC workers

Lieu de résidence	Nombre	%
Limonade	329	10.75
Caracol	347	11.34
Trou-du-Nord	664	21.70
Terrier Rouge	238	7.78
Quartier Morin	54	1.76
EKAM	246	8.04
Cap Haïtien	420	13.73
Ouanaminthe	131	4.28
Autres	87	2.84
Etrangers	56	1.83
Contractors	488	15.95
Total	3,060	100.00

5.2.5 Population Projections

The results of the previously presented data and analyses was used as a baseline from which to develop projections of the population of the NDC study area through to the year 2040. The methodology was as follows:

1. Calculation of the annual growth rate from 2000 to 2015 from the IHSI 2009b data introduced in *Section 5.2.3*, noting that the urban population in these documents is not disaggregated to represent the different urban centers in this study.

2. Adjustment of the annual growth rate (from 1 above) for the period 2015-2040. An adjusted growth rate was calculated by the following:

   - Calculate difference (variation) between the annual growth rate at the national level: 2005-2015 vs. 2015-2040.
   - Application of this variation in growth rate for 2010-2015 for the municipalities to generate an adjusted growth rate.
   - Using the adjusted growth rate, calculate the projection of municipal populations (total, rural and urban) in 2015 to obtain estimates for 2030 and 2040.
   - Populations in 2030 and 2040 are calculated as the base population of the study with the assumption that no development projects are implemented (slow scenario).

3. Disaggregation of the of the communal urban population agglomeration. For the urban municipalities, it provides the total urban population which in some cases includes several urban areas in the municipality

Slow Growth Scenario

Given the absence of municipal-level demographics projections for the post 2015 period, an adjusted growth rate was calculated that takes into account those trends observed at the national level (see *Section 5.2.3* above). The adjusted rate of growth has been applied to the 2012 population and projected through to generate population estimates for 2030 and 2040 in a scenario of non-implementation of development projects, as shown in *Table 10*.

High Growth Scenario

The AIA Study and the CIAT Strategic Plan estimate the demographic impacts of a similar scenario where development projects would be implemented. These estimates assumed strong regional planning controls to limit the expanding population and growth of the towns and urban centers in favor of the development of a new planned town in the Champin area (Nouvelle Caracol). The approach adopted for this ESCI Study has assumed a more realistic approach of recognizing the limited governmental capacity to steer growth and influx to the desired areas, and assumes to some extent that existing trends continue. The trends are defined by both settlement in already developed areas (agglomeration) and commuting patterns, and have taken into account the current growth trends at the local level, as well as data on migration flows (long-term and daily commuting).

Table 10 - Projections of the population base - scenarios of slow growth

Nom	Current 2012	AIA/ CIAT 2030 (Slow)	ESCI Projections (Slow Growth)	
			2030	2040
Quartier de Bord de Mer de Limonade	1,319	1,728	3,799	5,350
Quartier de Grand Bassin	8,379	12,156	15,449	19,702
Quartier de Petite Anse	93,586	137,779	118,636	132,666
Ville de Trou-du-Nord	24,154	33,697	44,534	56,792
Ville de Caracol	2,979	4,157	5,494	7,007
Ville de Derac	1,839	3,162	3,737	4,765
Ville de Ferrier	8,165	11,391	15,054	19,198
Ville de Fort Liberte	20,399	28,461	41,448	52,857
Ville de Limonade	17,556	23,005	50,569	71,205
Ville de Ouanaminthe	64,524	90,018	118,995	151,721
Ville de Quartier Morin	4,125	5,409	11,886	16,737
Ville de Terrier Rouge	13,876	18,894	25,585	32,627
Ville du Cap Haïtien	163,222	240,315	206,911	231,381
Ville de Sainte Suzanne	1,712	2,300	2,277	2,320
Total	425,835	612,472	664,373	804,326

The adjusted rate of growth has been applied to the 2012 population and projected through to generate population estimates for 2030 and 2040 in a scenario of non-implementation of development projects, as shown in *Table 11*.

5.3 Urban Area Needs

The area needs for urban development can be estimated based on the previously presented population projections and also the household numbers, average household size and housing density target.

Table 11 - Projections of the population base - scenarios of High growth

Nom	Current 2012	AIA/ CIAT 2030 (High)	ESCI 2040 Projections (High Growth)
Quartier de Bord de Mer de Limonade	1,319	4,617	7,589
Quartier de Grand Bassin	8,379	32,482	27,949
Quartier de Petite Anse	93,586	181,779	188,199
Ville de Trou-du-Nord	24,154	57535	80,564
Ville de Caracol	2,979	7,098	9,940
Ville de Derac	1,839	4,172	6,760
Ville de Ferrier	8,165	15,029	27,234
Ville de Fort Liberte	20,399	48,596	74,982
Ville de Limonade	17,556	39,279	101,010
Ville de Ouanaminthe	64,524	118,767	215,229
Ville de Quartier Morin	4,125	7,136	23,743
Ville de Terrier Rouge	13,876	32,260	46,285
Ville du Cap Haïtien	163,222	317,061	328,235
Ville de Sainte Suzanne	1,712	3,034.00	3,290
Total	425,835	868,846	1,141,008

The number of households was estimated by dividing the projected populations by the average household size, which was taken from IHSI data (IHSI 2012). This was performed for the baseline scenario and the high-growth scenario, and is detailed in Section 7.3 where the capacity of the existing townships to accommodate further growth and development is further explored.

6. GEOSPATIAL MODEL

6.1 Introduction

As stated in the *Section 1*, the goal of this study is to determine the areas in the NDC that should be preferentially considered for future urban growth and settlement, in such a way that this contributes to a sustainable setting. The fundamental principle is that the areas in which future urban settlement occurs should be those that result from protecting or setting aside key areas for cultural, ecological and environmental reasons, including those that are exposed to natural phenomena whose occurrence could not be mitigated, thus threating life.

This section provides an explanation of the method and criteria used in this ESCI Study to define suitable areas for future growth. The approach builds upon the AIA and the CIAT studies by:

- A number of the elements used to judge the suitability of land for development were defined with greater precision, through the work on risk and vulnerability as well as the update of a number of 'layers' provided by ESCI and CIAT.
- The 'combination' of all the pieces of information (or 'factors') which is the basis of a planner's decision about where to allocate development and where to protect, was not empirical but undertaken through a geo-spatial modelling process.

6.2 The Geospatial Modelling Process

In determining which areas ought to be transformed from their natural state to a developed state, communities, planners and decision makers are faced with the challenge of reaching a balance between the conservation of nature and economic development. The aim of all is to carry out this process by means of 'comprehensively' and 'equitably' considering all the elements that represent both pursuits, such that no one element ends up receiving, supporting or 'suffering' the negative effects of another. This is the basis of modern planning and is what regional planners have called multi criteria decision analysis. The 'art' of planning has always resided on how that balance is demonstrated to have been reached in a particular situation.

In the past this type of analysis was carried out with tools and references that had less precision that today, but in both cases we are faced with the same elements that represent the forces of economic development and nature conservation. Roads, schools, agglomerations, continue to be the elements that attract a settler, particularly for the way in which they positively impact the family or firm's economic bottom line. And wetlands, woods, areas of bio-diversity are all elements that could also attract the settler but should be preserved or protected because of their natural value to society.

Land suitability analysis through GIS modeling is a well-known computational tool that helps provide planners with a more precise delimitation of different elements as well as a clear delimitation of areas that would result through a simulated combination of all those elements under pre-determined combination criteria. In other words, it is a computational tool that rigorously applies multi criteria decision analysis.

Because of the scope of the study and the limited amount of information in Haiti, in the Northern Development Corridor study ERM made a fundamental, very conservative assumption: consider of equal value each element that was identified as an attraction or a restriction, such that no one element exercised a greater influence over the others. In a situation in which the scope of the work had been larger, the logical approach would have been to survey the area of study and engage the different communities so as to identify as to the specific forces that 'pull harder' than others and provide this as the balancing criteria.

As Joerin and Thériault (2001) demonstrate there is a vast array of 'models' or 'approaches' to the question of which elements and criteria to use in the running of the multicriteria tool. However, the aim of ERM in this particular project was not to adhere to any model in particular, but simply produce the land suitability map that would result from considering all elements in equality of circumstance. By applying this approach we are ensuring the arrival to at least the closest representation of the balanced result that would be drawn with or without the modelling tool – hence representing what would likely be the picture if it had been drawn following traditional mapping and planning techniques.

In determining which areas would be recommendable for human settlement in a given city and region, the approach carried out uses a geospatial modeling process that simulates what is commonly known as attraction and restriction factors. The attraction factors represent those elements that will encourage and attract development by virtue of the services or value they provide. For example, roads are a strong attracting factor for development given the access they provide, and similarly the presence of utilities due to the service they provide. Employment areas and social infrastructure facilities can also be strong attractors. Conversely, restriction factors are those elements that either needs protection due to the inherent value they provide e.g. areas of high biodiversity, cultural sites or aquifer recharge areas, or are areas where development should be actively discourage e.g. areas prone to natural hazards such as flooding. The baseline information presented in *Sections 3* and *4*, as well as the future growth and development considerations presented in *Section 5*, is used and categorized in terms of the attraction and/or restriction forces that they present.

By combining these attraction and restriction factors through geospatial modelling, an understanding can be gained in terms of preferable and less preferable locations for future urban development. Combining the attraction and restriction factors is undertaken through the lens of the different development or growth scenarios being envisioned.

For example, in a location with limited controls and enforcement of urban growth, the influence of the restrictions can be significantly diminished and therefore urban growth, or 'sprawl', can occur in an ad-hoc and uncontrolled way which is responding only to the attractions. This can produce a setting that tends to be marked by mid-density settlements inside the urban areas, surrounded by expanding, low to very-low density settlements. 'Informal' or 'extra-legal' settlements also occur on empty, unprotected public lands or in areas with little value because of their exposure to natural hazards or lack of public utilities and /or social services.

Conversely, in a scenario or strong planning controls and enforcement, the restriction factors can play a strong and influential role, limiting where future urban growth occurs. Growth will still follow and respond to the attractions; however it will also respect and avoid designated restricted areas. This latter scenario can be viewed as embracing sustainable planning principles in that it supports conservation and protection efforts and focuses development to appropriate areas. In this context, growth and new settlements tend to be steered towards already developed areas.

This approach is widely and almost universally recognized as the way to build sustainable cities and regions, for it fosters the following key results:

- It promotes densification (better known as compact cities), which, in turn, makes the delivery of water, sewer and other infrastructure, social services, transport much less costly and much more effective on a per capita basis.
- It tends to increases the mixture of land uses per unit of area, which, in turn, increases the likelihood of pedestrian or bicycle home-to-work travel, reduces travel distances that reduce emissions and enhances health, and others.

6.3 Modelling for the NDC

The modelling approach used builds off successful similar studies undertaken by ERM and ESCI for the metropolitan regions of Cochabamba and Managua. However, recognizing the unique characteristics of the NDC area and Haiti more broadly, a particular focus has been placed on the speed and/or pace in which development could occur in the area, recognizing both the recent growth due to investments like the PIC, and the many proposed additional development projects.

In addition, the modelling approach has sought to integrate from the beginning sustainable planning considerations (also referred to as 'smart' or 'intelligent' growth). This means that the geospatial modelling has sought at all times to recognize the importance of restrictions, and therefore respect and avoid the defined restrictions. In modeling terms, this means that the restrictions have been 'maximized' so that their influence in the selection of suitable land is very clear. The computational process selects and creates a hierarchy of all the areas with the highest degrees of attraction (from the baseline components that have been classified as such e.g. roads, infrastructure, schools), but discards, also hierarchically, all those areas affected or controlled by factors that should impede or prevent settlement (e.g. locations prone to flood or earthquake, or the presence rich agricultural soils or biodiversity).

The modeling outputs are computer generated maps of potential suitability based upon the applied attraction and restriction factors. These outputs are only a guide, and must not be used as a definitive output for suitability. The outputs must then undergo detailed analyses to then determine potentially suitable development areas based on a range of factors such as the capacity of the areas to absorb new development, current land uses, residential density and the general characteristics of the locations.

The analysis also includes due consideration of the expected population growth of the region and a calculation is made to derive the time horizon in which the suitable areas would be reaching capacity. This effort yields, among others, public policy recommendations with regards to the areas of the territory that should be considered urban, for-expansion, and rural or peri-urban, and when, if at all, should their boundaries and general terms of development be modified. This work is further described and presented in *Section 6.7*.

The modeling process used involved the following stages and components:

1. Using the baseline GIS information introduced in *Sections 3, 4 and 5*, attractions and restrictions are determined.

2. Assigning attraction/restriction scales to each one of the variables based on analyses of each layer according to the degree to which they influence (or should influence) development. For example, based on professional judgment, a road such as RN6 is given 1 km of influence on both sides, considering that there are no additional roads of similar status. Whereas secondary roads are given not more than 500 m of influence, considering as is the case with the roads that serve Trou-du-Nord that after that distance another road will probably appear.

3. Developing individual sub-models, one each for attraction factors and restriction factors. These sub-models combine all of the relevant factors to create composite restriction and attraction maps. This allows the “isolation” of the intensity of attraction from that of restriction, making it possible to understand the push and pull separately.

4. The restriction and attraction maps are then combined to generate an overall model map, which shows the land suitability based on the attractiveness of locations where no to minimal restrictions exist

This model map is then translated into a general land use scenario, and used to define the general regional planning policies and actions on land use, and road and transport infrastructure. This work is presented in *Section 7*.

6.4 Restriction Factors Sub-Model

6.4.1 Individual Restriction Factors

The topics and elements considered restrictions for development in the NDC Study Area are illustrated in *Figure 32*, where there are twenty-two elements assessed. Having defined the elements and parameters that will be considered as restriction factors, then they are analyzed and processed using a geo-spatial model. The analysis of each element enables an understanding of the degree with which it should be considered as a restriction in the model, as well as ideas about the more suitable areas for human settlement. This is explained further for each key restriction factor in *Table 12*, and the individual restriction maps are presented in detail in *Appendix 7*.

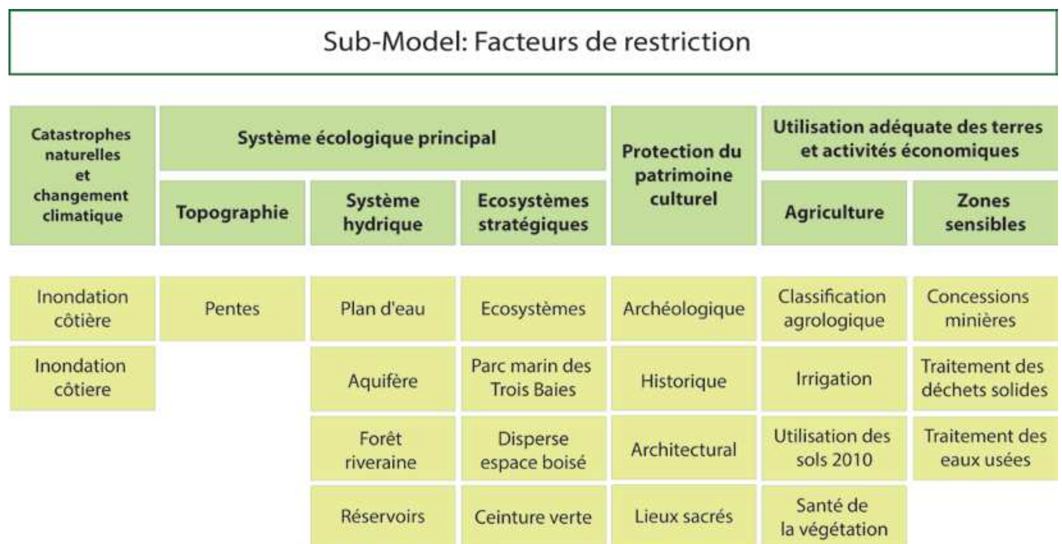

Figure 32 - Topics and elements considered to be restrictions for development

Table 12 – Summary of the main restriction factors

Risk	Topography	Hydrology
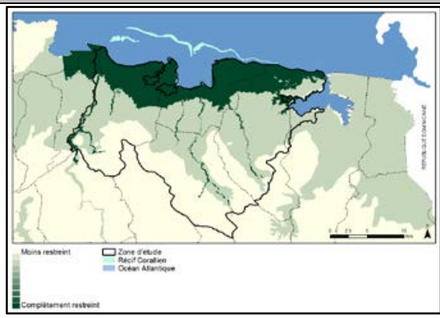		
Based upon the hazard maps generated in *Section 4.4*, principally for coastal and inland flooding and seismic, a restriction layer was developed, recognizing the higher risk areas identified along the coast due to coastal flooding and seismic, and the river corridors.	A restriction layer was prepared based upon gradient of slopes, where no restrictions were applied for slopes under 12%, moderate restriction were designated for slopes between 12-25%, stricter restriction between 25-50% and a complete restriction for slopes over 50%.	Restrictions were placed around key water features including reservoirs and watersheds for principal and secondary rivers. A moderate level of restriction was applied to the inferred Plaine du Nord/Massacre aquifer area.
Ecology	**Cultural**	**Agricultural and Land Use**
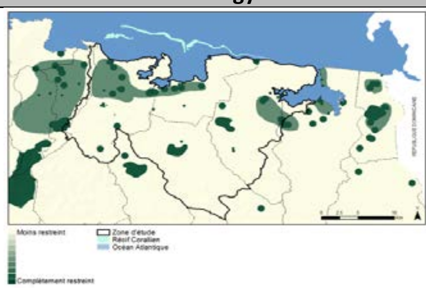	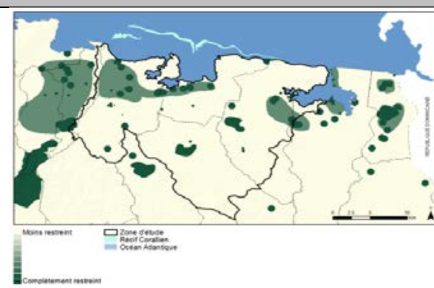	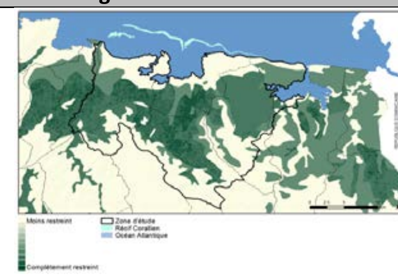
Key strategic ecosystems considerations including the Three Bays Marine Park, the coastal mangrove areas and the highlands ecosystem, which has been identified for reforestation and watershed protection, were used to build a restriction layer.	The cultural heritage variable implies that the coastal areas are the most sensitive, as well as recognizing the vernacular architecture areas and the sites identified in each of the in or near the urban cores. A restrictions map of these issues was constructed.	Using the agricultural soils classifications, areas of high quality soils were identified for protection, as well as considering other land use factors such as mining concessions.

Note: Further details of the resection layers and the full maps are contained in Appendix 7

6.4.2 Synthesis Map of the Restrictions Sub-model

The sub-model combines the levels of restriction, of each variable analyzed. The different elements described in the previous point were process together in the modelling application. The approach taken for the relative influence of the different restriction factors was a 'conservative' or 'balanced' one, which was to assign an equal influence to each element. The sub-model results are observed spatially through a map of ten restriction levels. The map in *Figure 33* show the final restrictions levels included in the suitability model. The darkest green shows the most restricted areas and as the green becomes lighter, the less restricted the area becomes.

This map shows the strong restrictions along the coastal areas and also in the mountainous areas in the south of the study area. In between are

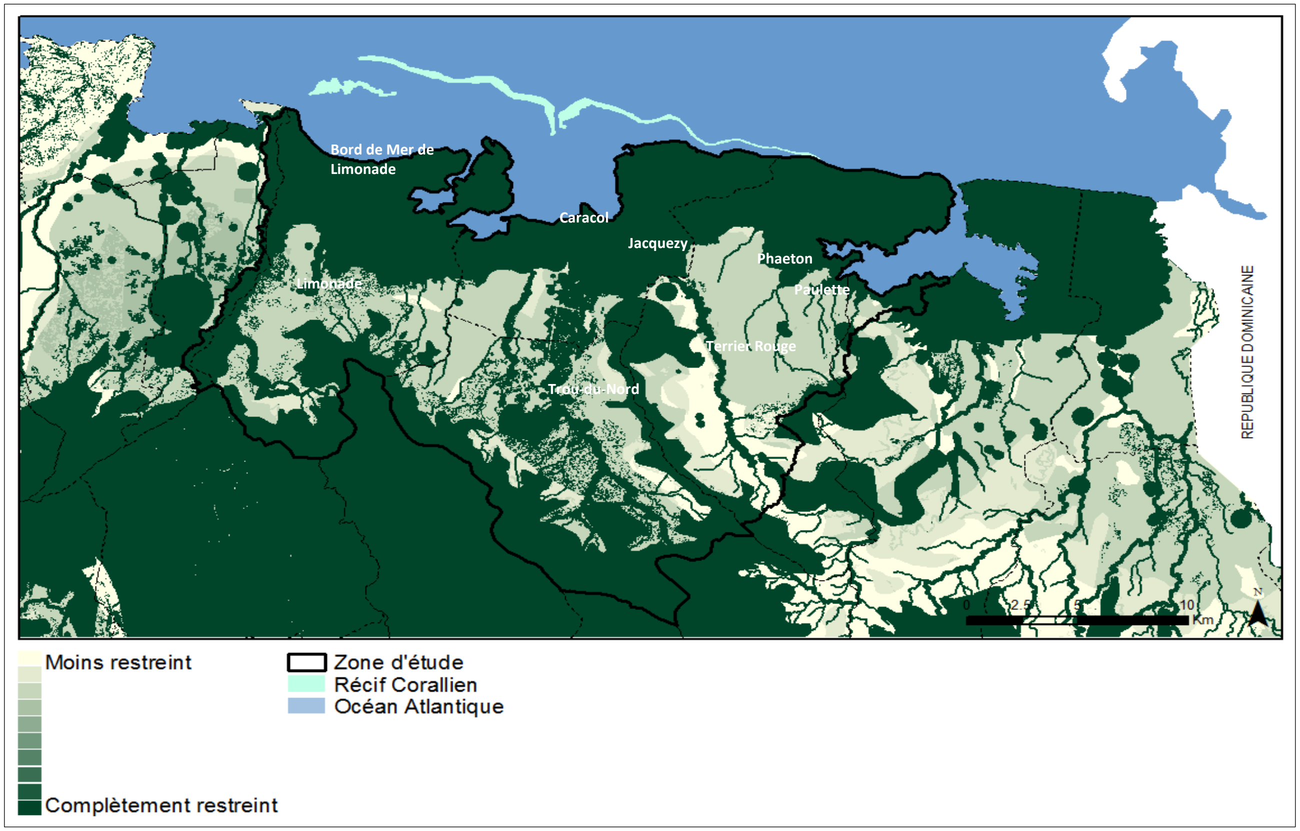

Figure 33 - Map of the restrictions sub-model: composite of maximum restrictions

Map source: Results from the restrictions sub-model. Variables built from geographic information layers by AIA (2012), CIAT (2012), CNGIS (c.2012), IADB (c.2013), NATHAT (2010), USAID-OFDA (c.2012), OSM (2013), OCHA (c.2010), PDNA (2010) and DTM (2013). Georeferencing digitizing and remote sensing analysis from satellite imagery 1986, 2010 and 2013.

intermitted restricted areas, but also many areas of limited restriction. These clearly imply where would be more convenient or suitable for development to be located.

6.5 Attractions Factors Sub-Model

The attractions sub-model includes variables related to existing agglomeration, access to roads, public facilities, social services and access to employment. This sub-model accounts for the attraction factors that will be considered by an individual, household or firm when locating within the area of study, as shown in *Figure 34*. While the importance of public lands and land value is noted, the absence of any available information on this topic has resulted in its exclusion from the model. The selected attractiveness factors are discussed as follows.

6.5.1 Individual Attraction Factors

Having defined the elements and parameters that will be considered as attraction factors, then they are analyzed and processed using the geo-spatial application. The analysis of each element enables an understanding of the degree with which it should be considered in the model, as well as ideas about the more suitable areas for human settlement. This is explained further for each key attraction factor in *Table 13*, and the individual attraction maps are presented in detail in *Appendix 8*.

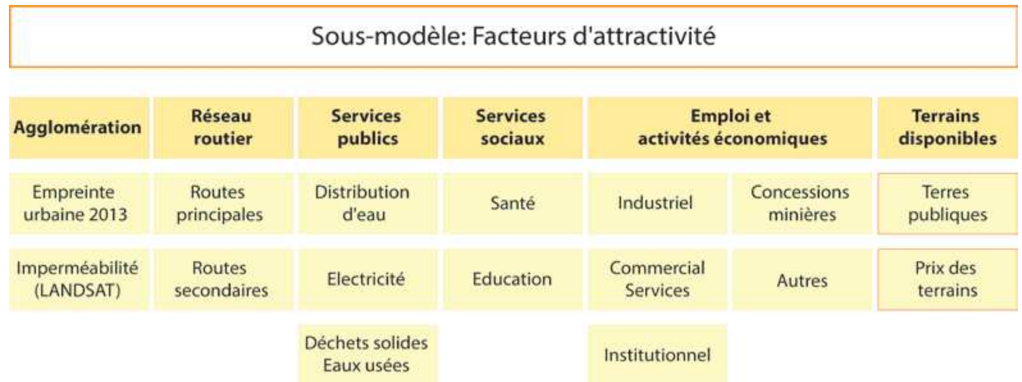

Figure 34 - Topics and elements considered to be attractions for development

Legend: Boxes that appear highlighted in red are components for which the identification of geographical data was not possible by ERM

Table 13 - Summary of the main attraction factors

Agglomeration	Roads	Public Utilities
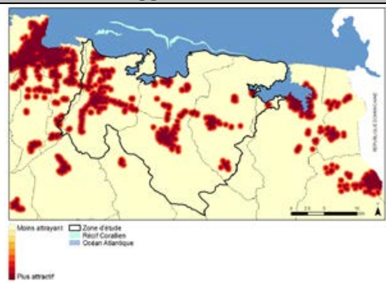 All the cities, towns, hamlets and even smaller groupings of houses were considered as agglomerations, which are an attraction feature for individuals and families.	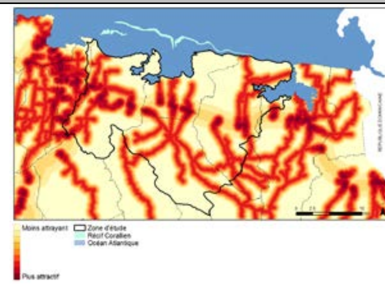 The modeling exercise included primary and secondary roads. The primary road was modelled to exercise recognize its greater influence as an attractor compared to secondary roads.	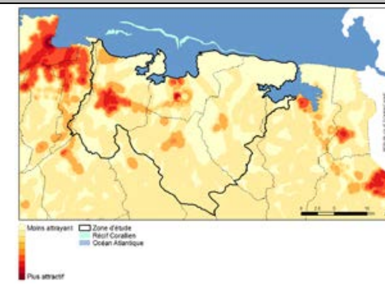 Public utilities included areas with access to water and sewer systems, water points, and areas with electricity. Each element, whether a line or a point, was modeled to exercise its influence
Social Services	**Employment and Economic Activities**	
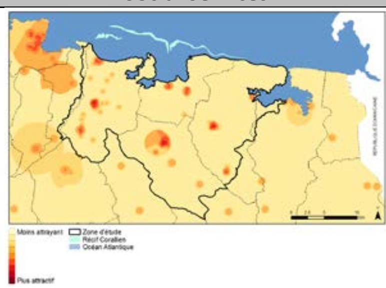 Social services included schools, universities, hospitals, and similar facilities, and the attractiveness also considered the relevant township or community in which they serve	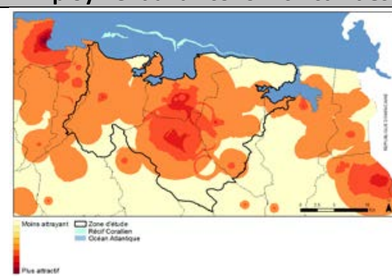 Economic activities that were brought together in the model included industries, mines, banks, agro industrial operations, retail centers, and others, recognizing both local and regional attractiveness.	

Note: Further details of the resection layers and the full maps are contained in Appendix 8

6.5.2 Synthesis Map of the Attractiveness Sub-model

Having defined th e restrictions and analyzed their components, each variable was processed, analyzed and consolidated into the attractions sub-model.

The different elements described in the previous point were also processed together in the modelling application. The approach taken was a 'conservative' or 'balanced' one, which was to assign an equal influence to each element. *Figure 35* shows the final sub-model results.

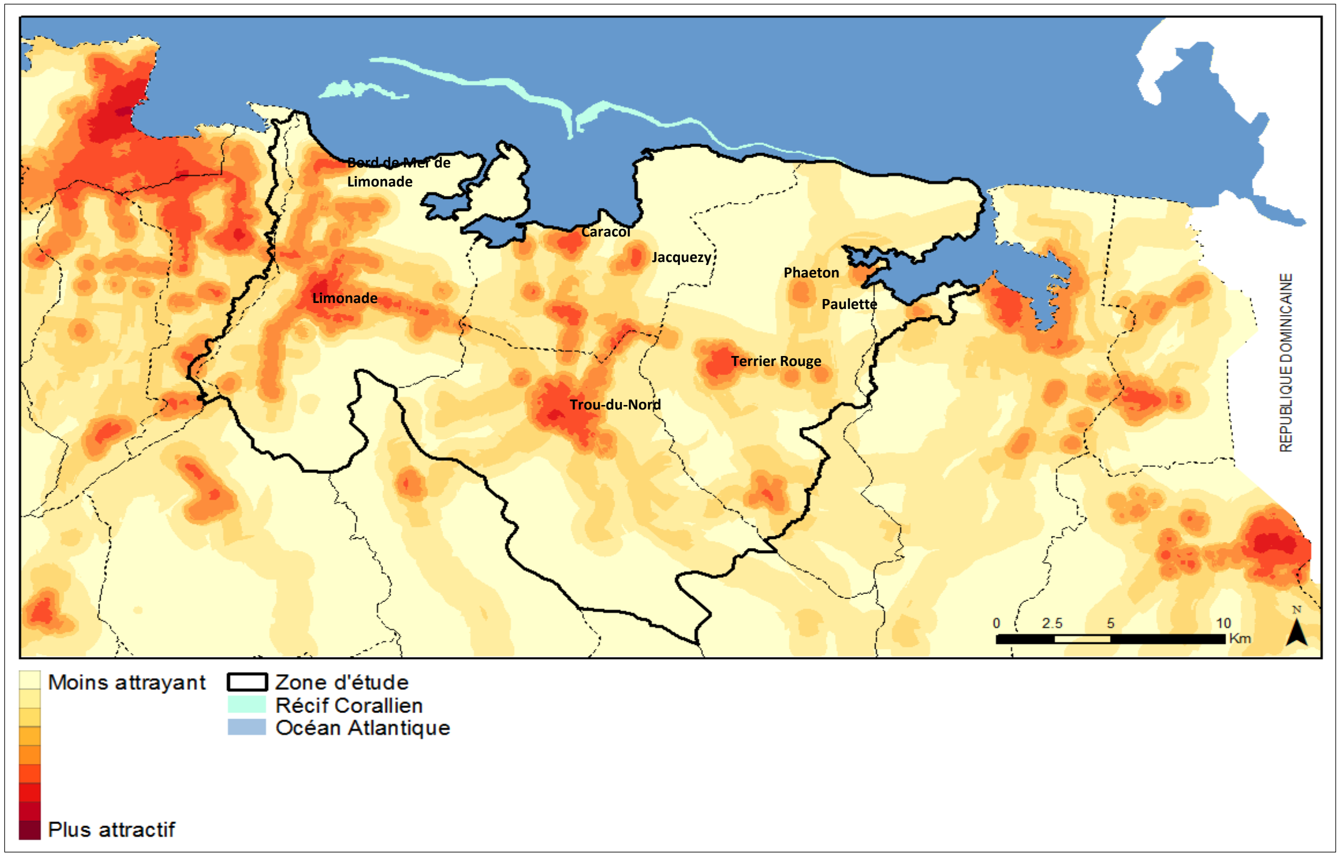

Figure 35 - Map of the attractions sub-model: composite of maximum attractiveness factors

Map source: Results from the attractiveness sub-model. Variables built from geographic information layers by AIA (2012), CIAT (2012), CNGIS (c.2012), IADB (c.2013), NATHAT (2010), USAID-OFDA (c.2012), OSM (2013), OCHA (c.2010), PDNA (2010) and DTM (2013). Georeferencing, digitizing and remote sensing analysis from satellite imagery 1986, 2010 and 2013.

6.6 Future Development Projects Sub-Model

The future development projects sub-model includes on-going and planned development projects as described in *Section 5.1*. Four main layers were developed for existing or on-going development projects: Caracol industrial park (PIC), National University of Haiti Roi Henri Christophe Campus in Limonade (UHN-RHC), housing (EKAM in Caracol: 750 Housing units and 535 plots, feed the poor projects along RN6 and fishing villages) and an existing quarry.

Four additional layers were developed for planned development projects: Sea Port expansion in Cap Haïtien, mining concessions, infrastructure projects (thermic plants, water networks, solid waste treatment plants and wastewater treatment plants) and projected housing (PIC resettlement called Calles or Faias): 572 housing units and food for the poor in Terrier rouge: 242 housing plots).

Appendix 9 shows the results of each one of the variables analyzed to compose the development projects sub-model. Each image shows the attractiveness levels of one or a group of development projects according to their impact and geographic location. The sub-model results are observed spatially through a map of nine attractive-ness levels as seen in *Figure 36*.

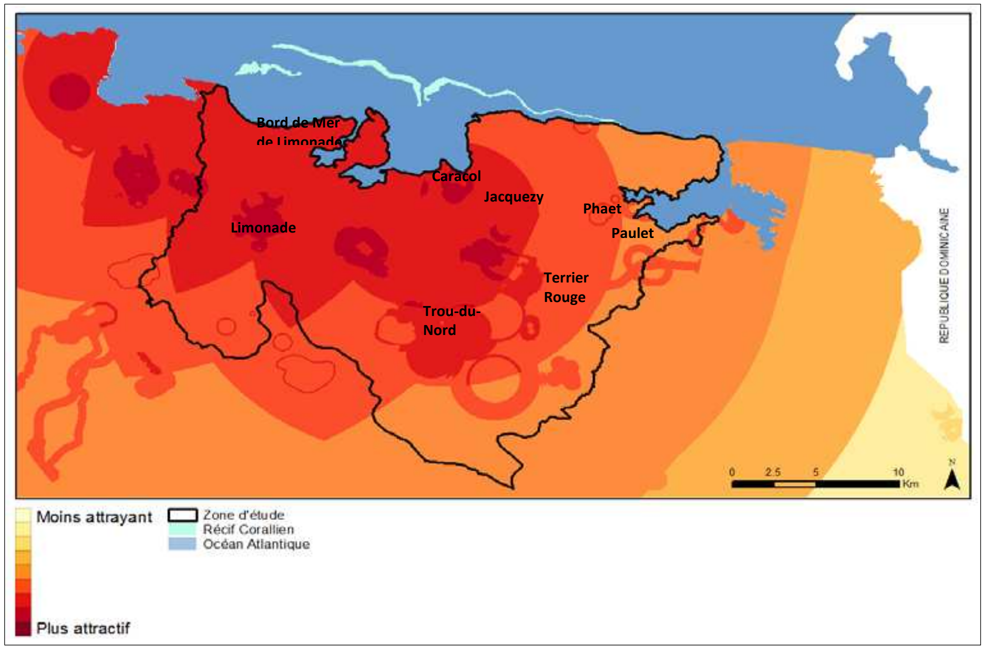

Figure 36 - Attraction factors: Development Projects

Map source: Results from the attractiveness sub-model. Variables built from geographic information layers by AIA (2012), CIAT (2012), CNGIS (c.2012), IADB (c.2013), NATHAT (2010), USAID-OFDA (c.2012), OSM (2013), OCHA (c.2010), PDNA (2010) and DTM (2013). Georeferencing, digitizing and remote sensing analysis from satellite imagery 1986, 2010 and 2013

6.7 Suitability Analysis

To determine the areas that should to be considered for sustainable human settlement in the future, a geo-spatial model has been used that simulates the interaction of attraction and restriction factors. This study's focus has utilized a proposed sustainable growth scenario through maximizing the restrictions (in order to protect key ecosystems and resources) and maximizing the attractiveness factors recognizing the importance they plan in the development area.

Combining the three sub-models presented above: restrictions, attractiveness factors and development projects, the geo-spatial model combines all variables relevant to identify areas potentially suitable for urban development as well as rural and natural land use.

The model results of combining the three components are shown in *Figure 37* with levels of attraction and restriction that range from the most attractive areas for development, appropriate for urbanization, to the most restricted for development, and therefore adequate for the protection of natural areas.

As highlighted at the beginning of this section, this analysis provides an indication only of potential land suitability, and cannot be used as a definitive result with respect to where development can and cannot occur.

What this map is depicting is what the regional and urban planners, as well as decision makers, should bear in mind when establishing where to locate the developments that would come in the future as well as the services that the growing and migrating population would demand.

On one end, the red areas are those in which development would be more attractive because they would be those areas in which a settling family or business would have the greatest levels of access to services, infrastructure, the economy of the agglomerations, transport services and others. And they would also be the places in which the natural resources would be less affected. On the other end, the green areas would be those that would need the greatest protection, for they are the ones in which most of the elements considered as restrictions are operating and in the greatest degree.

Consequently, the areas in between the dark green and the dark red zones, would be the threshold in which the planner and decision maker would have to base in order to define what areas could be allocated for development and the degree to which they would affect natural resources or be affected by natural hazards. For example, when and if considering that Terrier Rouge should expand because it does not have the area to provide housing for future generations inside its urban setting, it is clear from this map that this should be to the south of the urban area.

The map is also key at indicating how the city of Limonade should be looking at planning the areas to the East and Southeast, where a major agglomeration is beginning to appear, or how the EKAM – University of Limonade node is also beginning to create a pole of attraction, or where in the PIC area will new settlement likely occur.

The map also indicates how, if a new settlement pole was to be considered apart from the existing townships, the above mentioned areas ought to be considered first and foremost. Interestingly, the presence of a light green zone in between the two roads connecting Trou-du-Nord and the PIC tells us that these are amongst the more valuable agricultural lands of the area, from the points of view agrological quality of soils, vegetation health as well as the fact that they are being utilized precisely for the uses for which they have a vocation.

Finally, the map is clear in defining an inverted 'arc' of lands that could be useful for development between Terrier Rouge, Grande Bassin, Perches and Ouanaminthe. These areas would be attractive for development not only because of their agrological and soil conditions (less good for agriculture) but also because they would be least exposed to natural phenomena, would traverse almost no valuable ecological asset areas, and therefore would provide the ideal environment for developing roads, infrastructure and human settlement.

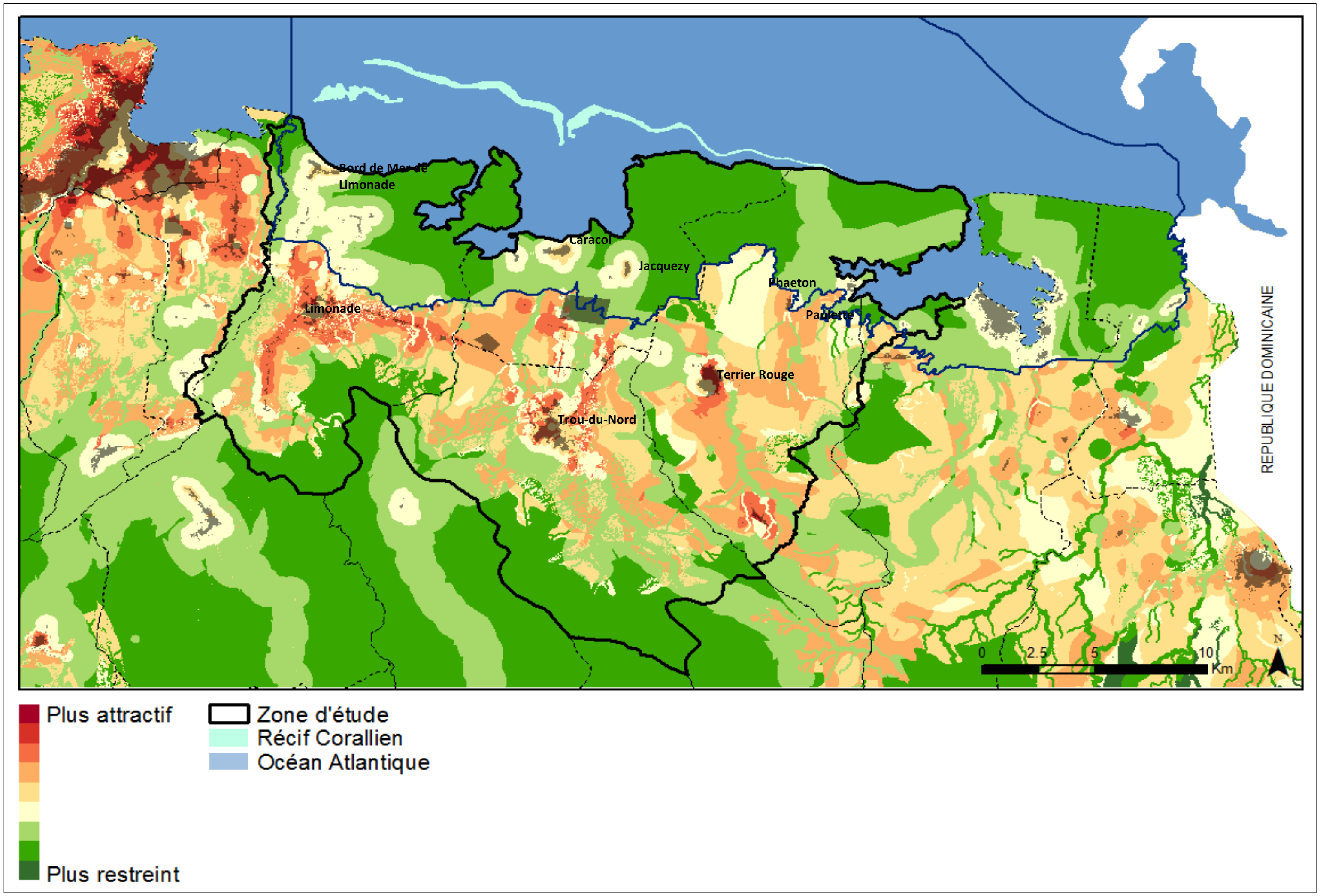

Figure 37 - Land Suitability Model Based on Attractions and Restrictions

Map source: Results from the attractiveness sub-model. Variables built from geographic information layers by AIA (2012), CIAT (2012), CNGIS (c.2012), IADB (c.2013), NATHAT (2010), USAID-OFDA (c.2012), OSM (2013), OCHA (c.2010), PDNA (2010) and DTM (2013). Georeferencing, digitizing and remote sensing analysis from satellite imagery 1986, 2010 and 2013.

7. DEVELOPMENT OF A SUSTAINABLE GROWTH SCENARIO

Based upon the results presented from the baseline analysis and the geo-spatial modelling, the preferable options for future development and growth of the NDC can be explored, with the aim of providing insights on where and how should future human settlement occur. Building in sustainability considerations, future development should seek to contribute to and make use of the economic opportunities of the region as a whole; not compromise opportunities in other areas such as agricultural development, environmental preservation; and not compromise the lives of people who could be exposed to serious natural phenomena.

This section presents the key findings from this work and specifically covers the following:

- Captures key findings and recommendations from the geo-spatial modelling presented in *Section 6* based on land suitability;
- Considers the existing form and trends of human settlement in the region (presented in *Section 3.1*), and the issue of densification, which can give insight on the capacity areas proposed for development and settlement;
- Explores the main townships and hamlets to determine their capacity to accommodate new development;
- Considers the approach to settlement under the 'slow' and 'high' population growth scenarios;
- Explore in more detail the area of influence or 'neighborhood' of the PIC and the potential for a new development; and
- A discussion of the Three Bays Marine Park and the associated protection opportunities and development restrictions.

7.1 Land Suitability

As presented in *Section 6* and Figure 37, the results of the geo-spatial modeling provides insight on the most attractive areas for development (appropriate for urbanization) through to the most restricted for development (appropriate for the protection of natural areas). In general, these results can be divided in three major zones: The northern coast and the southern highlands that ought be predominantly dedicated to ecosystem recovery; and the central plains, where most of the areas suitable for development are concentrated. The hydric system, running from the southern highlands to the Atlantic Ocean, works like a transversal element connecting the three zones.

This is illustrated in *Figure 38*, which shows an initial classification of the appropriateness of land use, and these broad areas are discussed further below.

7.1.1 Northern Coast Protection

Marine and coastal ecosystems and cultural heritage along the coast should be protected, while development should be restricted. Bord de Mer de Limonade, En Bas Saline, Caracol, Jaquezy and Phaéton, and in general coastal areas in the north, fall into the area where many of the restrictions overlap, such as the Three Bays Marine Park, coastal flooding zones, cultural heritage areas, marine and coastal strategic ecosystems and high agrological soil classes. Urbanization in the northern coast should be restricted, ideally limited to the current footprints.

Marine and coastal ecosystems and cultural heritage areas should be protected as part of the Three Bays Park management structure. Traditional economic activities, such as fishing, agriculture and salt exploitation should continue inside the park, but should be regulated to ensure compatibility with ecosystem recovery and conservations efforts. Sustainable tourism focused on ecological conservation and heritage preservation could become the main economic activity if the conservation efforts are successful and water supply and energy networks are consolidated.

7.1.2 Southern Highlands

The highlands ecosystems to the south of the study area should be restored as part of a watershed management priority. The highlands have potential for watershed management, focused on reforestation and the restoration of the hydric system, both crucial for the sustainability of the NDC.

Urban development in the highlands should be restricted and agriculture should be restricted to focus on ecosystem recovery. Charcoal and construction materials production should be replaced by silviculture and sustainable forestry. However, the success of these measures may depend on the capacity to generate and distribute energy to the communities across the NDC, in order to reduce the demand of charcoal.

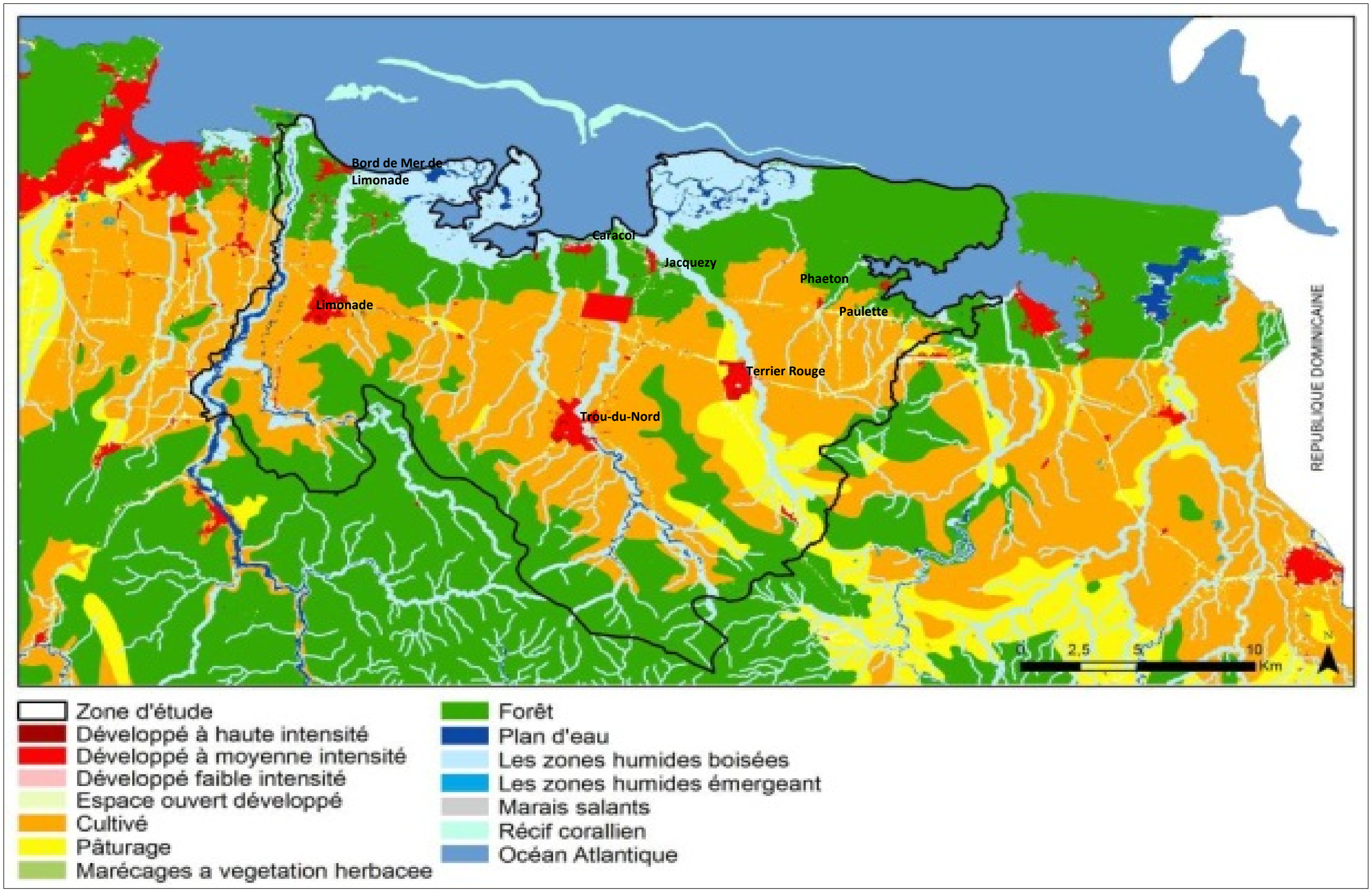

Figure 38 – Optimized land use map

Map source: Results from the attractiveness sub-model. Variables built from geographic information layers by AIA (2012), CIAT (2012), CNGIS (c.2012), IADB (c.2013), NATHAT (2010), USAID-OFDA (c.2012), OSM (2013), OCHA (c.2010), PDNA (2010) and DTM (2013). Georeferencing, digitizing and remote sensing analysis from satellite imagery 1986, 2010 and 2013.

7.1.3 The Central Plains

Development should concentrate in the central plains around existing settlements, balanced with the recovery of agriculture. Suitable areas for development concentrate in the communes of Limonade and Terrier Rouge and to a lesser degree in Trou-du-Nord and Caracol. The best areas for urbanization are south of Limonade towards Buclair, between the urban core of Limonade and the UNH-RHC and EKAM; southwest of the PIC, between Terrier Rouge and Gran Bassin and east of Trou-du-Nord.

The central plains are also the area best suited for agriculture; good quality agrological soils occupy a significant proportion of the central area. Ideally, the urbanization process of the NDC should increase densities in the existing urban footprint to optimize the use of land, balanced with urban and rural economic activities open space, public facilities and social services.

7.1.4 The Hydric System

The hydric system, including its riparian forests, should be restored to connect all areas from the highlands to the coast. The hydric system, running from the southern highlands to the Atlantic Ocean in the north, works like a transversal element connecting the three zones, its protection is crucial.

7.2 Densification

7.2.1 Settlement Patterns and Growth

While the majority of the Study Area can be considered rural, the urbanization and agglomeration patterns are important to understand in order to provide insights on future growth opportunities. These patterns are characterized by townships, hamlets, farms, 'linear' settlements along roads, and planned settlements. *Section 3.1* has already provided more details on these patterns as part of the baseline discussion. Given the land suitability analysis, with the results supporting land protection (for both natural resource protection and agriculture promotion), understanding the existing townships and urban areas, and their capacity to absorb future demand for land based on the growth projections in population becomes a very important consideration.

From social and economic perspectives, the most convenient approach to providing settlement opportunities for the growing and the migrating population of the NDC is to seek them in the human settlements that already exist. Existing agglomerations provide many attractions such as access to greater opportunities for exchanging goods, services and knowledge, as well as better public services of water, sanitation, education and health, than those that would be found in more rural areas.

7.2.2 Current Density Patterns

The general pattern of urbanization in the main existing urban areas is made by a single house in a small parcel in which approximately 50% of the plot is occupied by the dwelling. The number of parcels that may be found in one hectare of land typically ranges between 50 and 60, except the case of Limonade, in which the density is 105 dwelling units per hectare. (This will be demonstrated in the detailed analyses of the different townships). With an average 4.56 persons per household (as is the case for Limonade), this equates to a population density between 228 and 456 inhabitants per hectare.

However, as will also be seen in the township analyses that follow, there are clearly visible empty lands throughout the townships.

Based on these characteristics, in this study has made two important planning assumptions:

- The first is that as societal effort would be undertaken to promote the densification of already built plots of land. However, to remain in the conservative side, it has been assumed that throughout the 25 year period of analysis, this effort will yield an additional 20% homes in those areas.
- The second is that the empty lands within the urban setting and in the areas immediately adjacent would be developed to the highest possible density under the constraints posed by the local market.

To this end, the Zorange Housing Expo has been referenced. This was an effort undertaken following the 2010 disaster by GOH in collaboration with the IDB, the Clinton Foundation and other organizations, with the goal of presenting good examples of housing that could be used in the re-construction. The project was not only intended at offering such examples, but also to be configured as a new community. Several multi-housing proposals were built that could be thought for the NDC (see *Figure 39*), and a few were dwellings raised from the ground, a solution that would be interesting for flood-prone areas. Interestingly, in the Zorange community, where the expo took place, there are multi-dwelling complexes that are inhabited, as can be clearly visible from the lower center image.

Figure 39 - Examples of multi-dwelling and raised dwellings presented at the Zorange Expo

Source: http://archrecord.construction.com/news/2012/01/Haiti-Communities-Expo-slideshow.asp?slide=42. Photo credits: Jenna M. McKnight

According to the promoters of the Expo (see reference noted on photograph), each unit had to be developed within a budget that allowed either its purchase by donor organizations focused in providing shelter to Haitians such as USAID, or the purchase by working families with capacity to constitute a loan. Although the Expo was successful in demonstrating this, it was the absence of resources to develop infrastructure and services what prevented the Expo from becoming a living community.

These experiences demonstrate that not only technically but also financially there is a possibility to develop multi-dwelling solutions in the country. A solution such as the one depicted in the lower left image (of *Figure 39*) could perfectly be carried out in all townships of the area, which would result in the density of 100 to 150 dwelling units per gross hectare of land, or 150 – 200 dwellings per net hectare of land, that is factoring areas for roads, parks and community services.

Consequently, an aspiration of a density of about 150–200 dwelling units per hectare of net existing urban areas would be a reasonable measure.

7.3 Capacity of Existing Townships

7.3.1 Introduction

A key question in the pursuit of sustainability in the northern development corridor is whether the existing townships can afford, and to what extent, the increased population that organic growth and migration are expected to bring to the region. This should also be understood in terms of the two population scenarios developed in this study, the 'slow' and 'fast' growth scenarios.

7.3.2 Approach

To answer this question, two analyses were undertaken for each one of the main townships in the area as follows:

1. Establishing the net available land for building new residential developments inside the urban setting, taking into account two factors:
   - The demand generated by imagining that the activities taking place inside areas of high risk would relocate to non-risk areas; and
   - A distribution of land uses reflective of 'good practice' quantitative distribution of land uses.

2. The calculation, in terms of number of households that could fit inside the urban setting. This, in turn, is comprised by two analyses:
   - The capacity inside the net available land defined in the previous point.
   - The capacity inside parcels of land that currently exhibit residential buildings and therefore have one or more households currently living inside the premises.

   It was assumed that this will be the case because of the predominant pattern of land subdivision and residential settlement inside urban areas and the fact that when a family grows into an additional household, the latter usually develops its living space through construction of additional rooms or levels of the original house, or a new building on the original parcel.

These two analyses are further elaborated on below in *Sections 7.3.3* and *7.3.4*.

7.3.3 Net Land Available for Residential Development

In order to establish the availability of land for each town, the following analyses took place, which are also illustrated in *Figure 40*:

1. Definition of a polygon that could be regarded as the 'urbanized area' or 'urban perimeter' of the township. This was traced following the existing built form at the periphery of the town, including what could be defined as property lines of the built units, as defined from remote imagery plus other sources of information such as Google Earth and the Open Street Map project.

2. Land use distribution, including areas occupied by roads, woods, public open spaces, institutional facilities, commercial facilities, industrial operations, and residential settings. As a result a more precise measure could be achieved of the areas that could be considered as 'open' or 'not developed' within the urban setting. These areas could be considered as 'prime developable land', since they are located inside the setting with the most complete system of public utilities, social services, commercial and employment opportunities that the region has to offer, that is, the urban setting.

3. Land use break down of the areas that would be affected by floods according to the risk and vulnerability analyses presented in *Section 4*. This allows a determination of the demand in

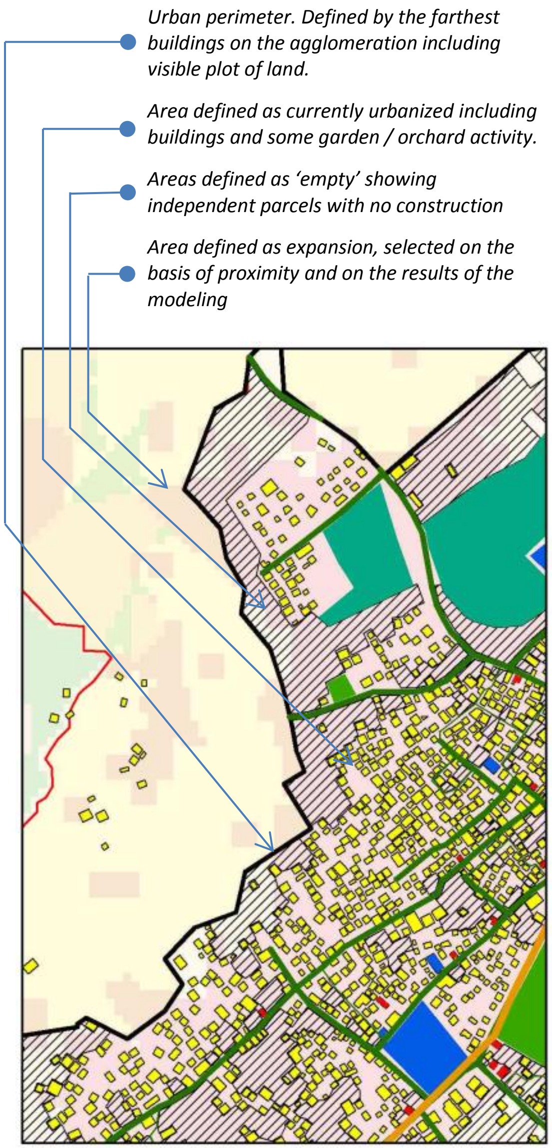

Figure 40 - Detail of elements analyzed for each one of the townships in the study area.

terms of these high risk areas that can then be added to the growth demand from future growth, should a program for progressive relocation be implemented for settlements in high-risk areas,

4. Land use outside flood area. This is the result of subtracting from the gross areas calculated in the second step described above, the areas defined as prone to flooding as determined in *Sections 4.4.3 and 4.4.4*. This is very important because it gives a measure of the 'true' area that is available for future development by avoiding risk areas.

5. An approximation to the distribution of urban land uses within the 'true' area previously mentioned, under a 'good practice' scenario. This considers that roads, wooded areas and public open space account for 45% of the area, solely institutional and solely commercial uses account for 10% of the area, industrial for 3% of the area, and 42% for residential activities, which would be mixed with commercial and other complementary uses. These approximate percentages are based on professional judgment and experience from cities in Latin America.

By applying these percentages to the 'true' available area previously identified, the net available lands for residential developments was is obtained for within the urban area, which is referred to as net available residential areas.

7.3.4 Establishing the Capacity for Additional Residential Units

The capacity of each township to hold additional residential units has been defined based upon establishing how many households could fit inside the net available residential areas and how many could do so inside areas currently exhibiting residential buildings. As discussed in *Section 7.2.2*, examples of multi-dwelling and raised dwelling prototypes (such as those developed at the Zorange Expo) that a reasonable measure would be 175 dwelling units per hectare. This is the density that is applied to the net available lands.

In order to determine the capacity of areas currently exhibiting residential buildings, the following have been calculated for each township:

- The average number of dwellings per hectare. This was done by selecting two to three sample areas in each town, one near or in the center, and the others in the periphery. The exact number of buildings inside each sample area was counted and divided into units of one hectare to arrive to the number of dwellings per hectare.
- The number of dwellings per hectare for each sample area was added and divided by the number of sample areas, to obtain the average number of dwellings per hectare for the town. The average number of dwellings per hectare in the different townships ranges between 60 and 105 dwelling units. Consequently, in calculating the number of houses for future projections, the average obtained for each town was applied.
- From the same polygons used as sample to determine the average number of residential units, the total built surface as well as the average built surface was calculated. This allowed the average footprint size of one hectare of developed residential land and the average open or unbuilt land within the same

hectare to be calculated. These two were found to range between 3,000 and 6,000 m^2 in the case of the built footprint and 7,000 to 4,000 m^2 for the open or unbuilt area.

A conservative stance on the amount of houses that exist and will emerge inside this setting was taken, assuming one household per building, and that only 20% additional houses would likely appear in the 25 years through to 2040 covered by this study. For illustration purposes, in a township in which the average number of homes per hectare is 60 inside the areas already built, it was assumed that there are 60 families (1 family per home) and that in the next 25 years a total of 12 new families and homes (20% of 60) will likely be formed in the same parcels of land in which these are located, for a total density of 72 dwelling homes at the end of the period.

In addition to development within the existing built footprint described above, development potential is also calculated and assessed (assuming 175 dwelling units per hectare) for the defined undeveloped areas, or prime developable land, that exists within the urban perimeter. This stance preferentially focuses on the 'net available residential areas' defined by these two components.

7.3.5 Expansion Areas

Once the capacity of both these areas was reached, the number of families whose houses would have to be developed on additional lands, the expansion areas, was calculated using the measure of 175 dwelling units per hectare. The resulting hectares of land per the calculation indicated in the previous point were distributed around the entire perimeter of the township, especially into areas defined as more attractive for development per the results of the modeling process.

7.4 Capacity in Trou-du-Nord

7.4.1 Total area and land use distribution

As illustrated in *Figure 41* and supporting *Table 15*, the township of Trou-du-Nord comprises an urban area of 212.91 hectares of land. In terms of surface, it is divided in order of size by empty lands comprising 44% of the total, followed by residential areas with 39%, roads with 8%, institutional services with 4%, wooded areas with 2% and commercial and public open space with 1% each.

7.4.2 Area and land uses under high risk conditions

However, as demonstrated in *Table 14*, 59.9 hectares, which equal 28% of the total urban area are located inside the high risk flood area as defined

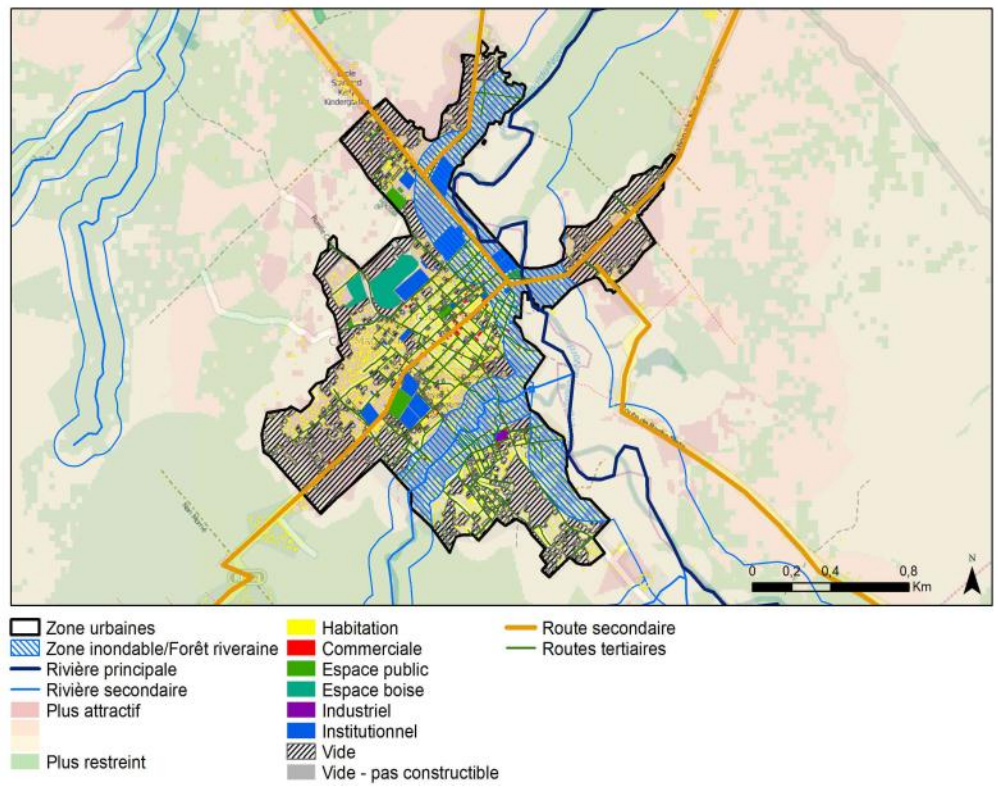

Figure 41 - Main land uses identified in the township of Trou-du-Nord.

Table 14 - Total area and current land use distribution in the township of Trou-du-Nord

CATEGORY	AREA (Ha)	%
Routes	17.82	8%
Espace Boise	4.13	2%
Espace Public	2.11	1%
Institutionnel	8.93	4%
Commerciale	1.23	1%
Industriel	0.27	0%
Vide	94.71	44%
Habitation	83.71	39%
TOTAL	212.91	
	100%	

by the studies conducted as presented in *Section 4.4.4*. These areas are comprised largely of unoccupied lands with 48% of the total, residential areas with 45%, and some institutional facilities with 7% of the area.

In an ideal scenario none of these areas would be occupied by buildings, since they are classified as high risk, in which mitigation measures would likely not be sufficient to protect life.

7.4.3 Available land

This leaves 72% of the urban setting or 153 hectares as the area in which future development could be planned within. Based on the data in *Table 14* for the total land outside the flood zone, the urban area within Trou-du-Nord would be able to receive new developments inside the identified 66 ha of empty lands.

While the specific land use breakdown of a city is closely associated to its economy, experience in several cities in Latin America suggests a sustainable urbanization model for land distribution would comprise: 45% for roads, public spaces, natural or naturalized areas; 42% for residential uses (in which small scale commerce and other complementary uses are included); 10% for institutional and commercial uses and 3% for other, industry-related uses.

If this model was applied in Trou-du-Nord, the 66 ha that constitute the 'gross' available land should be broken into the land uses and areas that appear in *Table 14* under 'availability for development'. Consequently, not more than 28 hectares ought to be destined for residential developments. This is referred to as 'net available residential land'.

7.4.4 Capacity to accommodate residential developments

In order to determine the capacity of already built areas, the two areas that appear illustrated in Figure *42* (a central city area and a more peripheral one) were used to measure the number of dwellings they contain, finding an average 59 units per hectare. Using the previously defined conservative approach to the growth of areas that are currently built (20% of the growth of the average number of houses over a 25 year period), a density of 71 dwelling units per hectare was derived, and when applied to the 57 hectares of residential land in which this could take place, a capacity of 4,024 homes was obtained. In addition, for the 28 hectares of net residential land defined in *Section 7.4.3*, applying the reasonable density of 175 dwelling units per hectare generates a further 4,868 dwelling units. Based on these two factors, the total capacity of dwelling units inside the urban setting would be 8,892.

Table 15 - Trou-du-Nord - Urban land uses inside and outside the high risk flood areas, and 'true' available land.

URBAN LAND USE INSIDE FLOOD AREA

CATEGORY	AREA (Ha)	%
Routes	0.00	0%
Espace Boise	0.00	0%
Espace Public	0.21	0%
Institutionnel	4.18	7%
Commerciale	0.25	0%
Industriel	0.01	0%
Vide	28.48	48%
Habitation	26.77	45%
TOTAL	59.91	
	28%	

URBAN LAND USE OUTSIDE FLOOD AREA

CATEGORY	AREA (Ha)	%
Routes	17.82	11.65%
Espace Boise	4.13	2.70%
Espace Public	1.90	1.24%
Institutionnel	4.74	3.10%
Commerciale	0.98	0.64%
Industriel	0.26	0.17%
Vide	66.23	43.29%
Habitation	56.94	37.21%
TOTAL	153.00	
	72%	

AVAILABILITY FOR DEVELOPMENT (NET VIDE)

CATEGORY	GOOD PRACTICE	AREA (Ha)	RELOCATED	NET AREA
Routes	15%	9.93	0	9.93
Espace Boise	15%	9.93	0	9.93
Espace Public	15%	9.93	0.04	9.89
Institutionnel	5%	3.31	0.82	2.49
Commerciale	5%	3.31	0.53	2.78
Industriel	3%	1.99	0.29	1.70
Vide	0%	0.00	0	0.00
Habitation	42%	27.82	11.22	16.60
TOTAL		66.23	12.9	

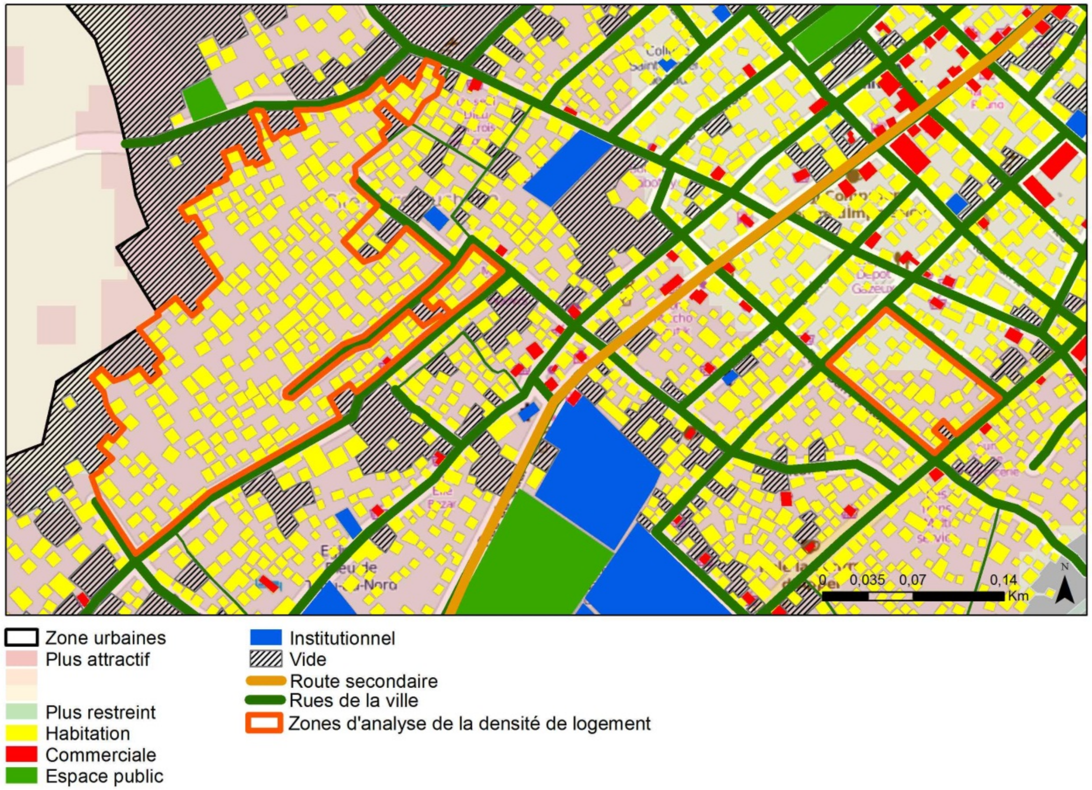

Figure 42 - Trou du Nord - Areas selected for calculating the building density.

Table 16 - Trou du Nord - Capacity for residential developments inside the urban setting and areas required for expansion in the 2040 fast growth scenario

TROU DU NORD	BASELINE	#
	No. of homes per ha in sample area 1	61
	No. of homes per ha in sample area 2	57
	Average number of homes per ha	59
	"Reasonable"density in areas currently occupied by residential use (current homes per ha + 20%)	71
	"Reasonable" density in non developed lands	175
SUPPLY	AVAILABLE OPEN LANDS	
	Area (Ha)	28
	Capacity in # of homes on non-developed lands at reasonable density (175)	4868
	DEVELOPED ZONES OUTSIDE RISK AREAS	
	Area (Ha)	57
	Capacity in # of homes on already developed zones at reasonable density (71)	4024
	TOTAL SUPPLY IN URBAN AREA	8892
DEMAND	Demand from relocation in Ha	27
	Demand from relocation in # of homes (at average density)	1577
	Total households by 2040 in the fast growth scenario*	17083
	TOTAL DEMAND BY 2040	18660
EXPANSION NEEDS	Total supply in urban area	8892
	Total housing needs in expansion areas	9768
	Area required for expansion in ha	56

* According to ERM population study and projections

Considering that by 2040, in the fast growth scenario Trou-du-Nord would reach a total demand of 18,660 housing units including existing households plus those that might be considered for relocation, and that 8,892 of those could be housed inside the current urban area, a total of 9,768 households would have to be located in expansion areas. At the reasonable density of 175 dwelling units per hectare, Trou-du-Nord would have to incorporate an additional 56 hectares of land to its perimeter. *Table 16* summarizes these calculations for Trou-du-Nord.

Based on these calculations, and as illustrated in *Figure 43*, a series of areas for future urban development around the perimeter of the city have been identified, which amount to 78 hectares. This provides an extra buffer against the 56 hectares identified above, and acknowledges that the area could be developed with varying density parameters that reduced the dwelling units per hectare parameter. These correspond with the areas surrounding the town and those that extend along the main roads that were classified as more attractive for development based on the modelling process presented in *Section 6.7*.

7.4.5 Next Step: Developing an Urban Design Vision

Having established the areas in Trou-du-Nord that should be considered for future urbanization inside and outside the urban setting, the next step would be to develop an urban design vision. This should be based on applying, for both the 'true' available land and the expansion areas, the distribution of land uses that is proposed under the 'good practice' model discussed previously.

Because of its size and location farthest from areas of high risk, the quadrant comprised by polygon D in *Figure 43* should be thought of as the one where the main institutional, commercial and recreational activities of the township ought to be developed. Mixed with reasonable density residential developments, this could provide the balance that the township is requiring in terms of public open spaces and other elements of a quality civic life.

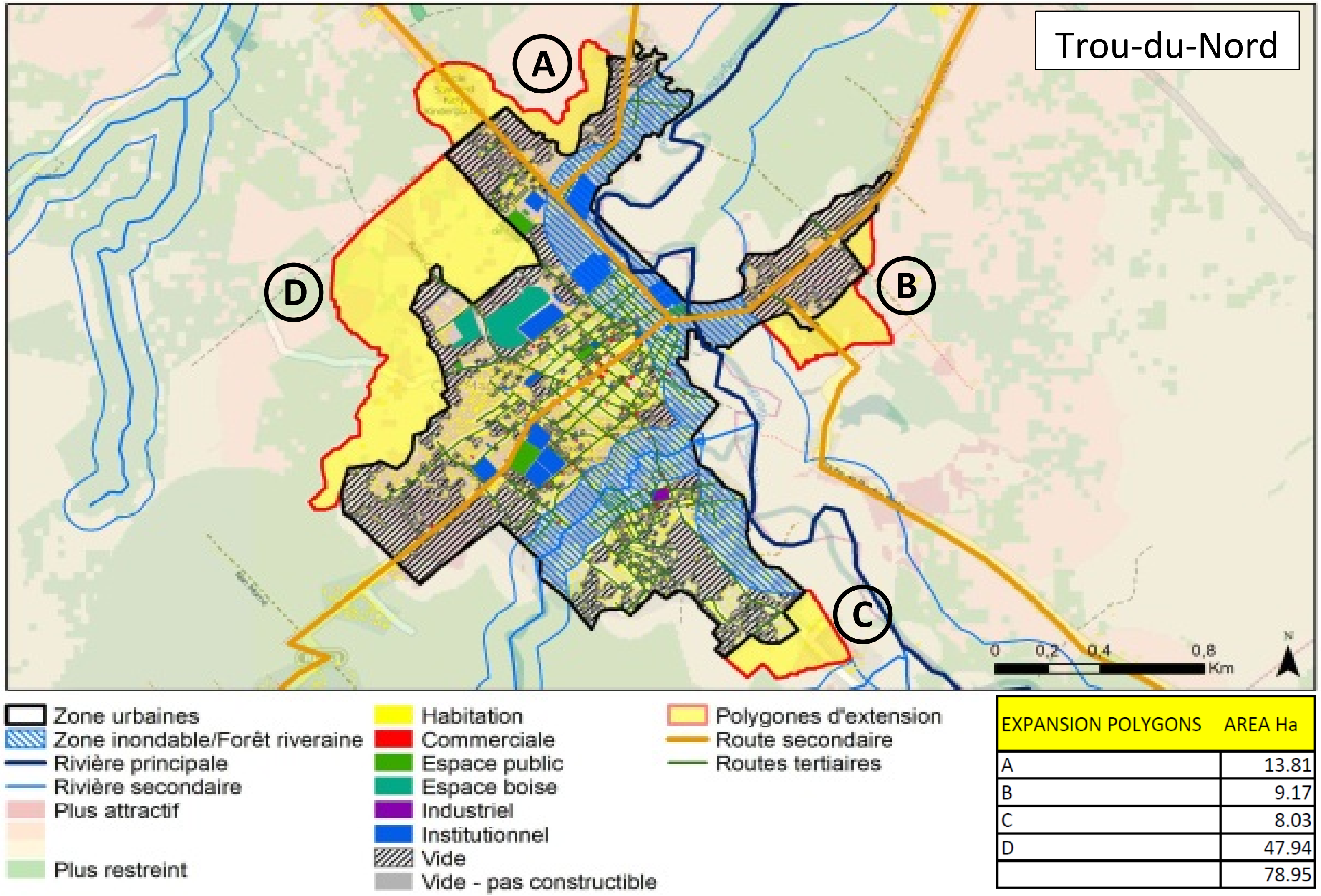

EXPANSION POLYGONS	AREA Ha
A	13.81
B	9.17
C	8.03
D	47.94
	78.95

Figure 43 – Trou-du-Nord - Current land uses, areas for densification within the urban setting and proposed expansion areas.

7.5 Capacity in Limonade

7.5.1 Total area and land use distribution

As illustrated in *Figure 44* and supporting Table 1 - 4, the township of Limonade comprises an urban area of 155 hectares of land. In terms of surface, it is divided in order of size by empty lands comprising 55% of the total, followed by residential areas with 26%, roads with 10%, wooded areas with 6%, public spaces with 2%, and commercial and institutional space with 1% each. Only one industrial operation was identified, with less than 1%.

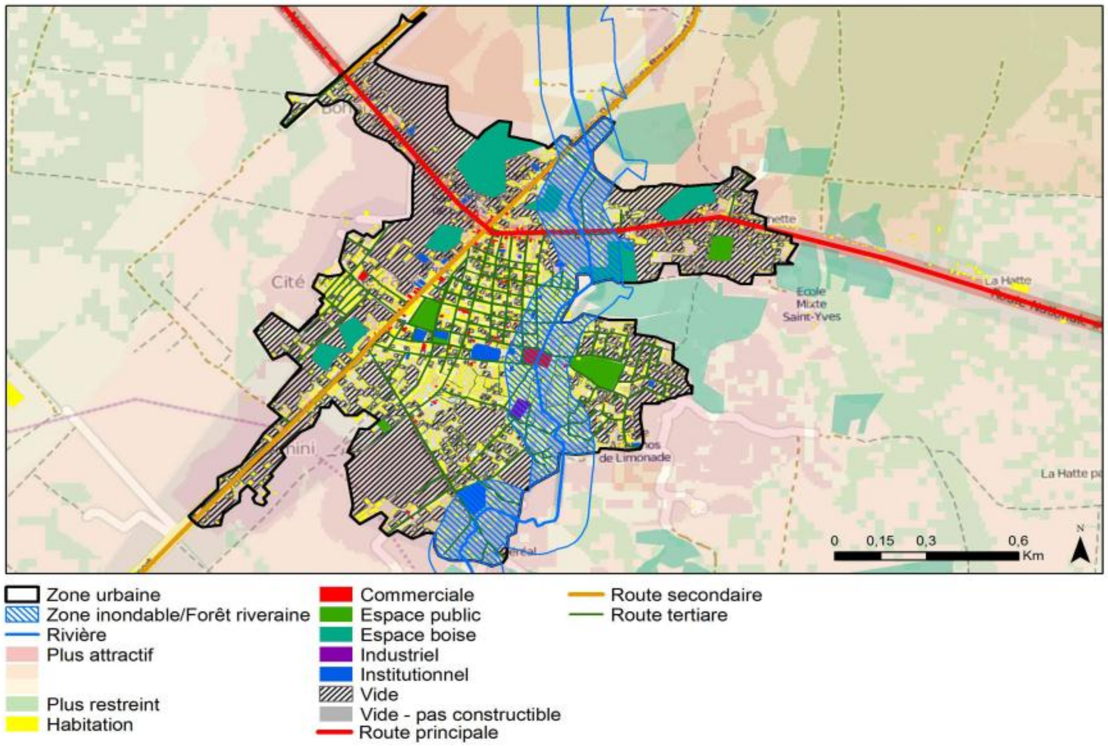

Figure 44 - Main land uses identified in the township of Limonade

7.5.2 Area and land uses under high risk conditions

As demonstrated in *Table 18*, 29.49 hectares, which equal 21% of the total urban area are located inside the high risk flood area as defined by the studies conducted as presented in *Section 4.4.4*. These are comprised largely by unoccupied areas with 42% of the total, residential areas with 38%, roads with 9%, wooded areas with 5% and some institutional, commercial and industrial facilities adding up to 6% of the area. As mentioned at the beginning of this Chapter, in an ideal scenario none of these areas would be occupied by buildings, since they are classified as high risk, in which mitigation measures would likely not be sufficient to protect life.

Table 17 - Total area and current land use distribution in the township of Limonade

CATEGORY	AREA (Ha)	%
Routes	15.27	10%
Espace Boise	9.13	6%
Espace Public	2.73	2%
Institutionnel	2.06	1%
Commerciale	1.37	1%
Industriel	0.29	0%
Vide	84.36	55%
Habitation	39.46	26%
TOTAL	154.66	
	100%	

7.5.3 Available land

The above leaves 81% of the urban setting or 125 hectares as the area in which future development could to be planned and fostered. As also indicated in *Table 18*, of the total land outside the flood zone (125 ha), 72.07 ha are empty (58%), followed by 28 ha of residential areas (23%), 13 ha of areas occupied by roads (10%) 7.55 areas occupied by wooded areas (6%), 3 ha of public open space (2%), and other land uses representing less than 2% of the area.

Based on these data, the urban area of Limonade would be able to receive new developments inside the 72 ha of empty lands previously mentioned.

Table 18 - Limonade - Urban land uses inside and outside the high risk flood areas, and 'true' available land.

URBAN LAND USE INSIDE FLOOD AREA			URBAN LAND USE OUTSIDE FLOOD AREA			AVAILABILITY FOR DEVELOPMENT (NET VIDE)				
CATEGORY	AREA (Ha)	%	CATEGORY	AREA (Ha)	%	CATEGORY	GOOD PRACTICE	AREA (Ha)	RELOCATED	NET AREA
Routes	2.72	9%	Routes	12.54	10.02%	Routes	15%	10.81	0	10.81
Espace Boise	1.58	5%	Espace Boise	7.55	6.03%	Espace Boise	15%	10.81	0	10.81
Espace Public	0.04	0%	Espace Public	2.69	2.15%	Espace Public	15%	10.81	0.04	10.77
Institutionnel	0.82	3%	Institutionnel	1.24	0.99%	Institutionnel	5%	3.60	0.82	2.78
Commerciale	0.53	2%	Commerciale	0.84	0.67%	Commerciale	5%	3.60	0.53	3.07
Industriel	0.29	1%	Industriel	0.00	0.00%	Industriel	3%	2.16	0.29	1.87
Vide	12.29	42%	Vide	72.07	57.58%	Vide	0%	0.00	0	0.00
Habitation	11.22	38%	Habitation	28.24	22.56%	Habitation	42%	30.27	11.22	19.05
TOTAL	29.49		TOTAL	125.17		TOTAL		72.07	12.9	
	19%			81%						

If the same model discussed in *Section 7.4* is applied in Limonade, the 72 ha that constitutes the 'gross' available land should be broken into the land uses and areas that also appear in *Table 18*. Consequently, not more than 30 hectares should be destined for residential developments.

7.5.4 Capacity to accommodate residential developments

In order to determine the capacity of already built areas, the two areas that appear illustrated in *Figure 45* (a central city area and a more peripheral one) were measured, finding an average of 105 units per hectare. Applying the conservative density (20% increase), a density of 126 dwelling units per hectare is derived, and applying this to the 28 hectares of residential land area, a future capacity of 3,558 homes is obtained. In addition, applying the 175 dwelling units per hectare to the 30 hectares identified in Section 7.5.3, a further 5,297 homes can be accommodated, giving a total capacity of dwelling units inside the urban setting of 8,855.

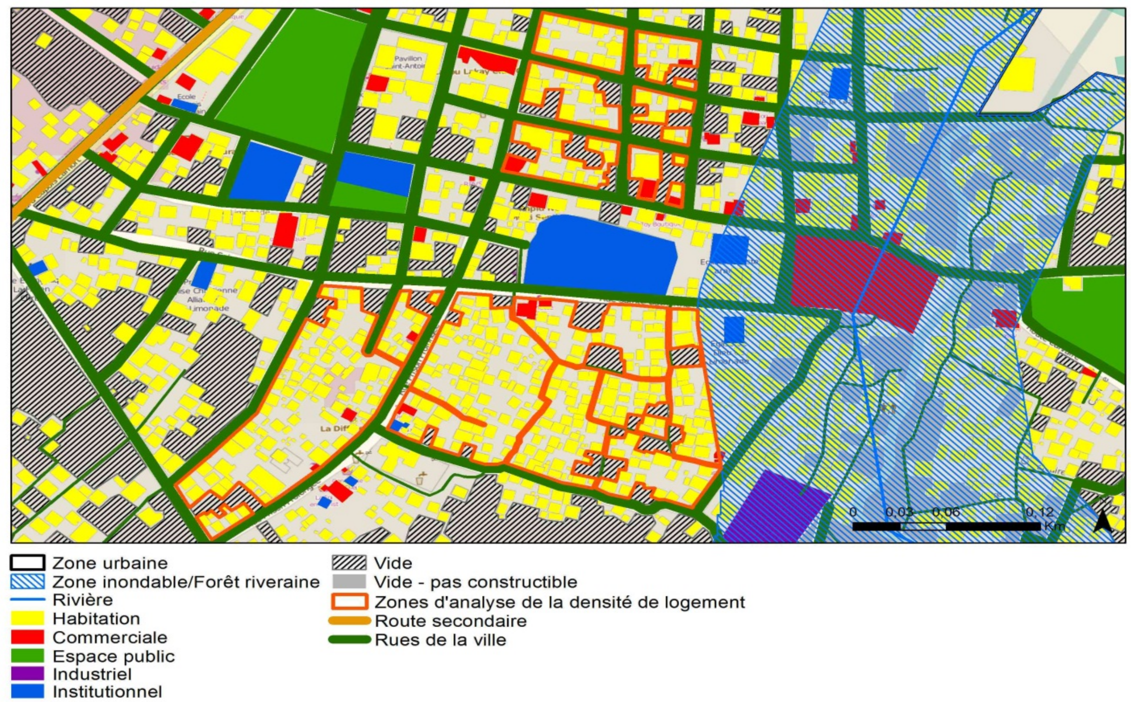

Figure 45 - Limonade - Areas selected for calculating the building density

Considering that by 2040, in the fast growth scenario Limonade would reach a total demand of

17,307 housing units including existing households plus those that might be considered for relocation, and that 8,855 of those could be housed inside the current urban area, a total of 8,452 households would have to be located in expansion areas. At the reasonable density of 175 dwelling units per hectare, Limonade would have to incorporate an additional 48 hectares of land to its perimeter. *Table 18* summarizes these calculations for Limonade.

Based on these calculations, and as illustrated in *Figure 46*, a series of areas for future urban development around the perimeter of the city have been identified. These correspond with the areas surrounding the town and those that extend along the main roads that were classified as more attractive for development based on the modelling process presented in *Section 6.7*.

Because of the presence of a significant process of settlement on the east side of Limonade, as well as a valuable wooded area in the same area, a planned expansion area that incorporates controls over the wooded area (polygon 'C' on the map) should be implemented. Coupled with providing expansion areas in all directions, this would yield a larger expansion area, which has been estimated at 111 hectares.

7.5.5 Next step: developing an urban design vision

Having established the areas in Limonade that ought to be destined for future urbanization inside and outside the urban setting, the next step would be to develop an urban design vision. This vision should be based on applying, for both the 'gross' available land and the expansion areas, the distribution of land uses that is proposed under the 'good practice' model discussed previously.

A major feature of Limonade visible in the figure is the presence of healthy, wooded areas surrounding the township. Considering that these could be major green assets in the area, the recommendable action would be to declare them as public space, integrating the western side of the city to this system. This should be thought of as the area where the main institutional, commercial and recreational activities of the township ought to be developed. Mixed with reasonable density residential developments, this could provide not only the balance that the township is requiring in terms of public open spaces but also become a major element of attraction to this township for new migrants or settlers.

Table 19 - Limonade - Capacity for residential developments inside the urban setting and areas required for expansion in the 2040 fast growth scenario

LIMONADE	BASELINE	#
	No. of homes per ha in sample area 1	122
	No. of homes per ha in sample area 2	88
	Average number of homes per ha	105
	"Reasonable" density in areas currently occupied by residential use (current homes per ha + 20%)	126
	"Reasonable" density in non developed lands	175
SUPPLY	AVAILABLE OPEN LANDS	
	Area (Ha)	30
	Capacity in # of homes on non-developed lands at reasonable density (175)	5297
	DEVELOPED ZONES OUTSIDE RISK AREAS	
	Area (Ha)	28
	Capacity in # of homes on already developed zones at reasonable density (126)	3558
	TOTAL CAPACITY IN URBAN AREA	8855
DEMAND	Demand from relocation in Ha	11
	Demand from relocation in # of homes (at average density)	1178
	Total households by 2040 in the fast growth scenario*	16129
	Total households by 2040 plus relocated households	17307
EXPANSION NEEDS	Total supply in urban area	8855
	Total housing needs in expansion areas	8452
	Area required for expansion in ha	48

* According to ERM population study and projections

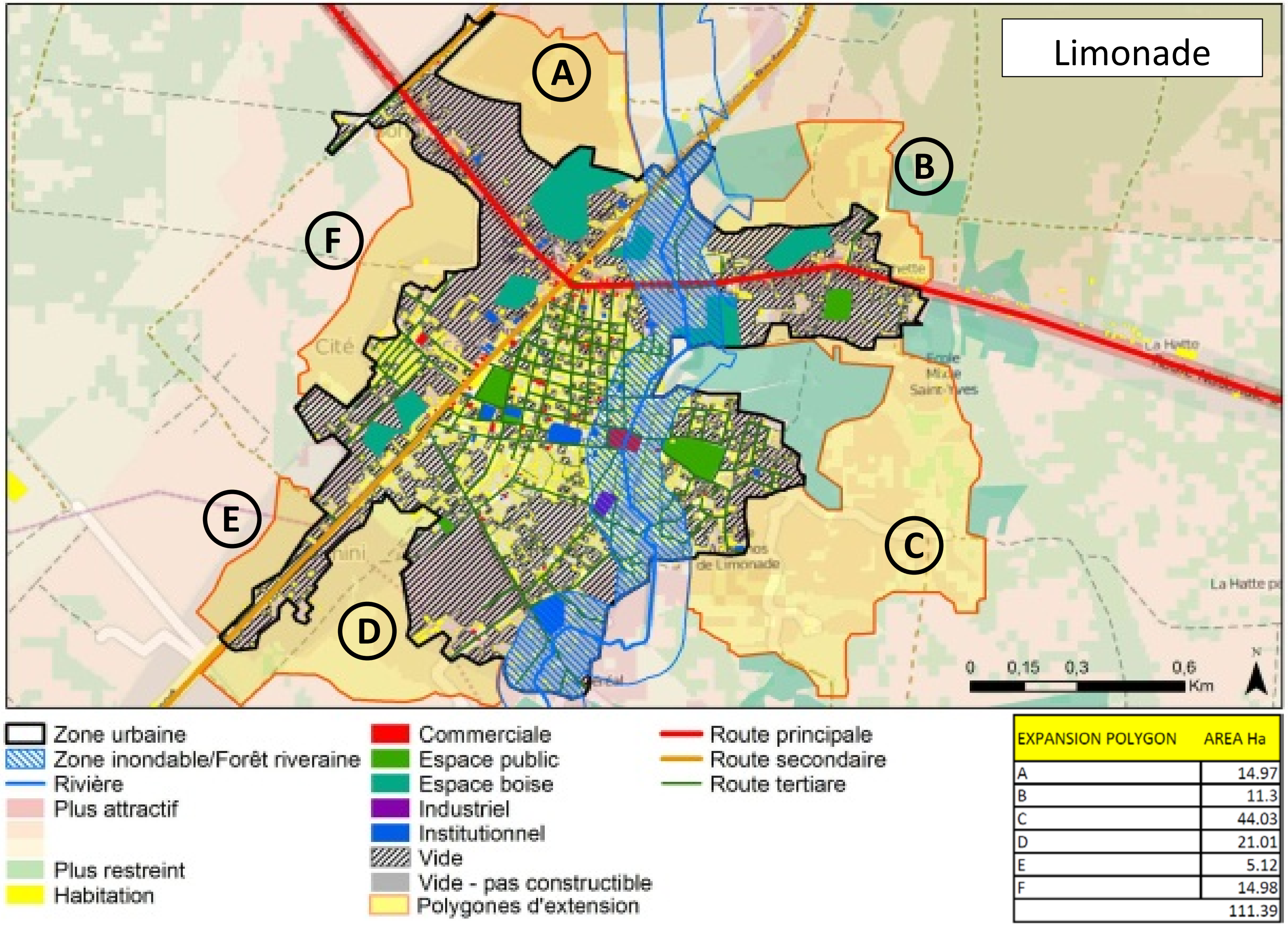

EXPANSION POLYGON	AREA Ha
A	14.97
B	11.3
C	44.03
D	21.01
E	5.12
F	14.98
	111.39

Figure 46 - Limonade - Current land uses, areas for densification within the urban setting and proposed expansion areas.

7.6 Capacity in Terrier Rouge

7.6.1 Total area and land use distribution

As illustrated in Figure 47 - Main land uses identified in the township of Terrier Rouge*Figure 47* and accompanying *Table 20*, the township of Terrier Rouge comprises an urban area of 130 hectares of land. In terms of surface, it is divided in order of size by empty lands comprising 45% of the total, followed by residential areas with 34%, roads with 12%, institutional services with 4%, public open spaces with 3% and very limited commercial areas.

7.6.2 Area and land uses under high risk conditions

As demonstrated in *Table 21*, just 2.56 hectares, which equal 2% of the total urban area are located inside the high risk flood area as defined by the studies conducted as presented in *Section 4.4.4*. The small flood zone is comprised by 1.12 ha of empty lands accounting for 44%, 0.78 ha of residential activity areas representing 31%, and some institutional facilities with 13% of the area. With these indicators, Terrier Rouge is clearly the least exposed township to flooding.

Table 20 - Total area and current land use distribution in the township of Terrier Rouge

CATEGORY	AREA (Ha)	%
Routes	15.35	12%
Espace Boise	0.86	1%
Espace Public	4.01	3%
Institutionnel	5.63	4%
Commerciale	0.55	0%
Industriel	0.00	0%
Vide	58.85	45%
Habitation	44.74	34%
TOTAL	129.98	
	100%	

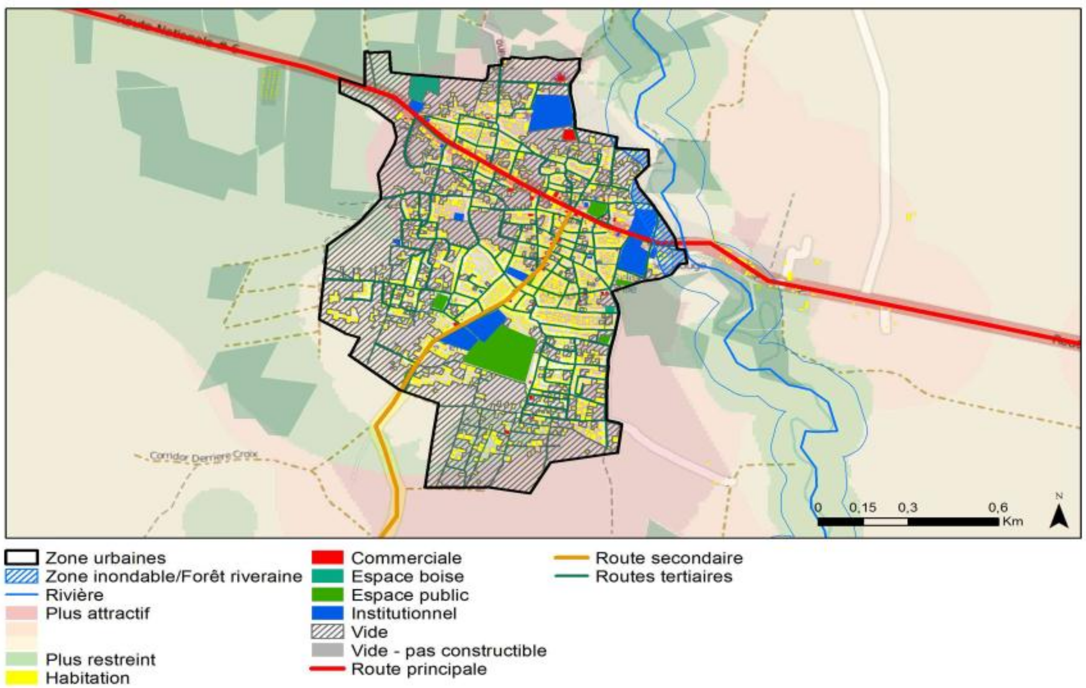

Figure 47 - Main land uses identified in the township of Terrier Rouge

Relocating, if selected as a measure, and implementing adaptation measures inside the areas would also be the least complex task to undertake in this town, compared to the other towns in the area of study.

7.6.3 Available land

The factors expressed above leave 98% of the urban setting or 127 hectares as the area in which future development could be planned. As indicated in the *Table 21*, of the total land outside the flood zone (127 ha), 58 are empty lands (45%), followed by 44 ha of residential areas (35%), 15 ha of roads (12%), institutional areas occupying 5 ha (4%), public open space occupying 4 ha (3%) and other land uses representing not more than 2% of the total area.

Based on these data, the urban area of Terrier Rouge would be able to receive new developments inside the 58 ha of empty lands previously mentioned.

Table 21 - Terrier Rouge - Urban land uses inside and outside the high risk flood areas, and 'true' available land.

URBAN LAND USE INSIDE FLOOD AREA			URBAN LAND USE OUTSIDE FLOOD AREA			AVAILABILITY FOR DEVELOPMENT (NET VIDE)				
CATEGORY	AREA (Ha)	%	CATEGORY	AREA (Ha)	%	CATEGORY	GOOD PRACTICE	AREA (Ha)	RELOCATED	NET AREA
Routes	0.32	13%	Routes	15.02	11.79%	Routes	15%	8.66	0	8.66
Espace Boise	0.00	0%	Espace Boise	0.86	0.67%	Espace Boise	15%	8.66	0	8.66
Espace Public	0.00	0%	Espace Public	4.01	3.15%	Espace Public	15%	8.66	0.04	8.62
Institutionnel	0.32	13%	Institutionnel	5.31	4.17%	Institutionnel	5%	2.89	0.82	2.07
Commerciale	0.01	0%	Commerciale	0.54	0.42%	Commerciale	5%	2.89	0.53	2.36
Industriel	0.00	0%	Industriel	0.00	0.00%	Industriel	3%	1.73	0.29	1.44
Vide	1.12	44%	Vide	57.73	45.30%	Vide	0%	0.00	0	0.00
Habitation	0.78	31%	Habitation	43.96	34.50%	Habitation	42%	24.25	11.22	13.03
TOTAL	2.56		TOTAL	127.43		TOTAL		57.73	12.9	
	2%			98%						

Applying the same approach for Terrier Rouge as has been applied to Limonade and Trou-du-Nord, the 58 ha that constitutes the 'gross' available land should be broken into the land uses and areas that appear in the availability for development part of *Table 21*. This results in 24 hectares identified for residential developments.

7.6.4 Capacity to accommodate residential developments

As in the previous townships, the determined the capacity of Terrier Rouge to accommodate new households was on the basis of a conservative approach to the growth (20% growth), together with the application of a 'reasonable' density of 175 dwelling units per hectare to the net available lands within the urban setting. The 24 net hectares that could be utilized for residential activities would therefore fit a total of 4,243 dwelling units.

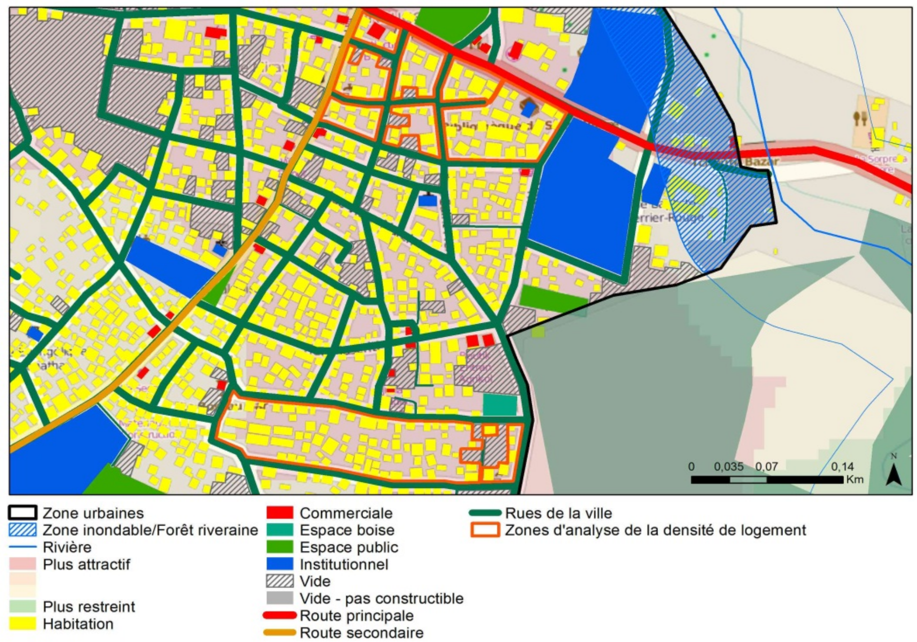

Figure 48 - Terrier Rouge - Areas selected for calculating the building density

In order to determine the capacity of already built areas, the two areas that appear illustrated in *Figure 48* (a central city area and a more peripheral one) were used to measure the number of dwellings they contain, finding an average 53 units per hectare. Consequently, by applying the conservative density of 64 dwelling units per hectare to the 44 hectares of residential land uses in which this could take place, a capacity of 2,796 homes is obtained. Based on these two factors, the total capacity of dwelling units inside the urban setting would be 7,039.

Considering that by 2040, in the fast growth scenario Terrier Rouge would reach a total demand of 11,190 housing units including existing households plus those that would have to be relocated, and that 7,039 of those could be built inside the current urban area, a total of 4,152 households would have to be located in expansion areas. At the reasonable density of 175 dwelling units per hectare, Terrier Rouge would have to incorporate an additional 24 hectares of land to its perimeter. Table 22summarizes these calculations for Limonade

Based on these calculations, and as illustrated in *Figure 49*, a series of areas for future urban development around the perimeter of the city have been traced. These correspond with the areas surrounding the town and those that extend along the main roads that were classified as more attractive for development based on the modelling process presented in *Section 6.7*.

7.6.5 Next step: urban design vision

Having established the areas in Terrier Rouge that ought to be destined for future urbanization inside and outside the urban setting, the next step would be to develop an urban design vision. This vision should be based on applying, for both the 'gross' available land and the expansion areas, the distribution of land uses that is proposed under the 'good practice' model discussed previously.

Table 22 - Terrier Rouge - Capacity for residential developments inside the urban setting and areas required for expansion in the 2040 fast growth scenario

TERRIER ROUGE	BASELINE	#
	No. of homes per ha in sample area 1	52
	No. of homes per ha in sample area 2	54
	Average number of homes per ha	53
	"Reasonable"density in areas currently occupied by residential use (current homes per ha + 20%)	64
	"Reasonable" density in non developed lands	175
SUPPLY	AVAILABLE OPEN LANDS	
	Area (Ha)	24
	Capacity in # of homes on non-developed lands at reasonable density (175)	4243
	DEVELOPED ZONES OUTSIDE RISK AREAS	
	Area (Ha)	44
	Capacity in # of homes on already developed zones at reasonable density (64)	2796
	TOTAL CAPACITY IN URBAN AREA	7039
DEMAND	Demand from relocation in Ha	1
	Demand from relocation in # of homes (at average density)	41
	Total households by 2040 in the fast growth scenario*	11149
	Total households by 2040 plus relocated households	11190
EXPANSION NEEDS	Total supply in urban area	7039
	Total housing needs in expansion areas	4152
	Area required for expansion in ha	24

* According to ERM population study and projections

Terrier Rouge is not significantly exposed to floods, and it is also a surrounded by very important natural wooded areas that should be protected.

Because of this factor, the expansion of the township should be thought of more towards the south (polygons C and D in *Figure 49*), which is also where the suitability analysis yielded the areas that should be developed. These should be the areas where the main institutional, commercial and recreational activities of the township ought to be developed. This proposition departs from the AIA Study's proposal to create a by-pass of RN6 towards the north of the township. That said, the south of Terrier Rouge and its connection with Grande Bassin is an area that should be looked for sustainable future development.

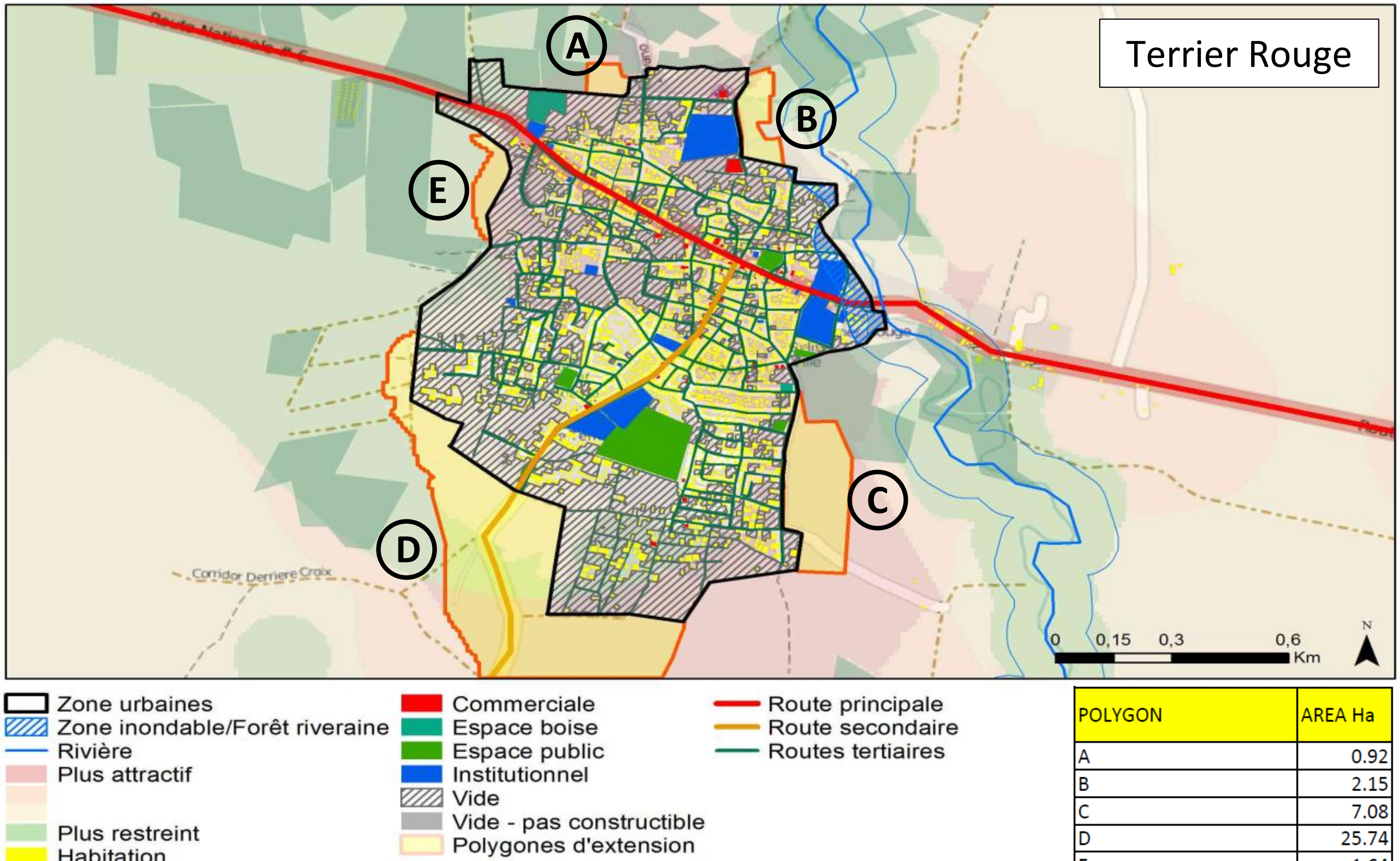

POLYGON	AREA Ha
A	0.92
B	2.15
C	7.08
D	25.74
E	1.64
	37.53

Figure 49 - Terrier Rouge - Current land uses, areas for densification within the urban setting and proposed expansion areas

7.7 Capacity in Bord de Mer de Limonade

7.7.1 Total area and land use distribution

As illustrated in *Figure 50* and supporting *Table 23*, the township of Bord de Mer de Limonade comprises an urban area of 52 hectares of land. In terms of surface, it is divided in order of size by empty areas comprising 51% of the total, followed by residential areas with 20%, roads with 7%, institutional areas with 3%, and commercial and public open space with 1% each.

7.7.2 Area and land uses under high risk conditions

The situation in Bord de Mer is critical because, as demonstrated in *Table 24*, 47 hectares, which equal 90% of the total urban area are located inside the high risk flood area as defined by the studies conducted as presented in *Section 4.4.4*.

In an ideal scenario none of these areas would be occupied by buildings, since they are classified as high risk, where mitigation effects could have limited impacts. However, it is very unlikely that a program to relocate 90% of the township will happen, and it is not possible to accommodate the current and future population demands in the 10% area that is not in situation of high risk.

As a consequence, the options for responses would be as follows:

1. Barr any expansion of the township and implement policies and incentives for new settlers to seek location elsewhere.

Table 23 - Total area and current land use distribution in the township of Bord de Mer de Limonade

URBAN LAND USE IN BDM de Limonade		
CATEGORY	AREA (Ha)	%
Routes	3.72	7%
Espace Boise	0.00	0%
Espace Public	0.66	1%
Institutionnel	1.41	3%
Commerciale	0.36	1%
Industriel	0.00	0%
Vide	26.77	51%
Habitation	19.57	37%
TOTAL	52.48	
	100%	

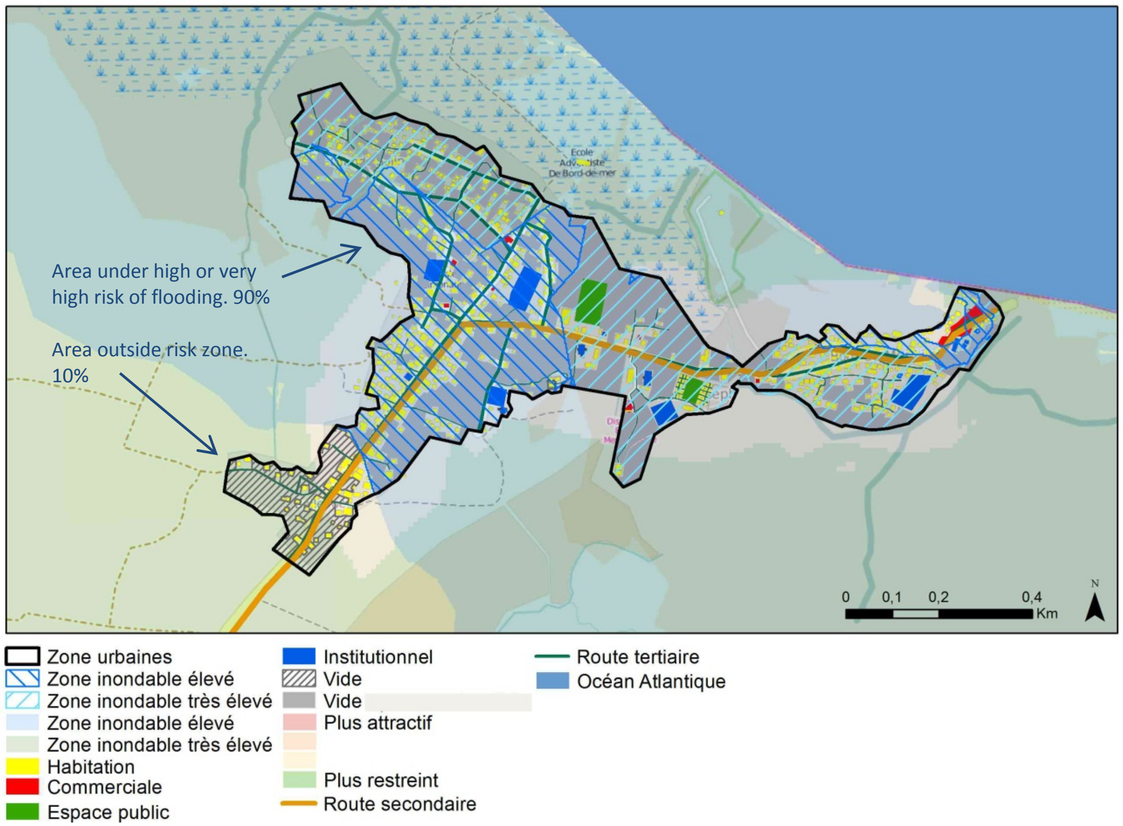

Figure 50 - Main land uses identified in the township of Bord de Mer de Limonade

Table 24 - Bord de Mer de Limonade - Urban land uses inside and outside the high risk flood areas, and 'true' available land.

URBAN LAND USE INSIDE FLOOD AREA			URBAN LAND USE OUTSIDE FLOOD AREA			AVAILABILITY FOR DEVELOPMENT (NET VIDE)				
CATEGORY	AREA (Ha)	%	CATEGORY	AREA (Ha)	%	CATEGORY	GOOD PRACTICE	AREA (Ha)	RELOCATED	NET AREA
Routes	3.37	7%	Routes	0.34	6.29%	Routes	15%	0.52	0	0.52
Espace Boise	0.00	0%	Espace Boise	0.00	0.00%	Espace Boise	15%	0.52	0	0.52
Espace Public	0.66	1%	Espace Public	0.00	0.00%	Espace Public	15%	0.52	0.04	0.48
Institutionnel	1.40	3%	Institutionnel	0.01	0.14%	Institutionnel	5%	0.17	0.82	-0.65
Commerciale	0.23	0%	Commerciale	0.13	2.31%	Commerciale	5%	0.17	0.53	-0.36
Industriel	0.00	0%	Industriel	0.00	0.00%	Industriel	3%	0.10	0.29	-0.19
Vide	23.30	50%	Vide	3.47	63.31%	Vide	0%	0.00	0	0.00
Habitation	18.04	38%	Habitation	1.53	27.96%	Habitation	42%	1.46	11.22	-9.76
TOTAL	47.01		TOTAL	5.48		TOTAL		3.47	12.9	
	90%			10%						

2. Consider the entire township for the application of the 'good practice' land use distribution model, which would be representative of a sustainable community in terms of economic activities. This would entail, as demonstrated in *Table 24*, doubling the surface occupied by roads, creating a public space realm of open spaces and wooded areas of 15.6 hectares in a place that just has 0.66 ha of this kind of space, doubling the area for institutional activities, and setting aside 4 hectares of land for a commercial operation. As a result, in terms of residential surface the township could only allocate 22 ha.

3. Develop a housing solution that adapts as maximum as possible to the potential hazards, in this case coastal floods and hurricanes. This could be possible, through housing models such as the one depicted in *Figure 50*. These should be implemented in the 22 ha that would be allocated for residential uses. This should be coupled with an intense program for changing the existing housing stock to these kinds of models.

4. Develop multi-family housing projects that maximize the density that solutions such as the one depicted in *Figure 50* could afford. Based on the analyses of the Zorange pilotis-supported structure and the EKAM project, the density in this case that could be reached would be 80 homes per hectare of net area.

5. Design and develop incentives for future households to settle outside the township, on areas that are less exposed to natural phenomena.

7.7.3 Capacity to accommodate residential developments

According to the analyses presented, and is demonstrated in *Table 25*, in Bord de Mer de Limonade there is a net availability of land for residential uses of approximately 23 hectares. This would yield a total 1,840 homes, which would be 196 units less than the 1,644 homes that would be expected to have arrived in the township by 2040. This is illustrated in *Table 23*

Figure 51 - A pilotis - supported house developed for the Zorange Housing Expo

Table 25 - Bord de Mer de Limonade - Capacity for residential developments inside the urban setting

Capacity Analysis	
Net land available for residential land uses	23
Multifamily density that could be reached	80
Total homes	1840
Total households by 2040 in the fast growth scenario*	1644
Remaining capacity by 2040	196

* According to ERM's population projections

7.7.4 Next step: developing an urban design vision

A re-thinking of the future of this township should be considered. However, this should be coupled with a program aimed at offering alternative settlement areas near the employment centers where its inhabitants work. For in the long term, a process of growth reflective of the current construction habits and trends would expose this township and its population to even more severe situations of risk.

7.8 Capacity in Caracol

7.8.1 Total area and land use distribution

As illustrated in *Figure 52* and supporting *Table 27*, the township of Caracol comprises an urban area of 43 hectares of land. In terms of surface, it is divided in order of size by empty areas comprising 48% of the total, followed by residential areas with 34%, roads with 10%, institutional areas and public open space with 3% each, wooded areas with 1%. There is only a minimal commercial activity near the town center.

7.8.2 Area and land uses under high risk conditions

The situation in Caracol is not as critical as in Bord de Mer, but still a concern, with 49% of the area of the township at risk of flooding (see *Table 28*). Again, in an ideal scenario none of these areas would be occupied by buildings. However, it is unlikely that a program to relocate 49% of the township will happen. Additionally, here it is also not possible to accommodate the current and future population demands in the half of the township that is not at risk of flooding.

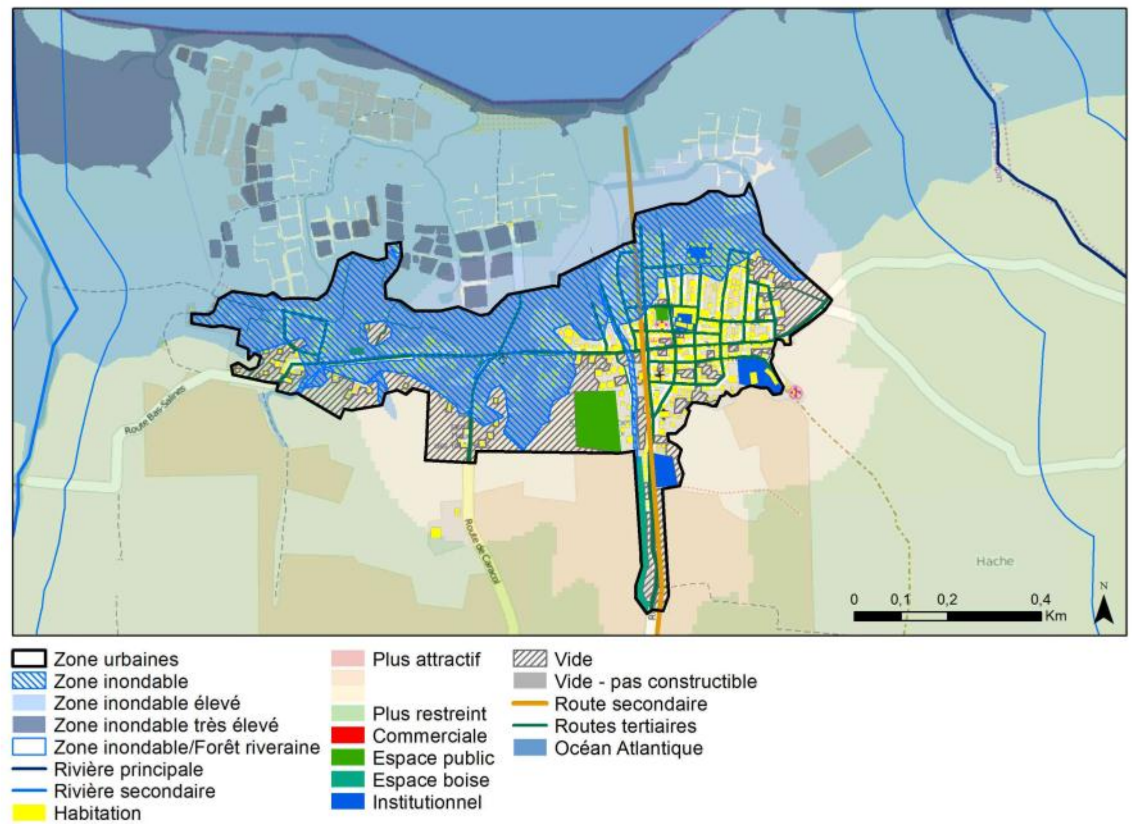

Figure 52 - Main land uses identified in the township of Caracol

Table 27 - Total area and current land use distribution in the township of Caracol

CATEGORY	AREA (Ha)	%
Routes	4.44	10%
Espace Boise	0.44	1%
Espace Public	1.27	3%
Institutionnel	1.40	3%
Commerciale	0.14	0%
Industriel	0.00	0%
Vide	20.96	48%
Habitation	14.73	34%
TOTAL	43.39	
	100%	

Furthermore, as will be shown in this section, due to the expected growth in the demand for housing in Caracol in the fast population growth scenario, the township will not have the necessary area to cover that demand if restricted areas are respected and adhered to.

As a result, the responses would have to the same as those proposed in Bord de Mer de Limonade, with an additional sense of urgency because of the demand issue, and would comprise:

1. Seek to prevent any expansion of the township and implement policies and incentives for new settlers to seek locations elsewhere. The proximity of the PIC and the fact that this is attracting workers from the entire region, calling for a local housing solution to be seriously thought, is an opportunity in this case.

2. Consider the entire township for the application of the 'good practice' land use distribution model, which would be representative of a sustainable community in terms of economic activities. With respect to the existing distribution of land uses (see *Table 27*), this would result (as shown in *Table 26*) in adding two more hectares of roads, creating a public space realm of open spaces and wooded areas of 13 hectares in a place that just has 2 ha of this kind of space, doubling the area for institutional and commercial activities, and setting aside 1 or 2 additional hectares of land for other productive activities. As a result, in terms of residential surface the township could only allocate 18 ha.

Table 26 - Bord de Mer de Limonade - Distribution of urban land uses under a 'good practice' scenario.

Routes	6.51	15%
Espace Boise	6.51	15%
Espace Public	6.51	15%
Institutionnel	2.17	5%
Commerciale	2.17	5%
Industriel	1.30	3%
Vide	0.00	0%
Habitation	18.23	42%
TOTAL	43.39	

Table 1 - 16. Caracol - Distribution of urban land uses under a 'good practice' scenario.

3. Develop a housing solution that adapts as maximum as possible to the potential hazards, in this case coastal floods and

Table 28 - Caracol - Urban land uses inside and outside the high risk flood areas, and 'true' available land.

URBAN LAND USE INSIDE FLOOD AREA			URBAN LAND USE OUTSIDE FLOOD AREA			AVAILABILITY FOR DEVELOPMENT (NET VIDE)				
CATEGORY	AREA (Ha)	%	CATEGORY	AREA (Ha)	%	CATEGORY	GOOD PRACTICE	AREA (Ha)	RELOCATED	NET AREA
Routes	1.61	7%	Routes	2.84	13.20%	Routes	15%	1.22	0	1.22
Espace Boise	0.00	0%	Espace Boise	0.44	2.05%	Espace Boise	15%	1.22	0	1.22
Espace Public	0.06	0%	Espace Public	1.20	5.61%	Espace Public	15%	1.22	0.04	1.18
Institutionnel	0.26	1%	Institutionnel	1.14	5.31%	Institutionnel	5%	0.41	0.82	-0.41
Commerciale	0.05	0%	Commerciale	0.10	0.45%	Commerciale	5%	0.41	0.53	-0.12
Industriel	0.00	0%	Industriel	0.00	0.00%	Industriel	3%	0.24	0.29	-0.05
Vide	12.85	59%	Vide	8.11	37.76%	Vide	0%	0.00	0	0.00
Habitation	7.09	32%	Habitation	7.64	35.60%	Habitation	42%	3.41	11.22	-7.81
TOTAL	21.92		TOTAL	21.47		TOTAL		8.11	12.9	
	51%			49%						

hurricanes. These should be implemented in the 18 ha that would be allocated for residential uses. This should be coupled with an intense program for changing the existing housing stock to these kinds of models.

4. Develop multi-family housing projects that maximize the density. Based on the analyses, the density in this case that could reached would be 80 homes per hectare of net area.

5. Design and develop incentives for future households to settle outside the township, on areas that are less exposed to natural phenomena.

7.8.3 Capacity to accommodate residential developments

According to the analyses performed, and as demonstrated in *Table 27*, in Caracol there is a net availability of land for residential uses of approximately 21 hectares. This would yield a total 1,680 homes, which would be 848 houses shy of the number of homes that would be expected to have arrived in the township by 2040. Figure

This means that, should the fast population growth scenario become a reality, the township of Caracol would not be in capacity to receive the population that is projected to arrive. Assuming that the densification program was successful, an additional 11 hectares of land would have to be found somewhere adjacent to Caracol (see *Table 29*). In a township of 43 hectares, this represents 25% of the surface. However, this would be contrary to the policies that are being sought through the implementation of the Three Bays National Park, which include zero land expansion of the urbanized areas.

Table 29 - Caracol - Capacity for residential developments inside the urban setting

Capacity Analysis	
Net land available for residential land uses	21
Multifamily density that could be reached	80
Total homes	1680
Total households by 2040 in the fast growth scenario*	2528
Remaining capacity by 2040	-848
Additional area required to house the 2040 housing demand at multifamily density	10.6

7.8.4 Next steps

As expressed in the previous paragraphs, a re-think of the future of this township should be carried out. An aggressive program to change the construction habits and to implement the density increases discussed would contribute to ease the pressures of this town in the next 25 years. However, in this case this should be coupled with a program aimed at offering alternative settlement in the vicinity of the PIC.

For in the long term, a process of growth reflective of the current construction habits and trends would expose this township and its population to even more severe situations of risk, and continue to expand the township into areas that are now protected by Law, threating the sustainability of the Three Bays National Park.

7.9 Capacity in Jacquezy

As illustrated in *Figure 53* and supporting *Table 30*, the township of Jacquezy comprises an urban area of 18 hectares of land. In terms of surface, it is divided in order of size by empty residential areas comprising 45% of the total, followed by empty lands with 34%, roads with 6%, public open space with 3% and institutional areas with 2%. There is only minimal commercial activity near the town center.

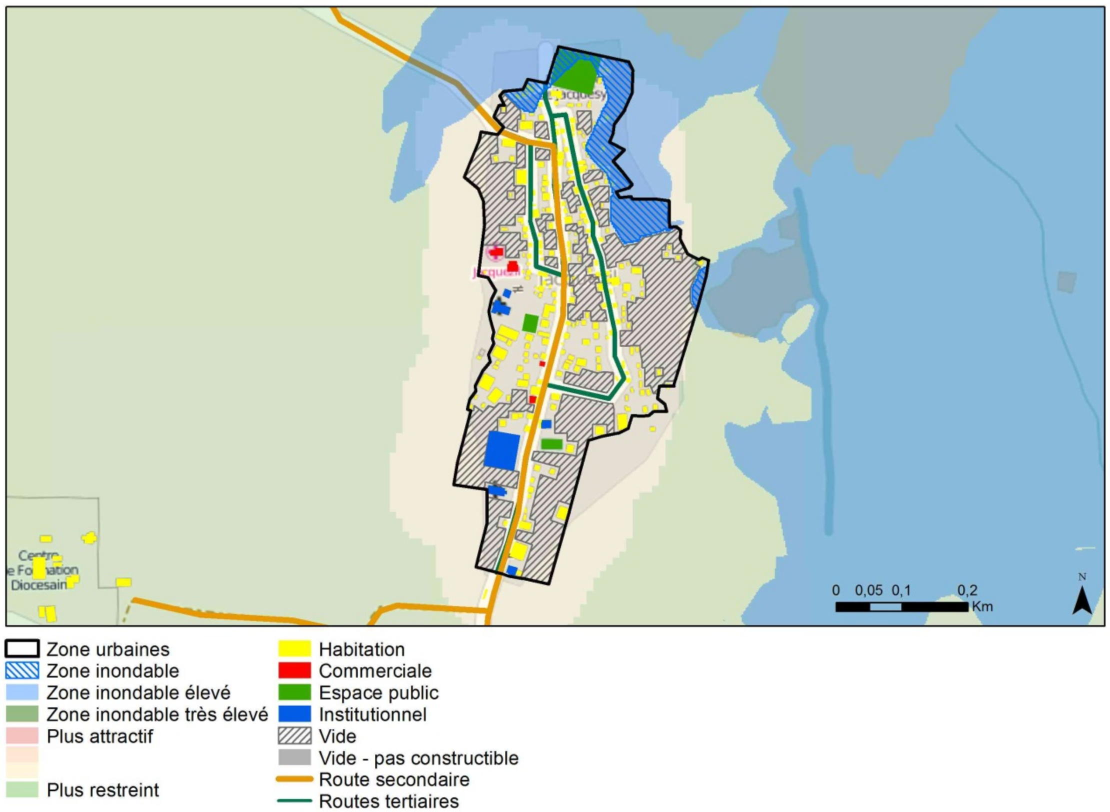

Figure 53 - Main land uses identified in the township of Jacquezy

Table 30 - Total area and current land use distribution in the township of Jacquezy

CATEGORY	AREA (Ha)	%
Routes	4.44	10%
Espace Boise	0.44	1%
Espace Public	1.27	3%
Institutionnel	1.40	3%
Commerciale	0.14	0%
Industriel	0.00	0%
Vide	20.96	48%
Habitation	14.73	34%
TOTAL	43.39 100%	

7.9.1 Area and land uses under high risk conditions

As a coastal town, Jacquezy is less at risk from flooding, with only 8% of the area of the township affected (see *Table 31*). Characteristics like the type of dwelling developed, the street and public open spaces scarcity are the same as Caracol and Bord de Mer de Limonade. With the creation of the Three Bays National Park, the ideal situation would be that this township did not expand, accommodating growth within its boundaries. The recommended responses would be the same as those proposed for Bord de Mer de Limonade and Caracol including avoiding expansion of the

1. Barr any expansion of the township and implement policies and incentives for new settlers to seek location elsewhere. The proximity of eastern exit of the Caracol Industrial Park and the fact that this is attracting workers from the entire region is also opportunity in this case. Furthermore, the Eastern entrance to the park could be planned more as the 'front' entrance with the Western one being the 'service' entrance. Together with the impressive landscape views at this side of the PIC, this could create an attraction for higher end residential solutions that will be required at some point.

Table 31 - Jacquezy - Urban land uses inside and outside the high risk flood areas, and 'true' available land.

URBAN LAND USE INSIDE FLOOD AREA			URBAN LAND USE OUTSIDE FLOOD AREA			AVAILABILITY FOR DEVELOPMENT (NET VIDE)				
CATEGORY	AREA (Ha)	%	CATEGORY	AREA (Ha)	%	CATEGORY	GOOD PRACTICE	AREA (Ha)	RELOCATED	NET AREA
Routes	1.61	7%	Routes	2.84	13.20%	Routes	15%	1.22	0	1.22
Espace Boise	0.00	0%	Espace Boise	0.44	2.05%	Espace Boise	15%	1.22	0	1.22
Espace Public	0.06	0%	Espace Public	1.20	5.61%	Espace Public	15%	1.22	0.04	1.18
Institutionnel	0.26	1%	Institutionnel	1.14	5.31%	Institutionnel	5%	0.41	0.82	-0.41
Commerciale	0.05	0%	Commerciale	0.10	0.45%	Commerciale	5%	0.41	0.53	-0.12
Industriel	0.00	0%	Industriel	0.00	0.00%	Industriel	3%	0.24	0.29	-0.05
Vide	12.85	59%	Vide	8.11	37.76%	Vide	0%	0.00	0	0.00
Habitation	7.09	32%	Habitation	7.64	35.60%	Habitation	42%	3.41	11.22	-7.81
TOTAL	21.92		TOTAL	21.47		TOTAL		8.11	12.9	
	51%			49%						

2. Consider the entire township for the application of the 'good practice' land use distribution model, which would be representative of a sustainable community in terms of economic activities. With respect to the existing distribution of land uses (see *Table 30*), this would entail, as demonstrated in *Table 32*, doubling the area covered by roads, creating a public space realm of open spaces and wooded areas of 5 hectares in a place that just has half a hectare this kind of space, tripling the area for institutional and commercial activities, and setting aside 1 or 2 additional hectares of land for other productive activities. As a result, in terms of residential surface the township could only allocate 8 ha.

3. As in the other cases, develop a housing solution that adapts as maximum as possible to the potential hazards, in this case coastal floods and hurricanes. These should be implemented in the 8 ha that would be allocated for residential uses as per the application of the model discussed previously.

4. Develop multi-family housing projects that maximize the density, which analysis suggests could reach would be 80 homes per hectare of net area.

5. Design and develop incentives for future households to settle outside the township, on areas that are less exposed to natural phenomena.

7.9.2 Capacity to accommodate residential developments

According to the analyses presented, and as demonstrated in *Table 31*, in Jacquezy there is a net availability of land for residential uses of approximately 8 hectares. This would yield a total 640 homes, which would be 418 houses shy of the number of homes that would be expected to have arrived in the township by 2040.

This means that, should the fast population growth scenario become a reality, the township of Jacquezy would not be in capacity to receive the population that today is expected to arrive under the assumption that the township does not expand. Assuming that the densification program was successful, an additional 5 hectares of land would have to be found somewhere adjacent to Jacquezy. In a township of 18 hectares, this represents 27% of the surface. However, as mentioned above this

Table 32 - Jacquezy - Distribution of urban land uses under a 'good practice' scenario

Routes	2.71	15%
Espace Boise	2.71	15%
Espace Public	2.71	15%
Institutionnel	0.90	5%
Commerciale	0.90	5%
Industriel	0.54	3%
Vide	0.00	0%
Habitation	7.59	42%
TOTAL	18.07	

would be contrary to the policies that are being sought with the implementation of the Three Bays National Park, which include zero land expansion of the urbanized areas.

7.9.3 Next steps

A re-think of the future of this township should be carried out. An aggressive program to change the construction habits and to increment the density could contribute to ease the pressures of this town in the next 25 years. However, in this case this should be coupled with a program aimed at offering alternative settlement in the vicinities of the PIC, which in the case of Jacquezy could take advantage of areas nearby less affected by risks, to develop a high quality settlement including residences for middle and upper middle income workers on the PIC, students attending the University of Limonade, and others.

7.9.4 "Fast' versus 'slow' growth scenarios.

The previous analyses were conducted using the housing demand that the townships would face in the 'fast growth' scenario as defined in the population and socioeconomic section (*Section 5.2*) of this study. As illustrated in *Table 33*, a total of 174 hectares would have to be incorporated into the urban setting and developed with infrastructure to accommodate the demand for housing in the fast growth scenario. This allocation would more than adequately cover the needs of the slow growth scenario (note that this does not include Jacquezy, as disaggregated baseline and projected information for this township is not provided by the IHSI).

Under both scenarios, the existing urban areas are insufficient and the allocated expansion areas would be needed. The existing urbanized setting would not be sufficient to accommodate the expected demand of either scenario, especially if the future of these townships was planned following the model of sustainable distribution of land uses that has been proposed in this study, in which residential development covers only 42% of the available areas outside the risk zones.

Consequently, it is appropriate and urgent to adopt an integrated policy of re-design and planning of the different townships sooner rather than later. The elements defined in this study - size and location of expansion areas, distribution of land uses, should serve as suitable reference points for tracing detailed urban designs for the future situations.

Table 33 - Total areas of expansion that would be required to accomodate the housing demand expected by 2040 in the 'fast' population growth scenario

Township	2040 HH in Fast Growth Scenario*	Expansion Requirement (ha)	2040 HH in Fast Growth Scenario*	Difference in HH	Ha of difference**
Trou-du-Nord	17083	56	11968	5115	29
Limonade	22289	83	15616	6673	38
Terrier Rouge	11149	24	7811	3338	19
BDM de Limonade	1644	0	1152	492	0
Caracol	2528	10.6	1771	757	4
Total	54693	173.6	38318	16375	91

* Source: ERM calculations
** Calculated using a density of 175 dwellings per net hectare of land.

7.10 The Neighborhood of the Caracol Industrial Park

An important consideration for this study, and as raised by both the AIA Study and the CIAT Strategic Plan, is whether or not a 'new city' is required to support future growth of the NDC, as well as whether this should be located in the neighborhood of the PIC or elsewhere. Drivers for such a decision include the presence and growth of the PIC, the University of Limonade, large agro-industrial operations that are beginning or expected to appear, and the aim of reducing as a minimum the urban growth of the coastal townships with the establishment of the Three Bays National Park.

From a purely quantitative point of view, and as presented in the above sections, it would be possible to accommodate inside the area townships and adjacent lands, the growing population at least until 2040. However, in Haiti there are two particular phenomena that must also be considered: one is the 'volatility' or 'ease' with which land uses change. This is largely associated with the absence of a secure, formal, system of property rights and the fact that the State is the owner of large extensions of land that are usually designated for different uses based on the priorities and projects of the government in turn. For example this is how settlements like that of EKAM or those promoted by aid organizations appear suddenly, in locations without any apparent linkages to a planning framework.

The second phenomenon is also the volatility with which population movements happen in the country. This is largely because the poverty conditions in which many live creates in families the need to go where employment is, regardless of this being temporary or permanent. So when a development such as the PIC appears, it is likely that many families will pursue settling in the area.

In consequence, the 'neighborhood' of the PIC and Caracol, the University of Limonade and EKAM, Trou du Nord, and Terrier Rouge, referred to hereinafter as the 'diamond', is an area that should to be considered for implementation of a planned process of human settlement.

Both the AIA and the CIAT call for the creation of such new center. This is proposed in the area of known as Champin, located to the south of the PIC and along the road that connects Caracol to Trou-du-Nord. While the CIAT document does not specifically indicate a location, the AIA does propose that it be built as a complementary and extended development to the community located half way between Champin and Trou-du-Nord.

However, based on the analyses carried out for this study, the following factors should be taken into consideration when defining the location of a potential new town:

i. Existing developments

As illustrated in *Figure 54*, the area exhibits numerous settlements such as the one where the AIA proposes its new town (see lettered boxes on map below):

A. The settlement that appears along RN6 before the municipal limits of Limonade and Trou-du-Nord.
B. The settlement located at the very intersection between RN6 and the roads that enters to Caracol.
C. The settlement along this same road, passed the entrance to the PIC.
D. There more scattered settlements along the road that enters Trou-du-Nord from the

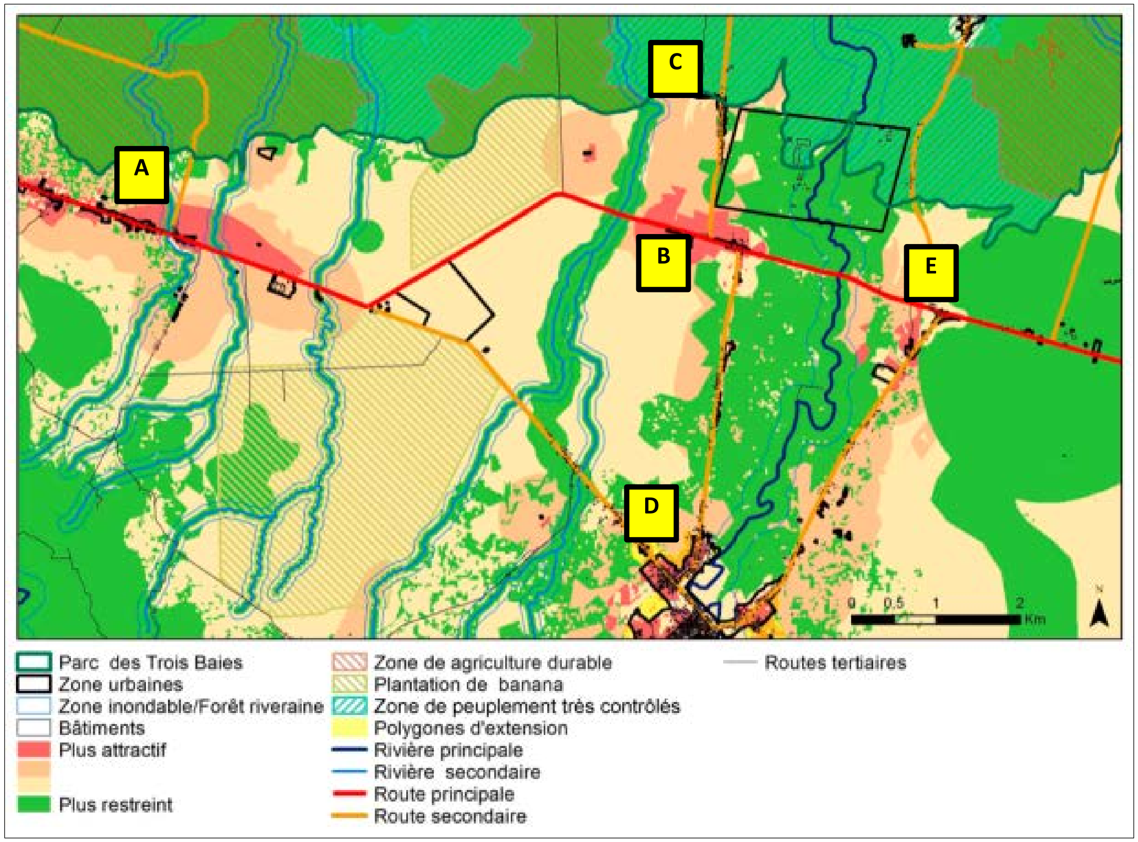

Figure 54 - The 'neighborhood' of the Caracol Industrial Park

Legend: The land use classifications 'Plantation de banana', 'Zone de peuplement très contrôlés' and 'Zone de agriculture durable' were established during conversations senior consultants from the Ministry of Tourism and the IDB. Map source: From geographic information layers by AIA (2012), CIAT (2012), CNGIS (c.2012), IADB (c.2013), NATHAT (2010), USAID-OFDA (c.2012), OSM (2013), OCHA (c.2010), PDNA (2010) and DTM (2013). Georeferencing, digitizing and remote sensing analysis from satellite imagery 1986, 2010 and 2013.

junction at the University of Limonade; and

E. The proto-township that is beginning to appear at the Jesus junction, where the old road between Trou-du-Nord and Terrier Rouge connects back to RN6.

In this context, there are numerous alternatives to consider for future settlements; the convenience of RN6, as well as proximity to the PIC and the University of Limonade, are considered to be the strongest drivers for growth.

ii. New plantations in the neighborhood

Also illustrated in *Figure 54* is a banana plantation of 1,000 that hectares is being set up in two major parcels: the first one is North of the RN6 junction that leads to the Champin area passed the University of Limonade, right in front of the EKAM project; the second one is East of the same junction extending approximately 1.5 km along the access road to Trou-du-Nord. This plantation will likely be demanding labor from area residents, in which case the vicinity to the EKAM area as well as that of the settlement at the Champing crossing would have a major advantage.

iii. The results of the geo-spatial modeling

Finally, in this setting it is recommended that the results of the geo-spatial modeling process for land suitability presented in *Section 6* also be considered, which indicate the area of the University of Limonade, the area of the Champin crossing and the area of Jesus to be the most attractive for development based on the maximization of the attractions and the maximization of the restrictions. The modeling process also yields a highly valuable area that should to be preserved and restricted between the two roads that link Trou-du-Nord with the Champin and Jesus crossings. As a result, the areas that appear highlighted in yellow in *Figure 55*, should be the ones in which more detailed urban planning analyses should be carried out.

To expand further, based upon the following considerations, it is considered that the areas that are depicted in the grey mesh pattern in *Figure 56* would be, together, the most convenient ones to develop integrated human settlements to absorb

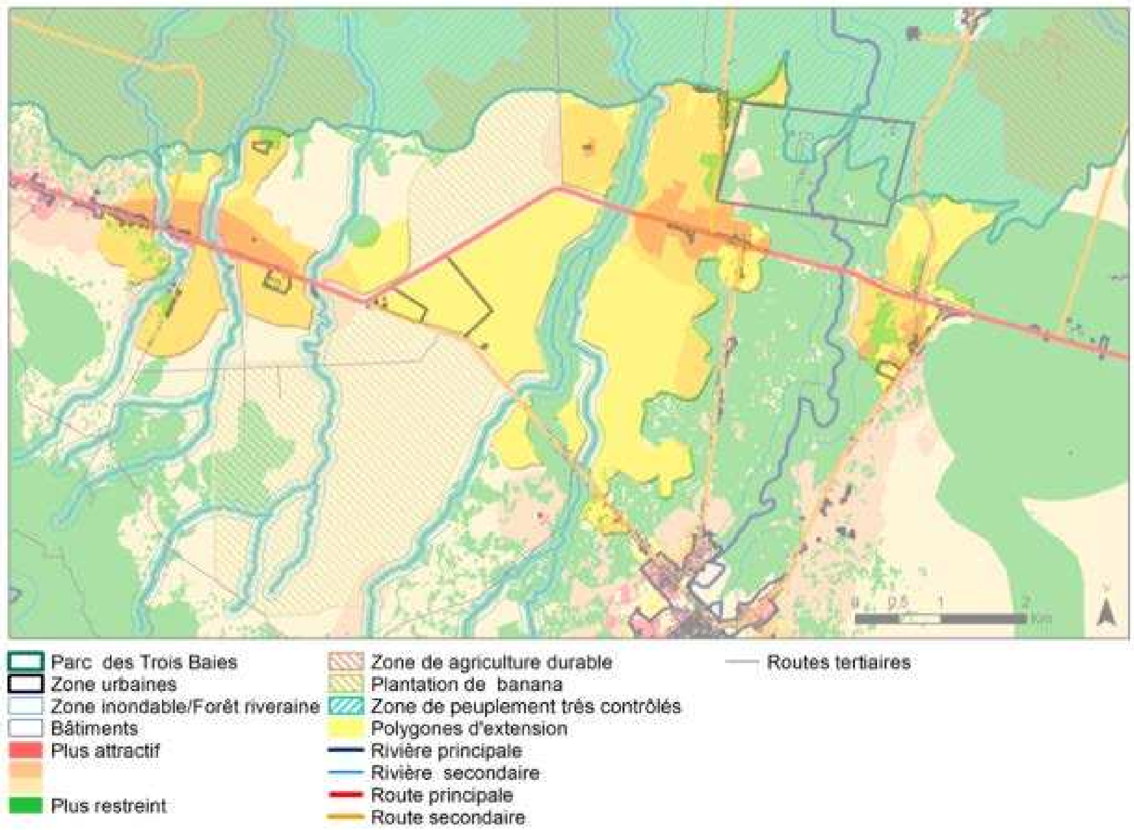

Figure 55 - Areas that should be considered for future development

Map source: From geographic information layers by AIA (2012), CIAT (2012), CNGIS (c.2012), IADB (c.2013), NATHAT (2010), USAID-OFDA (c.2012), OSM (2013), OCHA (c.2010), PDNA (2010) and DTM (2013). Georeferencing, digitizing and remote sensing analysis from satellite imagery 1986, 2010 and 2013.

future population:

- The policy recommended with regards to creating a buffer zone for the Three Bay National Park between its South limit and RN6, with activities of all types that could absorb all the pressures from outside as well as provide the necessary services and opportunities for economic exploitation associated to the Park;
- The clear presence of three highly attractive places human settlement as a result of the modeling, all of them inside or adjacent to the buffer zone;
- The significant demand that the University of Limonade will create in its immediate zone, and
- The very significant demand that the PIC is creating and will continue to create.

In the case of the settlement areas in the neighborhood of the University of Limonade the proposal would configure a linear continuum that not necessarily benefits the flow of goods and services that utilize RN6. It is also clear that under the present circumstances in Haiti it is difficult to determine if, in the near future, new road infrastructure will be developed. Therefore, a better approach is to develop a good plan that maximizes the opportunities of proximity and location while minimizing potential negative effects on traffic. This hypothesis will nevertheless be confirmed with a mobility study that is currently in progress for the same region.

In the area surrounding the PIC, and given the fact that this major facility has two access points at the east and west, it is very likely and recommendable that a functional loop be formed between the internal road of the facility and RN6. This calls, therefore, to the consolidation of both the Champin and the Jesus areas.

As illustrated in *Figure 56*, these three elements, the PIC, the Champin and the Jesus settlements, would serve as the basic articulating elements of a gridded system of roads and pathways that would structure a mixed use, mixed dwelling planned community. To successfully guarantee the consolidation of these nuclei of urban settlement and thus prevent further scattering of development the adaptation of the lands with road, water and sanitation infrastructure should be undertaken. This

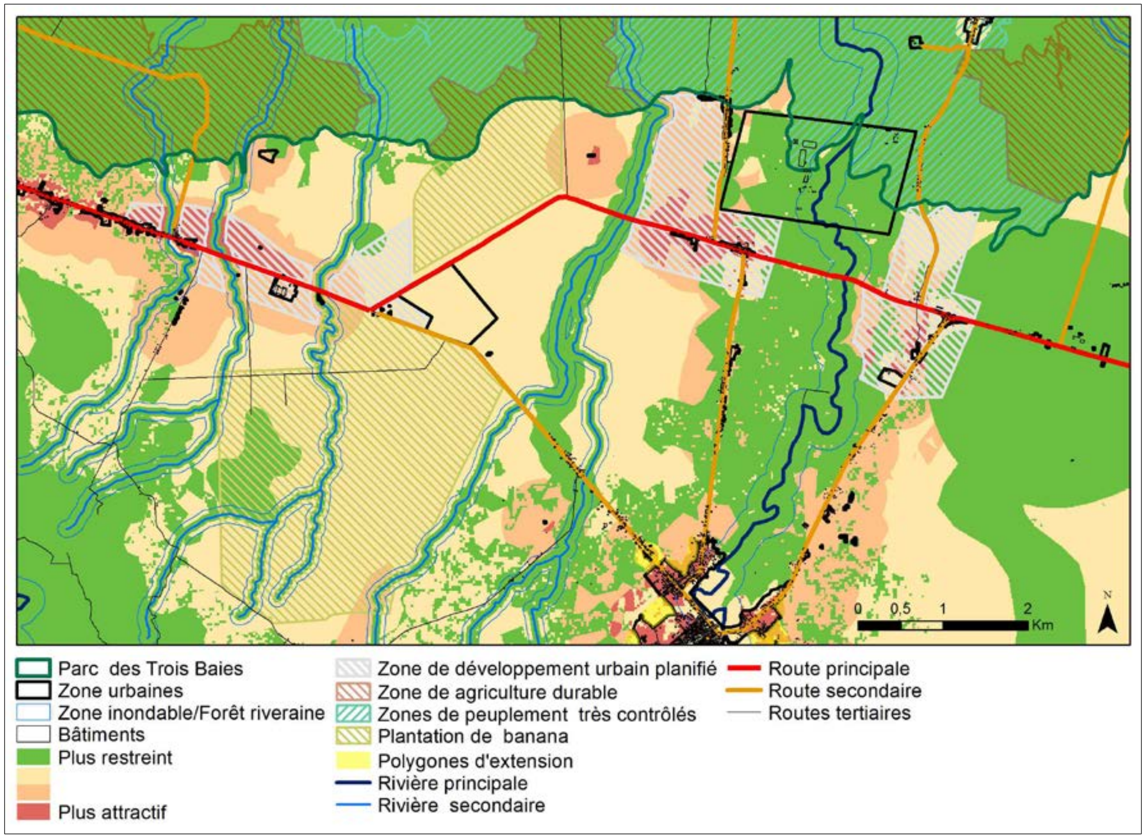

Figure 56 - Preferred locations for consolidating new urban settlements in the PIC area

Map source: From geographic information layers by AIA (2012), CIAT (2012), CNGIS (c.2012), IADB (c.2013), NATHAT (2010), USAID-OFDA (c.2012), OSM (2013), OCHA (c.2010), PDNA (2010) and DTM (2013). Georeferencing, digitizing and remote sensing analysis from satellite imagery 1986, 2010 and 2013 could begin a process in which different organizations could locate their individual efforts and projects in the neighborhood.

For the a proper evolution of the entire setting, a buffer zone surrounding the PIC should be implemented. In addition, a critical role would be played by the areas depicted in yellow between EKAM, Trou-du-Nord and Champin, which considers that, in order to prevent the consolidation of a linear urbanization along RN6 as well as the roads leading to Trou-du-Nord and Terrier Rouge, those areas would have to be rapidly destined to agro-industrial activities of the scale of the banana and sisal plantations that are being set up nearby.

The protection of the green zones that appear between the two roads connecting Trou-du-Nord with the PIC and Jesus would also be essential for the success of this scheme. These interventions would ensure a balanced, sustainable becoming of this region.

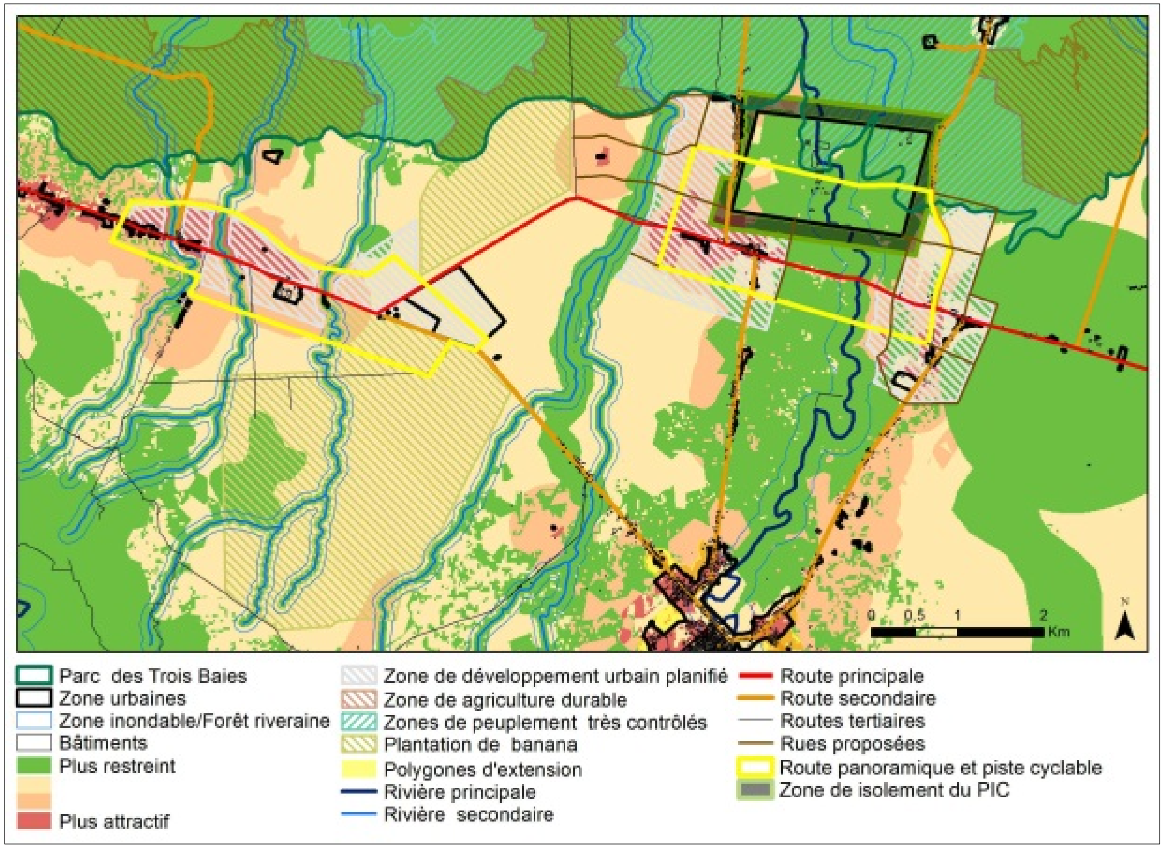

Figure 57 - Creating a planned, integrated community with the PIC as pivot.

Map source: From geographic information layers by AIA (2012), CIAT (2012), CNGIS (c.2012), IADB (c.2013), NATHAT (2010), USAID-OFDA (c.2012), OSM (2013), OCHA (c.2010), PDNA (2010) and DTM (2013). Georeferencing, digitizing and remote sensing analysis from satellite imagery 1986, 2010 and 2013

7.11 The Three Bays Marine Park

In December 2013, the Government of Haiti created the Parc National des Trois Baies or Three Bays Marine Park. This covers an area of approximately 90,000 hectares that includes the bays of Limonade, Caracol and Fort Liberté, as well as the Lagon aux Boeufs to the east of Fort Liberté.

This newly established marine protection area will help protect the mangroves, eel grass beds, reefs and habitats housing important fisheries that are crucial for providing livelihoods to nearby communities. It will also help protect the area from storm surges and provide local communities with ecosystem services such as carbon sequestration, tourism value and more. The area is also home to numerous threatened species, including sea turtles, whales, manatees and migratory birds.

To recognize and protect the Three Bays Marine Park, a series of 'preemptive zoning' classes has been developed in conjunction with the IDB's specialists who are supporting the Three Bays Marine Park development. *Figure 58* illustrates the proposed zoning as follows:

1. ***Coral reefs***. This a marine ecosystem of high economic value derived from the services it provides including i) fish, crustaceans and other marine species that sustain large portions of the local population and ex-ports; ii) shoreline protection, providing a barrier to storm surge and impacts of hurricanes on the shore. Coral reef health is closely linked to that of the sea grass and mangrove ecosystems, and iii) very important carbon sink, sequestering atmospheric carbon. Currently threatened by overfishing and sediment load from eroded watersheds.

2. ***See grasses***. Critical habitat for juvenile stage of fish species, turtles, manatees and other species. They play and important role in sequestering carbon. (not visible in map)

3. ***High flood zones***. This category covers the sea grasses zone, the man-grove areas, and extends beyond the latter into the mainland. The man-groves have been declared for complete protection, providing critical ecosystem services such as i) nurseries for commercially important fish species as well as crustaceans, mollusks and bird nesting habitat; ii) shoreline protection from storm surge, sea level rise and hurricanes. Currently threatened by charcoal production, firewood collection, salt production techniques and overfishing. Communities such as Jaquezy, Caracol, and Madrasse have been established in this area and are seriously threatened by increasing risk of flooding and storm damage. The risk is greatly exacerbated by illegal destruction of mangroves.

4. ***Zones where the population process needs to be highly controlled***. This corresponds to the areas identified as currently exhibiting any of the kinds of settlements discussed in the next Chapter. They correspond, largely, to the Bord de Mer de Limonade, La Chappelle, Borony, Monto-lon and La Genevré areas in the municipality of Limonade; in the municipality of Caracol, they include the Southwest areas of En Bas Saline, Car-acol, Jackezy and the Caracol Industrial Park. Additional areas not visible in the map in Paulette and Phaeton.

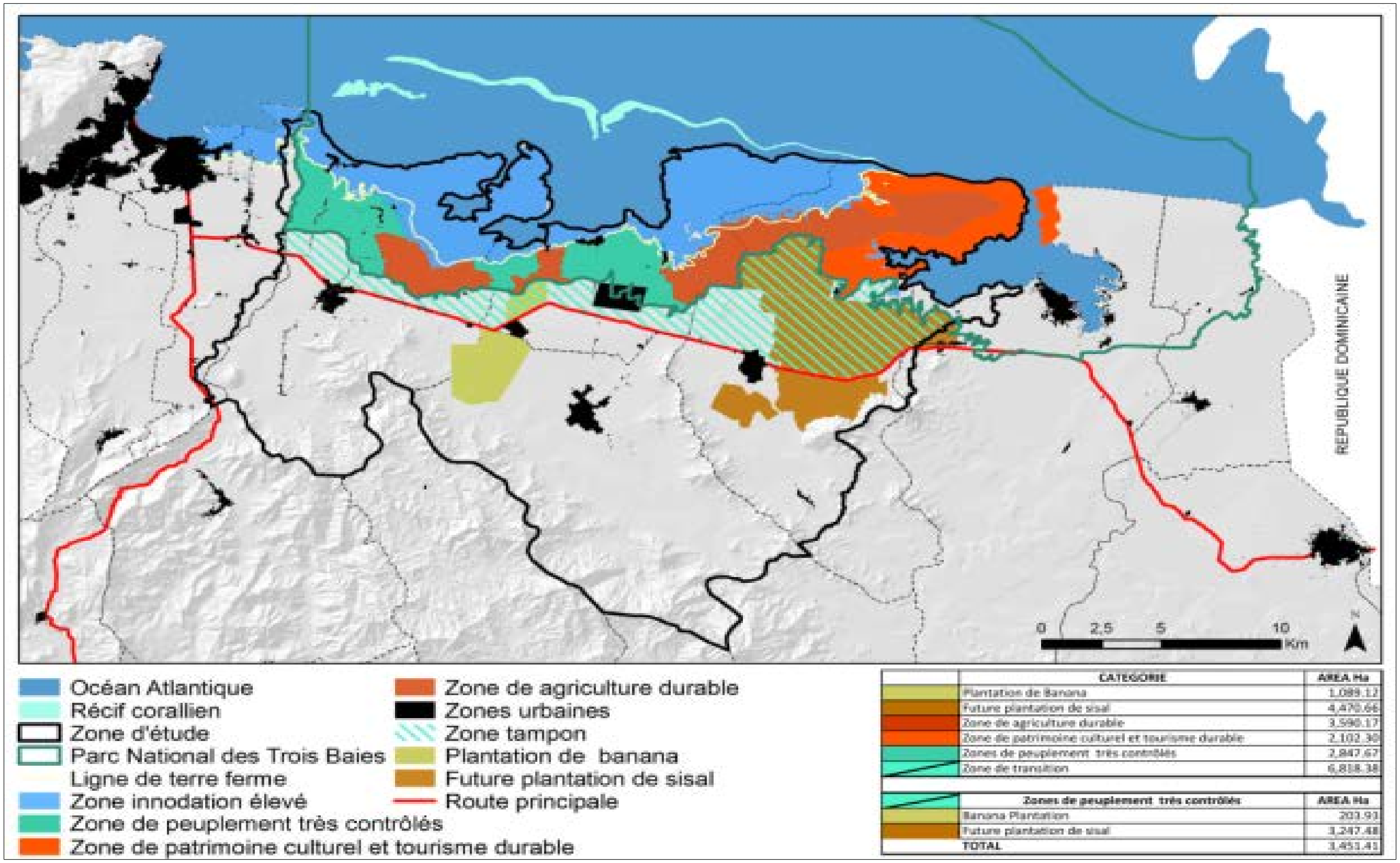

Figure 58 - Preemptive zoning classes proposed for the Three Bays Marine Park

Sources: Map source: From geographic information layers by AIA (2012), CIAT (2012), CNGIS (c.2012), IADB (c.2013), NATHAT (2010), USAID-OFDA (c.2012), OSM (2013), OCHA (c.2010), PDNA (2010) and DTM (2013). Georeferencing, digitizing and remote sensing analysis from satellite imagery 1986, 2010 and 2013.

5. ***Zones for the protection of cultural heritage and the promotion of sustainable tourism***. These correspond, largely, to the entire West coast of the Bay of Fort Liberté and the North shores of the area of study between the straight of the former bay and the point where the coral reefs begin. Inland, these areas extend between 500 m and 1 km inland, which is where a large number pre-Columbian and colonial era fortifications and other heritage elements are still visible. Additional areas of smaller size not visible in this map but accounted for in the modeling process would also be part of this class. Appropriate uses include restoration and man-aged visitation, guided walks etc. of cultural sites and small scale sustainable tourism infrastructure.

6. ***Zones of sustainable agriculture***. A large extension of the terrestrial area of the park consists of land that is appropriate for ecotourism, culture-focused tourism and other forms of sustainable tourism as well as sustainable agricultural practices which are compatible with the conservation of natural resources i.e. that conserve soil, water, biodiversity and ecological cycles and prevent run off into the bays. Plantations such as a banana or sisal or any other kind could take place in the former areas of the Dauphin plantation.

7. ***Urban areas***. Inside the park there would have to be a highly controlled mechanism of urban growth. The settlements located on areas affected by flooding ought to be re-located. The remaining areas ought to be re-developed with an adaptive architecture, such as pilotis. No expansion ought to be allowed, which would therefore require efforts to re-locate population outside the boundaries of the park. The urban areas outside the protected area, but nevertheless exerting direct and indirect impacts on it, require particularly strong planning and control structures in regard to solid waste management, water use and effluents. Finally,

8. ***A buffer zone*** to absorb and provide the necessary economic processes and settlements that would support and be supported by the park. A band of land and water immediately external to, but contiguous with, the park, where development is strictly managed to be low intensity and compatible with the conservation objectives of PN3B. Plantations of sisal, banana and others in this zone would have to certify production to be free from use of chemical inputs which negatively affect biodiversity in the Park such as pesticides and fertilizers. The park's regulations refer to a 5 km south of the boundary. This could be attained to the east of the park, but to the West, that is in the NDC area, this should be extended to the limits of RN6.

7.12 Risk Reduction Recommendations

7.12.1 Risk Ranking

Section hazard and risk assessment studies*4* presents the hazard and risk assessment for the prioritized natural hazards, and *Table 7* summarizes the hazard losses for each hazard. This section builds upon these results and compares and prioritizes the hazards and presents a series of general risk reduction recommendations. In addition, five mitigation strategies have been explored in more detail through a cost-benefit analysis.

To facilitate a prioritization of hazards, a simple methodology has been developed based on a comparison of the maximum probable losses for each hazard. A matrix is presented in that identifies the relative area of concern based on probability (expressed by the return period) and estimated impact (expected losses).

Hazards that tend to occupy the top left-hand quadrant of the chart, Quadrant A, have a high probability (occur with the most frequency) and have a potential high impact (high damage). Therefore, these are likely to be of greatest concern to stakeholders, and consequently should be a focus for risk reduction planning efforts. Areas of secondary concern are those hazards identified in Quadrants B and C.

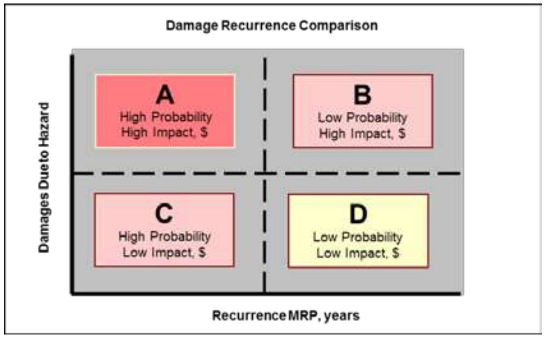

Figure 59 - Framework for Relative Risk Evaluation

Hazards in Quadrant B have a low probability of occurrence but have a potentially high impact, while hazards in Quadrant C have a high probability of occurrence but low impact. Hazards categorized in Quadrant D are likely to be of lowest relative concern because they are predicted to have both a low probability and a low impact; however, this framework does not necessarily negate the importance of addressing hazards that fall into Quadrant D (low probability, low impact).

Ranking hazards that fall into Quadrants A, B, and C depends on the level of risk tolerance or importance a specific hazard might have to the community.

Figure 60 provides a plot of the losses (general occupancy and infrastructure losses) vs. return period for each hazard and is an effective way to evaluate the relative risks.

Figure 60 maps hazards for which both recurrence and damage/loss estimates were calculated in this risk assessment: earthquake, hurricane, flooding, and coastal flooding. It provides a systematic framework from which to compare and prioritize hazards. It is important to keep in mind that the comparison does not represent an absolute ranking of hazards, but has been developed to assist in evaluation of the results so as to help decision makers prioritize mitigation measures.

The comparison is also presented in tabular form in and is based on an expected loss per year for each hazard, simply calculated as the total expected losses divided by the Mean Return Period, representing the amount of capital the local governments would have to set aside to cover the damages for such an event. shows a comparison of losses for different hazards based on the aggregate losses for a specific return period and the losses per year. For example, earthquake and hurricane hazards show highest losses. The coastal flood and inland floods have comparatively lower losses. When compared in terms of loss per 1000 USD/per year, coastal flooding and hurricane hazard are the top two hazards and followed by earthquake and inland floods.

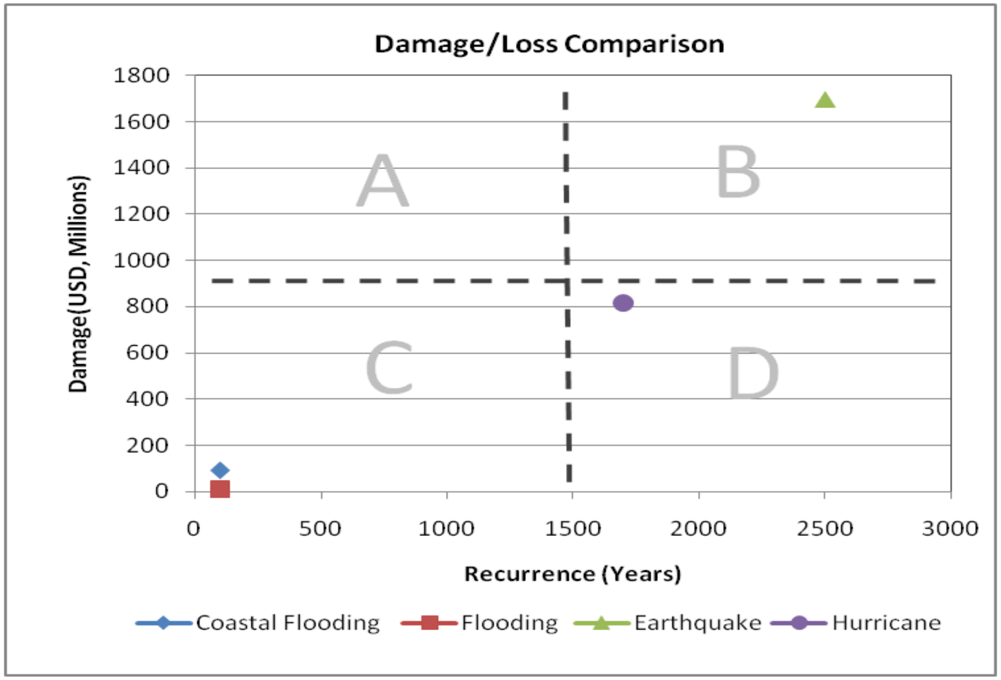

Figure 60 - Standardizing loss damage recurrence comparison for the study area

Table 34 - Comparison of Hazards for the study area

Hazard	MRP (Years)	Total Loss (10 ^ 6 US$)	Loss (US$)/ year
Flooding	100	10.78	2.53
Earthquake	2500	1694.47	2.58
Hurricane	1700	815.81	4.37
Coastal Flooding	100	93.47	5.50

7.12.2 General Risk Reduction Interventions

In Haiti, the most urgent risk reduction measure is to increase economic opportunity and alleviate poverty and improve living conditions to reduce risk to natural disasters. While increased wealth is not a save all for reducing the impact of natural hazards, it is often the poor that are less able to afford to relocate or resettle in areas that are less prone to natural hazards. The poor are also less prone to rebuild or reinvest after a disaster. This section lays out some general sustainability interventions to increase disaster resilience and reduce losses.

Earthquake Hazard

The section below highlights some high level interventions and mitigation measures, as well as recommendations, to improve the characterization of the earthquake hazard, should be considered.

The fact that most of the study area is comprised of deep, unconsolidated alluvial sediments, where the ground shaking hazard is high, the most important mitigation recommendation for reducing seismic risk is to develop a more detailed understanding of the hazard itself. Development a detailed seismic risk or zonation map for the entire study area, which details maximum accelerations and allow for the identification of high risk districts, will be critical for identifying specific risk areas and to prioritize risk reduction activities.

Another recommendation is to ensure that new construction is designed and built in accordance to international building standards and codes (residential, commercial, institutional and industrial). All construction should ensure that there is proper reinforcement in walls and that building connections including roof connections to the walls, wall connections to each other and the connection of walls to a strong foundation are present in all new construction.

For large construction projects and infrastructure developments, site specific seismic assessments should be undertaken to identify geologic constraints for the construction of critical facilities and major infrastructure.

Hurricane

Hurricanes tend not to be tied to a specific location, especially in such a small geographic study area as the study area. Nevertheless, there are areas where development should be restricted to a greater or lesser degree. Restricted areas should include locations in coastal areas and very steep hillsides. Again, building design standards and construction practices take precedence, however, there are a few specific and design considerations for hurricanes which include:

- Orientation of the building relative to site topography;
- Ensure that there are stabilizing measures incorporated into the design and construction of building, especially the connections between building parts;
- Debris removal in vacant lands to reduce flying projectiles, securing urban furniture, and the burying of utility lines, etc. are simple measures that can work to reduce damages during wind storms; and
- Reducing the amount of clear cutting as vegetation stabilizes soil and trees provide friction and stabilization from winds.

The general poor construction characterizing much of the study area is again tied to Haiti's poor economy and limited building code enforcement. Building codes have little relevance if they are not applicable to local construction practices, do not support known engineering solutions, and have not been tested.

Inland Flooding

The foremost consideration for flood hazard should be given to building a careful record of precipitation information within and surrounding the study region. The lack of reliable precipitation data has stymied the ability to understand in detail the local hydrologic regimes.

Several sustainability options for reducing or mitigating risk associated with in-land flooding hazards include:

- Development in the high hazard flood area should be restricted especially within identified floodway. High risk lands should not be considered for future development. If development occurs within high hazard flood areas, there should be detailed planning and development criteria that ensures that the property is built above base flood elevation.
- In high hazard areas where there is existing development (formal and informal settlements), bank stabilization should be pursued to help reduce flooding and erosion so as to help contain river flooding to watercourses. The re-vegetation of river banks is an important consideration for binding silt and soil to reduce water erosion due to flooding.
- In areas where there is urban flooding due to overland flows, drainage infrastructure should be improved to facilitate the flow of water away from settlements and back to water courses. In rural areas, special attention should be given to dredging irrigation channels and in some case surfacing with concrete bases so as to increase the flow of water to farmland and out of farmland.
- By far the most important measure for riverine flooding during intense rainfall events is awareness and education. The development of public awareness and public education campaigns should be targeted for high risk groups to increase hazard knowledge, improve risk perception and foster risk avoidance behavior such as evacuation.

Coastal Flooding

There are several sustainability options for reducing or mitigating risk associated with coastal flooding hazards. The ability to relocate settlements or adapt existing infrastructure for protection is limited by resources, but the physical expansion and the growth of settlements is not. Therefore, in coastal high hazard areas, the expansion of settlements should be discouraged and the construction of private and public infrastructure, including roads, energy sub-stations, drains and housing settlements should be limited. The location and nature of planned infrastructure should draw on forecasted inundation maps developed under this study.

The protection and expansion of coastal wetlands and estuaries is also an important measure that should be considered. Wetlands that are linked to the coast and estuaries serve as a natural buffer against storm surges, sea-level rise and wave action in particular. Natural features help to absorb large volumes of advancing water, and as a result, have a dissipating effect on wave energy. Further reduction to the size of wetlands and estuaries, is to discount their importance that these natural resources play in reducing the impact of coastal hazards.

The lack of an effective storm water system for discharging high volumes of water has hindered development meaningful responses to flooding and coastal flooding hazards. Drainage infrastructure needs to be improved to relieve coastal inundation caused by coastal storms or heavy rainfall events.

The coastal flooding hazard should be incorporated into disaster management prevention programs. There is a need to take into consideration coordinate responses for the evacuation of high risk populations, which will mean focusing resources toward prevention as opposed to response and recovery.

Other adaptive responses may include preventing hazard impacts by building strengthening protective structures.

Drought

The hydrological assessment has indicated that demand for water will increase and the water potential will diminish due to increased population and development pressures. Therefore, it will be paramount that policy makers consider actions that will help reduce the impact of water deficits in the study area, especially during dry periods.

In view future demands, a watershed management approach to mitigating the effects of drought should be pursued. Integrated watershed management should be incorporated into more diversified development planning for the region so as to address problems related to land degradation and unsustainable land use practices (i.e. deforestation).

The focus of a watershed management planning approach should be to increase ground infiltration so as to increase the water stock and reduce the impact of flooding. Many studies have shown that when local water catchment areas are protected, the vulnerability of local agriculture is reduced. Such approaches will help restore functions natural drainage areas and increase the supply of water and have an additional impact in reducing flooding impacts in low lying areas. Reforestation is a critical component in any watershed conservation program in Haiti. The planting of forest lands, even for tree crops (coffee) agroforestry (teak) purposes, will help developing sustainable water resources in the study area. The reforestation of upland areas should be pursued, along with a series of filtration ditches and natural walls to help in reducing the loss of land by erosion and will help in develop more stable hydrological cycle. For such approaches, financial or in-kind incentives to involve communities should be explored.

The construction of reservoirs and the revitalization of irrigation systems may also be another option for stabilizing the water supply in communities. While the construction of reservoirs for each community does not help restore natural resource area, they can be effective mechanisms for the storage of rainwater which can be used during dry seasons (June to October). Such investments will improve access to water for agriculture and rural households. If reservoirs are designed correctly, they can be linked to new or integrated into existing irrigation distribution systems. Attention should be given to the revitalization of a series of historic canals that are found throughout the study area.

Finally, more education and outreach is required to increase the efficiency of water utilization in the area. In this regard, effective institutional support (including assistance from international donors) will be paramount. Projects, particularly technical assistance focusing on increasing efficiency water utilization, must take into consideration local land use practices and farming methods so as to identify local adaptation measures that have a chance of being implemented. International donors can play a role in funding the required research needed to develop such local level approaches, as well as fund government institutions to disseminate information on innovative locally-based interventions that address drought and climate change.

7.12.3 Risk Reduction Case Studies

Specific recommendations and projects that are assessed in this section, were identified based upon field observations, stakeholder discussions and also from ensuring tangible and practical projects could be implemented. Given the intensity and frequency of flooding (both inland and coastal), these hazards have been given priority for risk reduction assessment.

A Cost Benefit Analysis (CBA) model has been used to assess the likely costs and benefits of identified mitigation measures, focusing on the following mitigation strategies in high risk areas:

- Upgrade Urban Drainage Infrastructure;
- Rural Drainage Infrastructure Implementation;
- Revitalize Historical Canal System To Alleviate Flooding;
- Upland Reforestation; and
- Mangrove Protection In the Three Bays Marine Park.

Appendix 10 contains the details of the five strategies explored and the methodology applied, and the results are summarized below in *Table 35*.

7.12.4 Land Use Planning to Manage Future Risks

The section above has elaborated on specific approaches to reducing risk by introducing and analyzing specific management options (structural and nonstructural). This section looks at the potential impacts of the introduction of land use planning as a method to reduce risks in the future.

A comparative assessment of future risks has been undertaken considering two situations so as to illustrate how decisions regarding the utilization of land may impact future losses in the study area. The two situations are as follows:

- A: takes into consideration the targeted development projects and utilizes a linear extrapolation of population growth and land use to project spatial development and growth on its current trajectory and assumes that there are not any interventions that are put in place to limit urban expansion and/or the further deterioration of the natural resource base within and around the study area; and
- B: all targeted development projects for the study areas are accelerated, but where growth is controlled by taking into consideration sustainability opportunities and constraints as projected this report.

By comparing future risk for a growth projection without the consideration of land use planning recommendations (A) to a fast growth development scenario that takes into consideration land use planning recommendations (B), the impact of introducing sustainable land use planning as a risk reduction measure is clearly demonstrated. For this comparison, a risk projection model was used, which combines three different components to understand the potential future losses for each hazard for a projected time period to 2040:

- Hazard - The hazard intensity/frequency relationship is assumed to increase due to climate change. To provide a consistent basis from which to compare hazards a 100-year return period is used.
- Vulnerability—The general characteristics of the built environment are expected to change over time due to the introduction of better building practices and improvements in construction materials. A vulnerability multiplier was used to update/modify the building performance from the present to 2040. The vulnerability parameter used for situation A is based on an assumption that the development pressures will continue on the current trajectory and that urbanized areas will increase by 7.45% and that little improvements will be made to existing infrastructure, while the situation B, assumes the same rate of population increase, but urban expansion will be limited and only increase by 2.6% due to increased density requirements for future development. B also considers that future development in hazard prone areas will be limited and/or reduced. Both include assumptions that construction practices, in terms of workmanship and materials, will improve incrementally over time.
- Exposure—population growth estimates is used to predict future exposure (value of buildings and infrastructure) across the study region and used a linear regression analysis to estimate the increased value of assets (i.e. buildings infrastructure, etc.). Therefore, the model assumes that exposure values will increase proportional to population growth and will be uniform across different land use categories in the study region as defined in for different development scenarios.

Table 35 provides a benchmark for decision makers to understand the implications of implementing the urban land use planning recommendations, which incorporates mitigation measures and introduces a

Table 35 - Potential Losses, 10^6USD

Hazard	2012	Situation A		Situation B	
	Agg. Potential Future Loss	Agg. Potential Future Loss	Loss as a % of Aggregate Exposure Value	Agg. Potential Future Loss	Loss as a % of Aggregate Exposure Value
Seismic Hazard	1694.47	2947.67	51.69%	1784.13	31.29%
Flooding Hazard	10.97	14.86	0.26%	8.95	0.16%
Hurricane Hazard	815.81	1023.62	17.95%	615.89	10.80%
Coastal Flooding	93.47	133.94	2.35%	80.79	1.42%

sensible utilization of land as a way of reducing the negative consequences of reducing risks.

The total aggregated loss estimates for 2013 amounted to 2.61B USD (i.e. a summation of the aggregate losses for each hazard). Under situation A, aggregate losses for each hazard are expected to increase substantially. However, if the urban land use planning and sustainability recommendations from this study are incorporated, which have utilized hazard and risk maps generated as part of this study to minimize future growth in more vulnerable areas, the projected potential aggregate losses for most hazards is greatly reduced from the loss estimates for 2013 and represent approximately 44% of the projected total exposure values in 2040 (2.48B USD).

Therefore, a substantial amount of potential future losses can be avoided if the land use recommendations are implemented.

7.12.5 Risk Reduction Summary

The information outlined in this section should be used to inform citizens and decision makers about hazards and the risks. This section in particular provides a basis for understanding the hazard impacts and prioritizing actions by laying out general sustainability interventions that should be considered for building more sustainably in the study area.

These analyses are preliminary and they indicate options to be taken forward for more detailed analysis. The mangrove protection in the Three Bays Marine Park, urban drainage infrastructure upgrade, and upland reforestation are three most promising interventions. The mangrove protection and upland reforestation, being non-structural measures, will also start providing benefits to the wider environment in terms of supporting environmental protection, aquifer recharge and biodiversity enhancement, in addition to the flood management and hazard protections. The urban and rural drainage upgrade will be beneficial immediately after implementation. It is necessary to note that while the canal revitalization appears to be low yielding investment due to the lesser beneficiary areas (sparse settlements and low exposure at risk), it does not preclude conducting such analysis in areas with denser populations, which may yield different results. Considering the satisfactory benefit cost ratio of top four scenarios, these options should be taken forward for possible planning and pre-feasibility studies.

Finally the analysis provides a basis for examining how risks may increase significantly if growth continues in an unplanned fashion, and how through the smart growth scenarios, where the hazard maps are considered and factored into future growth models, the future losses can be significantly reduced and citizens can meet the following goals:

- Provide information to planners and reviewers who make land use decisions to channel development to low hazard areas and/or flag development proposed in high hazard areas.
- Recommend sustainable locations for major developments projects and/or infrastructure projects, including public facilities, and residential, commercial, and industrial development.
- Support the conservation of natural resources, and the designation of critical areas, agricultural land, or historical resources.

To avoid losses occasioned by these hazards, there is a need for the new approaches and strategies to be put in place. The International Strategy for Disaster Reduction (ISDR -http://www.unisdr.org) recognizes this and emphasizes the importance of understanding local risk patterns, developing strategies to decentralize responsibilities at the relevant sub-national or local levels, and supports and integration of risk reduction, as appropriate, into development and planning policies.

Table 36 – Summary of risk mitigation measures

Upgrade Key Urban Drainage Infrastructure	**Rural Drainage Infrastructure Implementation**	**Revitalize Historical Canal System to Alleviate Flooding**	**Upland Reforestation of the Trou Du Nord Watershed**	**Mangrove Reforestation in the Parc National Trois Baies**
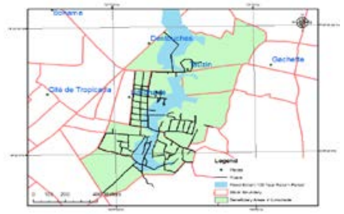		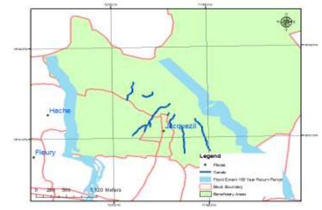	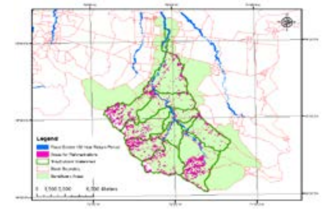	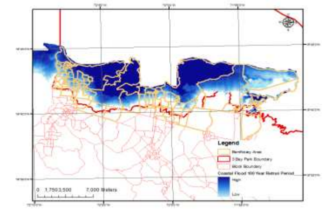
• Limonade used as a case study • Upgrade drainage to cope with flooding during heavy rain (increase capacity) • Increase in open drainage (assumed 18km)	• Example of land drain west of Caracol • Address overland flows in rural areas • Install new drainage to cope with overland flooding during heavy rain	• The revitalization of the canals in northern Haiti • Comprise dredging to remove silt and increasing the cross-sectional area of the canals • A length of 3.8 km is evaluated (near Jacquezil)	• Sustainable mitigation measure to increase the interception of water in the upper reaches of watershed • Will also work to prevent soil erosion and contribute to forest conservation • Benefits will be tied to a longer time horizon	• Serve as a natural buffer against storm surges, sea-level rise and wave action. • Proposed that a 5km strip of mangrove be reforested along coast line. • This would mean about 300 sq.km of area would be planted.
Over 20 years: • Costs: $3m • Benefits: $7.7m • CBA: 2.5, which represents a good investment	Over 20 years: • Costs: $0.9m • Benefits: $1.1m • CBA: 0.7, which represents an okay investment	Over 20 years: • Costs: $0.2m • Benefits: $0.1m • CBA: 0.7, which represents an okay investment	Over 20 years: • Costs: $1.2m • Benefits: $2.8m • CBA: 2.3, which represents a good investment	Over 20 years: • Costs: $6.7m • Benefits: $60.4m • CBA: 9, which represents an excellent investment

8. CONCLUSIONS AND RECOMMENDATIONS: A SMART GROWTH SCENARIO

8.1 Study Focus

This study seeks to address the complex question of where and how should development occur in the NDC of Haiti, with special emphasis on how human settlement should occur in light of the different dynamics and forces that will shape population growth and migration in the area. This ESCI study has sought to address the question through different angles that included the following:

- Understanding the context from physical, socio-spatial and socio-economic points of view.
- Analyzing recent planning efforts that have been key in tracing orientations with regards to the area; contrasting, comparing and building on their conclusions.
- Conducting additional supplementary population analyses and projections with regards to the residential land demand. This was undertaken for a slow and a fast growth scenario projected to 2040, based on the patterns that would be seen in the region following the implementation development projects that are being planned.
- Determining, through geo-spatial suitability modelling applied with a 'balanced approach' of restrictions and attractions, what lands would be more suitable for urbanization, where should the existing patterns of agriculture be preserved, which areas should be preserved for their bio-diversity and/or vegetation quality index, and other land use decisions of similar nature.
- Understanding and defining the 'pre-emptive' zoning classes that should be considered in the Three Bays National Park.
- Seeking to define the 'geography' of what could be called 'human settlement for a sustainable future' of the region. This has been assessed by understanding existing patterns, building efforts, levels of urban density that could realistically be pursued in the different townships of the region, and most importantly, testing these parameters in each one of the townships to determine how would they perform in terms of their capacity to accommodate the projected land demands. In the cases in which areas of expansion would be required for the townships, the exercise included tracing them in accordance with the results of the modeling.
- Attempting to define the areas in which new, planned settlements should be pursued, as a result of the significant impact that the PIC is having in the region, the increased economic activities associated to the University of Limonade, the large plantations that are appearing in the area and the need to provide alternatives for the coastal townships.

8.2 Smart Development Scenario

The results of putting these pieces together are presented in *Figure 61* which outlines recommendations for the Northern Development Corridor Smart Development Scenario.

In terms of human settlement, as illustrated therein, the scenario is that in which the urban footprints of the main townships that comprise the region outside the Three Bays National Park are expanded between 5 and 100 hectares each, in all cases on surrounding areas identified as the most suitable for urbanization. In this scenario, the urban footprints of Bord de Mer de Limonade, Caracol, and Jacquezy, are kept with their current dimensions in response to the Three Bays National Park intention to limit and if possible reduce the urban footprint inside its territory. In all three cases, a program of re-densification based on an architecture of pilotis (which is also applied to the non or low risk flooding areas in Caracol and Bord de Mer de Limonade) is also proposed in order to establish a culture of edification that is more resilient.

In this scenario, in which it is assumed that the Government of Haiti will be able to control the expansion of Caracol and Bord de Mer de Limonade, and has acquired resources to carry out a gradual, integrated socio-economically equitable and creative process of resettlement, two new areas have emerged as contemporary towns. One of them is in the Champin and Jesus areas, and the other in the University of Limonade – EKAM area. These contemporary towns are well designed, with a variety of mid to high density dwelling solutions, connected between themselves and with the townships in the area through a system of bicycle and landscaped paths.

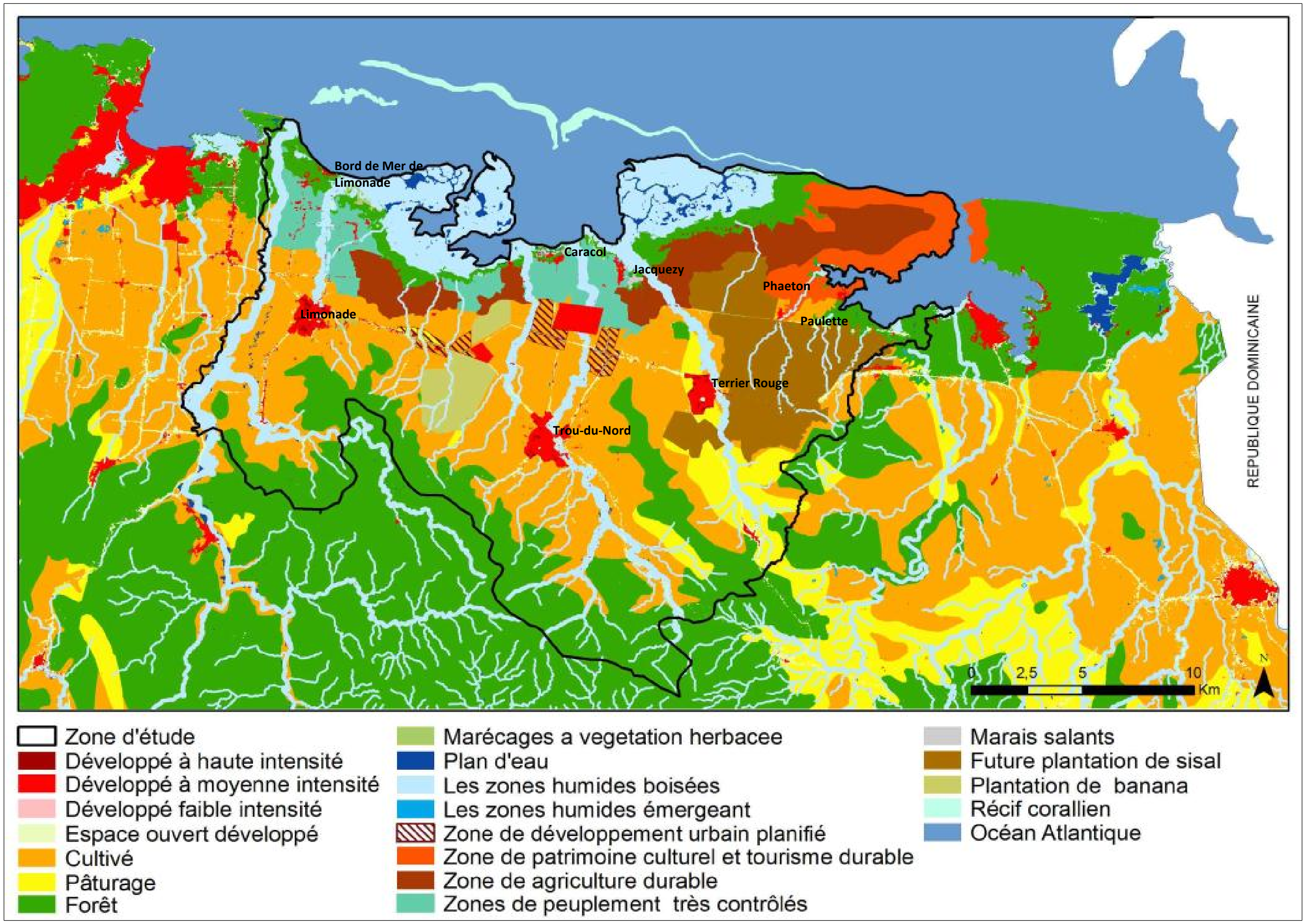

Figure 61 - Smart Development Scenario for Haiti's Northern Development Corridor

Map source: From geographic information layers by AIA (2012), CIAT (2012), CNGIS (c.2012), IADB (c.2013), NATHAT (2010), USAID-OFDA (c.2012), OSM (2013), OCHA (c.2010), PDNA (2010) and DTM (2013). Georeferencing, digitizing and remote sensing analysis from satellite imagery 1986, 2010 and 2013

Inside the Three Bays National Park, the mangrove areas so critical for the survival of this biodiverse Caribbean hotspot are healthy and are not suffering the pressures posed by those seeking their livelihood in their exploitation for charcoal. This is in part thanks to the emergence of alternative sources. Consequently, the mudflats next to the mangroves are preserved, which are followed by a continuous protection forest.

The elements described above manage to coexist in a balanced way, the system of zones of sustainable agriculture, of cultural heritage and sustainable tourism will have greater opportunity for thriving, providing new and better alternatives for native settlers and farmers. This includes the renewed, massive sisal plantations that have given more prime matter for the industries in the PIC, as well as the banana plantations.

Outside the park, the agricultural lands whose vocation is for this activity, together with those that have been traditionally used as such continue to do so, with no additional scattered settlements appearing on this realm thanks to the efforts and attraction created by the new, integrated planned settlements in the PIC and University areas. In all three realms, the coast and Park, the valley, and the mountainous areas all the elements are protected that require this as a result of their environmental or ecological valie. Consequently, fresh water will flow from peaks, through natural channels, before reaching the wonderful biodiversity area that the mangroves form.

8.3 Challenges to be Addressed

For a proper implementation of the proposed sustainable development scenario, there are a series of fundamental issues that would need to be proactively addressed by the relevant governmental, aid organizations and key economic stakeholders in the region:

- Address the land property rights system in the sense of creating a cadaster formalizing parcel boundaries, land uses, owner information, assessed value, and similar elements that are essential for planners and decision makers to properly understand the situation. This element is also fundamental for creating a visible, transparent and effective land and real estate market, which would be a key driver of a 'better' or more 'sustainable' territorial order, as well a major contributor to raising peoples and families from poverty. A cadaster would also bring clarity with respect to the lands belonging to the public realm, which would play a key role in defining where would it be less costly for society as a whole to plan and program interventions such as the 'new city' that has been discussed for this region. Finally, the cadaster should be implemented in equal terms for both the rural and the urban settings.

- Focus governmental and aid work on infrastructure, social services and productive operations such as the PIC. An important discovery was to find that there is an active and significantly large market of construction materials (although some of them are produced or extracted with negative environmental consequences) as well as a good array of engineering and construction firms with good capacity to build complete urbanizations. Should these factors be put at play in a transparent and private entrepreneurship context such as the one discussed in the previous point, there would be no need for the Government or aid organizations to directly provide housing solutions, at least for the lower middle and superior income levels. The limitations for a more varied housing and socially diverse setting appear to be the lack of infrastructure and social services that could drive families and individuals to establish in a given setting. Consequently, efforts to build large housing complexes could be put to a more effective and sustainable use by enhancing the infrastructure and social services in cities and townships, as well as creating two new infrastructure and social services ready areas around the University of Limonade and around the PIC.

- The efforts of the many aid organizations and the IDB could be put together for the creation of a sustainable setting in the region. Instead of dividing the actions of different organizations by sector and within that by locale, a concerted plan acting on existing townships and future areas of integrated development such as the ones proposed in this study, would yield much better results.

- This study has demonstrated the unused opportunities and capacity that existing cities and townships have to accommodate growth and its demands. Consequently, there should be a proactive move at intervening in these places, not only through the land regularization and formalization process discussed above, but also on the different mechanisms that are needed to unlock the urban land and real estate markets.

- Developing one or two integrated planned settings in the neighborhood of the PIC and the University of Limonade is essential for reducing the pressures on the coastal townships, because of the proximity to the opportunities for employment and services that these facilities create, which could deter the pursuit of those townships as places to live or even induce migration from them. It is important to base these planned settings on the land suitability analyses presented in this report to protect and enhance environmental resources.

- The long term sustainability of this region also depends on the pursuit of alternative routes connecting Cap Haïtien, Ouanaminthe and the Dominican Republic. This scenario shows the path that one of such routes could take, in which many a benefit would be accrued: reduced impact on environmentally or agriculturally productive lands, better access to markets by mountain communities, and lesser use of the flood, hurricane and other hazard exposed areas along the coast.

9. BIBLIOGRAPHY

AIA Legacy, American Institute of Architects. Cap Haïtien - Ouanaminthe Development Corridor Regional Comprehensive Plan. Vol. 1. 3 vols. Port-Au-Prince: AIA - IADB - USAID, 2012.

—. Cap Haïtien - Ouanaminthe Development Corridor Regional Comprehensive Plan. Vol. 2. 3 vols. Port-Au-Prince: AIA - IADB - USAID, 2012.

CNGIS (c.2012)

Comité Interministériel d'Aménagement du Territoire. La Gestion Intégrée Des Bassins Versants en Haïti: - Méthodologie de délimitation cartographique des bassins versants. Rapport final , Port-au-Prince: CIAT, 2010.

—. Plan d'Aménagement du Nord / Nord-Est: Couloir Cap - Ouanaminthe. Port au Prince: CIAT, 2012.

DTM (2013)

Famine Early Warning Systems Network, HAITI Food Security Outlook Update, June 2012

Food and Agriculture Organization of the United Nations, 2004. Technical Cooperation Programme. Project Title: Assistance to improve Local Agricultural Emergency Preparedness in Caribbean countries highly prone to hurricane related disasters.

Glaeser, Edward. Triumph of the City: How Our Greatest Invention Makes Us Richer, Smarter, Greener, Healthier and Happier. New York, NY: The Penguin Press, 2011.

IADB (c.2013)

IHSI 2012. Total Population, Population 18 years and older households and Densities Are times in 2012, IHSI, Departments of Vital Statistics and Social, January 2012

IHSI 2009a. Total Population, Population 18 years and older households and Densities Are times in 2009, IHSI, Departments of Vital Statistics and Social, January 2009

IHSI 2009b. Trends and Prospects of Population in Haiti at the Departments and Commons 2000-2015, IHSI, Directions of Demographic and Social Statistics, February 2009

IHSI and CELADE / ECLAC 2008. Estimates and Projections of the Total Population, Urban and Rural and economically active, IHSI - Census Bureau and Latin American Demographic Centre, CELADE / ECLAC, May 2008

IHSI 2009c. Socio-demographic Large Lessons learned from 4th RGPH, IHSI - Bureau of the Census, February 2009

IHSI 2004. Results of the Fourth General Census of Population and Housing, IHSI 2004

IPCC SRES

IPCC AR4 and 5

Joerin and Thériault (2001). Joerin, Florent and Thériault, Marius. Using GIS and outranking multicriteria analysis for land use suitability assessment. International Journal on Geographic Information Science, 2001, VOL. 15, No. 2, 153-174

NATHAT (2010)

NATHAT 2012

OSM (2013)

OCHA (c.2010)

PDNA (2010)

USAID-OFDA (c.2012)

APPENDIX 1: Individual GIS Maps for the Ecological System

Figure A1 – Topography of the NDC

Map source: From geographic information layers by AIA (2012), CIAT (2012), CNGIS (c.2012), IADB (c.2013), NATHAT (2010), USAID-OFDA (c.2012), OSM (2013), OCHA (c.2010), PDNA (2010) and DTM (2013). Georeferencing, digitizing and remote sensing analysis from satellite imagery 1986, 2010 and 2013.

Figure A2 – NCD Hydric System: Superficial water

Map source: From geographic information layers by AIA (2012), CIAT (2012), CNGIS (c.2012), IADB (c.2013), NATHAT (2010), USAID-OFDA (c.2012), OSM (2013), OCHA (c.2010), PDNA (2010) and DTM (2013). Georeferencing, digitizing and remote sensing analysis from satellite imagery 1986, 2010 and 2013.

Figure A3 – NCD Hydric System: Watersheds

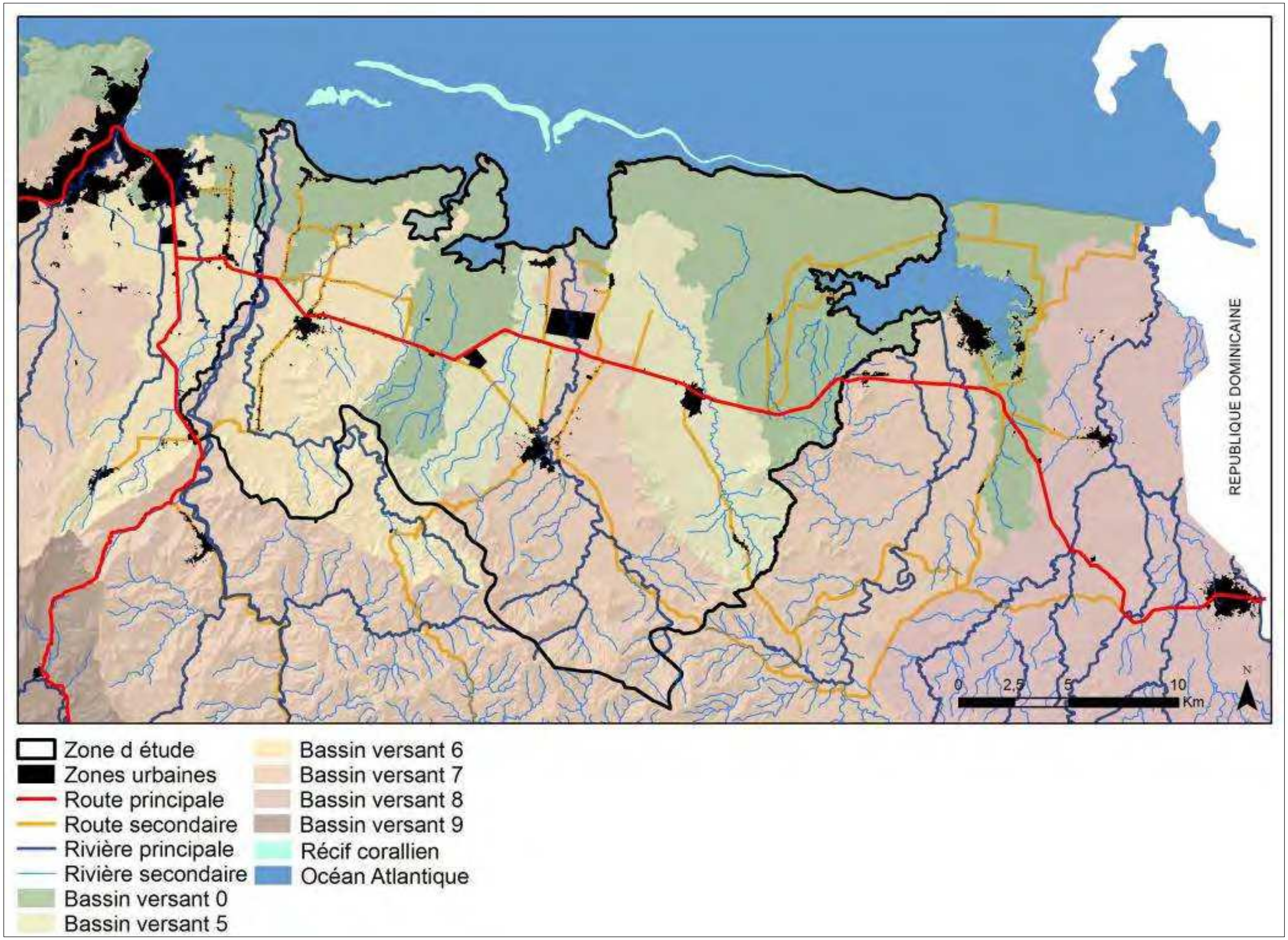

Map source: From geographic information layers by AIA (2012), CIAT (2012), CNGIS (c.2012), IADB (c.2013), NATHAT (2010), USAID-OFDA (c.2012), OSM (2013), OCHA (c.2010), PDNA (2010) and DTM (2013). Georeferencing, digitizing and remote sensing analysis from satellite imagery 1986, 2010 and 2013.

Figure A4 – NCD Hydric System: Superficial and underground water

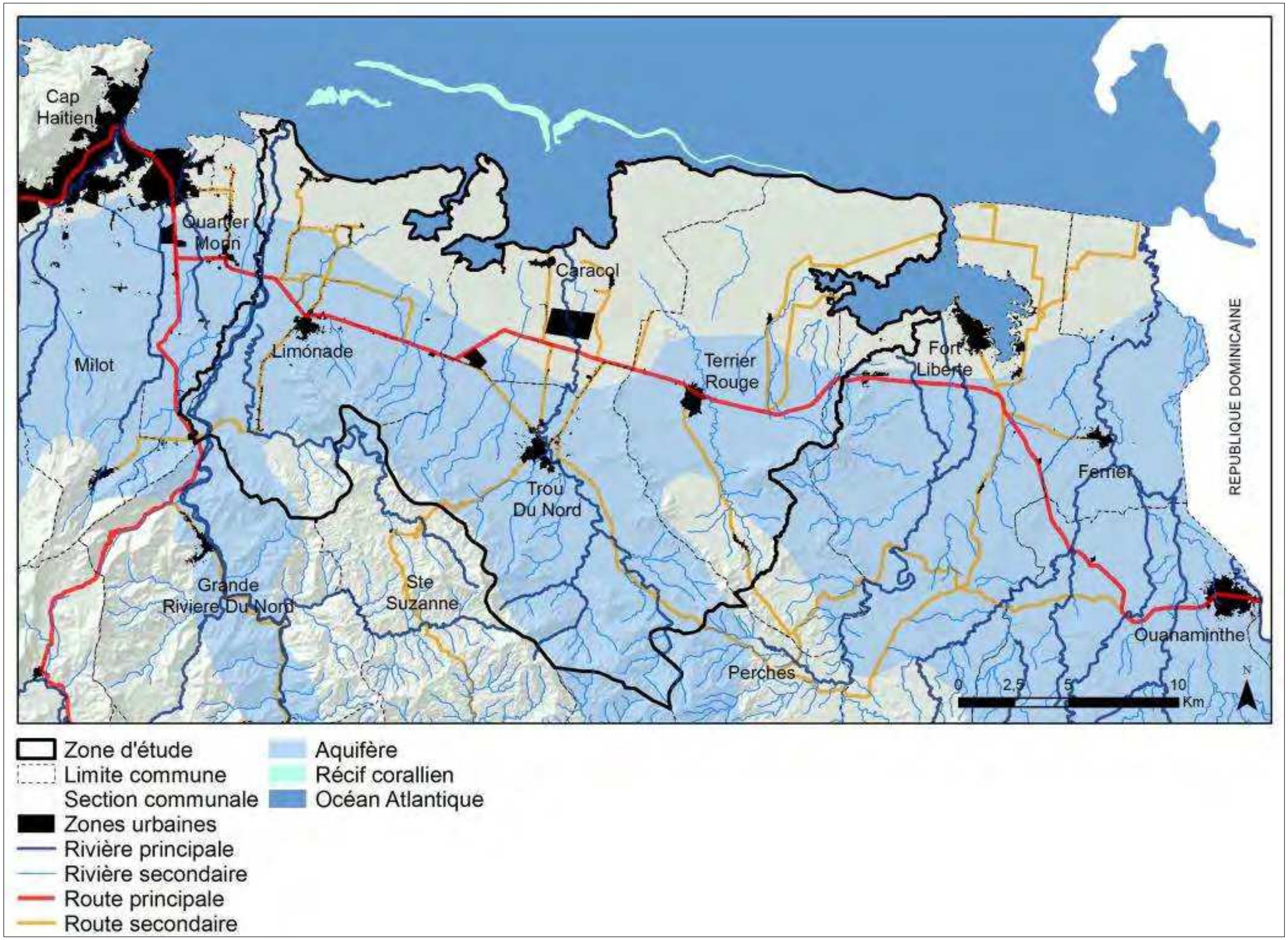

Map source: ERM (2014) from geographic information layers by AIA (2012), CIAT (2012), CNGIS (c.2012), IADB (c.2013), NATHAT (2010), USAID-OFDA (c.2012), OSM (2013), OCHA (c.2010), PDNA (2010) and DTM (2013). Georeferencing, digitizing and remote sensing analysis from satellite imagery 1986, 2010 and 2013.

Figure A5 – NCD Strategic Ecosystems

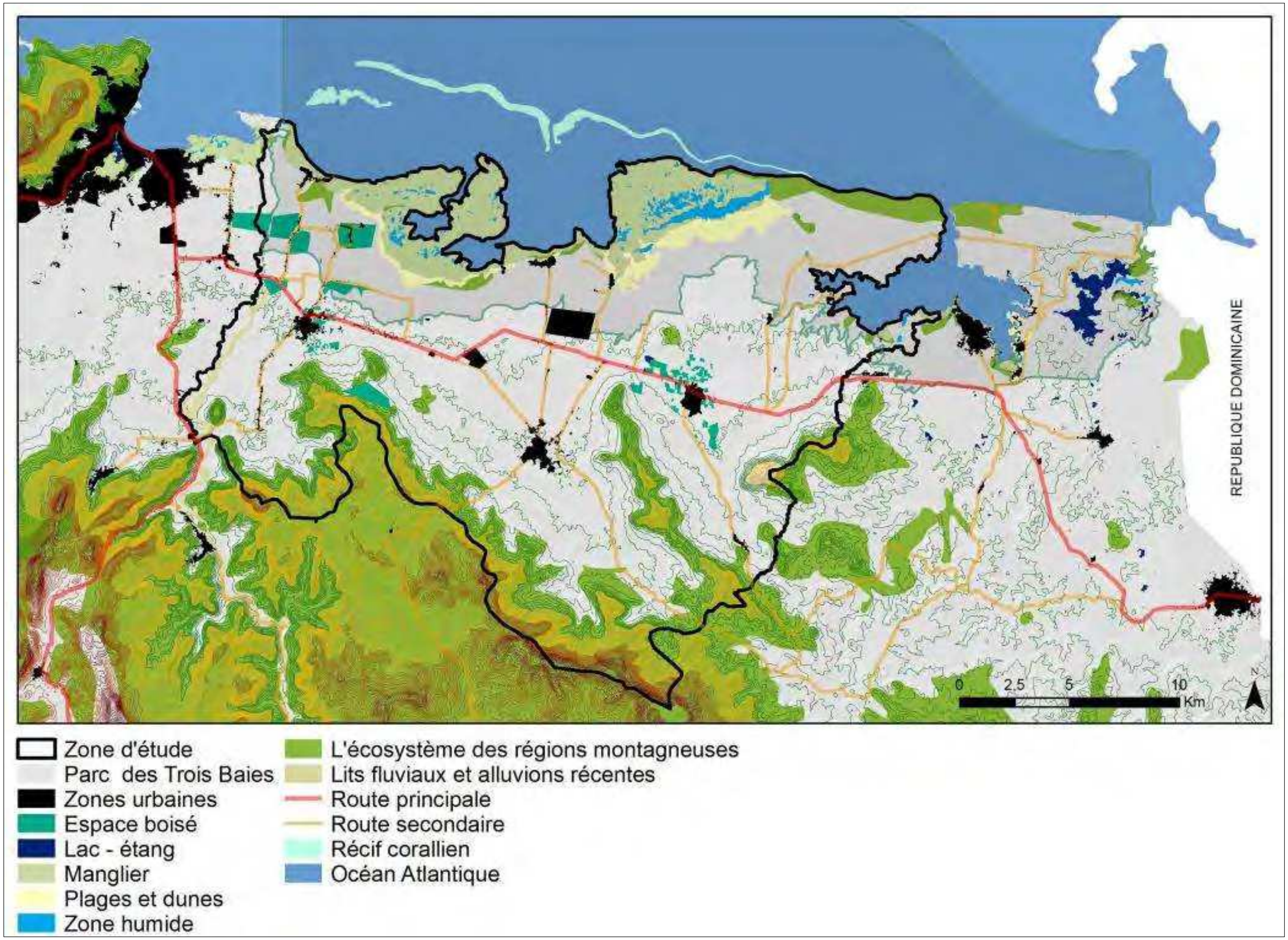

Map source: From geographic information layers by AIA (2012), CIAT (2012), CNGIS (c.2012), IADB (c.2013), NATHAT (2010), USAID-OFDA (c.2012), OSM (2013), OCHA (c.2010), PDNA (2010) and DTM (2013). Georeferencing, digitizing and remote sensing analysis from satellite imagery 1986, 2010 and 2013.

Figure A6 – NDVI: Normalized difference vegetation index

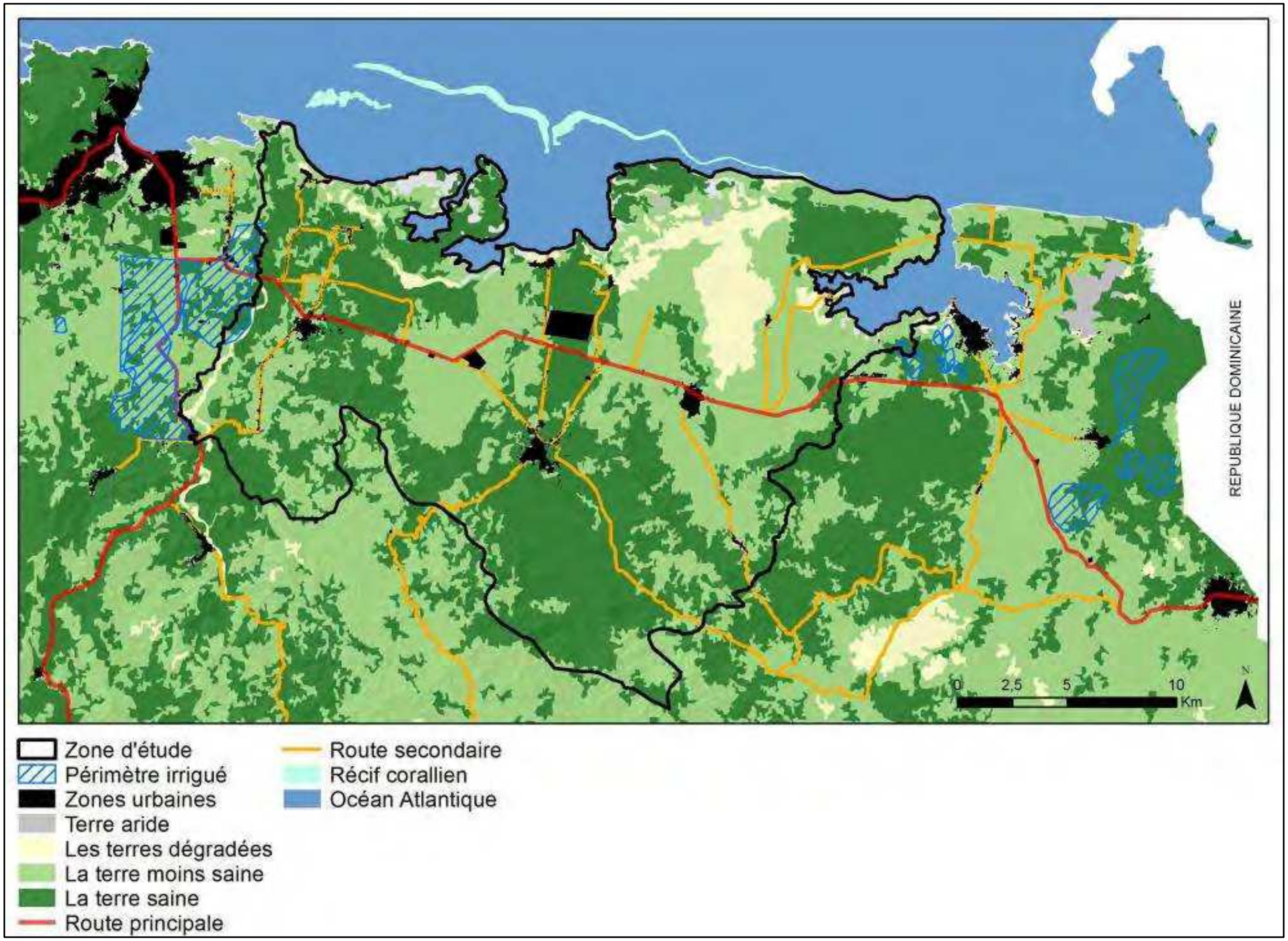

Map source: From geographic information layers by AIA (2012), CIAT (2012), CNGIS (c.2012), FAO(c.2012), IADB (c.2013), NATHAT (2010), USAID-OFDA (c.2012), OSM (2013), OCHA (c.2010), PDNA (2010) and DTM (2013). Georeferencing, digitizing and remote sensing analysis from satellite imagery 1986, 2010 and 2013.

Figure A7 - Parc Marin des Trois Baies and Main Ecological Structure

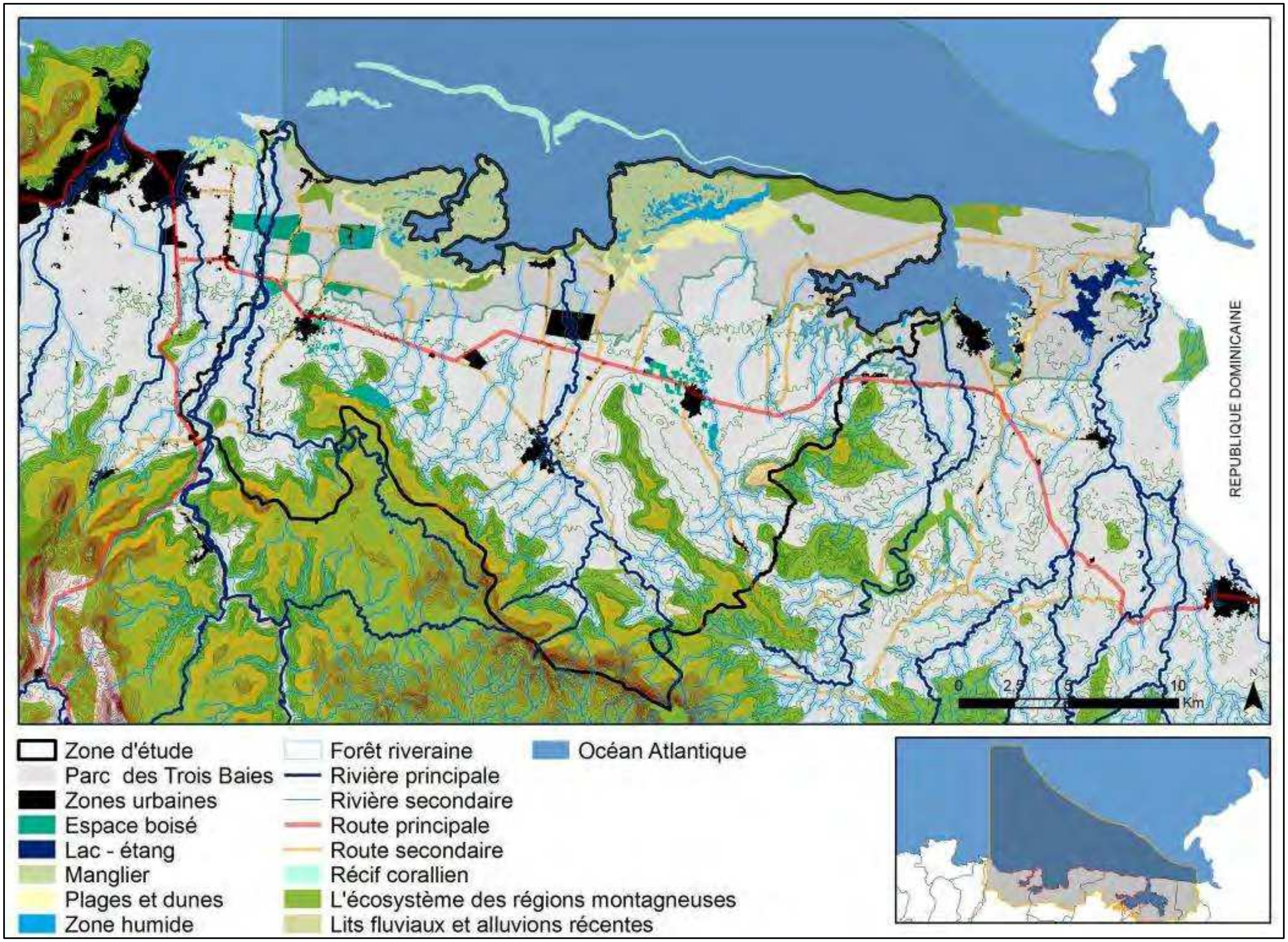

Legend: From geographic information layers by AIA (2012), CIAT (2012), CNGIS (c.2012), IADB (c.2013), NATHAT (2010), USAID-OFDA (c.2012), OSM (2013), OCHA (c.2010), PDNA (2010) and DTM (2013). Georeferencing, digitizing and remote sensing analysis from satellite imagery 1986, 2010 and 2013.

Figure A8 – Agrological Quality of Soils Classification

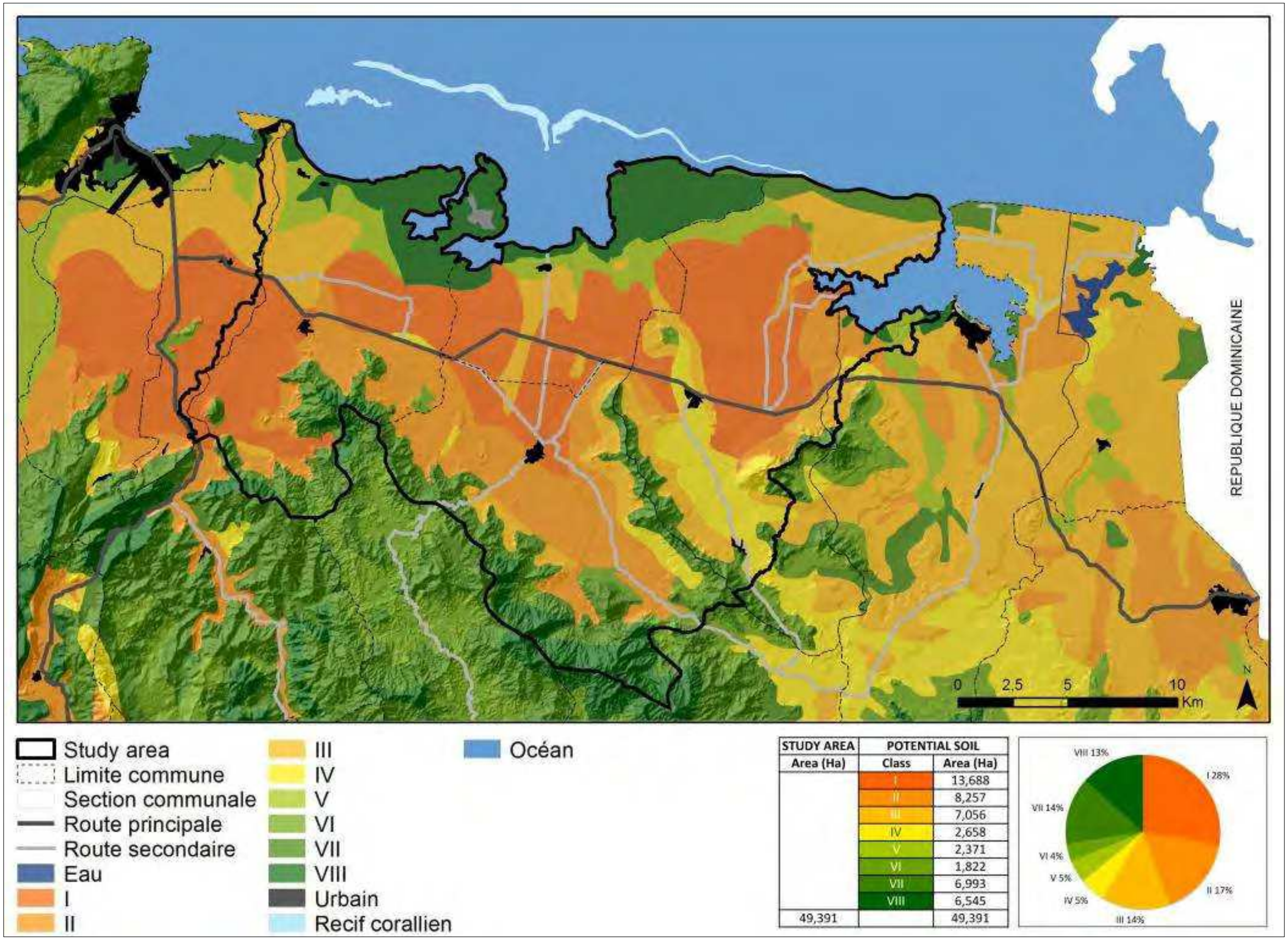

Map source: From geographic information layers by AIA (2012), CIAT (2012), CNGIS (c.2012), IADB (c.2013), NATHAT (2010), USAID-OFDA (c.2012), OSM (2013), OCHA (c.2010), PDNA (2010) and DTM (2013). Georeferencing, digitizing and remote sensing analysis from satellite imagery 1986, 2010 and 2013.

APPENDIX 2: Individual GIS Maps for Urban and Infrastructure Development

Figure B1 – Mining Concessions

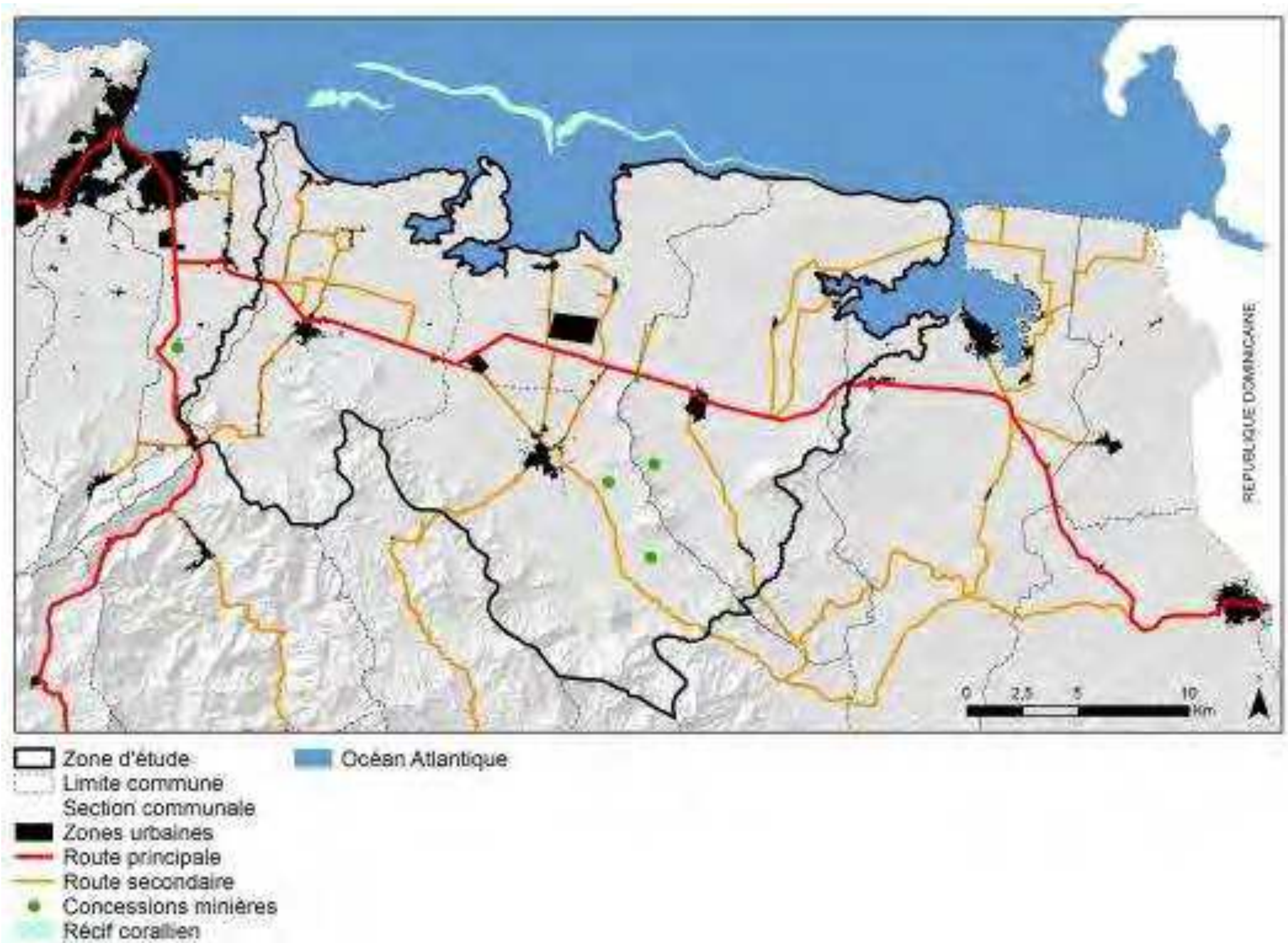

Figure B2 – Road Network Hierarchy

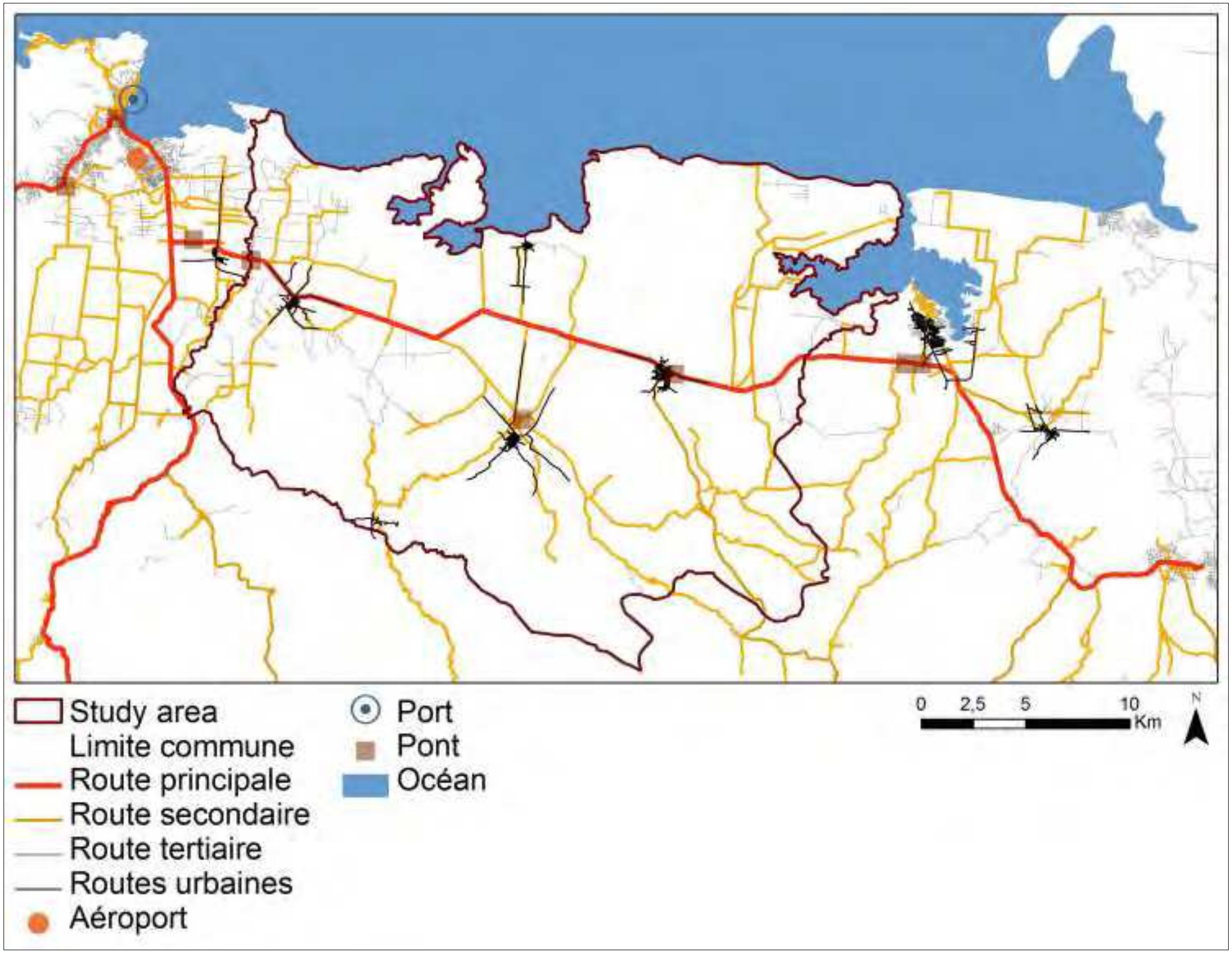

Map source: Variables built from geographic information layers by AIA (2012), CIAT (2012), CNGIS (c.2012), IADB (c.2013), NATHAT (2010), USAID-OFDA (c.2012), OSM (2013), OCHA (c.2010), PDNA (2010) and DTM (2013). Georeferencing, digitizing and remote sensing analysis from satellite imagery 1986, 2010 and 2013.

Figure B3 – Solid Waste and Waste Water System

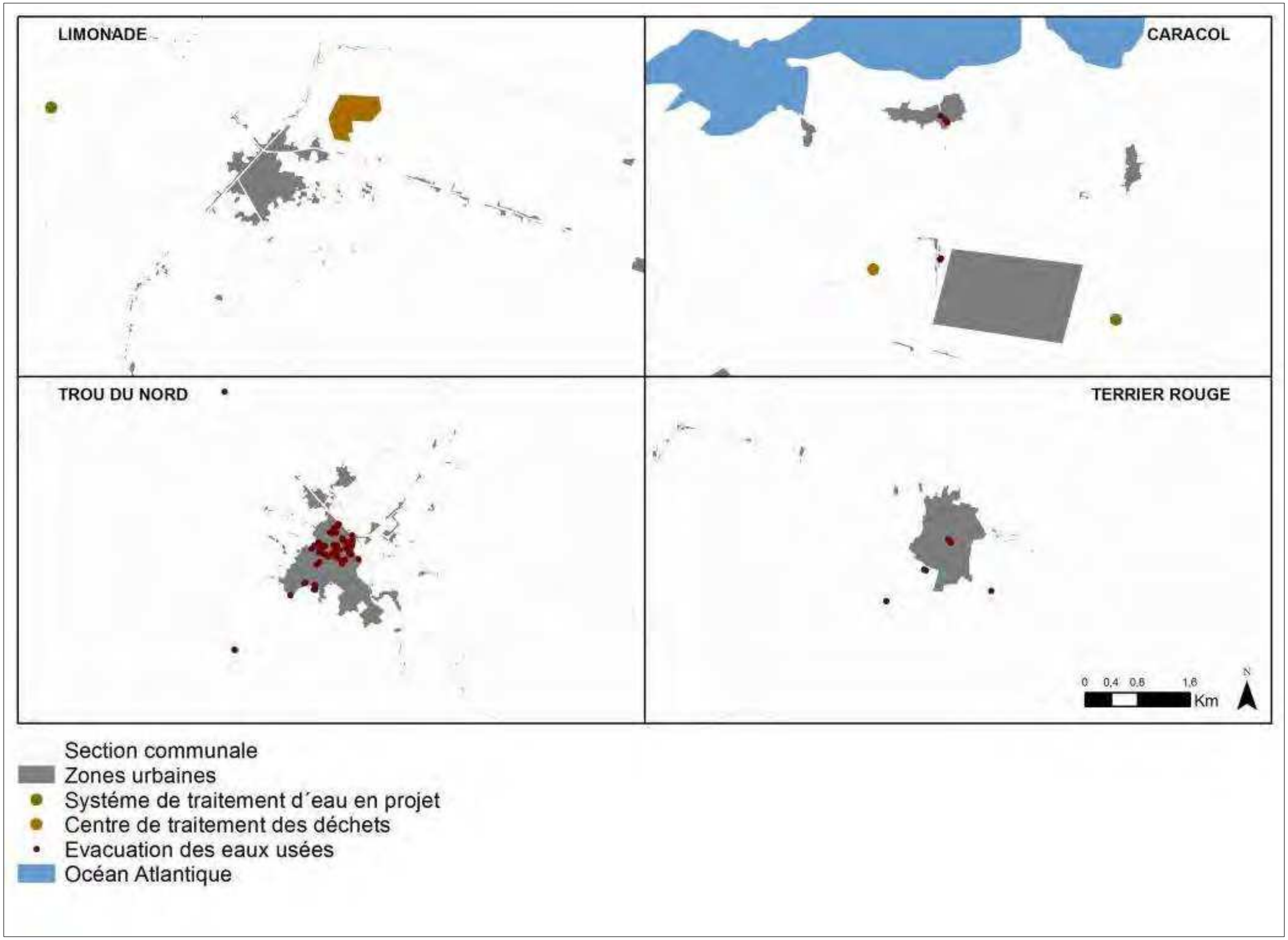

Map source: Variables built from geographic information layers by AIA (2012), CIAT (2012), CNGIS (c.2012), IADB (c.2013), NATHAT (2010), USAID-OFDA (c.2012),

Figure B4 – Water Supply System

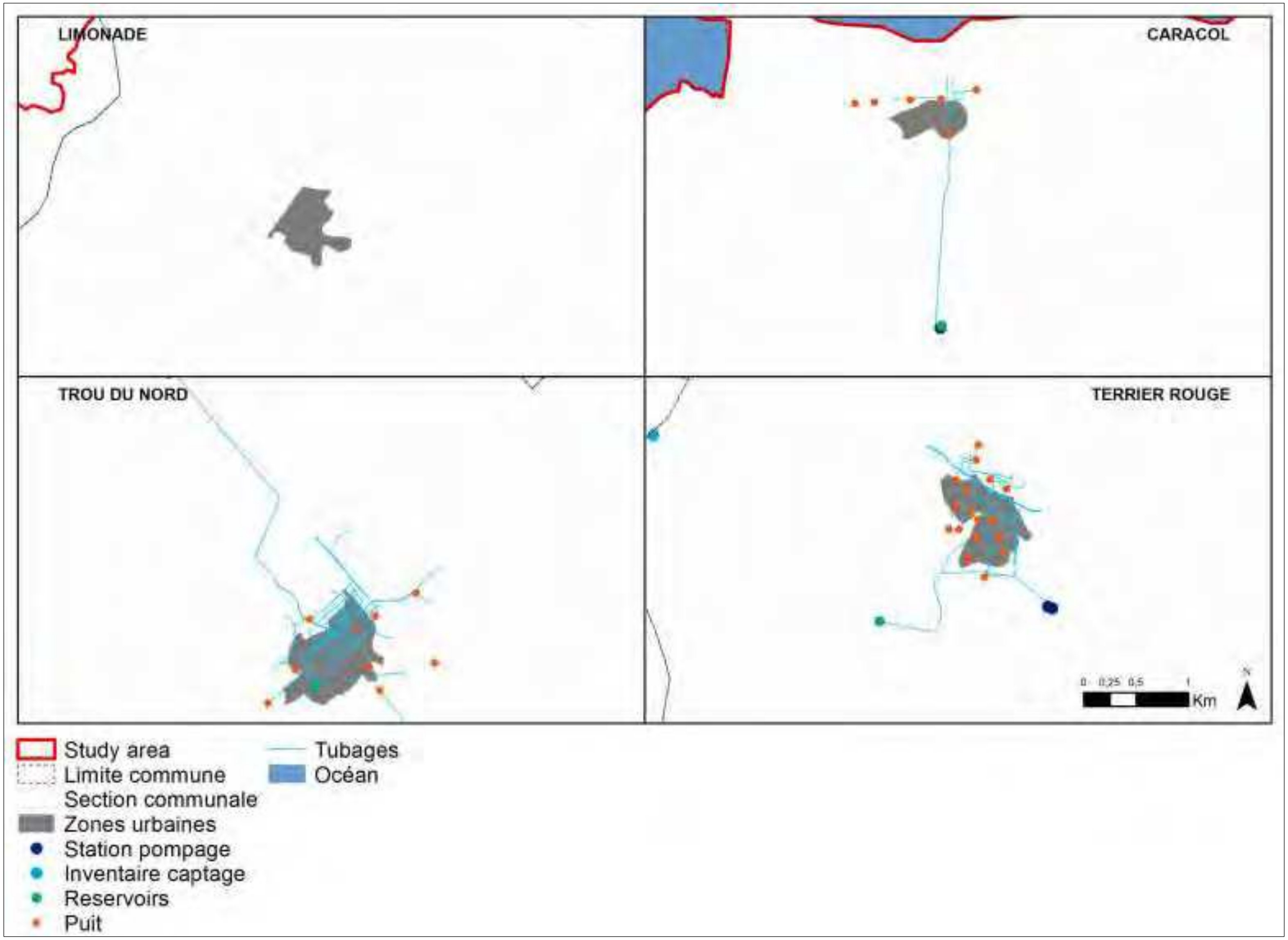

Map source: Variables built from geographic information layers by AIA (2012), CIAT (2012), CNGIS (c.2012), IADB (c.2013), NATHAT (2010), USAID-OFDA (c.2012), OSM (2013), OCHA (c.2010), PDNA (2010) and DTM (2013). Georeferencing, digitizing and remote sensing analysis from satellite imagery 1986, 2010 and 2013.

Figure B5 – Waste Water System

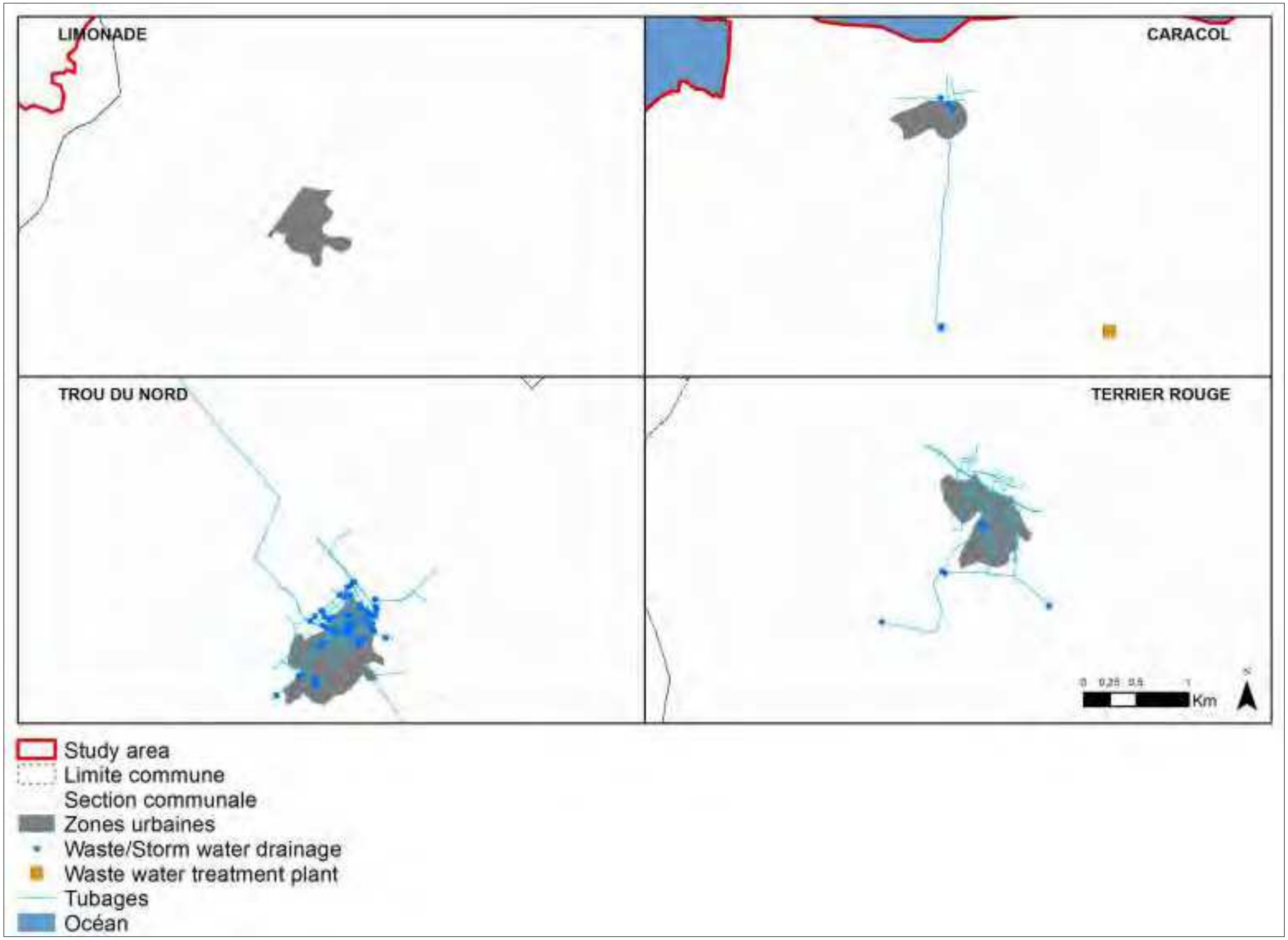

Map source: Variables built from geographic information layers by AIA (2012), CIAT (2012), CNGIS (c.2012), IADB (c.2013), NATHAT (2010), USAID-OFDA (c.2012), OSM (2013), OCHA (c.2010), PDNA (2010) and DTM (2013). Georeferencing, digitizing and remote sensing analysis from satellite imagery 1986, 2010 and 2013.

Figure B6 – Health Facilities System

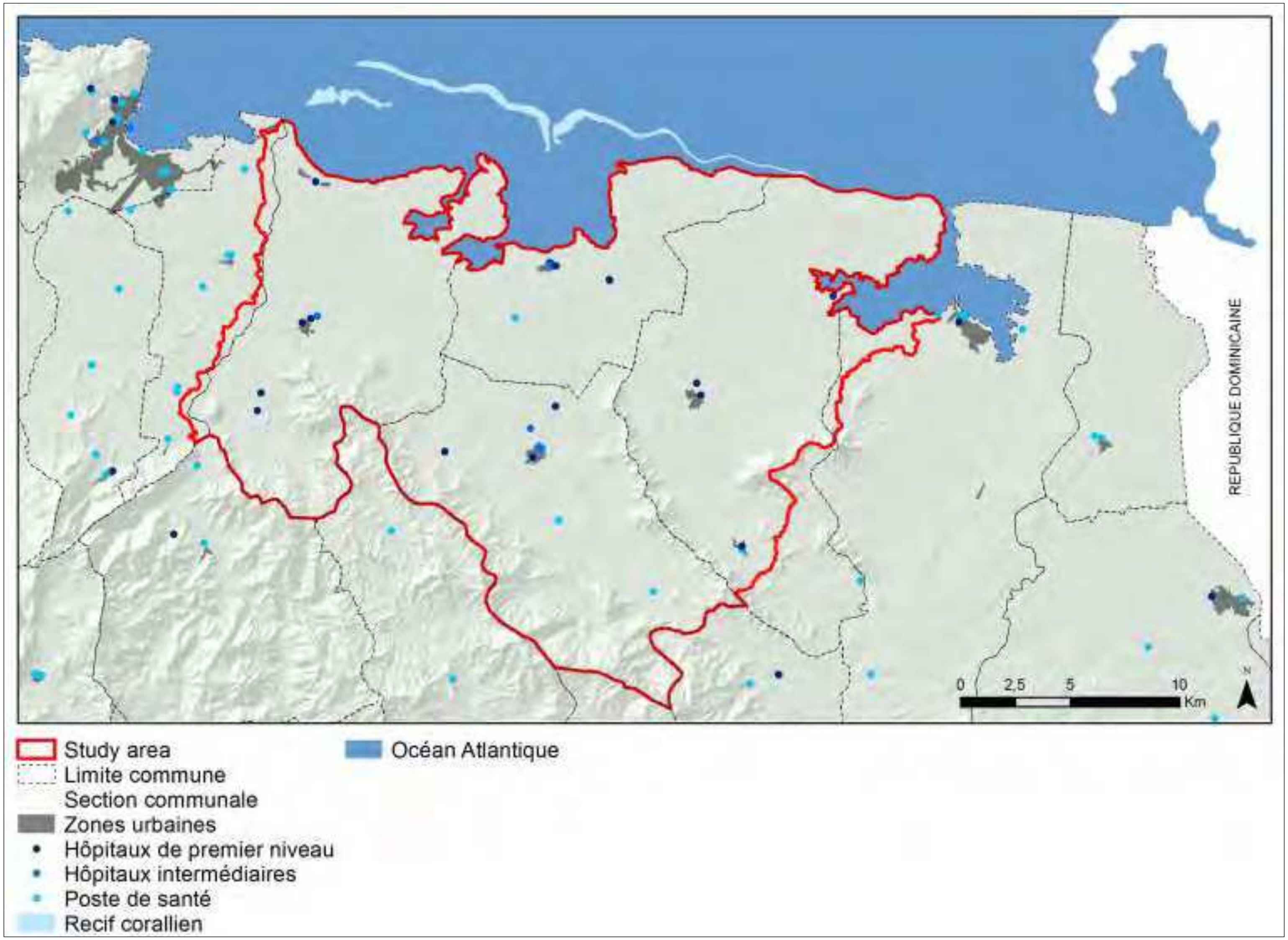

Map source: Variables built from geographic information layers by AIA (2012), CIAT (2012), CNGIS (c.2012), IADB (c.2013), NATHAT (2010), USAID-OFDA (c.2012), OSM (2013), OCHA (c.2010), PDNA (2010) and DTM (2013). Georeferencing, digitizing and remote sensing analysis from satellite imagery 1986, 2010 and 2013.

Figure B7 – Health Facilities System, urban core mosaic

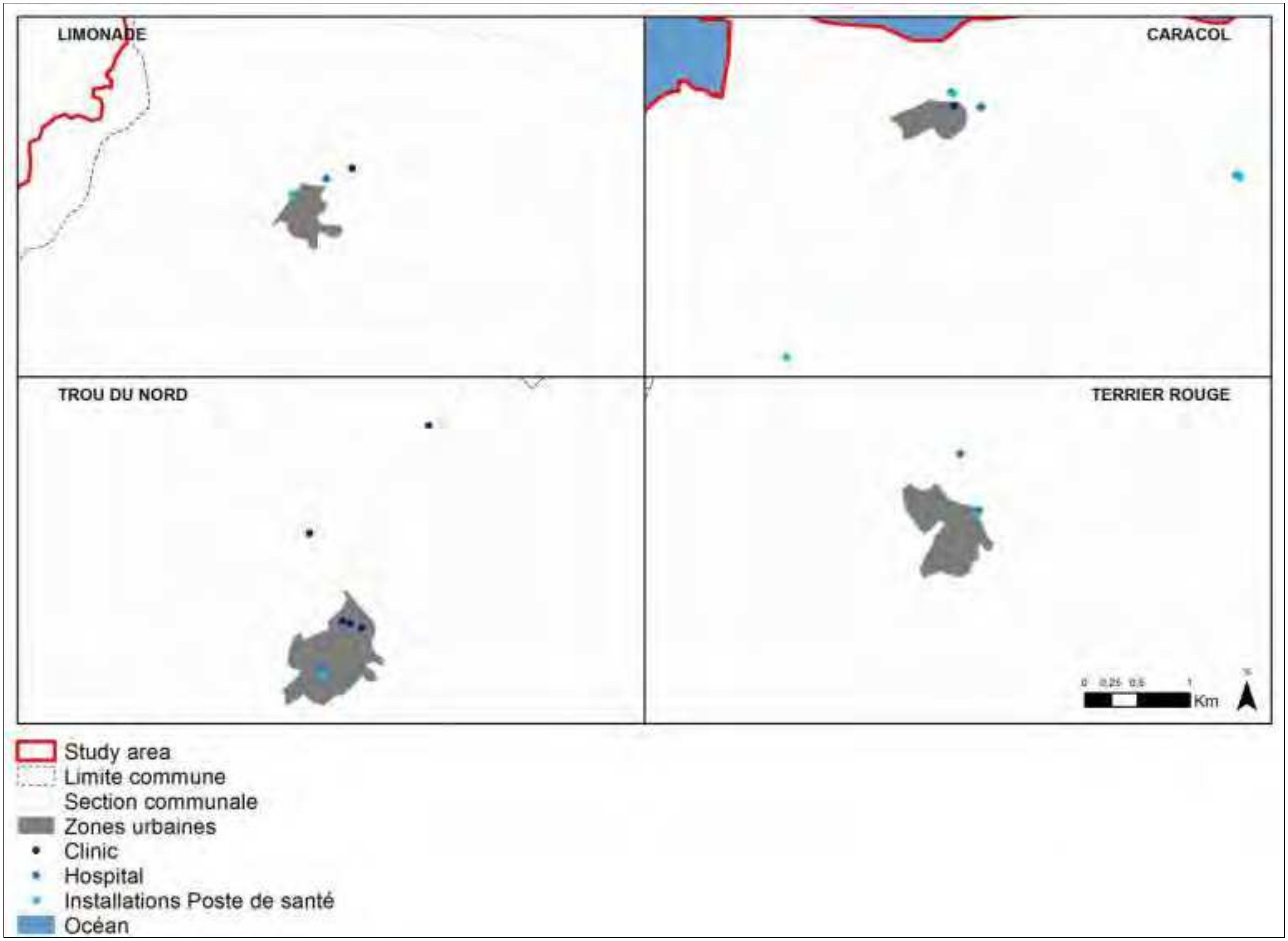

Map source: Variables built from geographic information layers by AIA (2012), CIAT (2012), CNGIS (c.2012), IADB (c.2013), NATHAT (2010), USAID-OFDA (c.2012), OSM (2013), OCHA (c.2010), PDNA (2010) and DTM (2013). Georeferencing, digitizing and remote sensing analysis from satellite imagery 1986, 2010 and 2013.

Figure B8 – Education Facilities System

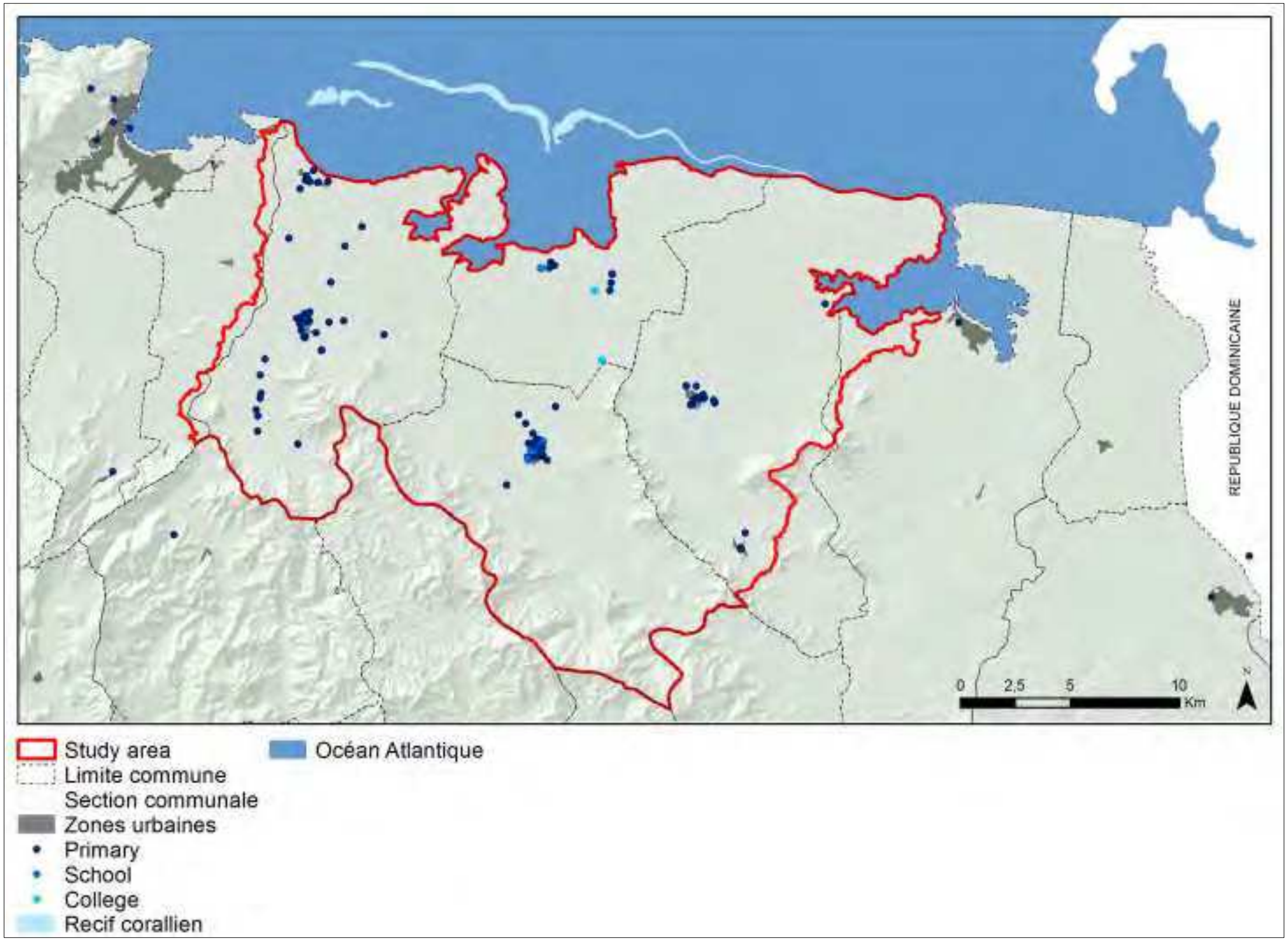

Map source: ERM (2014). Results from the restrictions sub-model. Variables built from geographic information layers by AIA (2012), CIAT (2012), CNGIS (c.2012), IADB (c.2013), NATHAT (2010), USAID-OFDA (c.2012), OSM (2013), OCHA (c.2010), PDNA (2010) and DTM (2013). Georeferencing, digitizing and remote sensing analysis from satellite imagery 1986, 2010 and 2013.

Figure B9 – Education Facilities System, urban core mosaic

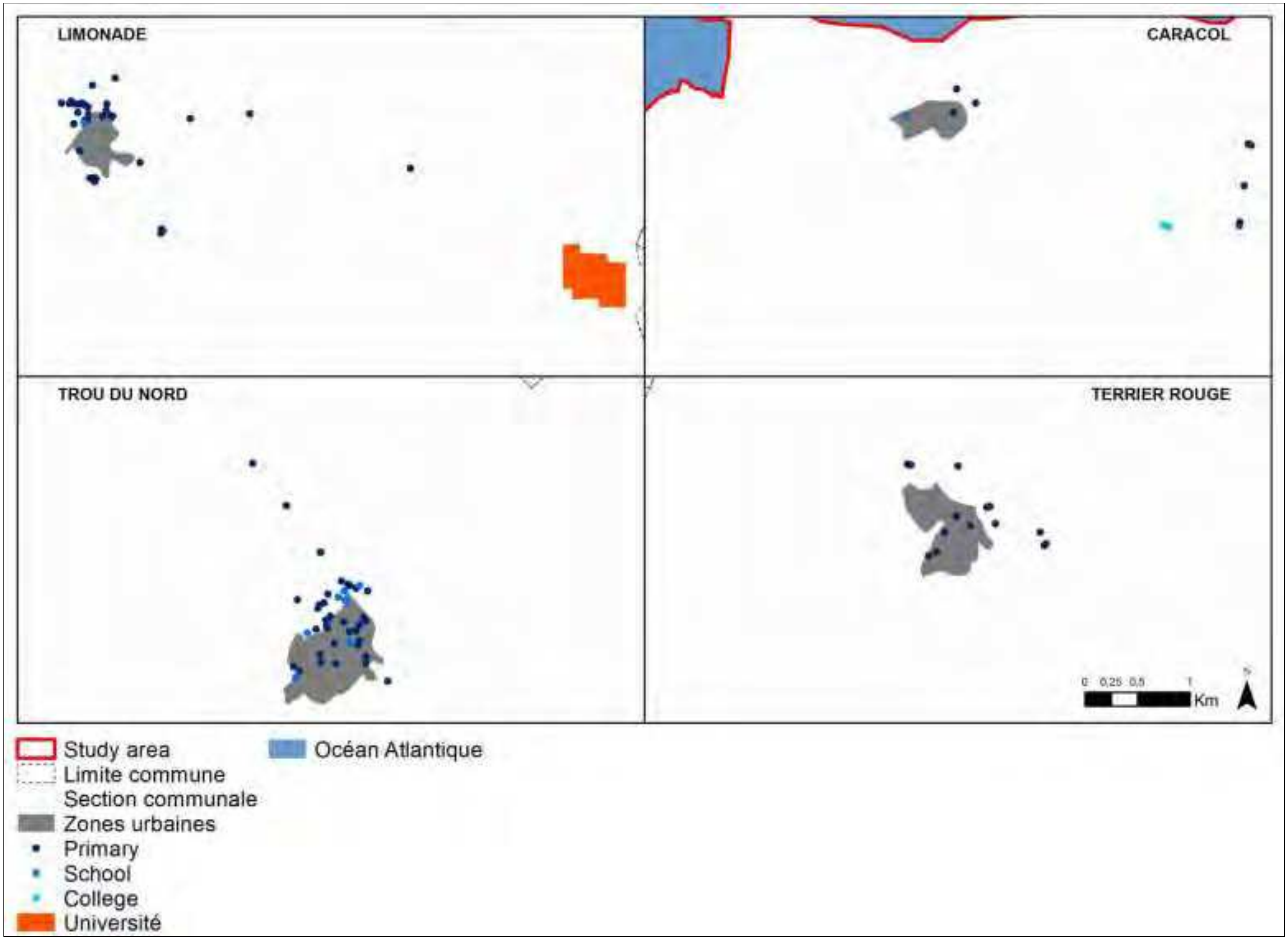

Map source: Variables built from geographic information layers by AIA (2012), CIAT (2012), CNGIS (c.2012), IADB (c.2013), NATHAT (2010), USAID-OFDA (c.2012), OSM (2013), OCHA (c.2010), PDNA (2010) and DTM (2013). Georeferencing, digitizing and remote sensing analysis from satellite imagery 1986, 2010 and 2013.

Figure B10 - Economic development projects that have been identified in the North and Northeast region of Haiti

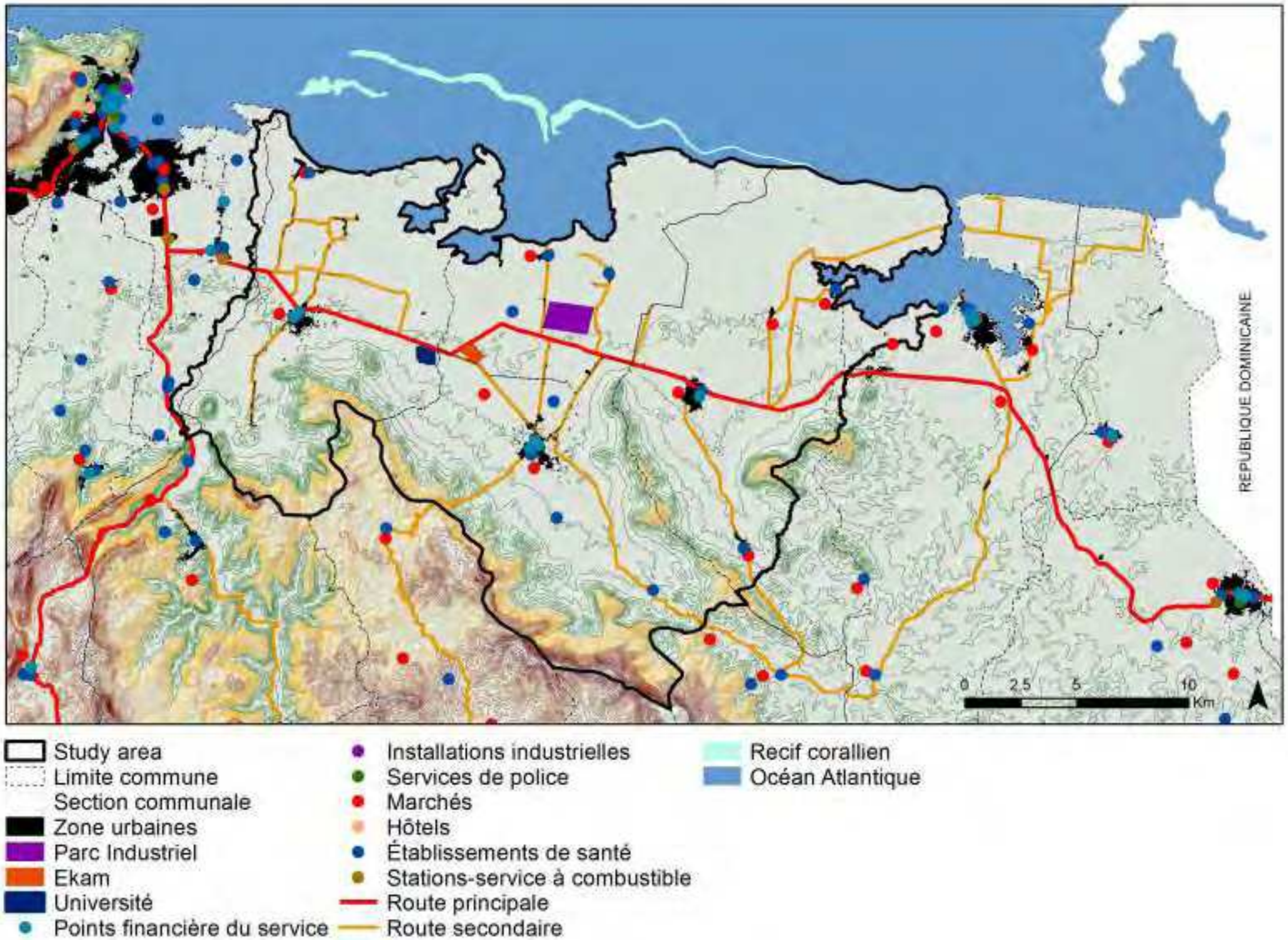

Note: It is important to note, however, that this criterion does not mean that beyond the municipality of Terrier Rouge, into Fort Liberté and Ouanaminthe, there is no economic activity of significance, especially along RN6. What it means is that it is likely that land and settlement changes which may occur, will likely respond to economic factors other than those associated with the development of the Caracol Industrial Park, thus falling outside the realm of this study

APPENDIX 3: Climate Studies by the University of West Indies

Projected Changes in 5 Atmospheric Variables for selected grid boxes over Haiti from the PRECIS RCM

Prepared by

Climate Studies Group, Mona

The University of the West Indies

February 2014

1. About the Model

PRECIS was developed by the Hadley centre (UK) in order to help generate high-resolution climate change information for as many regions of the world as possible. PRECIS is made freely available to groups of developing countries in order that they may develop climate change scenarios at national centres of excellence, simultaneously building capacity and drawing on local climatological expertise. http://www.metoffice.gov.uk/precis/intro.

PRECIS is a hydrostatic primitive equations grid point model. It contains 19 levels in the vertical and has horizontal resolutions of 0.44°x0.44° (~50 km) and 0.22°x0.22° (~25 km). Initial and lateral boundary forcing are taken from reanalysis or from outputs of General circulation Models (GCMs). The sea surface temperatures (SSTs) and sea-ice fractions surface boundary conditions are from a combination of monthly HadISST1 dataset and weekly NCEP observed datasets. Observed values of greenhouse gases are also fed into the model. PRECIS utilises a relaxation technique across a four point buffer zone at each vertical level. Dynamical flow, the atmospheric sulphur cycle, clouds and precipitation, radiative processes, the land surface and the deep soil are also described in the model. A full description of the model's physics is found in Jones et al. (2004).

Validation of the PRECIS Model for the Caribbean is offered in a number of papers including Campbell et al. (2011) and Taylor et al. (2013). Campbell et al. (2011) '*compared PRECIS's modeled patterns of temperature and precipitation with reanalysis datasets and available observations. They showed the mean Caribbean climatologies to be generally captured by the model, with the relative timing of temperature and precipitation maxima and minima being reproduced. This included the model's reproduction of the Caribbean midsummer rainfall minimum, which is a significant feature of many of the larger Caribbean islands. There was, however, also a general underestimation of rainfall amounts across the main Caribbean basin during the wet season and a simulation using temperatures that were too warm over the Caribbean islands but too cold over Central America and northern South America' (Taylor et al. 2013).*

2. About the Perturbed Physics Experiments (PPEs)

The first set of results presented are from the perturbed physics ensembles (PPE). PPEs are designed by varying uncertain parameters in the model's representation of important physical and dynamical processes. PPEs are used to capture some major sources of modelling uncertainty by running each member using identical climate forcings. It provides an alternative to using GCMs developed at different modelling centres around the world (e.g. a multi-model ensemble, MME), like those in the CMIP3 (Coupled Model Intercomparison Project 3). The Hadley Centre's PPE includes 17 members which are formulated to systematically sample parameter uncertainties under the ***A1B emissions scenario*** – this is referred to as the QUMP (Quantifying Uncertainties in Model Projections) ensemble. The QUMP ensemble was designed for use in the UK's own climate projections and is described in detail in the UKCP report available online at http://ukclimateprojections.defra.gov.uk/content/view/944/500/. Globally, and for many regions and variables, the range of climate futures projected by the QUMP PPE is equivalent or greater than those based on the CMIP3 MME. The PPE systematically samples the parameter uncertainties, exploring a wider range of possible variation in the formulation of a single model, leading to a wider range of physically plausible future climate outcomes than the MME. It is important to remember that PPE (similarly for MME) does not account for all of the sources of model uncertainty. [1]

The following 6 QUMP experiments were evaluated: Q0, Q3, Q4, Q10, Q11, and Q14. All were run at 25 km and from 1960 through 2100. For each experiment the deviation of a future decade e.g. 2020s, 2030s, 2040s from the experiments baseline (1960-1990) were determined. This gave an ensemble of 6 future changes for each decade. The ensemble results are summarised and presented in Tables below for the 2040s (as requested).

2.1. Grid Boxes

The model grid boxes over Haiti are as shown in Figure 1 below. Projections for grid boxes 46, 47, 53, 54, 60 and 61 are provided as requested.

[1] Portions of the narrative are adapted from narrative on the PRECIS webpage http://www.metoffice.gov.uk/precis/qump

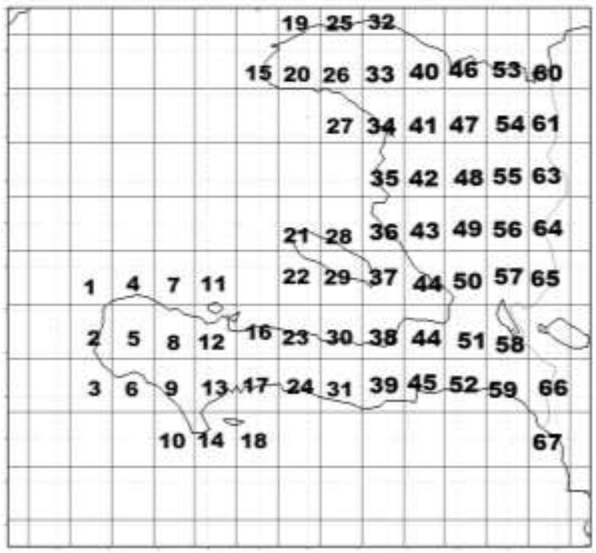

Figure 1: PRECIS 25 km model grid boxes over Haiti.

Table 1: Coordinates for each grid box.

Grid Box #	Longitude	Latitude
61	71.75 W	19.5 N
60	71.75 W	19.75 N
54	72 W	19.5 N
53	72 W	19.75 N
47	72.25 W	19.5 N
46	72.25 W	19.75 N

2.2. About the Data

Future change data are provided for five variables. For four of the five variables the data are provided as absolute change. These variables are: minimum temperature (^{o}C), maximum temperature (^{o}C), mean temperature (^{o}C) and 10 m wind speed (m/s). Percentage change is provided for precipitation. Data is averaged for over three month seasons: November-January (NDJ), February-April (FMA), May-July (MJJ) and August–October (ASO), roughly consistent with the Caribbean dry season and wet season (Taylor et al. 2002). The mean annual change is also given. The change for each variable and for each period is calculated for the 2040s for each member of the ensemble. The minimum, maximum and mean values of the 6 member ensemble are provided.

2.2.1. Data by Variable

Table 2: Projected absolute change in minimum temperature (^oC) for the 2040s relative to the 1960-1990 baseline. Data presented for minimum, maximum and mean value of a six member ensemble. Values are for 25 km grid boxes shown in Figure 1.

Change in Minimum Temperature (^oC)							
GRID BOX		**61**	**60**	**54**	**53**	**47**	**46**
NDJ	MIN	1.17	1.08	1.21	0.84	1.20	0.98
	MEAN	1.79	1.79	1.83	1.62	1.80	1.85
	MAX	2.08	2.07	2.16	2.04	2.09	2.58
FMA	MIN	1.38	1.38	1.41	1.24	1.44	1.45
	MEAN	1.81	1.81	1.82	1.63	1.80	1.94
	MAX	2.08	2.03	2.11	2.01	2.05	2.72
MJJ	MIN	1.42	1.46	1.43	1.29	1.43	1.42
	MEAN	2.00	1.94	1.99	1.73	1.95	2.06
	MAX	2.40	2.34	2.42	1.94	2.38	3.37
ASO	MIN	1.13	1.04	1.07	0.95	1.06	0.95
	MEAN	1.94	1.92	1.95	1.72	1.91	2.02
	MAX	2.50	2.48	2.54	2.50	2.48	2.54
ANN	MIN	1.48	1.43	1.47	1.22	1.45	1.37
	MEAN	1.88	1.87	1.89	1.67	1.87	1.97
	MAX	2.21	2.20	2.22	1.98	2.17	3.02

Table 3: Projected absolute change in maximum temperature (^{o}C) for the 2040s relative to the 1960-1990 baseline. Data presented for minimum, maximum and mean value of a six member ensemble. Values are for 25 km grid boxes shown in Figure 1.

Change in Maximum Temperature (^{o}C)							
GRID BOX		**61**	**60**	**54**	**53**	**47**	**46**
NDJ	MIN	1.22	1.09	1.23	0.76	1.22	1.07
	MEAN	1.62	1.55	1.62	1.41	1.59	1.76
	MAX	2.01	1.88	1.97	1.87	1.93	3.13
FMA	MIN	0.86	0.93	0.95	1.05	1.04	1.01
	MEAN	1.51	1.49	1.51	1.45	1.52	1.78
	MAX	2.16	2.05	2.14	2.01	2.09	2.99
MJJ	MIN	1.43	1.36	1.45	1.23	1.46	1.35
	MEAN	1.90	1.72	1.89	1.54	1.86	2.11
	MAX	2.29	2.04	2.29	1.86	2.24	4.52
ASO	MIN	0.09	0.05	0.17	0.56	0.17	0.08
	MEAN	1.84	1.62	1.86	1.51	1.83	2.07
	MAX	2.63	2.28	2.61	1.99	2.57	4.71
ANN	MIN	1.33	1.20	1.30	1.04	1.28	1.17
	MEAN	1.72	1.59	1.72	1.48	1.70	1.93
	MAX	2.01	1.88	2.00	1.83	1.94	3.84

Table 4: Projected absolute change in mean temperature (^{o}C) for the 2040s relative to the 1960-1990 baseline. Data presented for minimum, maximum and mean value of a six member ensemble. Values are for 25 km grid boxes shown in Figure 1.

Change in Mean Temperature (^{o}C)							
GRID BOX		**61**	**60**	**54**	**53**	**47**	**46**
NDJ	MIN	1.30	0.19	1.49	0.12	1.49	0.75
	MEAN	1.69	1.48	1.73	1.37	1.74	1.54
	MAX	2.01	1.94	2.02	1.93	1.95	1.90
FMA	MIN	1.06	0.54	1.12	0.60	1.19	0.99
	MEAN	1.54	1.39	1.57	1.36	1.60	1.47
	MAX	2.06	1.96	2.06	1.94	2.03	1.93
MJJ	MIN	0.72	-1.32	1.09	-0.21	1.33	-0.09
	MEAN	1.65	1.25	1.70	1.30	1.77	1.40
	MAX	2.21	2.09	2.22	1.78	2.20	2.02
ASO	MIN	1.09	-0.07	1.26	0.31	1.54	0.50
	MEAN	1.89	1.60	1.91	1.48	1.91	1.65
	MAX	2.46	2.28	2.45	1.88	2.38	2.20
ANN	MIN	1.13	-0.16	1.33	0.21	1.47	0.54
	MEAN	1.69	1.43	1.73	1.38	1.76	1.51
	MAX	1.99	1.92	2.00	1.84	1.97	1.87

Table 5: Projected absolute change in 10 m wind speed (m/s) for the 2040s relative to the 1960-1990 baseline. Data presented for minimum, maximum and mean value of a six member ensemble. Values are for 25 km grid boxes shown in Figure 1.

Change in Wind Speed at 10m (m/s)							
GRID BOX		**61**	**60**	**54**	**53**	**47**	**46**
NDJ	MIN	-0.23	-0.34	-0.27	-0.32	-0.35	-0.42
	MEAN	-0.03	-0.04	-0.04	-0.06	-0.04	-0.15
	MAX	0.12	0.15	0.13	0.16	0.16	0.14
FMA	MIN	-0.07	-0.19	-0.06	-0.18	-0.07	-0.50
	MEAN	-0.01	0.01	0.00	0.00	0.01	-0.06
	MAX	0.08	0.20	0.11	0.14	0.15	0.09
MJJ	MIN	-0.05	-0.14	-0.07	-0.14	-0.09	-0.14
	MEAN	0.08	0.14	0.06	0.10	0.05	0.07
	MAX	0.23	0.31	0.22	0.25	0.27	0.23
ASO	MIN	0.07	0.15	0.07	0.15	0.06	0.13
	MEAN	0.19	0.27	0.19	0.26	0.22	0.21
	MAX	0.28	0.44	0.29	0.39	0.37	0.30
ANN	MIN	-0.06	-0.07	-0.07	-0.07	-0.12	-0.13
	MEAN	0.06	0.10	0.05	0.07	0.06	0.02
	MAX	0.15	0.19	0.15	0.17	0.20	0.15

Table 6: Projected percentage change in precipitation (%) for the 2040s relative to the 1960-1990 baseline. Data presented for minimum, maximum and mean value of a six member ensemble. Values are for 25 km grid boxes shown in Figure 1.

Change in Precipitation (%)							
GRID BOX		**61**	**60**	**54**	**53**	**47**	**46**
NDJ	MIN	-19.14	-28.09	-19.12	-34.16	-20.88	-25.72
	MEAN	-3.01	-8.60	-5.76	-5.61	-6.54	-11.33
	MAX	5.85	7.51	4.12	9.61	6.80	7.89
FMA	MIN	-22.51	-32.84	-24.98	-32.40	-23.32	-31.88
	MEAN	4.03	9.98	2.80	7.00	3.00	-0.83
	MAX	28.56	41.57	24.66	47.66	21.80	16.15
MJJ	MIN	-11.44	-23.03	-14.42	-30.62	-14.55	-50.38
	MEAN	-4.75	-9.96	-5.59	-6.47	-4.43	-10.14
	MAX	8.42	3.05	4.01	34.49	4.05	6.37
ASO	MIN	-13.98	-25.56	-17.63	-29.04	-14.20	-41.20
	MEAN	-11.03	-11.96	-11.89	-11.82	-7.14	-15.72
	MAX	-3.82	10.48	-4.93	29.27	0.71	11.76
ANN	MIN	-13.08	-22.99	-16.23	-20.70	-12.89	-25.48
	MEAN	-3.69	-5.13	-5.11	-4.23	-3.78	-9.50
	MAX	0.43	5.64	0.24	7.17	1.17	2.23

2.2.2. Data by Grid Box

Tables 7-12: Mean projected absolute change in minimum, maximum, and mean temperature and 10 m wind speed and mean projected percentage change in precipitation for the 2040s relative to the 1960-1990 baseline for each 25 km grid box. Data presented for mean value of the six member ensemble. Grid boxes are as shown in Figure 1.

Table 7: Grid Box 61					
Variable	**Mean Temp**	**Min T**	**Max T**	**Wind**	**Precip**
NDJ	1.69	1.79	1.62	-0.03	-3.01
FMA	1.54	1.81	1.51	-0.01	4.03
MJJ	1.65	2.00	1.90	0.08	-4.75
ASO	1.89	1.94	1.84	0.19	-11.03
Annual	1.69	1.88	1.72	0.06	-3.69

Table 8: Grid Box 60					
Variable	**Mean T**	**Min T**	**Max T**	**Wind**	**Precip**
	^oC	^oC	^oC	m/s	%
NDJ	1.48	1.79	1.55	-0.04	-8.60
FMA	1.39	1.81	1.49	0.01	9.98
MJJ	1.25	1.94	1.72	0.14	-9.96
ASO	1.60	1.92	1.62	0.27	-11.96
Annual	1.43	1.87	1.59	0.10	-5.13

Table 9: Grid Box 54					
Variable	Mean T	Min T	Max T	Wind	Precip
	°C	°C	°C	m/s	%
NDJ	1.73	1.83	1.62	-0.04	-5.76
FMA	1.57	1.82	1.51	0.00	2.80
MJJ	1.70	1.99	1.89	0.06	-5.59
ASO	1.91	1.95	1.86	0.19	-11.89
Annual	1.73	1.89	1.72	0.05	-5.11

Table 10: Grid Box 53					
Variable	Mean T	Min T	Max T	Wind	Precip
	°C	°C	°C	m/s	%
NDJ	1.37	1.62	1.41	-0.06	-5.61
FMA	1.36	1.63	1.45	0.00	7.00
MJJ	1.30	1.73	1.54	0.10	-6.47
ASO	1.48	1.72	1.51	0.26	-11.82
Annual	1.38	1.67	1.48	0.07	-4.23

Table 11: Grid Box 47					
Variable	Mean T	Min T	Max T	Wind	Precip
	°C	°C	°C	m/s	%
NDJ	1.74	1.80	1.59	-0.04	-6.54
FMA	1.60	1.80	1.52	0.01	3.00
MJJ	1.77	1.95	1.86	0.05	-4.43
ASO	1.91	1.91	1.83	0.22	-7.14
Annual	1.76	1.87	1.70	0.06	-3.78

Table 12: Grid Box 46					
Variable	Mean T	Min T	Max T	Wind	Precip
	°C	°C	°C	m/s	%
NDJ	1.54	1.85	1.76	-0.15	-11.33
FMA	1.47	1.94	1.78	-0.06	-0.83
MJJ	1.40	2.06	2.11	0.07	-10.14
ASO	1.65	2.02	2.07	0.21	-15.72
Annual	1.51	1.97	1.93	0.02	-9.50

3. About the SRES Experiments

The results presented in this section come from experiments in which the PRECIS model was forced by the ECHAM4 Global Climate Model at its lateral boundaries. In these experiments the model was run from 1960-2100 and a baseline of 1960-1990 used to determine change for future years. The model was run at 50 km resolution and for one run each of the A2 and B2 scenarios described by the Intergovernmental Panel on Climate Change's (IPCC) Special Report on Emissions Scenarios (Nakićenović et al. 2000).

3.1. Grid Boxes and Data

Data is presented for one 50 km grid box centered on 72W and 19.5 N. The pattern follows that of the previous Tables. Data are only presented for the 2040s.

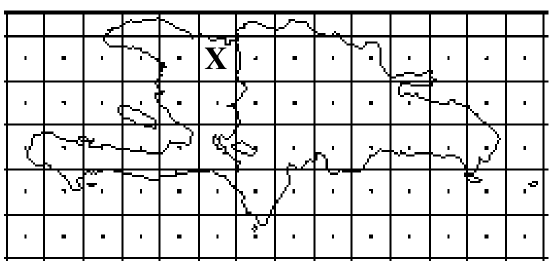

Figure 2: PRECIS 50 km model grid boxes over Haiti. Box with **X** denotes grid box used.

3.2. Data

Table 13: Projected absolute change in mean, maximum and minimum temperature (^{o}C) for the 2040s relative to the 1960-1990 baseline. Data presented for A2 and B2 scenarios (one run each). Values are for a 50 km grid box centered on 72W and 19.5 N.

	Mean T		**Min T**		**Max T**	
	A2	B2	A2	B2	A2	B2
NDJ	2.0	1.7	2.5	2.2	1.6	1.3
FMA	2.0	1.6	2.4	1.9	1.8	1.5
MJJ	2.2	1.9	2.4	2.2	2.2	1.8
ASO	2.2	2.3	2.6	2.6	2.1	2.3
Annual	2.1	1.9	2.5	2.2	1.9	1.7

Table 14: Projected percentage change in precipitation (%) and absolute change in 10 m wind speed (m/s) for the 2040s relative to the 1960-1990 baseline. Data presented for A2 and B2 scenarios (one run each). Values are for a 50 km grid box centered on 72W and 19.5 N.

	Precipitation (%)		**Wind Speed (m/s)**	
	A2	B2	A2	B2
NDJ	37.6	58.9	-0.11	-0.25
FMA	-1.3	15.0	-0.08	0.24
MJJ	-13.4	-5.6	0.17	0.18
ASO	0.8	-13.4	0.09	0.17
Annual	5.9	13.7	0.02	0.08

4. References

Campbell, J. D., M. A. Taylor, T. S. Stephenson, R. A. Watson, and F. S. Whyte, 2011: Future climate of the Caribbean from a regional climate model. *Int. J. Climatol.*, **31**, 1866–1878, doi:10.1002/joc.2200

Jones, R. G., M. Noguer, D. Hassell, D. Hudson, S. Wilson, G. Jenkins, and J. Mitchell, 2003: Workbook on generating high resolution climate change scenarios using PRECIS. UNDP, GEF, and Met Office Hadley Centre Manual, 32 pp.

Nakićenović, N., and R. Swart, Eds., 2000: *Special Report on Emissions Scenarios*. Cambridge University Press, 599 pp

Taylor, M. A., D. B. Enfield, and A. A. Chen, 2002: The Influence of the tropical Atlantic vs. the tropical Pacific on Caribbean Rainfall. *J. Geophys. Res.*, 107(C9) 3127, doi:10.1029/2001JC001097

Taylor, M. A., and Coauthors, 2007: Glimpses of the future: A briefing from the PRECIS Caribbean Climate Change Project. Caribbean Community Climate Change Centre, 24 pp.

Taylor, M. A**.,** A. Centella, J. Charlery, A. Benzanilla, J. Campbell, I. Borrajero, T. Stephenson, and R. Nurmohamed, 2013: The PRECIS-Caribbean Story: Lessons and Legacies. *Bull. Amer. Meteor. Soc* doi: 10.1175/BAMS-D-11-00235.

Evaluation of trends in sea levels and tropical storm intensities

Prepared by

Climate Studies Group, Mona

The University of the West Indies

February 2014

ACKNOWLEDGEMENT

The following authors contributed to the compilation of this report:

Tannecia S. Stephenson

Jhordanne Jones

Michael A. Taylor

ABOUT THIS DOCUMENT

This report presents an assessment of current literature on current and projected trends in sea level rise and storm intensities with particularly emphasis (where possible) on future values for the Caribbean region. Specifically the document reviews:

1. Current and projected trends of mean and extreme sea levels globally and regionally.
2. Current and projected trends in storm intensities as characterized by the Accumulated Cyclone Energy (ACE) and the Power Dissipation Index (PDI)

Table of Contents

List of Figures

List of Tables

At A Glance

Future Projections for 3 key variables are shown below:

A. Mean sea Level

Table A1 Historical rates and absolute change in global mean sea levels. Rates are obtained from IPCC (2013). [Referenced as Table 2.1 in text]

Period	Rate (mm yr^{-1})	Total sea level rise	IPCC Likelihood
1901 – 2010	1.7 ± 0.2	0.19 ± 0.02	Very likely
1971 – 2010	2.0 ± 0.2	-	Very likely
1993 – 2010	3.2 ± 0.4	-	Very likely

Table A2 Projected increases in global mean surface temperature and global and Caribbean mean sea level from the IPCC (2007) contrasted with those of Rahmstorf (2007). Projections are by 2100 relative to 1980-1999. Source: CARIBSAVE Climate Change Risk Atlas – Jamaica (2011). [Referenced as Table 2.3 in text.]

Scenario	**Global mean surface temperature (°C)**	**Global mean sea level rise (m)**	**Caribbean mean sea level rise (±0.05 m) relative to global mean**
IPCC B1	1.1 – 2.9	0.18 – 0.38	0.14 – 0.43
IPCC A1B	1.7 – 4.4	0.21 – 0.48	0.16 – 0.53
IPCC A2	2.0 – 5.4	0.23 – 0.51	0.18 – 0.56
Rahmstorf, 2007	-	Up to 1.4 m	Up to 1.4 m

Table A2 Projected increases in global mean surface temperature and global mean sea level. Projections are taken from IPCC (2013) and are relative to 1986-2005. [Referenced as Table 2.4 in text.]

		2046 – 2065		**2081 – 2100**	
Variable	**Scenario**	**Mean**	**Likely range**	**Mean**	**Likely range**
Global Mean Surface Temperature Change(°C)	RCP2.6	1.0	0.4 – 1.6	1.0	0.3 – 1.7
	RCP4.5	1.4	0.9 – 2.0	1.8	1.1 – 2.6
	RCP6.0	1.3	0.8 – 1.8	2.2	1.4 – 3.1
	RCP8.5	2.0	1.4 – 2.6	3.7	2.6 – 4.8
Variable	Scenario	Mean	Likely range	Mean	Likely range
Global Mean Sea Level Rise (m)	RCP2.6	0.24	0.17 – 0.32	0.40	0.26 – 0.55
	RCP4.5	0.26	0.19 – 0.33	0.47	0.32 – 0.63
	RCP6.0	0.25	0.18 – 0.32	0.48	0.33 – 0.63
	RCP8.5	0.30	0.22 – 0.38	0.63	0.45 – 0.82

B. Tropical cyclones

Projections relating to intensities suggest the following:

- Simulations with high resolution dynamical models and statistical-dynamical models consistently find that greenhouse warming causes tropical cyclone intensity to shift towards stronger storms by the end of the 21st century (2 to 11% increase in mean maximum wind globally).

- Applying 21st century sea surface temperature projections to statistical relationships between local or relative SST and tropical cyclone power dissipation, suggests power dissipation increasing by about 300% in the next century for one relationship but suggesting no change in the other relationship. Both relationships can be reasonably defended based on physical arguments but it is not clear which, if either is current.

- When simulating 21st century warming under A1B, the present models and downscaling techniques suggest increases in intensity and fraction increases in the number of most intense storms. Of concern however is the limited ability of global models to accurately simulate upper-tropospheric wind which modulates vertical wind shear and tropical cyclone genesis and intensity evolution.

1. BACKGROUND

1.1 Introduction

The Caribbean region has been characterized as among the most vulnerable to climate change and climate extremes. This is in the context of limited natural and human resources, restricted lands, densely populated urban and coastal areas, economic dependence on international funders, and heavy reliance on fragile sectors such as tourism. In response, small island states are compelled to undertake assessments towards characterizing present and future climate trends, evaluating possible impacts and proposing possible adaptation and mitigation strategies.

One of the major challenges facing island states is that posed by tropical cyclone events and sea level rise. Sea-level rise greatly impacts human activity near the coastal zone (IPCC, 2007) since in many cases the majority of human settlements, economic activity, infrastructure and services are located at or near the coast and local economies are often reliant on just a few sectors such as tourism and agriculture (Nicholls, 1998). Sea level rise therefore exacerbates the vulnerability of coastal regions to other physical processes (e.g. storm surges, storm waves). Another direct influence of sea-level rise is the inundating of low level coastal areas which is of concern. It is anticipated however that ocean waves and storm surges of the future will exhibit changes in characteristics from the present climate and are the dynamic side issue of climate change. It is necessary to seriously consider the impacts of these dynamic phenomena for coastal disaster prevention and reduction, if extreme weather events will become stronger than those in the present climate (Mori et al., 2010).

This review examines the current state of knowledge of trends in (i) sea level rise, and (ii) tropical cyclone intensities. The report concentrates on these factors since the relative sea level and its rise over time influences the extent to which the surge and wave heights generated by hurricanes impact coastal areas. In the past relative sea level rise was included in coastal protection design by raising design water levels an amount equivalent to the relative sea level rise. But surge generation and propagation are nonlinear processes and linear addition of relative sea level rise to design water levels underestimates the impact in many areas. In addition to the surge elevation, wave heights also increase with water level in coastal areas where wave height is limited by water depth.

1.2 SRES and RCP Scenarios

Long term projections discussed in this report are premised on assumptions made with respect to human activities or natural effects that could alter the climate over decades and centuries. Future anthropogenic emissions of greenhouse gases (GHG), aerosol particles and other forcing agents such as land use change are dependent on socio-economic factors, and may be affected by global geopolitical agreements to control those emissions to achieve mitigation. The Intergovernmental Panel on Climate Change (IPCC) Fourth Assessment Report (AR4) made extensive use of the SRES scenarios that do not include additional climate initiatives, which means that no scenarios were included that explicitly assume implementation of the United Nations Framework Convention on Climate Change (UNFCCC) or the emissions targets of the Kyoto Protocol. However, GHG emissions are directly affected by non-climate change policies designed for a wide range of other purposes. The SRES scenarios were developed using a sequential approach, i.e., socio-economic factors fed into emissions scenarios, which were then used in simple climate models to determine concentrations of greenhouse gases, and other agents required to drive the more complex atmosphere-ocean global climate models. The SRES scenarios were labelled A1, A2, B1 and B2, describing the relationships between the forces driving greenhouse gas and aerosol emissions and their evolution during the 21st century for large world regions and globally. Each storyline represents different demographic, social, economic, technological, and environmental developments that diverge in increasingly irreversible ways (Nakicenovic et al., 2000). See Figure 1.1 and Table 1.1.

In the IPCC Fifth Assessment Report (AR5), outcomes of climate simulations that use new scenarios (some of which include implied policy actions to achieve mitigation) referred to as "Representative Concentration Pathways" (RCPs) are assessed. These RCPs represent a larger set of mitigation scenarios and were selected to have different targets in terms of radiative forcing at 2100 (about 2.6, 4.5, 6.0 and 8.5 Wm^{-2}). They are defined by their total radiative forcing (cumulative measure of human emissions of greenhouse gases from all sources expressed in Watts per square metre) pathway and level by 2100. The scenarios should be considered plausible and illustrative, and do not have probabilities attached to them.

The SRES scenarios resulted from specific socio-economic scenarios from storylines about future demographic and economic development, regionalization, energy production and use, technology, agriculture, forestry and land use (IPCC, 2000). The RCPs are new scenarios that specify concentrations and corresponding emissions, but not directly based on socio-economic storylines like the SRES scenarios. The four RCP scenarios are identified by the 21st century peak or stabilization value of the RF derived from the reference model (in Wm^{-2}). Table 1.1 provides a summary of the RCPs.

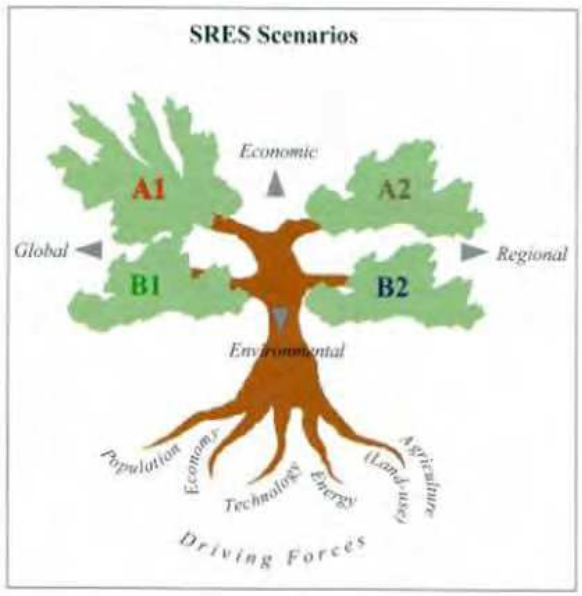

Figure 1.1: Schematic illustration of the four SRES storylines

Table 1.1 Summary of SRES Storylines.

SRES scenario family	Storylines
A1	A future world of very rapid economic growth, global population that peaks in mid-century and declines thereafter, and rapid introduction of new and more efficient technologies. A1FI (fossil intensive), A1T (predominantly non-fossil) and A1B (balanced across energy sources).
A2	A very heterogeneous world with continuously increasing global population and regionally oriented economic growth that is more fragmented and slower than in other storylines
B1	A convergent world with the same global population as in the A1 storyline but with rapid changes in economic structures toward a service and information economy, with reductions in material intensity, and the introduction of clean and resource-efficient technologies.
B2	A world in which the emphasis is on local solutions to economic, social, and environmental sustainability, with continuously increasing population (lower than A2) and intermediate economic development.

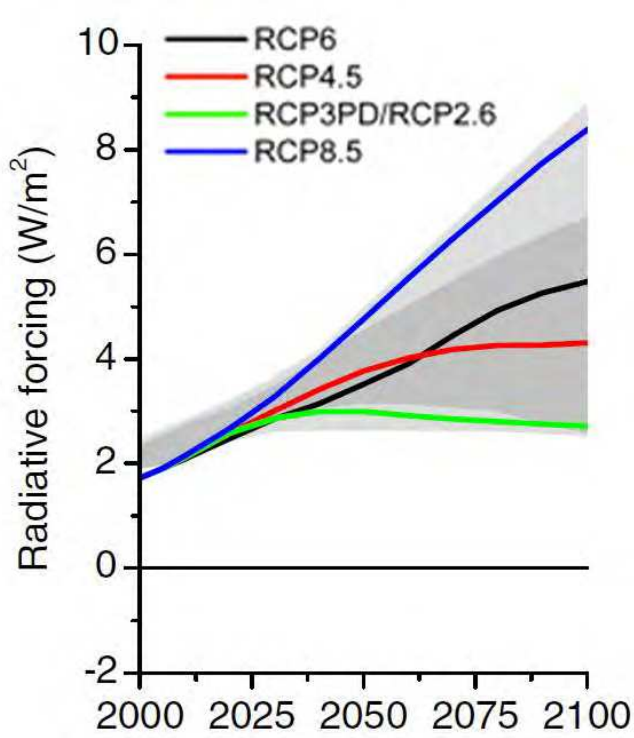

Figure1.2: Radiative Forcing of the Representative Concentration Pathways. Taken from van Vuuren et al (2011). The light grey area captures 98% of the range in previous IAM scenarios, and dark grey represents 90% of the range.

Table 1.2 Descriptions of the Representative Concentration Pathway (RCP) Scenarios.

RCP	Comments	Radiative Forcing Behaviour
RCP2.6	Lowest	Peaks at 3 Wm^{-2} and then declines to approximately 2.6 Wm^{-2}
RCP4.5	Medium-low	Stabilization at 4.5 Wm^{-2}
RCP6	Medium-high	Stabilization at 6 Wm^{-2}
RCP8.5	Highest	RF of 8.5 Wm^{-2} by 2100 but implies rising RF beyond 2100

2. SEA LEVEL RISE

2.1 Introduction

Global sea levels have risen through the 20th century. The rising levels are expected to accelerate through the 21st century and beyond because of global warming, but their magnitude remains uncertain. Key uncertainties include the possible role of the Greenland and West Antarctic ice sheets and the amplitude of regional changes in sea level. In many areas, non-climatic components of relative sea level change (mainly subsidence) can also be locally appreciable. Cooper and Pilkey (2004) suggests that factors which cause changes in the morphology of coasts are numerous and include sediment supply, variations in wave energy, tidal currents, wind action, sediment type, tidal inlet dynamics, morphological feedback, etc. Therefore isolating the influence of sea-level rise from these other factors is perhaps the biggest challenge in discerning the impact of sea level rise.

2.2 Causes

Two main factors contribute to SLR: (i) thermal expansion of sea water due to ocean warming and (ii) water mass input from land ice melt and land water reservoirs. Thermal expansion is the physical response of the water mass of the oceans to atmospheric warming. Ocean temperature data collected during the past few decades indicate that ocean thermal expansion has significantly increased during the second half of the 20th century. Thermal expansion accounts for about 25% of the observed SLR since 1960 (Domingues et al., 2008) and about 50% from 1993 to 2003 (for e.g. IPCC 2007, Nicholls and Cazenave 2010). Ice sheets have the largest potential effect, because their complete melting would result in a global sea-level rise of about 70 m. Yet their dynamics are poorly understood, and the key processes that control the response of ice flow to a warming climate are not included in current ice sheet models. The interplay of these factors and their action on different timescales makes understanding of global sea level rise dynamics very difficult.

The mechanism of thermal expansion can be gauged relatively accurately through an analysis of global temperatures and their rate of increase through GCMs. However, there is a great uncertainty in predicting the melting rate of the ice sheets and ice caps. Analysis of observed data suggests that the decay rate of ice sheets is non-linear. Simpson et al (2009) further highlights that rapid collapses of ice sheets have occurred previously that bear no correlation, whether contemporaneous or lagged, to any climate forcing that may have triggered it.

2.3 Current Trends

2.3.1 Global

Using proxy and instrumental data, it is virtually certain (i.e. with 99-100% probability) that the rate of global mean sea level rise has accelerated during the last two centuries, marking the transition from relatively low rates of change during late Holocene (order tenths of mm yr^{-1}) to modern rates (order mm $year^{-1}$). Rates and absolute changes in global mean sea level are shown in Table 2.1

Table 2.1 Rates and absolute change in mean sea level. Rates are obtained from IPCC (2013).

Period	Rate (mm yr^{-1})	Total sea level rise	IPCC Likelihood
1901 – 2010	1.7 ± 0.2	0.19 ± 0.02	Very likely
1971 – 2010	2.0 ± 0.2	-	Very likely
1993 – 2010	3.2 ± 0.4	-	Very likely

Tide-guage and satellite altimeter data both reflect the rate represented in the 1993-2010 period. It is likely that rates similar to this period also occurred between 1930 and 1950. It is also likely that global mean sea level has accelerated since the early 1900s, with estimates ranging from 0.000 to 0.013 [-0.002 to 0.019] mm yr^{-2} (IPCC, 2013). Accelerations in the rate of increase over the 20th century are have been detected in most regions. See for example Woodworth et al. (2009), and Church and White (2006)

2.3.2 Caribbean

Estimates of observed sea level rise from 1950 to 2000 suggest that sea level rise within the Caribbean appears to be near the global mean. Table 2.2 shows the rates of sea level rise for a number of locations in the Caribbean. All values suggest an upward trend. It is important to note that due to shifting surface winds, expansion of warming ocean water and the addition of melting ice, ocean currents can be altered which, in turn leads to changes in sea level that vary from place to place. Additionally more localized processes such as sediment compaction and tectonics may also contribute to additional variations in sea level.

Table 2.2 Observed rates of sea level rise for some Caribbean stations. Source: The State of the Jamaican Climate (2013).

Tidal gauge Station	Observation Period	Rates (mm yr^{-1})
Bermuda	1932 –2006	2.04 ± 0.47
San Juan, Puerto Rico	1962 –2006	1.65 ± 0.52
Guantanamo Bay, Cuba	1973 –1971	1.64 ± 0.80
Miami Beach, Florida	1931 –1981	2.39 ± 0.43
Vaca Key, Florida	1971 –2006	2.78 ± 0.60

2.4 Projected Trends

2.4.1 Global and Caribbean

Estimates of future global mean sea level were obtained from observations and GCM results reported by IPCC Working Group1 for IPCC Fourth and Fifth Assessment Reports (IPCC 2007, IPCC 2013). According to the Fourth Assessment Report by the end of the century, sea levels are also expected to rise by 0.21m to 0.48m under an A1B (medium emissions) scenario or by 0.26-0.59 m under the highest emissions scenario, A1F1, but the models exclude future rapid dynamical changes in ice flow. One study suggests that the rate of rise may actually double as noted for A1B (Science Daily, Feb. 12, 2008).

Higher projections of sea level rise are noted in the IPCC Fifth Assessment Report (AR5) in comparison to the Fourth Assessment Report (AR5). This is considered to be primarily due to the improved modeling of land-ice contributions. There is also higher confidence in the projections of sea level rise in the latter report due to improved understanding of the components of sea level, improved agreement of process-based models with observations, and the inclusion of ice-sheet dynamical changes. Projections and Graph are shown below. In the RCP projections, thermal expansion accounts for 30 to 55% of the 21st century global mean sea level rise, and glaciers for 15 to 35%. AR5 notes that the basis for higher projections of global mean sea level was considered but it was concluded that there is currently insufficient evidence to evaluate the probability of specific levels above the assess *likely* rate. Finally the point is made in AR5 that sea level rise will not be uniform. It is *very likely* that sea level will rise in more than about 95% of the ocean area. Approximately 70% of the coastlines worldwide are projection to experience sea level change within 20% of the global mean sea level change.

It is useful to note that for the SRES A1B which was assessed in AR4, the likely range bases on the science assessed in the AR5 is 0.60 [0.41-0.79] m by 2100 relative to 1986-2005 and 0.57 [0.40-

0.75]m by 2090-2099 relative to 1990. Compared with the AR4 projection of 0.21-0.48 m for the same scenario and period, the largest increase is from the inclusion of rapid changes in Greenland and Antarctic ice-sheet outflow.

Table 2.3 Projected increases in global mean surface temperature and global and Caribbean mean sea level from the IPCC (2007) contrasted with those of Rahmstorf (2007). Projections are by 2100 relative to 1980-1999. Source: CARIBSAVE Climate Change Risk Atlas – Jamaica (2011).

Scenario	**Global mean surface temperature (°C)**	**Global mean sea level rise (m)**	**Caribbean mean sea level rise (±0.05 m) relative to global mean**
IPCC B1	1.1 – 2.9	0.18 – 0.38	0.14 – 0.43
IPCC A1B	1.7 – 4.4	0.21 – 0.48	0.16 – 0.53
IPCC A2	2.0 – 5.4	0.23 – 0.51	0.18 – 0.56
Rahmstorf, 2007	-	Up to 1.4 m	Up to 1.4 m

Table 2.4 Projected increases in global mean surface temperature and global mean sea level. Projections are taken from IPCC (2013) and are relative to 1986-2005.

		2046 – 2065		**2081 – 2100**	
Variable	**Scenario**	**Mean**	**Likely range**	**Mean**	**Likely range**
Global Mean Surface Temperature Change(°C)	RCP2.6	1.0	0.4 – 1.6	1.0	0.3 – 1.7
	RCP4.5	1.4	0.9 – 2.0	1.8	1.1 – 2.6
	RCP6.0	1.3	0.8 – 1.8	2.2	1.4 – 3.1
	RCP8.5	2.0	1.4 – 2.6	3.7	2.6 – 4.8
Variable	Scenario	Mean	Likely range	Mean	Likely range
Global Mean Sea Level Rise (m)	RCP2.6	0.24	0.17 – 0.32	0.40	0.26 – 0.55
	RCP4.5	0.26	0.19 – 0.33	0.47	0.32 – 0.63
	RCP6.0	0.25	0.18 – 0.32	0.48	0.33 – 0.63
	RCP8.5	0.30	0.22 – 0.38	0.63	0.45 – 0.82

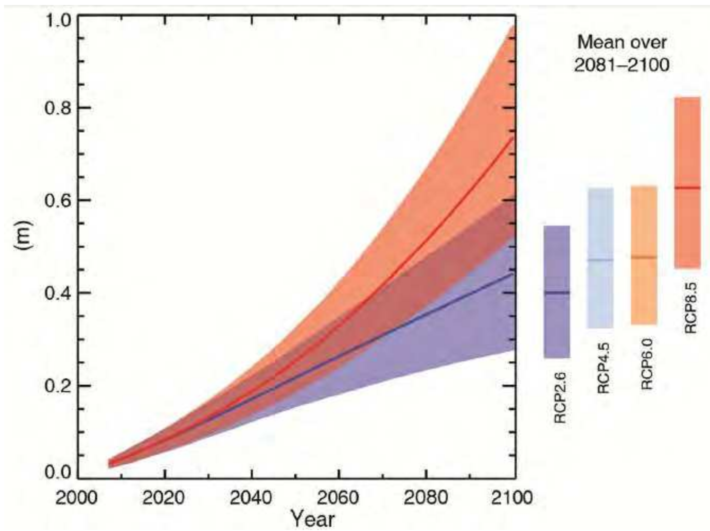

Figure 2.1 Projections of global mean sea level rise over the 21st century relative to 1986–2005 from the combination of the CMIP5 ensemble with process-based models, for RCP2.6 and RCP8.5. The assessed *likely* range is shown as a shaded band. The assessed *likely* ranges for the mean over the period 2081–2100 for all RCP scenarios are given as coloured vertical bars, with the corresponding median value given as a horizontal line.

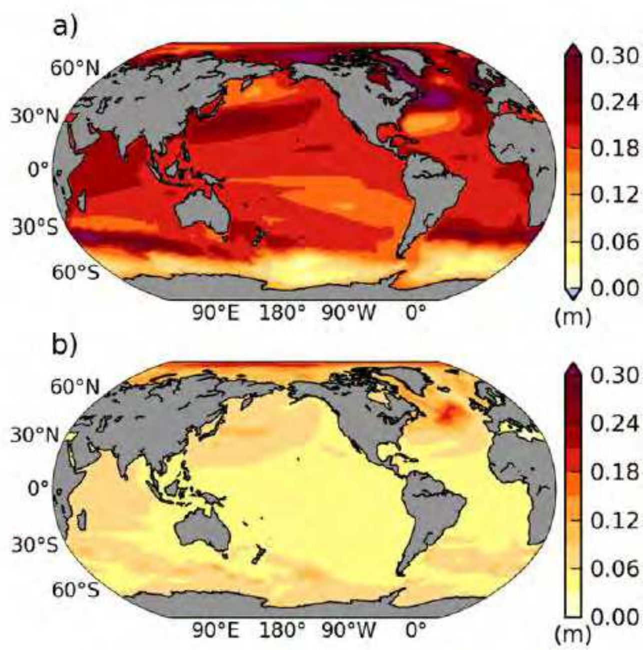

Figure 2.2 (a) Ensemble mean projection of the time-averaged dynamic and steric[1] sea level changes for the period 2081–2100 relative to the reference period 1986–2005, computed from 21 CMIP5 climate models (in m), using the RCP4.5 experiment. The figure includes the globally averaged steric sea level increase of 0.18 ± 0.05 m. (b) RMS spread (deviation) of the individual model result around the ensemble mean (m). Source: IPCC AR5.

[1]The term 'steric' pertains to the temperature, salinity and pressure dependent specific volume of the ocean. (Lauderer et al. 2006)

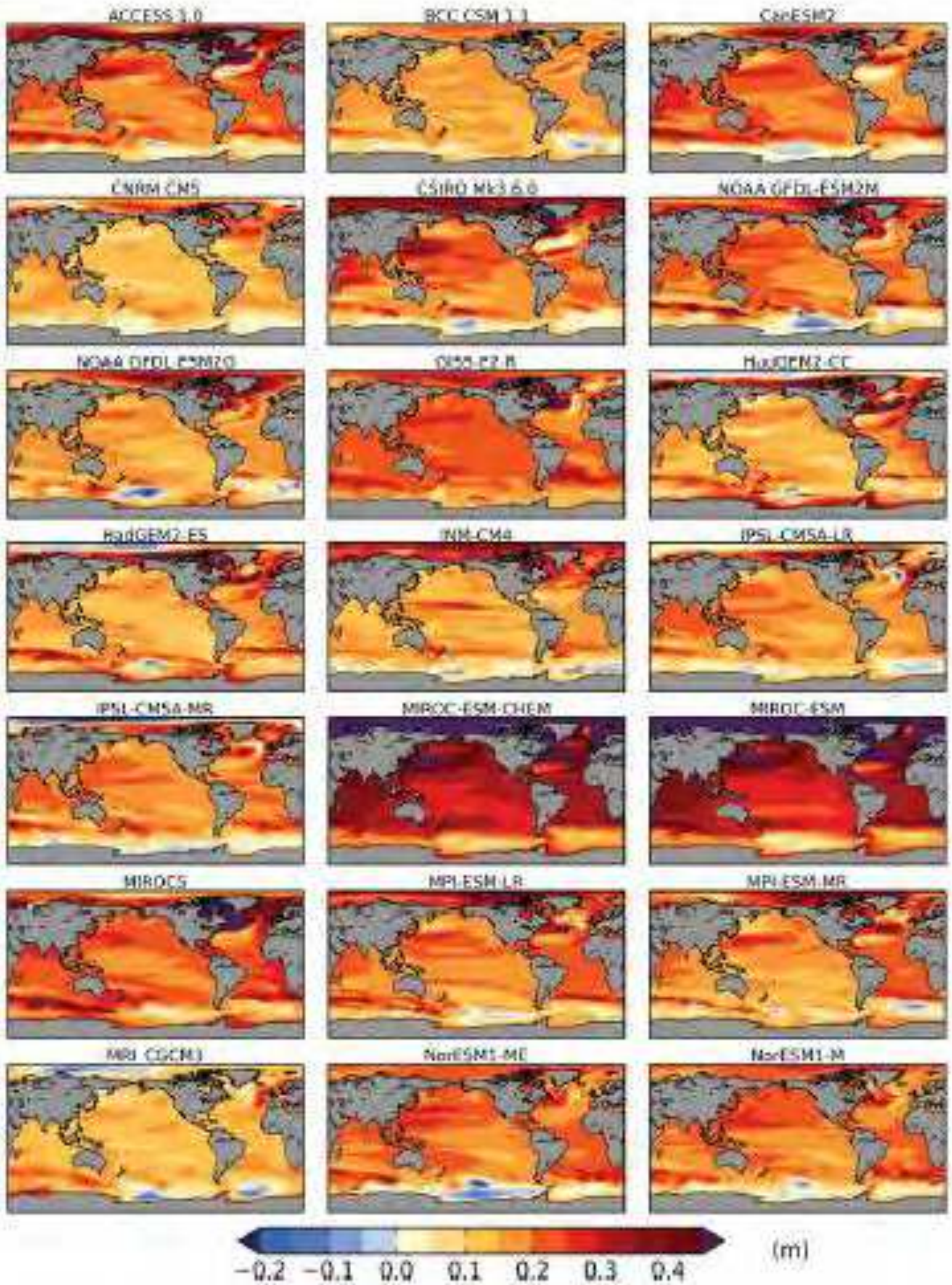

Figure 2.3: Projected relative sea level change (in m) from the combined global steric plus dynamic topography and glacier contributions for the RCP4.5 scenario over the period from 1986–2005 to 2081–2100 for each individual climate model used in the production of Figure 2.2 Source: IPCC AR5.

2.5 Observations and Projections of Sea Level Extremes

2.5.1 Observations of sea level extremes

Tsunamis aside, extremes in sea level (i.e. coastal flooding, storm surge, high water events, etc.) tend to be caused by large storms, especially when they occur at times of high tide. In fact any low pressure system off shore with associated high winds can cause a coastal flooding event depending on duration and direction of winds. Table 2.5 highlights several examples of major storms impacting the US east coast and shows the peak pressure, storm size, continental slope and storm surge measurements. The table highlights that the maximum sustained wind (represented by the category of the storm) is not necessarily a good indication of storm surge values, though some correlation exists between the two.

Table 2.5: Major storms affecting the east coast of the United Sates from 1970-2005. Adapted from Irish et al. (2008)

Storm Date (Name)	Central pressure (mb)	Radius to maximum wind (km)	Saffir-Simpson Category	Estimated influencing continental shelf slope	Observed open coast surge (m)
July 1970 (Celia)	944	17	3	1:800-1:1,100	2.7 - 2.8
August 1974 (Carmen)	943	28	3	1:2,500	
August 1979 (Frederic)	950	46	3	1:1,500-1:1,900	3.5 - 3.8
July 1980 (Allen)	945	37	3	1:800-1:1,100	2.1 - 3.7
August 1992 (Andrew)	949	30	5	1:750-1:1,500	2.4
October 1995 (Opal)	940	69	3	1:750-1:1,000	3.1 - 3.7
August 1999 (Bret)	953	19	3	1:800-1:1,100	0.9 - 1.5
September 2002 (Lili)	966	28	1	1:4,000-1:7,500	3.2 - 3.6
September 2004 (Charley)	950	19	4	1:500-1:1,000	2.1
September 2004 (Ivan)	955	56	3	1:1,500-1:1,900	3.0 - 3.1
July 2005 (Dennis)	952	11	3	1:750-1:1,500	1.7 - 2.5
August 2005 (Katrina)	919	47	3	1:5,000-1:10,000	7.5 - 8.5

September 2005 (Rita)	946	40	3	1:2,500-1:3,000	3.0 - 4.6
October 2005 (Wilma)	951	73	3	1:500-1:1,000	1.8 - 2.4

The AR4 noted that highest water levels have been increasing since the 1950s in most regions of the world, caused mainly by increasing mean sea level. Higher regional extremes are also associated with climate fluctuations such as ENSO, the North Atlantic Oscillation and the Atlantic Multidecadal Oscillation, among others. Since the publication of AR4 most analyses have focused on specific regions and find that extreme values have increased since the 1950s, using various statistical measures such as annual maximum surge, annual maximum surge-at-high-water, monthly mean high water level, changes in number of high storm surge events or changes in the 99th percentile events. Global analysis of tide gauge data that spans 1970s to the present, also suggests that the magnitude of extreme sea level events has increased in all regions studies. The height of a 50-year flood event has increased anywhere from 2 to more than 10 cm per decade since 1970 although some areas have seen a negative rate because of the vertical land motion is much larger than the rate of mean sea level rise.

The height of a 50-year flood event has increased anywhere from 2 to more than 10 cm per decade since 1970 (Figure 2.4a), although some areas have seen a negative rate because vertical land motion is much larger than the rate of mean sea level rise. However, when the annual median height at each gauge is removed to reduce the effect of local mean sea level rise, interannual and decadal fluctuations, and vertical land motion, the rate of extreme sea level change drops in 49% of the gauges to below significance (Figure 2.4b), while at 45% it fell to less than 5 mm yr^{-1}. Only 6% of tide gauge records evaluated had a change in the amplitude of more than 5 mm yr^{-1} after removing mean sea level variations, mainly in the southeast United States, the western Pacific, southeast Asia, and a few locations in northern Europe. The higher rates in the southeastern United States have been linked to larger storm surge events unconnected to global sea level rise (Grinsted et al., 2012, IPCC, 2013).

2.5.2 Projections of Sea Level Extremes

Lowe et al. 2010 suggest that increases in the observed sea level extremes in the 20th century and increases projected for the 21st century occur mainly through an increase in mean sea level.

Projected changes in storm surges (relative to mean sea level) have been assessed by applying climate-model forcing to storm-surge models. Return periods of sea level extremes, exceeding a given threshold level, referred to as return levels, are used in quantifying projected changes. Table 2.6 summarizes the results of studies examining projections of sea level extremes. The results show that projections are sensitive to the choice of global climate model or regional climate model.

Table 2.6 Summary of studies examining projections of sea level extremes. Compiled from IPCC (2013).

Tool	Scenario	Result	Reference
Regionally downscaled GCM	A2, B2, A1B	8–10% increase in the 99th percentile surge heights between 1961-90 and 2071-2100, mainly during the winter season along the coastlines of the eastern North Sea and the northwestern British Isles, and decreases south of Iceland.	Debernard and Roed (2008)
Downscaled GCM	A1B	Significant increase in wintertime storm surges around most of Ireland between 1961–1990 and 2031–2060	Wang et al. (2008)
3 climate models	A2	Changes in the 95th percentile sea level height across the southern Australian coast in 2081–2100 compared to 1981–2000 were small (±0.1 m), mostly negative, and despite some inter-model differences, resembled the changes in wind patterns simulated by the climate models	Colberg and McInnes (2012)
Numerical ocean model	-	For the tropical east coast of Australia, a 10% increase in tropical cyclone intensity for 2050 led to increases in the 100-year return level (including tides) that at most locations were smaller than 0.1 m	e.g. McInnes et al. (2013)
GCM		Sea level rise has a greater potential than meteorological changes to increase sea level extremes by the end of the 21st century for southeastern coast of Australia, eastern Irish Sea, North Sea and the United Kingdom coast	Brown et al. (2010) Woth et al. (2006) Lowe et al. (2009)
RCM	A2	The combined effect of MSL rise of 4 mm/yr and RCM projections for winds and atmospheric pressure gave an increase in 100-year return levels of total sea level (including tides) between 0.40–0.67 m (about 15–20%) along the northern part of the east coast of India, except around the head of the bay for 2071–2100 compared to 1961–1990.	Unnikrishnan et al. (2011)
Numerical surge and wave models	-	The effect of MSL rise on simulated surges was linear. Yet in the regions of moderate surges (2–3 m), particularly in wetland-fronted areas, the increase in surges was larger by 1–3 m than the present values. They showed that sea level rise alters the speed of propagation of surges and their amplification in different regions of the coast.	Smith et al. (2010)

Statistical model	-	The dynamic interaction of surge and sea level rise lowered or amplified the surge at different points within a shallow coastal bay for the Gulf of Mexico. Higher mean sea levels can significantly decrease the return period for exceeding given threshold levels.	Mousavi et al. (2011)

For a network of 198 tide gauges covering much of the globe, Hunter (2012) determined the factor by which the frequency of sea levels exceeding a given height would be increased for a MSL rise of 0.5 m. The calculations were repeated in the AR5 using regional relative sea level projections and their uncertainty using the RCP4.5 scenario. This multiplication factor depends exponentially on the inverse of the Gumbel scale parameter (a factor which describes the statistics of sea level extremes caused by the combination of tides and storm surges) (Coles and Tawn, 1990). The scale parameter is generally large where tides and/or storm surges are large, leading to a small multiplication factor, and vice versa.

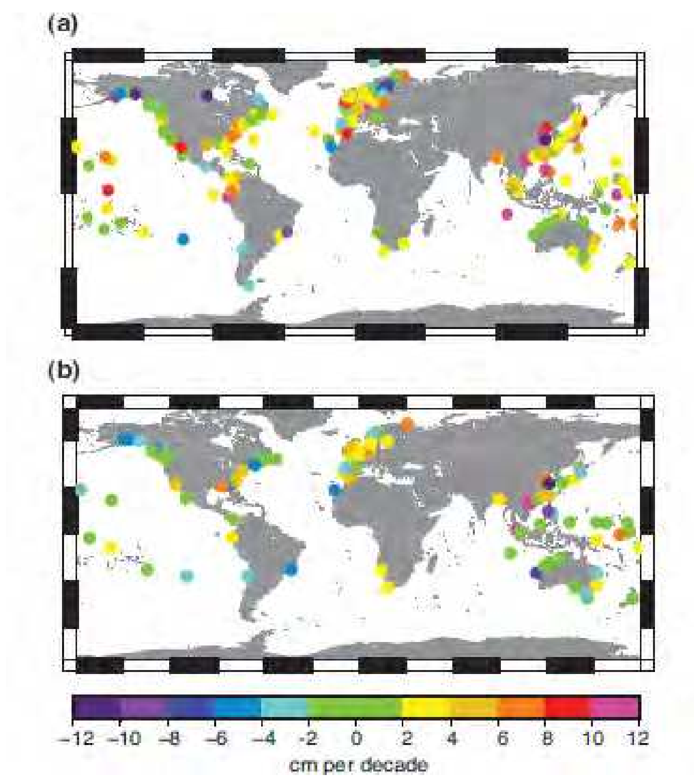

Figure 2.4: Estimated trends (cm per decade) in the height of a 50-year event in extreme sea level from (a) total elevation and (b) total elevation after removal of annual medians. Black dots indicate trends are not significant at the 95% confidence level. Data are from Menéndez and Woodworth (2010).

Another useful study is that of Ali (1996). The study showed that storm surge heights increase with an increase in wind speed and SST (Table 2.7). On the other hand, sea level rise tends to reduce the surge heights if wind speed remains constant. It is to be noted here that the model had a fixed boundary and as a result could not simulate the surge height for a moving shoreline. Sea level rise will convert the hitherto land area into a part of the sea which will then become a shallow water area where the surge will be amplified. Thus, although the sea level rise will apparently reduce the surge height in the present sea water, it will increase the surge height in the newly converted (from land to sea) sea area.

Table 2.7 Storm surge heights under different sea surface temperature and sea level rise scenarios. (Wind speed of 225 km h^{-1} corresponds to that of the April 1991 cyclone impacting Bangladesh.) Taken from Ali (1996).

	Current temp. (27°C)	2°C increase	4°C increase
Wind speed (km h^{-1})	225	248	275
Surge height in m (% change)			
Sea level rise = 0.0 m	7.6 (0)	9.2 (21)	11.3 (49)
Sea level rise = 0.3 m	7.4 (-3)	9.1 (20)	11.1 (46)
Sea level rise = 1.0 m	7.1 (-7)	8.6 (13)	10.6 (40)

Table 2.8 Storm surge under different sea level rise and sea surface temperature rise conditions. (Scenario I represents base condition that corresponds to wind speed and central pressure as observed during the 1991 cyclone) Derived from Emanuel (2005) and Ali (2000).

Climate Scenarios	Sea level rise (m)	SST rise (°C)	Wind speed (km/h)	Central pressure (hPa)	Surge height (m, mean sea level)
Scenario I	0.0	0	225	926	7.6
Scenario II	0.0	2	246	924	9.2
Scenario III	0.0	4	274	921	11.3
Scenario IV	0.3	0	225	926	7.4
Scenario V	0.3	2	246	924	9.1
Scenario VI	0.3	4	274	921	11.3
Scenario VII	1.0	0	225	926	7.1
Scenario VIII	1.0	2	246	924	8.6
Scenario IX	1.0	4	274	921	10.6

Karim and Mimura (2008) examined different scenarios of sea surface temperature and sea level rise increases and the impact they have on storm surge height (Table 2.8). Scenario I represents the base condition, while Scenario V is considered as an average climate condition by 2050. It shows that storm surge height may increase as much as 21% if SST rises by 2 °C (Scenario II) and 49% if SST rises by 4 °C (Scenario III). Another analysis based on continental shelf length and wind speed (Chowdhury, 1994) also produced similar surge heights at the coast. These predictions are relatively large compared with the results of Mitchell et al. (2006) in which they predicted 0.5–0.7m increase in surge height of a 50-year return period storm surge. It is interesting to note that surge height reduces by 7% if sea level rise by 1.0m, but SST remains unchanged (Scenario VII). The reason is that the amplification of the surge is less if the water depth is increased, due to the differences in bottom friction on the propagating waves.

2.6 Uncertainties

The range of uncertainty cones from a combination of emissions uncertainty and methodology uncertainty as follows:

- Emissions uncertainty arises because the future is uncertain and there are a range of plausible futures (with respect to for example technologies and energy requirement). This is addressed by presenting results for a range of projections that attempt to cover the range of plausible futures.
- Methodological uncertainty arises because of the inability to create perfect models of the climate system even if future emissions were known. Additionally some processes depend on parameters that have not yet been accurately measured or one may discover are entirely missing from the models. This uncertainty is addressed by either running simple models for a range of climate sensitivities or by looking at a range of values from the few available complex climate models.

3. Tropical Cyclones

3.1 Hurricane Metrics

Several publications and reports outline the damage sustained by countries due to hurricanes during the annual North Atlantic hurricane season throughout history. It is not surprising then, the initiative shown by several institutions to characterize and, thus, predict the yearly trend. Institutions such as the National Oceanic and Atmospheric Administration (NOAA) have led research into hurricane dynamics and have developed several important tools and datasets that are used today to characterize hurricane activity. This report highlights two metrics for intensity (accumulated cyclone energy [ACE], power dissipation index [PDI]). In addition to intensity, it should be noted that the structure and areal extent of the wind field in tropical cyclones is largely independent of intensity and play an important role on potential impacts, particularly from storm surge (Irish and Resio, 2010), but measures of storm size are largely absent in historical data

3.1.1 Accumulated Cyclone Energy (ACE)

The ACE proposed by the National Oceanic and Atmospheric Administration (NOAA) is defined as the sum of squares of the maximum sustained wind speed in knots (v_{max}) measured every six hours for all named storms while they are at least tropical storm strength (Bell et al. 2000). The ACE is calculated by the formula below and is of the order of 10^4 kt^2.

(1)

NOAA classifies a season as above-normal, normal or below-normal as illustrated in Figure.3.1:

- Above-normal: above $111x10^4$ kt^2 (corresponding to 120% of the 1981-2010 median), 13 or more named storms, 4 or more hurricanes, 3 or more major hurricanes
- Below-normal: below $66x10^4$ kt^2 (corresponding to less than 71.4% of the 1981-2010 median), 9 or fewer named storms, 4 or fewer hurricanes, 1 or fewer major hurricanes.
- Near-normal: ACE values lies in the range of $66x10^4$ - $111x10^4$ kt^2 (between 71.4%-120% of the 1981-2010 median), 10-15 named storms, 4-9 hurricanes, 1-4 major hurricanes.

  Klotzbach (2006) suggests that the ACE is proportional to the kinetic energy generated by the storm.

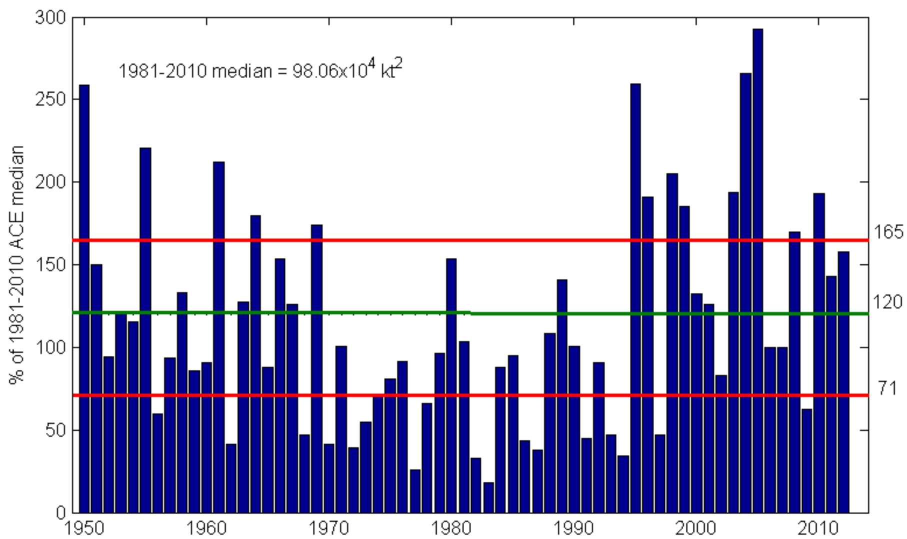

Figure 3.1 Showing the total ACE value per year as a percentage of the 1981-2010 median for the period 1950-2012. Years falling above 120% are considered to be above-normal, years falling in between 71 - 120% are considered to be normal activity, while years falling below an 71% are considered to have below-normal activity. Years exceeding 165% is deemed to be very active.

3.1.2 Power Dissipation Index (PDI)

Emanuel (2005) introduced the power dissipation index (PDI), the cubed of the maximum sustained wind speed at the standard altitude of 10 m, integrated over the lifetime of the storm. Theory provides that a hurricane loses power at a rate per unit area of

(2)

where ρ is the air density, C_D is the surface drag coefficient and V is the surface wind speed (Emanuel, 1998). Assuming a circularly symmetric hurricane, the dissipative rate D is integrated over the radius (from the center to an outer limit r_0) and over the lifetime τ of the storm to give the total power dissipation PD, shown below.

(3)

The equation is further simplified due to unavailability of accurate records of hurricane radii and the variability of C_D and ρ within the radius of maximum wind speeds. Another limitation is that there is very little relation between the peak winds and the size of the hurricane (Emanuel, 2005), and so may provide a less than accurate picture of the intensity of the storm. Taking the values for the drag coefficient and sea-level air density to be constant, the final equation arises as:

(4)

It is however important to note that both ACE and PDI are based on the assumption that velocity varies linearly with radius inside the radius of maximum winds. Yu et al (2009) point out that the radial wind structure within a tropical cyclone varies and that the formulae proposed for the two indices results in an overestimation of the total activity. For this reason, both indices were revised (Yu et al., 2009; Yu and Chiu, 2012).

The revised ACE (RACE) and revised PDI (RPDI) indices are constructed based on a modified Rankine vortex structure proposed by Yu et al(2009). The algorithm outlining their construction is described in detail in Appendix A. The RACE index and RPDI index are defined by equations (5) and (6), respectively.

(5)

(6)

where is the cut-off radius (dimensionless) in which the wind energy is measured and is the decaying tendency of wind beyond the radius of maximum wind. Like the ACE and PDI indices, the revised versions are strongly influenced by strong tropical cyclones. This is due to the inclusion of the intensity and duration of the storms, and is thus a better indicator of the strength of the storms within a given season. Yu and Chiu (2009) concludes that the ACE, PDI, RACE and RPDI indices may not give a clear trend in frequency. These metrics have recently become a popular tool of characterizing overall hurricane activity. However, no publications as of yet outlines the use of the revised metrics in projections of future tropical cyclone activity. Additionally, Klotzbach (2006) notes that ACE and PDI correlate globally at 0.97. Therefore to examine the trend in either index at the global level should yield virtually the same results.

3.2 Current trends in North Atlantic Hurricane intensities

Intensity measures in historical records are especially sensitive to changing technology and improving methodology. Over the satellite era however, increases in the intensity of the strongest storms in the Atlantic are quite robust (Kossin et al., 2007; Elsner et al. 2008). Time series of cyclone indices such as power dissipation show upward trends in the North Atlantic since the late 1970s (Emmanuel, 2007) but interpretation of longer-term trends is constrained by data quality concerns (Landsea et al., 2012). The AR5 notes that evidence suggests a virtually certain increase in the frequency and intensity of the strongest cyclones in the Atlantic since the 1970s. Wu et al. (2008) suggest that the magnitude of the statistically significant linear trend in PDI over 1975-2004 is 0.024 $m^3 s^{-3} year^{-1}$. It is further noted that the average lifetime of North Atlantic tropical cyclones show an increasing trend of 0.07 day $year^{-1}$ for the same period which is statistically significant. The variability and trend in power dissipation can be related to sea surface temperature and other local factors such as tropopause temperature and vertical wind shear (Emanuel, 2007), but there is debate to whether local sea surface temperature or the difference between local sea surface temperature and mean tropical sea surface temperature is the more physically relevant metric (Swanson, 2008). The distinction becomes important when making projections of changes in power dissipation based on projections of SST changes particularly in the tropical Atlantic where SST has been increasing more rapidly than in the tropics as a whole (Vecchi et al., 2008). ACE has shown declines globally since reaching a high point in 2005, and is presently at a 40 year low point (Maue, 2009) (IPCC SREX 2012).

3.3 Projected trends in North Atlantic frequencies and intensities

The AR4 concluded that a range of modeling studies project a likely increase in peak wind intensity and near storm precipitation in future tropical cyclones. Simulations with high resolution dynamical models (e.g. Oouchi et al., 2006; Bengtsson et al., 2007; Gualdi et al., 2008; Knutson et al., 2008; Sugi et al., 2009; Bender et al., 2010) and statistical-dynamical models (Emanuel, 2007) consistently find that greenhouse warming causes tropical cyclone intensity to shift towards stronger storms by the end of the 21^{st} century (2 to 11% increase in mean maximum wind globally).

Applying 21^{st} century sea surface temperature projections to a relationship between local SST and tropical cyclone power dissipation (constructed by Emmanuel, 2007), power dissipation is projected to increase by about 300% in the next century (Vecchi et al., 2008; Knutson et al., 2010). Alternatively when using a similar strong relationship between power dissipation and relative SST (which represents the difference between local and tropical mean SST), projections indicate almost no change in power dissipation in the next century (Vecchi et al., 2006). Both relationships can be reasonably defended based on physical arguments but it is not clear which, if either is current (Ramsay and Sobel, 2011).

When simulating 21st century warming under A1B, the present models and downscaling techniques suggest increases in intensity and fraction increases in the number of most intense storms. The frequency of the most intense storms is more likely than not to increase by more than +10% (IPCC 2013, AR5), while the annual frequency of tropical cyclones are projected to decrease or remain relatively unchanged for the North Atlantic (See Figure 3.2). Of concern however is the limited ability of global models to accurately simulate upper-tropospheric wind (Cordero and Forster, 2006) which modulates vertical wind shear and tropical cyclone genesis and intensity evolution.

Knutson et al (2013) conclude that there is likely to be an increase in radius-averaged precipitation rainfall rates near the hurricane core. The conclusion follows from an expected increase in atmospheric water-vapour content, and thus an increase in moisture convergence that results in convective systems, such as hurricanes. Increases of approximately 20% are projected for radii within 100km from the hurricane core. However, an accurate quantification of positive changes for smaller radii prove to be difficult due to complex dynamics near the centre of the hurricane (Knutson et al, 2010).

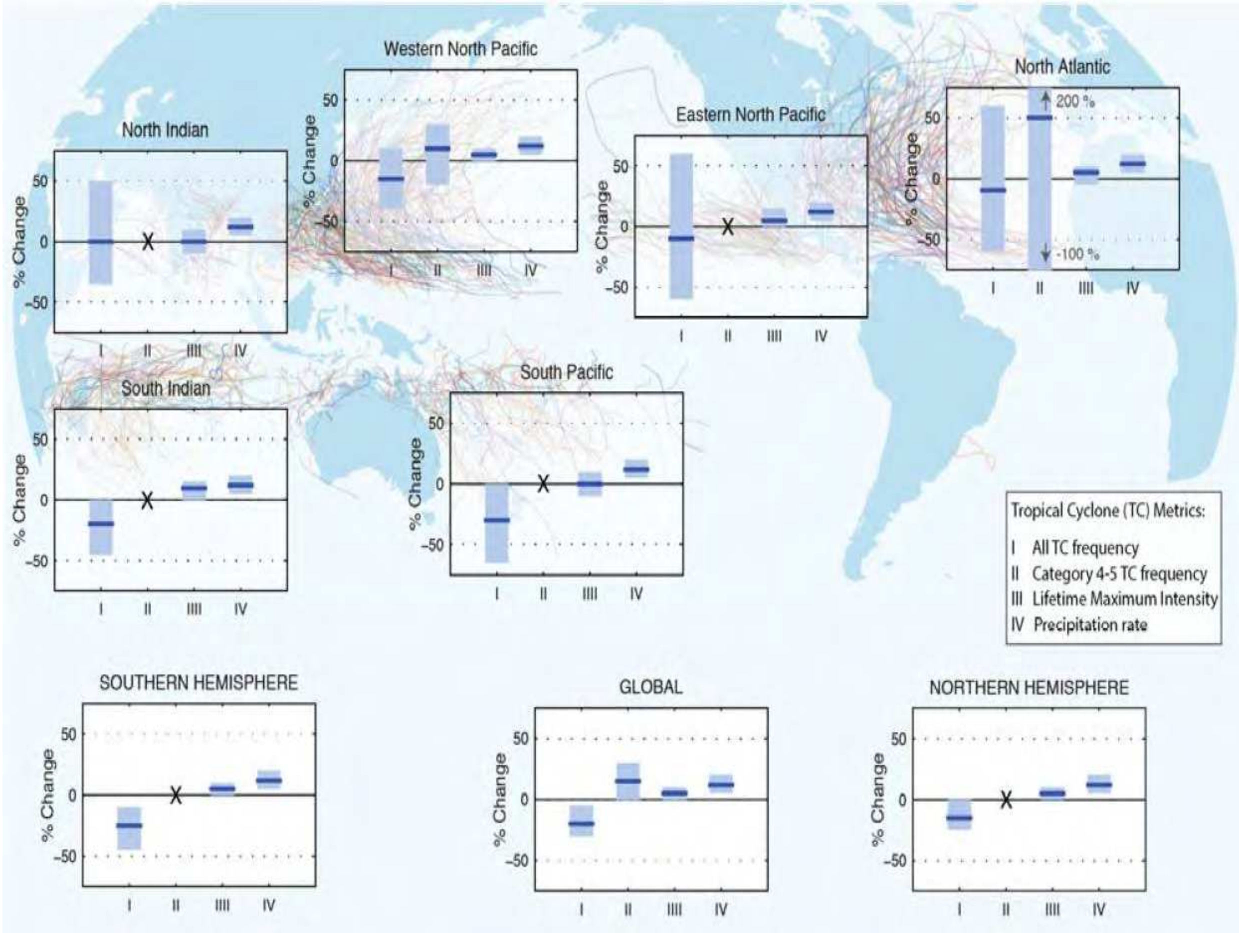

Figure 3.2 Projected changes in tropical cyclone statistics. All values represent expected change in the average over period 2081-2100 relative to 2000-2019, under an A1B-like scenario, based on expert judgment after subjective normalisation of the model projections. Four metrics were considered: the percent change in I) the total annual frequency of tropical storms, II) the annual frequency of Category 4 and 5 storms, III) the mean Lifetime Maximum Intensity (LMI; the maximum intensity achieved during a storm's lifetime), and IV) the precipitation rate within 200km of storm center at the time of LMI. For each metric plotted, the solid blue line is the best guess of the expected percent change, and the coloured bar provides the 67% (likely) confidence interval for this value (note that this interval ranges across -100% to +200% for the annual frequency of Category 4 and 5 storms in the North Atlantic). Where a metric is not plotted, there is insufficient data (denoted "X") available to complete an assessment. A randomly drawn (and coloured) selection of historical storm tracks are underlaid to identify regions of tropical cyclone activity. Source: IPCC AR5.

4. Some References

Ali, A. (1996). *Vulnerability of Bangladesh to climate change and sea level rise through tropical cyclones and storm surges*. In *Climate Change Vulnerability and Adaptation in Asia and the Pacific* (pp. 171-179). Springer Netherlands.

Ali, A. (2000). *Climate change impacts and adaptation assessment in Bangladesh*. *Climate Research*, *12*(2-3), 109-116.

Bender, M.A., Knutson, T.R., Tuleya, R.E., Sirutis, J.J., Vecchi, G.A., Garner, S.T., Held, I.M. (2010). *Modeled Impact of Anthropogenic Warming on the Frequency of Intense Atlantic Hurricanes*, Science 327, 454-458, doi:10.1126/science.1180568.

Bengtsson, L., Hodges, K. I., Esch, M., Keenlyside, N., Kornblueh, L., LUO, J. J., & Yamagata, T. (2007). *How may tropical cyclones change in a warmer climate?*. *Tellus A*, *59*(4), 539-561.

Brown, J. M., & Wolf, J. (2009). *Coupled wave and surge modelling for the eastern Irish Sea and implications for model wind-stress*. *Continental Shelf Research*, *29*(10), 1329-1342.

Boldingh Debernard, J., & Petter Røed, L. (2008). *Future wind, wave and storm surge climate in the Northern Seas: a revisit*. *Tellus A*, *60*(3), 427-438.

Campbell, J.D., Taylor, M.A., Stephenson, T.S., Watson, R.A., Whyte, F.S. (2010). *Future climate of the Caribbean from a regional climate model*, International Journal of Climatology 31, 1866-1878, doi:10.1002/joc.2200.

Chowdhury, J. U. (1994). *Determination of shelter height in a storm surge flood risk area of Bangladesh Coast*. *Water Resources Journal*, *182*, 93-99.

Colberg, F., & McInnes, K. L. (2012). *The impact of storminess changes on extreme sea levels over southern Australia*. *JGR-Oceans, doi*, *10*.

Coles, S. G., & Tawn, J. A. (1990). *Statistics of coastal flood prevention*. *Philosophical Transactions of the Royal Society of London. Series A: Physical and Engineering Sciences*, *332*(1627), 457-476.

Cooper, J. A. G., & Pilkey, O. H. (2004). *Sea-level rise and shoreline retreat: time to abandon the Bruun Rule*. *Global and planetary change*, *43*(3), 157-171.

Cordero, E. C., & Forster, P. D. F. (2006). *Stratospheric variability and trends in models used for the IPCC AR4*. *Atmospheric Chemistry and Physics*, *6*(12), 5369-5380.

Domingues, C. M., Church, J. A., White, N. J., Gleckler, P. J., Wijffels, S. E., Barker, P. M., & Dunn, J. R. (2008). *Improved estimates of upper-ocean warming and multi-decadal sea-level rise*. *Nature*, *453*(7198), 1090-1093.

Elsner, J. B., Kossin, J. P., & Jagger, T. H. (2008). *The increasing intensity of the strongest tropical cyclones*. *Nature*, *455*(7209), 92-95.

Emanuel, K.A. (1998). *The power of a hurricane: An example of reckless driving on the information superhighway*. Weather 54, 107-108.

Emanuel, K.A. (2005). *Increasing destructiveness of tropical cyclones over the past 30 years*. Nature 436, 686-688, doi:10.1038/nature03906.

Fish, M.R., Côté, I.M., Gill, J.A., Jones, A. P., Renshoff, S. and Watkinson, A. R (2005). *Predicting the impact of sea level rise on Caribbean sea turtle nesting habitat,* Conservation Biology, 19, 482-491.

Goldenberg, S.B., Landsea, C.W., Mestas-Nuñez, A.M., Gray, W.M. (2001). *The recent increase in Atlantic Hurricane Activity: Causes and Implications*, Science 293, 474-478.,

Gualdi, S., Scoccimarro, E., & Navarra, A. (2008). *Changes in tropical cyclone activity due to global warming: Results from a high-resolution coupled general circulation model*. *Journal of climate*, *21*(20), 5204-5228.

Hunter, J. (2012). *A simple technique for estimating an allowance for uncertain sea-level rise*. *Climatic change*, *113*(2), 239-252.

IPCC, (2012). *Managing the Risks of Extreme Events and Disasters to Advance Climate Change Adaptation. A Special Report of Working Groups I and II of the Intergovernmental Panel on Climate Change* [Field, C.B., V. Barros, T.F. Stocker, D. Qin, D.J. Dokken, K.L. Ebi, M.D. Mastrandrea, K.J. Mach, G.-K. Plattner, S.K. Allen, M. Tignor, and P.M. Midgley (eds.)]. Cambridge University Press, Cambridge, UK, and New York, NY, USA, 582 pp.

IPCC, (2013). *Climate Change 2013: The Physical Science Basis. Contribution of Working Group I to the Fifth Assessment Report of the Intergovernmental Panel on Climate Change* [Stocker, T. F., D. Qin, G.-K. Plattner, M. Tignor, S. K. Allen, J. Boschung, A. Nauels, Y. Xia, V. Bex and P. M. Midgley (eds.)]. Cambridge University Press, Cambridge, United Kingdom and New York, NY, USA, **in press**

Irish, J.L., Resio, D.T., Ratcliff, J.J. (2008). *The influence of storm size on hurricane surge*, Journal of Physical Oceanography 38, 2003-2013, doi: 10.1175/2008JPO3727.1.

Irish, J. L., & Resio, D. T. (2010). A hydrodynamics-based surge scale for hurricanes. *Ocean Engineering*, *37*(1), 69-81.

Karim, M. F., & Mimura, N. (2008). Impacts of climate change and sea-level rise on cyclonic storm surge floods in Bangladesh. *Global Environmental Change*, *18*(3), 490-500.

Knutson, T. R., Sirutis, J. J., Garner, S. T., Vecchi, G. A., & Held, I. M. (2008). *Simulated reduction in Atlantic hurricane frequency under twenty-first-century warming conditions*. *Nature Geoscience*, *1*(6), 359-364.

Knutson, T. R., et al., (2010). *Tropical cyclones and climate change*. *Nature Geoscience*, **3**, 157-163.

Knutson, T. R., et al., (2013). *Dynamical downscaling projections of 21st century Atlantic hurricane activity: CMIP3 and CMIP5 model-based scenarios*. *Journal of Climate*, in press.

Kossin, J. P., Knapp, K. R., Vimont, D. J., Murnane, R. J., & Harper, B. A. (2007). *A globally consistent reanalysis of hurricane variability and trends*.*Geophysical Research Letters*, *34*(4).

Landsea, C. W., Feuer, S., Hagen, A., Glenn, D. A., Sims, J., Perez, R., ... & Anderson, N. (2012). *A Reanalysis of the 1921-30 Atlantic Hurricane Database**. *Journal of Climate*, *25*(3), 865-885.

Lowe, J., Howard, T., Pardaens, A., Tinker, J., Holt, J., Wakelin, S., ... & Bradley, S. (2009). *UK Climate Projections science report: Marine and coastal projections*.

Mann, M.E., Emanuel, K.A. (2006). *Atlantic Hurricane trends Linked to Climate Change*, EOS 87 (24), 233-244.

Maue, R. N. (2009). *Northern Hemisphere tropical cyclone activity*. *Geophysical Research Letters*, *36*(5).

McInnes, K. L., Macadam, I., Hubbert, G., & O'Grady, J. (2013). *An assessment of current and future vulnerability to coastal inundation due to sea-level extremes in Victoria, southeast Australia*. *International Journal of Climatology*, *33*(1), 33-47.

McKenzie, A. (2012). *Beach Responses to Hurricane Impacts: A Case Study of Long Bay Beach, Negril, Jamaica*. *Caribbean Journal of Earth Science*, *43*, 51-58.

Meehl, G.A., T.F. Stocker, W.D. Collins, P. Friedlingstein, A.T. Gaye, J.M. Gregory, A. Kitoh, R. Knutti, J.M. Murphy, A. Noda, S.C.B. Raper, I.G. Watterson, A.J. Weaver and Z.-C. Zhao, (2007). *Global Climate Projections. In: Climate Change 2007: The Physical Science Basis. Contribution of Working Group I to the Fourth Assessment Report of the Intergovernmental Panel on Climate Change* [Solomon, S., D. Qin, M. Manning, Z. Chen, M. Marquis, K.B. Averyt, M. Tignor and H.L. Miller (eds.)]. Cambridge University Press, Cambridge, United Kingdom and New York, NY, USA.

Menéndez, M., & Woodworth, P. L. (2010). *Changes in extreme high water levels based on a quasi-global tide-gauge data set*. *Journal of Geophysical Research: Oceans (1978–2012)*, *115*(C10).

Mitchell, J. F., Lowe, J., Wood, R. A., & Vellinga, M. (2006). *Extreme events due to human-induced climate change*. *Philosophical Transactions of the Royal Society A: Mathematical, Physical and Engineering Sciences*, *364*(1845), 2117-2133.

Mori, N., Yasuda, T., Mase, H., Tom, T., & Oku, Y. (2010). *Projection of extreme wave climate change under global warming*. *Hydrological Research Letters*, *4*(0), 15-19.

Mousavi, M. E., Irish, J. L., Frey, A. E., Olivera, F., & Edge, B. L. (2011). *Global warming and hurricanes: the potential impact of hurricane intensification and sea level rise on coastal flooding*. *Climatic Change*, *104*(3-4), 575-597.

Nakicenovic, N., Alcamo, J., Davis, G., De Vries, B., Fenhann, J., Gaffin, S., ... & Dadi, Z. (2000). *Emissions scenarios*.

Nicholls, R. J. (1998). *Assessing erosion of sandy beaches due to sea-level rise*. *Geological Society, London, Engineering Geology Special Publications*,*15*(1), 71-76.

Nicholls, R. J., & Cazenave, A. (2010). *Sea-level rise and its impact on coastal zones*. *science*, *328*(5985), 1517-1520.

Oouchi, K., Yoshimura, J., Yoshimura, H., Mizuta, R., Kusunoki, S., & Noda, A. (2006). *Tropical cyclone climatology in a global-warming climate as simulated in a 20 km-mesh global atmospheric model: Frequency and wind intensity analyses*. *J.Meteorol.Soc.Jpn*, *84*(2), 259-276.

Rahmstorf, S. (2007). *A Semi-Empirical approach to projecting future sea-level rise*, Science 315, 368-370, doi:10.1126/science.1135456.

Ramsay, H. A., & Sobel, A. H. (2011). *Effects of relative and absolute sea surface temperature on tropical cyclone potential intensity using a single-column model*. *Journal of Climate*, *24*(1), 183-193.

Simpson, M.C., Scott, D., New, M., Sim, R., Smith, D.,Harrison, M., Eakin, C.M., Warrick, R.,Strong, A.E.,Kouwenhoven, P., Harrison, S., Wilson, M., Nelson, G.C., Donner, S., Kay, R.,Geldhill, D.K., Liu, G.,Morgan, J.A., Kleypas, J.A., Mumby, P.J., Christensen, T.R.L., Baskett, M.L., Skirving, W.J., Elrick, C., Taylor, M., Bell, J., Rutty, M., Burnett, J.B., Overmas, M., Robertson, R. and Stager, H., (2009) *An Overview of Modeling Climate Change Impacts in the Caribbean Region with contribution from the Pacific Islands*, United Nations Development Programme (UNDP), Barbados, West Indies

Simpson, M. C., Clarke, J. F., Scott, D. J., New, M., Karmalkar, A., Day, O. J., Taylor, M., Gossling, S., Wilson, M., Chadee, D., Stager, H., Waithe, R., Stewart, A., Georges, J., Hutchinson, N., Fields, N., Sim, R., Rutty, M., Matthews, L., and Charles, S. (2012). *CARIBSAVE Climate Change Risk Atlas (CCCRA) - Jamaica.* DFID, AusAID and The CARIBSAVE Partnership, Barbados, West Indies

Smith, J. M., Cialone, M. A., Wamsley, T. V., & McAlpin, T. O. (2010). *Potential impact of sea level rise on coastal surges in southeast Louisiana*. *Ocean Engineering*, *37*(1), 37-47.

Sugi, M., Murakami, H., & Yoshimura, J. (2009). *A reduction in global tropical cyclone frequency due to global warming*. *Sola*, *5*(0), 164-167.

University at Buffalo, (2008, February 12). *Global Warming: Sea Level Rise Could be Twice As High as Current Projections, Greenland Ice Sheet Study Suggests. ScienceDaily*. Retrieved from November 30,2013, from http://www.sciencedaily.com/release/2008/02/080211172517.htm

Unnikrishnan, A. S., RameshKumar, M. R., & Sindhu, B. (2011). *Tropical cyclones in the Bay of Bengal and extreme sea-level projections along the east coast of India in a future climate scenario*. *Current Science*, *101*(3), 327-331.

Van Vuuren, D. P., Edmonds, J., Kainuma, M., Riahi, K., Thomson, A., Hibbard, K., ... & Rose, S. K. (2011). *The representative concentration pathways: an overview*. Climatic Change, 109(1-2), 5-31.

Vecchi, G. A., B. J. Soden, A. T. Wittenberg, I. M. Held, A. Leetmaa, and M. J. Harrison, (2006). *Weakening of tropical Pacific atmospheric circulation due to anthropogenic forcing*. *Nature*, **441**, 73-76.

Vecchi, G.A., Swanson, K.L., and Soden, B.J. (2008). Whither Hurricane Activity?, 322 (October).

Villarini, G., Vecchi, G.A. (2012b). *Twenty-first-century projections of North Atlantic tropical storms from CMIP5 models*, Nature Climate Change (online publication), doi: 10.1038/NCLIMATE1530.

Villarini, G., Vecchi, G.A. (2013). *Projected increases in North Atlantic tropical cyclone intensities from CMIP5 models*, Journal of Climate 26, 3231-3240.

Wang, S., McGrath, R., Hanafin, J., Lynch, P., Semmler, T., & Nolan, P. (2008). *The impact of climate change on storm surges over Irish waters*. *Ocean Modelling*, *25*(1), 83-94.

Webster, P.J., Holland, G.J., Curry, J.A., Chang, H.-R. (2005). *Changes in Tropical Cyclone Number, Duration, and Intensity in a Warming Environment*, Science 309, 1844-1846, doi:10.1126/science.1116448

Woth, K., Weisse, R., & von Storch, H. (2006). *Climate change and North Sea storm surge extremes: an ensemble study of storm surge extremes expected in a changed climate projected by four different regional climate models*. *Ocean Dynamics*, *56*(1), 3-15.

Yu, J.Y., C.Chou, and P.G. Chiu. (2009) *A revised accumulated cyclone energy index*. Geophys.Res.Lett. 36, L14710, doi:10.1029/2009GL039254.

Yu, J.Y., Chiu, P.G. (2012). *Contrasting various metrics for measuring tropical cyclone activity*, Terr.Atmos.Ocean.Sci 23 (3), 303-316, doi:10.3319/TAO.2011.11.23.01(A).

APPENDIX 4: Hazard Profiles

A4 HAZARD PROFILES

A4.1 Introduction

The hazard profile in the pursuant sections characterizes each of the hazards in the Area of Study. A brief outline of each hazard and its potential manifestation within the area of study is presented. A description of the main elements utilized to determine or characterize each hazard is provided as is a map that delineates the spatial extent of the hazard to identify hazard prone areas within the study area. The incorporation of long-term meteorological data from regional climate change models is used to better understand the potential impact of climate variability on natural hazards.

The distinction of natural hazards must be made between those hazards that are potentially affected by climate change and those that are not. In general, all hazards that are of hydro-meteorological origin are potentially affected by climate change, while geo-hazards are generally not influenced by climate variability. Table AError**! No text of specified style in document.**.1 provides a characterization of hazards identified for this study effort.

*Table A**Error! No text of specified style in document.**.1 Categorization of Natural Hazards*

Natural Hazards		Affected by Climate Change
Hydrometeorological hazards	**Seismic**	**No**
	In-land Flooding	**Yes**
	Coastal Flooding	**Yes**
	Hurricane	**Yes**

Source: Revisado de Schmidt-Thomé 2006

It is necessary to note that regional models provide generalized understanding of changes to precipitation, temperature and sea level rise, which are critical inputs to applicable hazard models (coastal flood, in-land flood, hurricane wind, and drought). All hazards have been determined or mapped using the best available data. Hazard maps, where applicable, are developed to identify the areas of general susceptibility. The hazard mapping utilizes a qualitative classification scheme that identifies hazard prone areas as very low, low, moderate, high and very high.

A4.2 Seismic Hazard

Context

An earthquake is caused by a sudden motion or trembling of the earth due to an abrupt release of stored energy in the rocks beneath the earth's surface. When stresses due to underground tectonic forces exceed the strength of the rocks, they will abruptly break apart or shift along existing faults. The energy released from this process results in vibrations known as seismic waves that are responsible for the trembling and shaking of the ground during an earthquake. Earthquakes are also caused by tremendous rock slides that occur along the ocean floor.

The seismic hazard in Haiti has its origin in the interaction of the North American and Caribbean plates (Figure AError**! No text of specified style in document.**.1), which have a relative eastward movement of 2 cm/year (20 mm/yr).

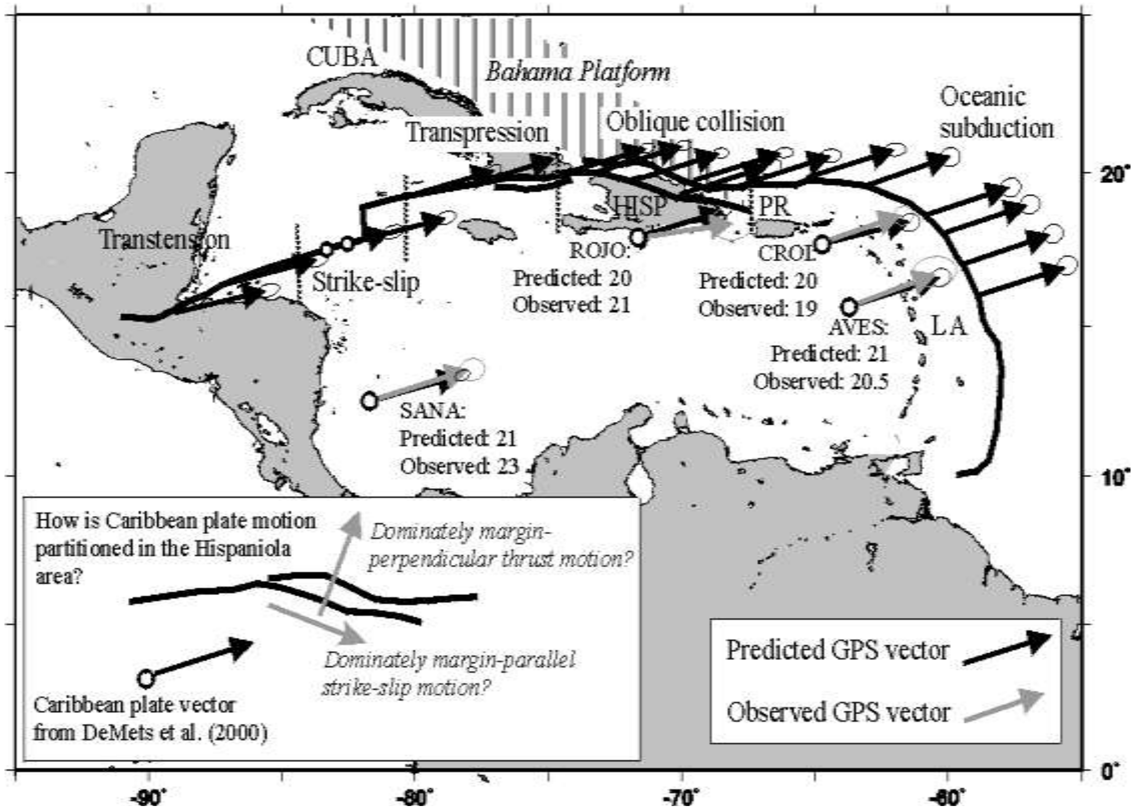

*Figure A**Error! No text of specified style in document.**.1 Relative vectorial displacement of the Caribbean tectonic plate*

Source: (Calais; 2001)

The island of Hispaniola is considered a complex area of deformation which presents both subduction zones off the northern and southeastern coast and strike-slip fault zones that transect the northern and southern portion (Figure AError**! No text of specified style in document.**.2). It also has thrust faults within the island (Frankel et. al., 2010).

The strike-slip component of the motion is due to the eastward movement of the Caribbean Plate relative to the North American Plate. On Hispaniola, the majority of the strike-slip plate motion is accommodated across two major features: the Septentrional fault zone, which runs across the northern boundary of the island, and the Enriquillo-Plantain Garden fault zone, which extends from southern-central Hispaniola to Jamaica. The location and characteristics of the significant seismic event that occurred in Haiti in January 2010 indicate that it occurred on a segment of the Enriquillo-Plantain Garden fault zone (RMS FAQ, 2010). The Matheaux Neiba Fault is a thrust fault that underlies the mountain ranges of Haiti.

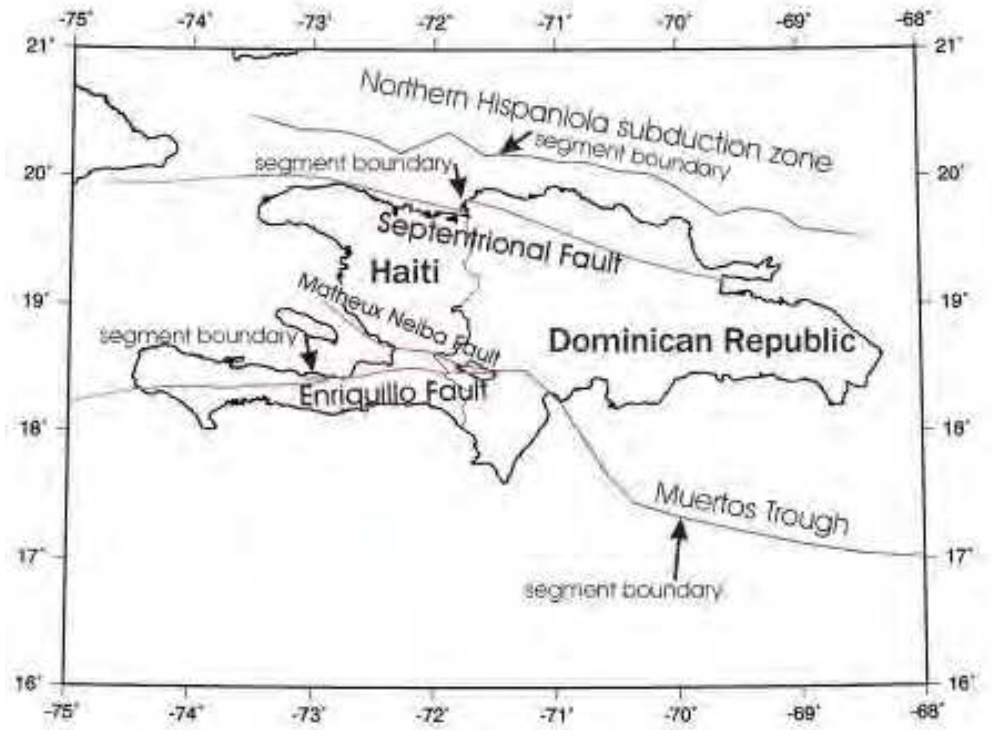

*Figure A**Error! No text of specified style in document.**.2 Crustal faults and subduction zones used in the hazard maps.*

Source: USGS, 2010; note: Red lines denote the portions of the Septentional and Enriquillo Faults. Green lines denote the western portions of the Septentrional and Enriquillo Faults that are treated separately. Blue lines denote the traces of the uppermost portion of the subduction zone faults considered. Locations of the inferred segment boundaries used in the hazard maps are marked by arrows.

Active subduction zones are located off the northern and southern coasts of Hispaniola. The Northern Hispaniola subduction zone has produced a series of powerful earthquakes from 1946 and 1953 (USGS, 2010). The focal mechanisms for these earthquakes indicate a southwestward subduction of the North American Plate. The Muertos Trough subduction zone is located south of Hispaniola and extends eastward to south of Puerto Rico and there is evidence that this zone ruptured in 1751 in a large earthquake and produced a tsunami (McCann, 2006).

There is a verifiable record of earthquake occurrences dating back more than 500 years in the Caribbean (Table AError**! No text of specified style in document.**.2). In general, the occurrence of seismic events in Haiti has been poorly recorded. A review of the information available has indicated that since 1750 the following major events have occurred:

*Table A**Error! No text of specified style in document.**.2 The most important seismic events in the island of Hispaniola*

Date		Magnitude	Cities affected
	1564	7 + 6.2	Conception de la Vega, Santo Domingo
	1615	7.0	Santo Domingo
	1684	6.5	Santo Domingo, Ázua
	1691	7.0	Santo Domingo
9 Nov	1701	6,0	Léogane

Date		Magnitude	Cities affected
15 Sept	1751	8 + 7.5	Port-au-Prince, Santo Domingo, Ázua
18-25 Oct	1751	7.5	Port-au-Prince
3 Jun	1770	7	Port-au-Prince, Léogane, 250 killed
29 Jul	1785	6.5	Port-au-Prince
20 Nov	1818	6.5	Cap Henri
7 May	1842	6.5	Cap Haïtien & Port-de-Paix
7 May	1842	8.0	Port-au-Prince
8 May	1842	6.9	Cap-Haïtien, 2500 killed
23 Sept	1887	7.0 + 7.75	Môle Saint-Nicolas, Cap Haïtien, 5500 killed
22-Sept	1904	6.5	Port-de-Paix
6 Oct	1911	7.1	Hinche, San Juan, Azua, 12 killed
4 Aug	1946	7 + 8.1 + 7.4	Puerto Plata
20 Apr	1962	6.75	Cap Haïtien
12 Jan	2010	7.0	Port-au-Prince and others, 200,000 killed

Source: After McCann 2001; Calais 2001

Note: The impacts of these seismic events can be wide-ranging and therefore this table includes key events across Haiti, not just those for the north.

Hazard Determination

Seismic hazard maps were developed by USGS in response to the urgent need for seismic hazard information as a result of from the catastrophic earthquake of January 2010. The probabilistic maps were assembled based on the current available information on historical and instrumental seismicity and followed the general methodology developed for the 1996 U.S. national seismic hazard maps (Frankel and others, 2000). The methodology provided in the USGS report authored by Frankel et. al, 2010 is concisely summarized in the sections below, and consisted of adding seismic hazard calculated from crustal faults, subduction zones and spatially smoothed seismicity for shallow earthquakes and Wadati-Benioff- zone earthquakes (Frankel et al., 2010).

Faults

The fault zones included in the seismic hazard model are the Septentrional fault, Enriquillo-Plantain Garden fault zone, and the Matheux Neiba fault (see Figure AError**! No text of specified style in document.**.2). The Septentrional Fault and the Enriquillo-Plantain Garden faults are crustal faults, while the Matheaux Neiba fault is a thrust fault. For each fault, a frequency-magnitude distribution was applied to account for the random uncertainty in accounting for the magnitude of future earthquakes. Seismic moment rates were estimated for each fault from its estimated slip rate, segment length and width. Maximum magnitude of rupture were determined from the segment lengths and empirical relation between surface rupture length and moment magnitude were utilized following Wells and Coppersmith (1994).

Subduction Zones

The Northern Hispaniola and the Muertos Trough subduction zones were considered in the hazard model. The Northern Hispaniola subduction zone is thought to continue along the entire coast of Hispaniola. The Muertos Trough subduction zone is located south of Hispaniola and extends eastward to Puerto Rico. It appears that the Enriquillo fault merges into this trough.

Spatially Smoothed Seismicity Model

The spatial smoothed seismicity model, which was developed by Frankel (1995), was utilized to determine the earthquake hazard for Hispaniola. This assumes that future moderate and large earthquakes will occur near areas that have had significant historic seismic activity in the past. The analysis of historic seismicity is based on a review of background source zones and a review of historical and observed data. The model also utilizes attenuation relations (ground motion prediction equations) for each of the source zones.

Slip rates and recurrence rates were determined for each fault segment and subduction zone. A historical catalog, derived from U.S. Geological Survey PDE catalog, the Engdahl and Villasensor Catalog (2002) and the International Seismic Cennter (ISC) catalog, was reviewed and divided into thresholds based on the completeness of data[1] The seismicity was then further divided into depth ranges. Three depth ranges were utilized to develop a seismicity rate grid: 0-40km, 41-100km, and 101km and deeper).

The data was combined and interpolated using Gaussian distribution methods and integrated into a mapping grid to calculate the hazard. The results were then combined with attenuation relations (ground motion prediction equations) for each of the crustal faults and subduction zones to determine the seismic hazard for Hispaniola for firm rock site conditions and with site amplification.

Hazard Maps

The published USGS hazard maps based on fault slip rates and historical and instrumental seismicity have been used to generate the contours having Peak Horizontal Ground Acceleration (PGA) Rock (firm-rock conditions) values for Haiti (Frankel and others, 2010). These hazard maps are for PGA (percent g) for 10 percent and 2 percent probabilities of exceedance (PE) in 50 years, respectively (Figure AError**! No text of specified style in document.**.3 and Figure AError**! No text of specified style in document.**.3 PGA (% g) with 10% probability of exceedance in 50 years (475 years return periods)

Figure A**Error! No text of specified style in document.**.4).

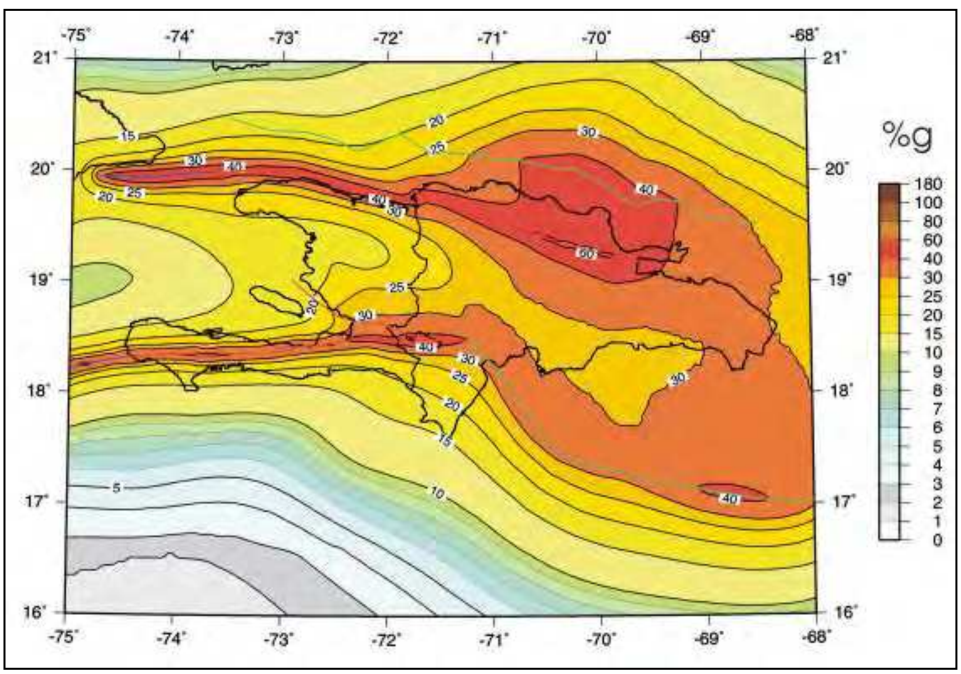

*Figure A**Error! No text of specified style in document.**.3 PGA (% g) with 10% probability of exceedance in 50 years (475 years return periods)*

[1] Complete 1960 > M4.0 and 1915 for larger events.

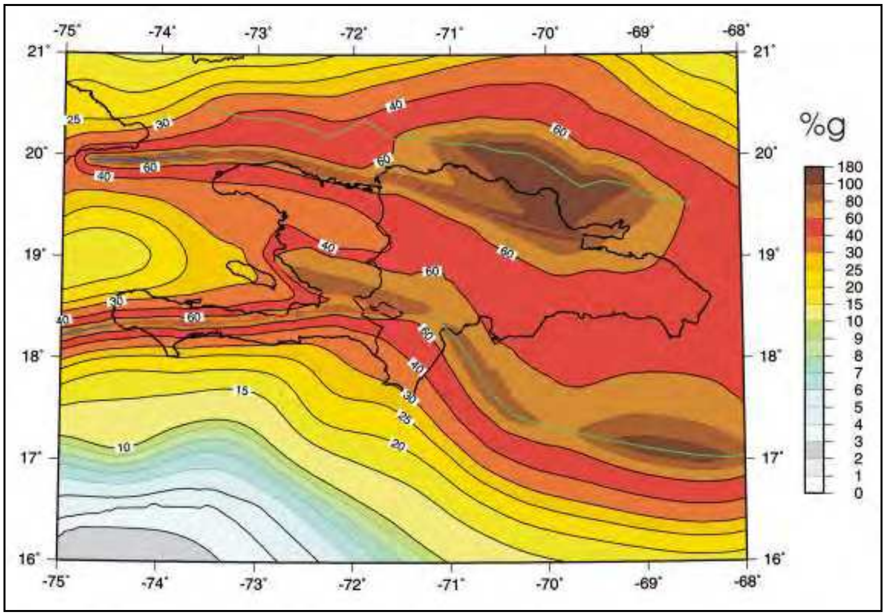

*Figure A**Error! No text of specified style in document.**.4 PGA (% g) with 2% probability of exceedance in 50 years (2500 years return periods)*

In the data conversion process, these maps have been first geo-referenced using GIS tools and then the contours present in these maps have been captured as polyline features with necessary attribute values associated with them. The contours are then processed using suitable interpolation techniques and PGA Rock data are distributed in raster grid format for the study area. The following figures (Figure AError**! No text of specified style in document.**.5 and Figure AError**! No text of specified style in document.**.5 Distribution of PGA (in g) with 10% probability of exceedance in 50 years (475 years return periods) for the study area

) present the PGA at Rock level developed by USGS.

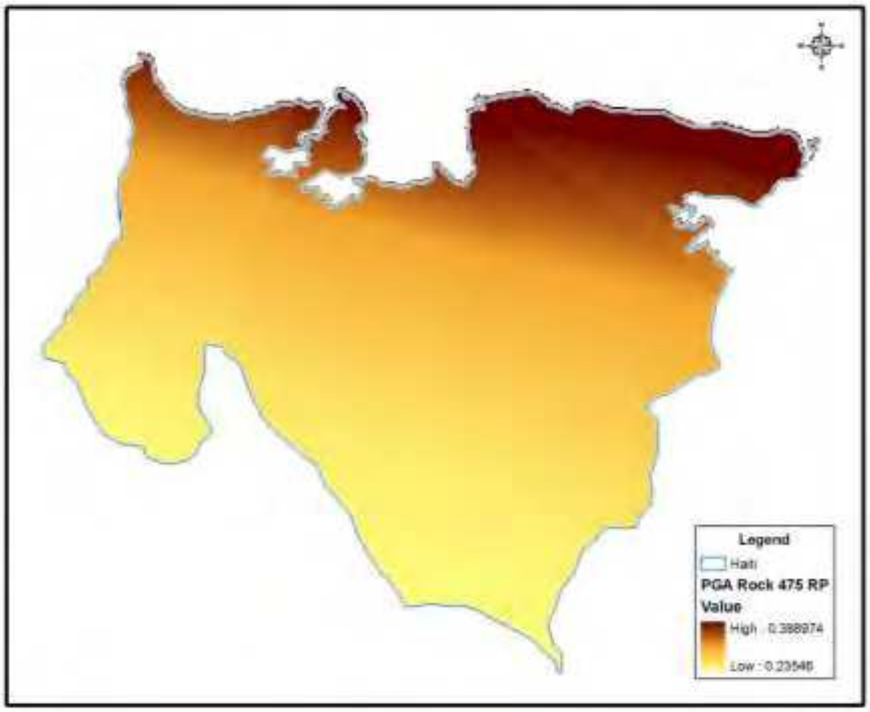

*Figure A**Error! No text of specified style in document.**.5 Distribution of PGA (in g) with 10% probability of exceedance in 50 years (475 years return periods) for the study area*

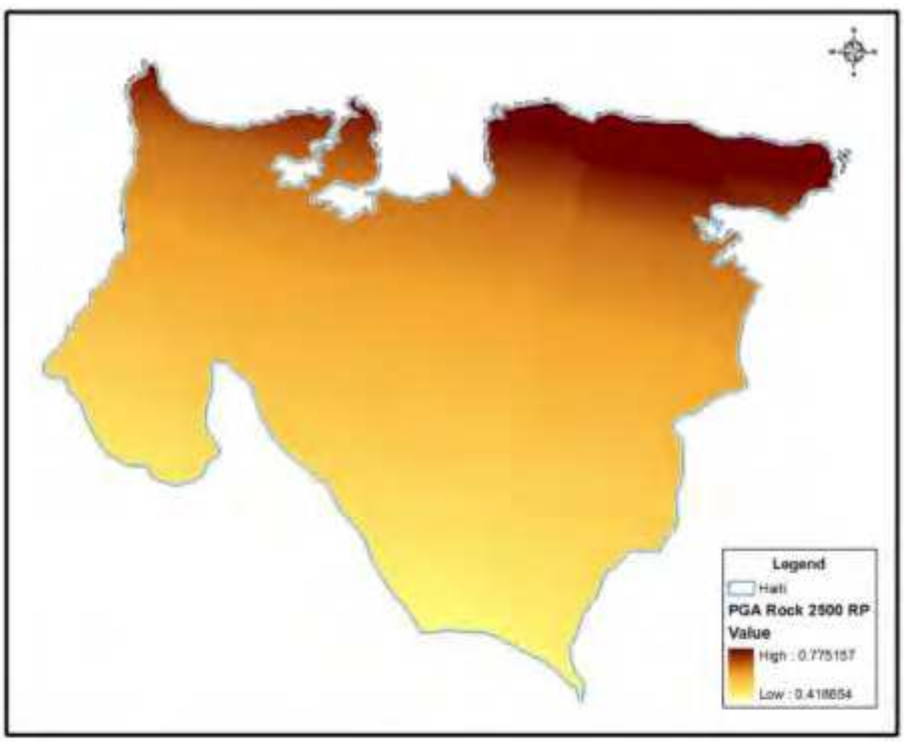

*Figure A**Error! No text of specified style in document.**.6 Distribution of PGA (in g) with 2% probability of exceedance in 50 years (2500 years return periods)*

To validate the results initially, ERM has performed a comparison of the USGS PGA values with data derived from the UN Global study for the study area. It has been observed that the distribution and range of PGA values have similarity for the study area, e.g. the range of PGA (in g) values found in USGS data varies between 0.235 and 0.389, whereas, the UN Global data values vary between 0.402 and 0.419 for 475 years return period. Similarly, in the same area, the PGA for 2,500 years return period varies from 0.417 to 0.775 (in g) in USGS hazard data while PGA values in the UN Global data vary from 0.744 and 0.758 (less variation due to coarser resolution of about 38 km grid).

After required data validation and quality checks, the USGS PGA rock data has been carried out to generate PGA Soil values using appropriate site amplification factors for the study area.

Soil Modifications

Local soil conditions can significantly affect earthquake ground motion of an earthquake. The soil top layers act as filters that can modify the ground motion as a function of their dynamic characteristics. Soft, weak soils tend to amplify long-period seismic motions and thus generally impart large ground displacements to structures, while very stiff soil and rock tend to de-amplify the ground motion.

For dynamic purposes, soils are classified in terms of their shear wave velocity. A majority of authors, including the European and NGA developers (Schott et al., 2004; Campbell et al., 2009; Boore et al., 2011; Sandıkkaya et al., 2013) have used the average shear-wave velocity in the upper 30 meters of sediments, Vs_{30}, as the parameter for characterizing effects of sediment stiffness on ground motions. Use of this parameter is considered to be diagnostic in determining site amplification than the broad and ambiguous soil and rock categories used in the earlier studies [with the exception of the relation of Boore et al. (1997), who used Vs_{30}].

Therefore, the site amplifications of ground motions relative to a reference rock condition are continuous functions of Vs_{30} and have been used for the study area, due to the absence of Haiti-specific relationships between site classes and amplification effects, and coarse surficial geology at 1:250,000 scale. The widely used NEHRP's site amplification procedure based on shear wave velocities (Wills et al, 2000, BSSC, 2001) has been applied in this study (Table AError**! No text of specified style in document.**.3).

*Table A**Error! No text of specified style in document.**.3 Soil classification scheme based on shear wave velocities*

Soil Index value	NEHRP /CDMG Class	Brief Description	Shear Wave Velocities (Vs,30) m/s
1.0	AB	Very hard to firm rocks mostly metamorphic and igneous rocks	>760
1.5	BC	Firm sedimentary rocks (mid Miocene age) and weathered metamorphic	760
2.0	C	Sedimentary Formation Mid-Lower Pleistocene age	550-760
2.5	CD	Weak rock to gravelly soils - Deeply weathered and highly fractured bedrock	270-550
3.0	D	Holocene Alluvial soils	180-270
3.5	DE	Young alluvium / Water-saturated alluvial deposits	90-180
4.0	E	Non-engineered artificial fill, soft clays, peat and swamp deposits	< 90

Topographic Slope Based Seismic Site Conditions

Wald et al. (2004), and Wald and Allen (2007), describe a general methodology for deriving maps of seismic site conditions using topographic slope as a proxy. Vs_{30} measurements (the average shear-velocity down to 30 m depth) are correlated against topographic slope to develop two sets of coefficients for deriving Vs_{30} at grids. The site-specific Vs_{30} values have been recommended to be used at finer scales or at particular locations.

The basic premise of the method is that the topographic slope can be used as a reliable proxy for Vs_{30} as an alternative method in the absence of geologically and geo-technically based site-condition maps by correlating Vs_{30} measurements and topographic gradient. Based on the past seismicity in northern part of Haiti, the seismic sources and the potential events in the region, the stable coefficient was utilized for Haiti site amplification and spatially interpolated the Vs_{30} data using GIS tools.

Due to the size of the study area, the evaluation of seismic site conditions could not rely on the USGS published Vs_{30} data, which is available at 30 m resolution, or the average shear velocity to 30 m depth (Vs_{30}). Therefore, a high resolution (2m) digital elevation model (DEM) has been used to compute topographic slope based site conditions.

In this process, the USGS published Vs_{30} data has been plotted against the high resolution (2m) DEM and correlation has been established between these two parameters (Figure AError**! No text of specified style in document.**.7).

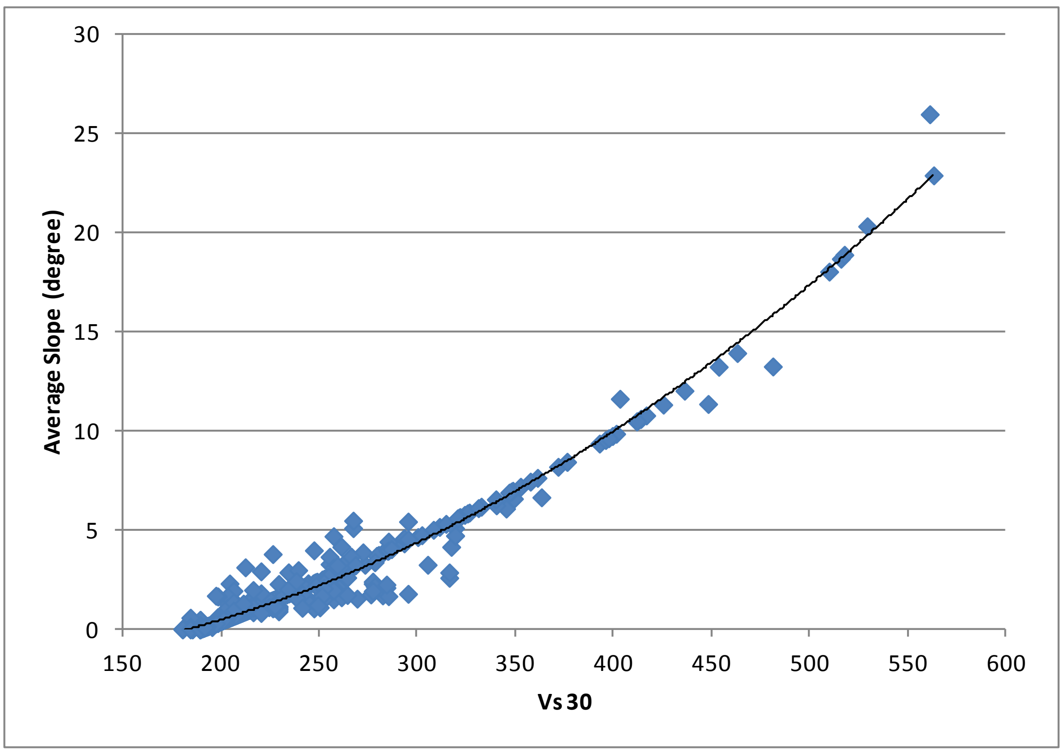

*Figure A**Error! No text of specified style in document.**.7 Average slope and Vs 30 relationship for the study area*

This correlation provides the basis for establishing site specific values for the higher resolution elevation data which facilitated the calculation of a soil index map using the NEHRP's classification (Figure AError**! No text of specified style in document.**.8).

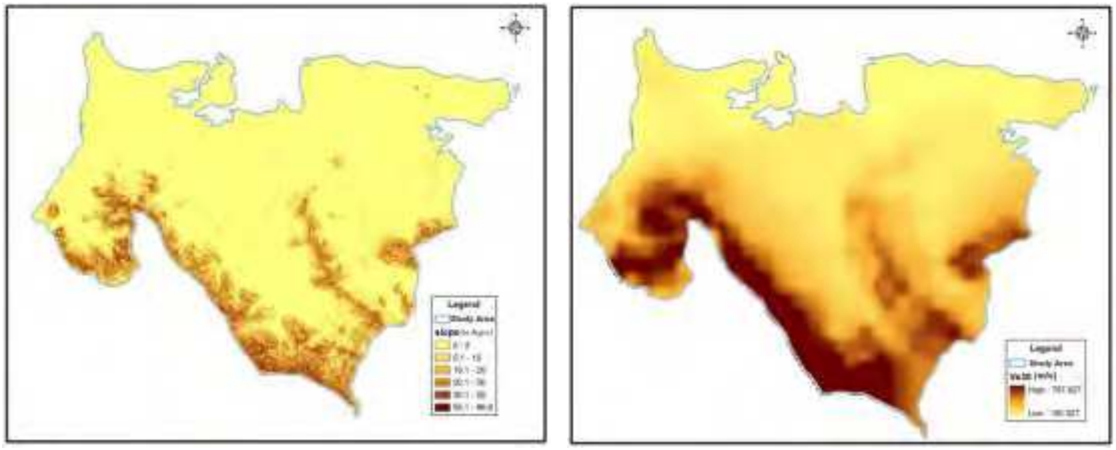

*Figure A**Error! No text of specified style in document.**.8 The slope map derived from high resolution DEM (left) and distribution of Vs 30 within the study area*

In the next step, ERM has performed sample review of the distribution of Vs_{30} values with the topography. The values of Vs_{30} at specific sites like foothills, riverine plains have been compared to validate their correlation.

The soil classification scheme follows the NEHRP scheme of 7 soil classes and their associated Vs_{30} distribution. The results of the analysis is presented in the below figure (Figure AError**! No text of specified style in document.**.9).

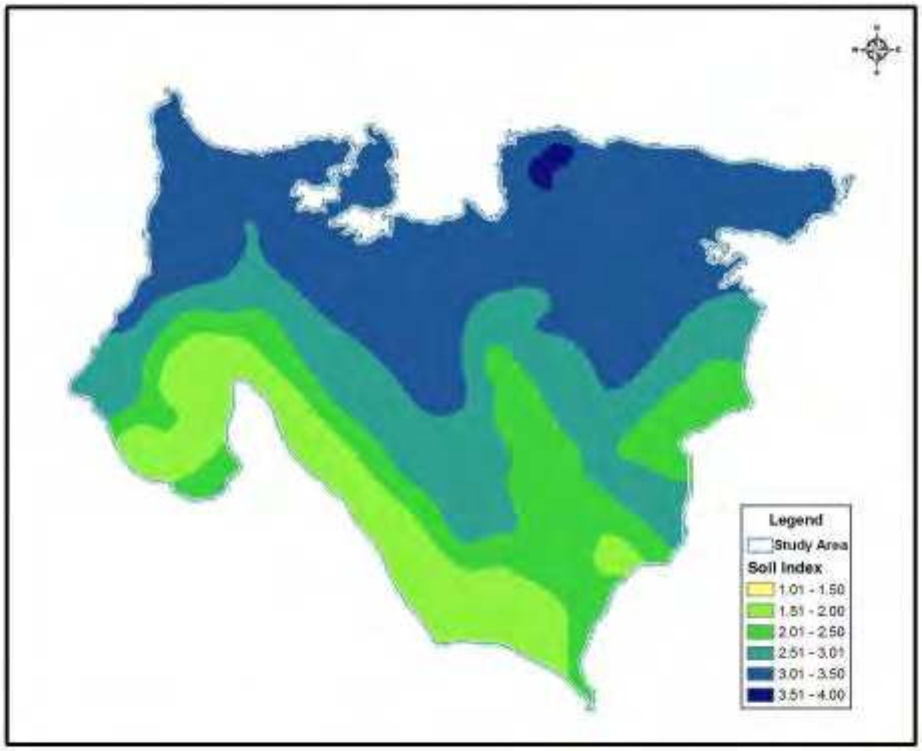

*Figure A***Error! No text of specified style in document.***.9 Topographic slope based soil classification for the study area, Haiti*

Site Conditions Validation from Geological Maps

The soil index developed for the study area as per NEHRP classes (Table AError**! No text of specified style in document.**.2) has been validated against the available geological maps for the study area in Haiti. Since, the units in the geological map are not so detailed and the extent of the study area considerably small in size, the classified soil index map developed shows broad relationship with the geological classes, though the overall trend of the boundaries shows similarity.

Site Amplifications

To derive a more detailed understanding of the seismic hazard in the study area, specifically an understanding of amplification, site amplification factors were applied to the soil index values adopted from NEHRP. The site–dependent amplification factors have followed the non-linear two-dimensional soil amplification factors modified from Choi and Stewart (2005); and Walling, M, Walter Silva, and Norman Abrahamson (2008), which relate non-linear multipliers based on the level of ground motion (PGA) and averaged soil index assigned for a given location.

The plot of amplification factors for different soil index classes (corresponding to respective Vs_{30} values) normalized by the amplification for reference BC soil Vs_{30}=760 m/s (soil index 1.5), used in the study is shown in Figure AError**! No text of specified style in document.**.5Distribution of PGA (in g) with 10% probability of exceedance in 50 years (475 years return periods) for the study area

.

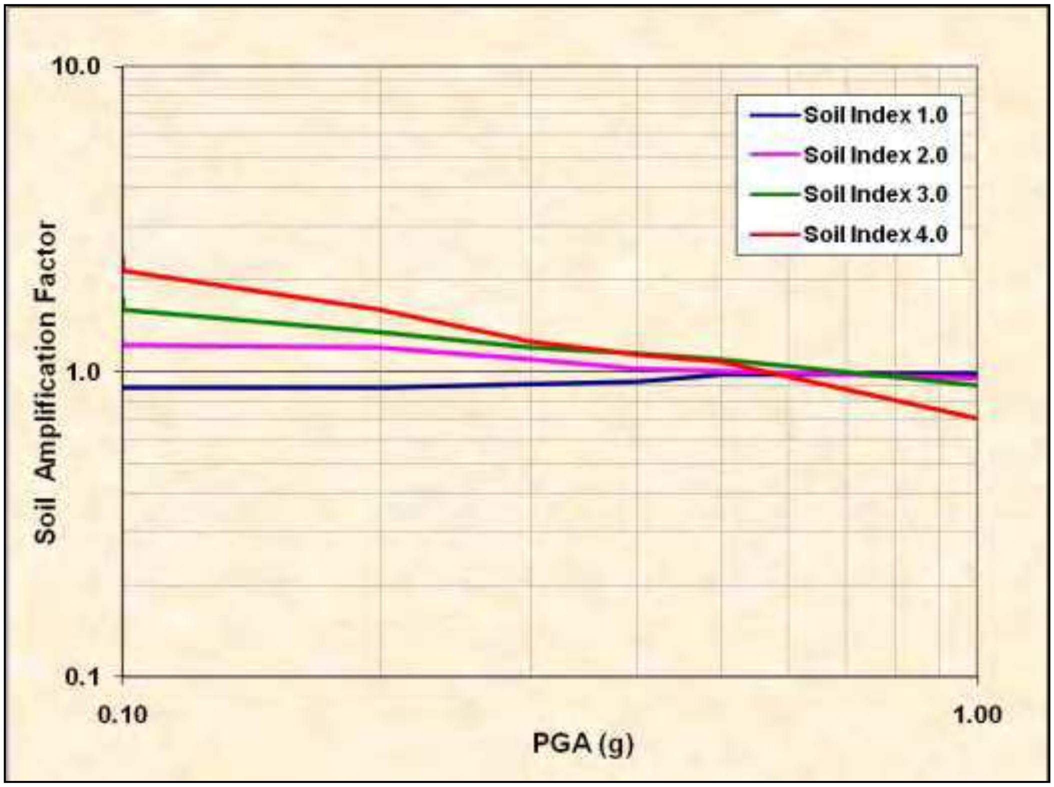

*Figure A**Error! No text of specified style in document.**.10 Site amplification factors for different soil index values (= VS30 values)*

The PGA values derived from USGS for the study area were multiplied with site amplification factors that were derived from the Vs_{30}based soil index map. The site amplification factors that were derived from the Vs_{30} data were correlated with values from the high resolution topography to derive appropriate site amplification factors for the soils in the study area (Figure AError**! No text of specified style in document.**.10).

The outcomes are earthquake hazard maps, expressed in terms of PGA Soil values at 10 m horizontal resolution[2]. The final hazard maps developed for the study area is shown in the following figures (**Error! Reference source not found.** and).

2 Note that the average slope derived from 2m DTM has been used to correlate with corresponding Vs 30 values. The result was at satisfactory level and was expressed in a 10m mapping resolution.

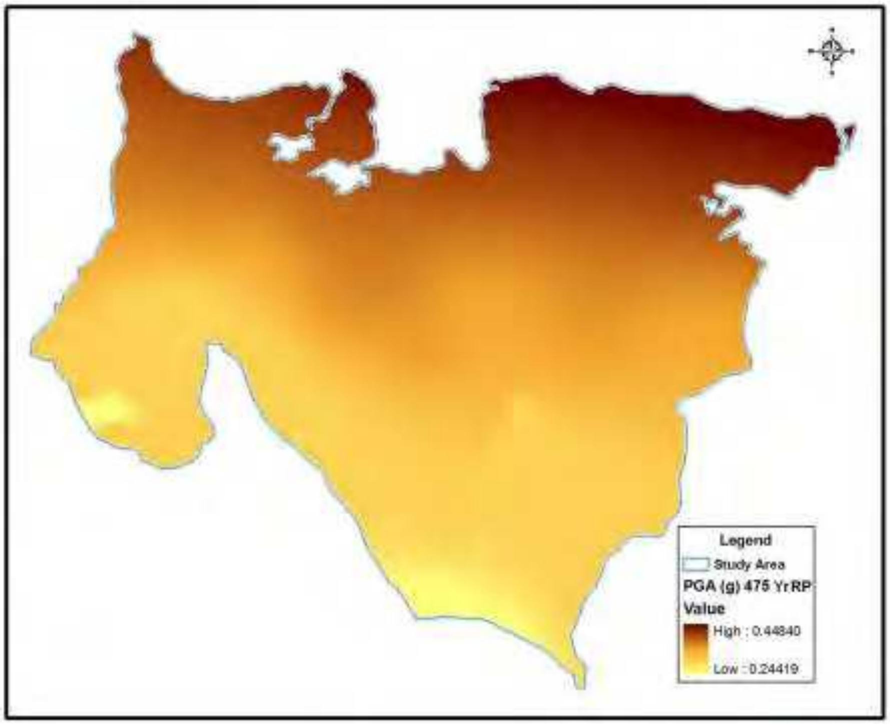

*Figure A**Error! No text of specified style in document.**.11 PGA probabilistic seismic hazard map for 10% probability in 50 years, i.e. 475-year return period*

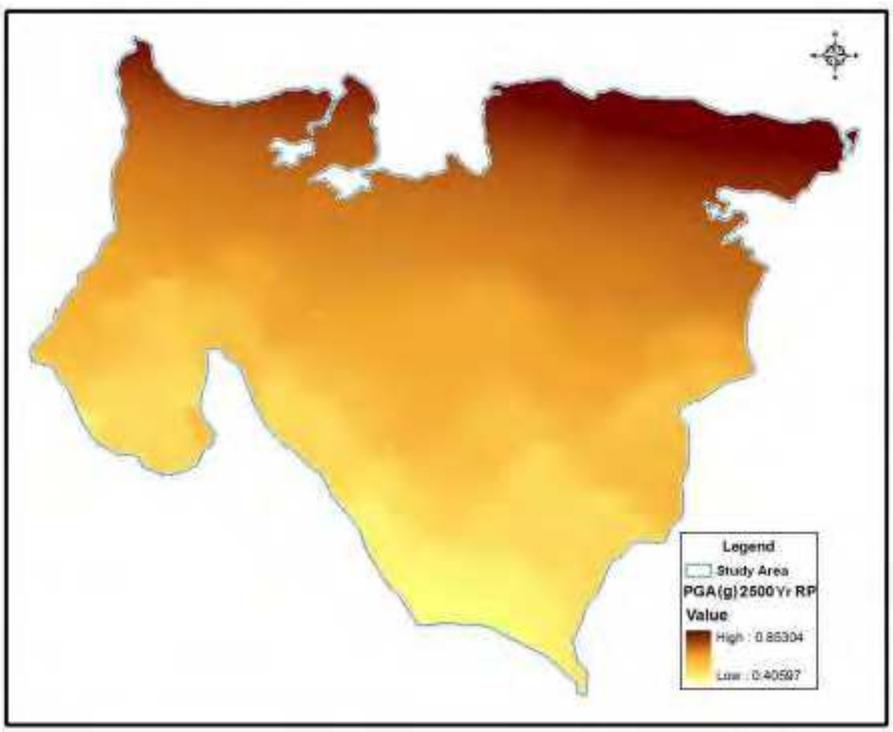

*Figure A**Error! No text of specified style in document.**.12 PGA probabilistic seismic hazard map for 2% probability in 50 years, i.e. 2,500 year return period*

Hazard Frequency and Magnitude

The basis of the understanding of the frequency and magnitude of a seismic hazard lies in the probabilistic data using modeled information concerning stochastic events.

It has been observed that the peak ground acceleration (PGA in g) with site amplification varies from 0.244 to 0.448 within the study area for 475 years return period. In the same area, the PGA for 2,500 years return period varies from 0.406 to 0.853 (in g). Values for the cited return periods are expressed in tabular form in Table A4.4.

*Table A**Error! No text of specified style in document.**.4 Return Period and Peak Ground Acceleration*

Return Period	PGA (ranges within data set)	Annual Probability
475	0.244 to 0.448	1/475%
2500	0.406 to 0.853	1/2500%

The frequency and magnitude of a seismic event is interpreted by rating the level of PGA, i.e. to a return period of 2500 years, with the annual probability of occurrence. The annual probability of experiencing an event with a range of acceleration of a 2500-year event, then, is 0.04 percent.

A4.3 Hurricane Hazard

Context

Hurricanes and tropical storms are large-scale systems of severe thunderstorms that develop over tropical or subtropical waters and have a defined, organized circulation. Hurricanes have a maximum sustained (meaning 1-minute average) surface wind speed of at least 74 mph; tropical storms have wind speeds of 39 mph to 74 mph.

Hurricanes get their energy from warm waters and lose strength as the system moves inland. Hurricanes and tropical storms can bring severe winds, inland riverine flooding, storm surges, coastal erosion, extreme rainfall, thunderstorms, lightning, and tornadoes. Hurricanes and tropical storms typically have enough moisture to cause extensive flooding throughout a large geographical area, or in the case of Haiti, the entire country.

Hurricane magnitude is measured on the Saffir-Simpson hurricane scale, shown in Table AError**! No text of specified style in document.**.5, which categorizes hurricane magnitude by wind speeds and storm surge above normal sea levels.

*Table A**Error! No text of specified style in document.**.5 Saffir-Simpson Hurricane Scale*

Category	Wind Speed	Expected Damage
1	74–95 mph	Minimal: Damage primarily to shrubbery and trees; unanchored mobile homes damaged; some damaged signs; no real damage to structures.
2	96–110 mph	Moderate: Some trees toppled; some roof coverings damaged; major damage to mobile homes.
3	111–130 mph	Extensive: Large trees toppled; some structural damage to roofs; mobile homes destroyed; structural damage to small homes and utility buildings.
4	131–155 mph	Extreme: Extensive damage to roofs, windows, and doors; roof systems on small buildings completely fail; some curtain walls fail.
5	> 155 mph	Catastrophic: Considerable and widespread roof damage; severe window and door damage; extensive glass failures; entire buildings may fail.

Haiti is among the most hurricane-prone locations in the world. In 2004, the Food and Agriculture Organization (FAO) reported that during a period from 1909 - 2004, forty-seven (47) tropical storms and hurricanes hit Haiti, of which nineteen (19) hurricanes or major climatic events (FAO, 2004). From 2004 to 2012, twelve (12) wind storms have made landfall in Haiti (See Table AError**! No text of specified style in document.**.6 below).

Data from the Prevention Web[3], which provides information on human and economic losses from disasters, indicates that between 1980 and 2010, over four million (4,171,407) persons have been affected by hurricanes. For this same period, Prevention Web furthers that there were 4,990 deaths caused by hurricanes and that the estimated economic impacts for the same period reached over USD$ 822 Million in Haiti. Dr. Jeffrey Masters, in a summary of Hurricanes in Haiti entitled "*Hurricanes and Haiti: A Tragic History*"[4] indicates that the 2008 hurricane season was the cruelest for Haiti, with four (4) named storms making landfall and dumping heavy rains. He estimates that in 2008 alone, economic damages exceeded $1 billion US dollars.

*Table A**Error! No text of specified style in document.**.6 Hurricane History in Northern Haiti*

Year	Event	Description
1954	Hurricane Hazel	11–12 October: Hurricane Hazel affected every part of Haiti. Grand Anse, Ouest, Arbonite, Nord-Ouest
1979	Hurricane David	August; Location: limited impact on Nord-Ouest
1998	Hurricane Georges	23 September: Hurricane Georges; Location: Sud-Est and Nord-Ouest departments.
2008	Hurricane/ Tropical Storm Fay	16 August: Tropical Storm Fay crossed the entire country.
2008	Hurricane Hanna	1 September: Hurricane Hanna; Location: Artibonite and Nord-Est
2008	Hurricane Ike	6 September: Hurricane Ike; Location: Nord, Ouest and Nord-Ouest

Source: NATHAT, 2012, National Meteorological Center of Haiti;

One of the most serious components of hurricanes is high winds. Because of the extensive size of a catastrophic hurricane, a storm need not pass directly over Haiti to cause severe damage. A hurricane passing within close proximity to the island of Hispaniola can also cause major damage to property and even loss of life. Essentially there are no areas of Haiti that are free from hurricane force winds. The coastal and low lying areas, such as those of the study area, experience the first effects of damaging winds.

This subsection is focused on Hurricane Winds and effects (inland and coastal) flooding are covered in Sections 4.4 and 4.5 respectively. The rains that accompany hurricanes are intense and last for several days. Intense and prolonged rainfall can cause flooding by which water overflows river banks and puts at risk all low-lying areas along with structures and critical facilities and infrastructure. Coastal flooding or storm surges are also prevalent during hurricanes and have the potential to severely impact low-lying coastal villages and overwhelm homes and other buildings near the ocean.

Hazard Determination

The methodology developed for the identification of wind hazards for this study was based on numerical modeling of hurricane motion and procedures developed by Vickery, 2008 in an assessment entitled "*Development of Design Wind Speed Maps for the Caribbean for Application with Wind Load Provisions of ASCE 7*. The reference study, which was performed for the Pan American Health Organization (PAHO) under a special grant from the Office of Foreign Development Assistance of the United States Agency for International

[3] (http://www.preventionweb.net/english/countries/statistics/?cid=74)

[4] http://www.wunderground.com/resources/education/haiti.asp?MR=1

Development (OFDA/USAID), extended a hurricane simulation model that was originally developed and tested for the Gulf and Atlantic coasts in the United States, to the Caribbean. The models have been calibrated to capture variations of storm characteristics throughout the Caribbean Basin, with specific attention being placed on the Greater Antilles. The technical methodology of the report is concisely summarized below, which forms the basis for the hazard maps utilized in this study.

Track and Intensity Modeling

The hazard model incorporated the associated wind field for historical cyclones in the Atlantic basin. The initial step was to understand the wind speeds for various return periods for locations distributed over the Atlantic and Hispaniola as described in (Vickery et al., 2000, 2008). Central pressure was calculated for each storm and a one dimension model was used to calculate ocean feedback as described in Emanuel et al. (2006). The relative intensity of each storm was then calculated and intensity values were incorporated into a statistical model to understand vertical wind shear.

Storm Filling

Unlike the United States, there is insufficient data to calculate the effects of roughness on reducing the central pressure of hurricanes in the Caribbean. A filling model is usually used to compute the variation of central pressure of a storm during landfall and to take into consideration the time that the storm is over land and the variation in the intensity of the storm. The limited data that is available is associated with the HURDAT[5] data, which only has six (6) hour temporal resolution and that lack of landfall and exit pressures when storms make landfall and cross islands in the Caribbean (Vickery, 2012). Instead, a filling model that was developed by Vickery (2005) for the New England coast was utilized to model storm weakening as it provided the best data comparisons of storm central pressure statistics when compared to other models utilized in the region (Vickery, 2005). For the purposes of this study, it was assumed that the wind speed will equal the basic values from the hurricane model due to small size of study area and sparse development (i.e. limited roughness).

Model Validation

Vickery, as part of the hazard model developed for PAHO/OFDA/USAID implemented a validation procedure that compared the statistics of storm heading, translation speeds, and distance of closest approach, central pressure and annual occurrence rates of modeled and historical storms passing within 250 kilometers of a grid point (Vickery 2008).

The tropical cyclones from the period of 1900 to 2007 from HURDAT were used in model validation process. To verify the ability of the model to reproduce the historical storms, statistical tests were performed. The statistical tests include t-tests for equivalence of means, f-test for equivalence of variance and the Kolmogorov-Smirnov (K-S) tests for equivalence of cumulative distribution functions (CDF).

The results indicate that overall model reproduces the observed heading data very well and the variance of the observed data is strongly dependent on a few outliers. In most cases, these outliers were associated with one/two storms heading in easterly direction in the southern part of the Caribbean. The modeled values of central pressure represent the minimum pressures anywhere within 250 kms of an established model grid point that is likely to be exceeded, on average, once in 50 years.

Quantitative comparison of central pressure shows that the model reproduces wind speeds expected from an intense hurricane passing to the south of the greater Antilles and up through the Yucatan channel. The magnitude of modeled 50 year return period pressures are similar to the observed values, but reflects the smoothing expected for predicted mean values rather than single point observations from 50 year record. In

[5] The North Atlantic hurricane database, or HURDAT, is the database for all tropical cyclones in the Atlantic Ocean, Gulf of Mexico and Caribbean Sea, since 1851.

terms of the peak gust, the model and observed wind speeds are in good agreement, however there are relatively few measured gusts with wind speeds greater than 100 mph.

While Vickery provides a summary of how the actual hurricane simulation model was validated, ERM also compared the results to a wind hazard data provided in a recent United Nations Strategy for Disaster Reduction (UNISDR) and Global Assessment Report on Disaster Risk Reduction (GAR) report entitled "*Probabilistic Modeling of Natural Risks at the Global Level: Global Risk Model, 2013*". This global assessment models the cyclonic winds based on previous trajectories recorded for the main oceanic basins of the world. The hazard model used in the UN model forecasts the maximum intensities associated with the potential occurrence and track of a tropical cyclone in the Atlantic region. The calculations are performed for each of the selected historical tracks and for a set of "children" tracks obtained through the use of a statistical procedure known as disturbance, which allows generating random tracks that conserve the main characteristics of the historical ones so as to produce probabilistic wind speeds for a series of return periods (i.e. 50-, 100-, 250-, 500- and 1,000- year return periods). The data is available at a resolution of 30 km for wind speed.

A comparison of the PAHO/OFDA/USAID data with that of the UN model indicates that the UN global wind hazard maps show only minor variation in wind speed over Haiti (See Table AError**! No text of specified style in document.**.7). For instance, for a 50 year return period the variation between minimum and maximum wind speed was only 3 km/h. For 100 year return period variation between minimum and maximum wind speed was only 3.2 km/h. The data from the PAHO/OFDA/USAID wind hazard maps show a much better variation and distribution of wind speeds over Haiti. Since these maps are derived from wider area maps of Hispaniola region, they provide a good distribution and variation in the study area. For 50 and 100 year return period variation between minimum and maximum wind speed is about 70 km/ h.

The PAHO/OFDA/USAID wind speed data and hazard maps provide a more refined model for Hispaniola, the spatial resolution of this data is quite good.

*Table A**Error! No text of specified style in document.**.7 Comparison of PAHO/OFDA/USAID and UN Wind Hazard Map over Entire Haiti*

Source	Minimum Wind (Km/PH)	Maximum (Km/PH)	Range (Km/PH)
UN 50 Year	159.4	162.4	3
USAID 50 Year	114.2 (71)	185 (115)	70.8
UN 100 Year	188.1	191.3	3.2
USAID 100 Year	130.3 (81)	201.1 (125)	70.8

***Values in Parenthesis are Wind speed in MPH*

Climate Variability, Hazard Frequency and Magnitude

Climate Change Variability

The structure and areal extent of the wind field in tropical cyclones is largely independent of intensity storms and play an important role on potential impacts. With the use of satellite imagery and other instruments, intensity measurements have become more accurate, and as a result, the recorded intensities of wind storms in the Atlantic have been increasing (Kossin et al., 2007; Elsner et al. 2008). Time series of cyclone indices such as power dissipation show upward trends in the North Atlantic since the late 1970s (Emanuel, 2007) but interpretation of longer-term trends is constrained by data quality concerns (Landsea et al., 2012).

The IPCC Fourth Assessment Report of the Intergovernmental Panel on Climate Change (IPCC AR4) concluded that a range of modeling studies project a likely increase in peak wind intensity and near storm precipitation in future tropical cyclones. Simulations with high resolution dynamical models (e.g. Oouchi et al., 2006; Bengtsson et al., 2007; Gualdi et al., 2008; Knutson et al., 2008; Sugi et al., 2009; Bender et al., 2010) and statistical-dynamical models (Emanuel, 2007) consistently find that greenhouse warming causes tropical cyclone intensity to shift towards stronger storms by the end of the 21st century, with an expected 2 to 11% increase in mean maximum wind globally.

Frequency and Magnitude

The IPCC Fifth Assessment Report of the Intergovernmental Panel on Climate Change (IPCC AR5) indicates that the frequency of the most intense storms is more likely than not to increase by more than +10% (IPCC 2013, AR5), while the annual frequency of tropical cyclones are projected to decrease or remain relatively unchanged for the North Atlantic.

This suggests no major change in the frequency of hurricanes in North Atlantic region comprising Haiti. The SRES scenario B2 for study area of Haiti suggests that the wind speeds are projected to decrease by very small magnitude of 0.25 m/s (0.559 mph) over the projected for the 2040s relative to the 1960-1990 baseline. These projected changes have applied to model wind speed over the return period to develop wind hazard maps for Haiti that reflect projected climate change scenarios. The resultant maximum wind speed with projected climate change scenario are compared to modeled wind speeds for Haiti and are outlined in Table AError**! No text of specified style in document.**.8.

*Table A**Error! No text of specified style in document.**.8 Hazard Wind Speeds with Climate Change*

Return Period	Wind Speed (mph)Without Climate Change	Wind Speed (mph) With Climate Change
50	114.826	114.267
100	124.855	124.296
700	157.361	156.802
1700	170.000	169.441

With negligible change in the wind speed (intensity) and no major change in frequency of hurricanes, there should be little effect in terms of climate change on the wind storm hazard that will be used for the risk assessment.

Results

Hurricanes in their nature are difficult to model for their all associated parameters. It is also very difficult to quantify the impact of climate change on frequency and intensity due to complex nature of phenomenon and interrelations with other variables such as sea surface temperature and changes in land use and climate in inland areas.

The summary of the impact of the climate variability is best explained by looking at the changes in wind speed levels found throughout the study region. Presented below are a series of figures which provide an overview of hazard maps in terms of wind speed for three second gusts for a height of 10 meters for a flat terrain for return periods of 50, 100, 700 and 1700 years.

50 Year Wind Hazard Map without climate change

50 Year Wind Hazard Map with climate change

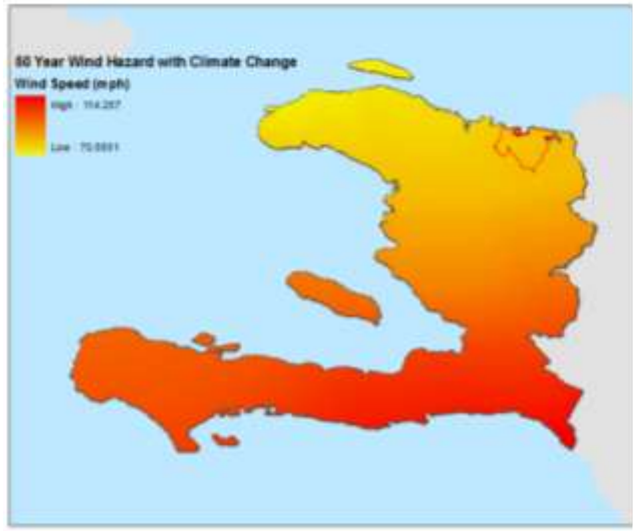

100 Year Wind Hazard Map without climate change

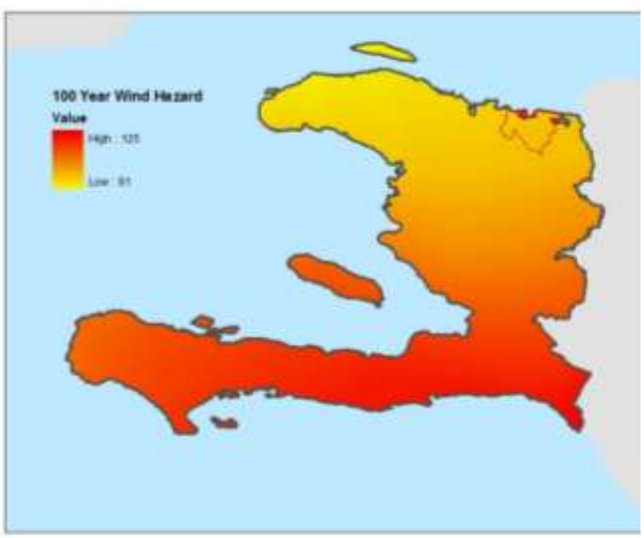

100 Year Wind Hazard Map with climate change

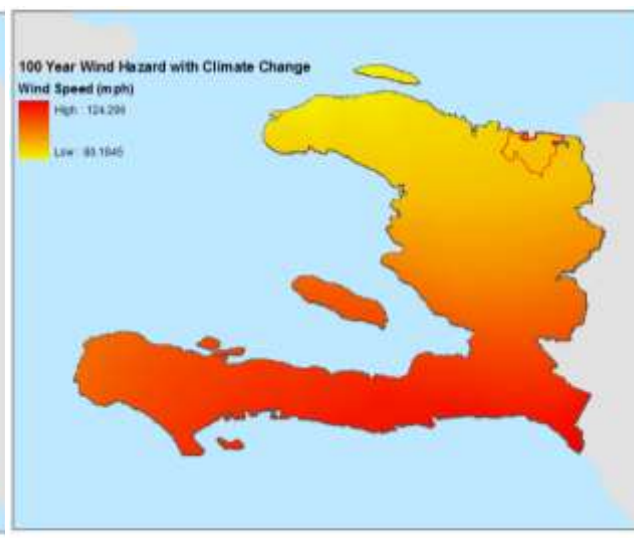

700 Year Wind Hazard Map without climate change

700 Year Wind Hazard Map with climate change

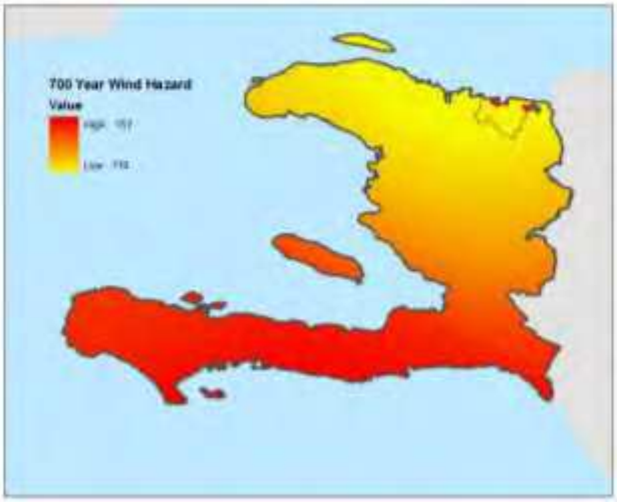

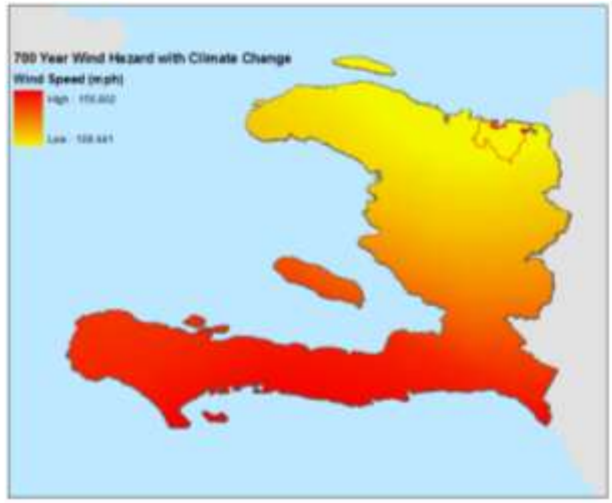

1700 Year Wind Hazard Map without climate change

1700 Year Wind Hazard Map with climate change

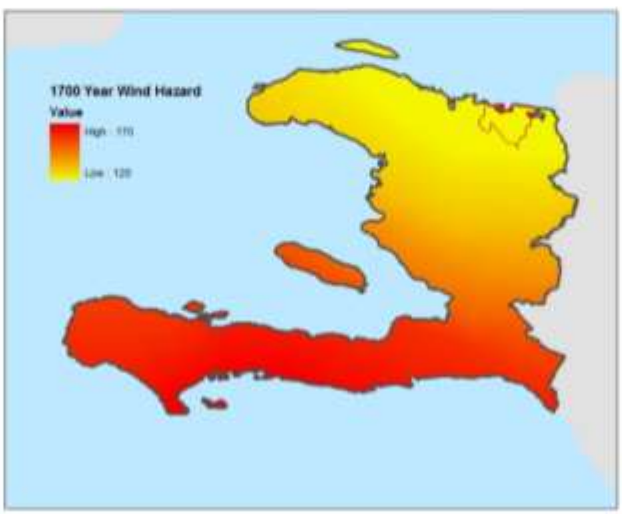

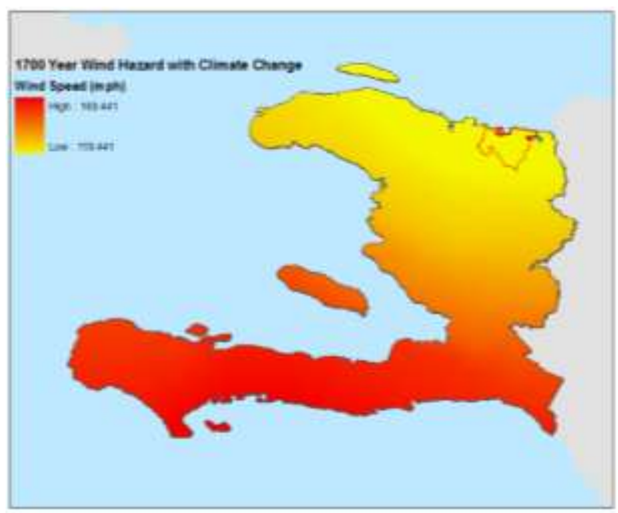

A4.4 Inland Flood Hazard

Floods can arise from a variety of causes. The most commonly understood floods occur when water levels in rivers rise and the waters overtops their banks, and adjacent floodplains and lowlands are subject to recurring floods. This type of flooding usually occurs after intense or prolonged rainfall. There also occurs in Haiti land flooding due to heavy rains where infiltration of rainfall is impeded (through either impermeable soils or development impacts). This form of localized flooding has not been assessed in this study.

Floods in Haiti, as in other Caribbean islands, follow tropical weather patterns. Haiti has two distinct rainy seasons, one from April to June and another from October to November. There have been a number of large-scale devastating flooding events in Haiti through time (see Table AError**! No text of specified style in document.**.9 below). Historically, most of the flooding events have been tied to large-scale climatic events (i.e. tropical cyclones) and have historically had the greatest impact. Recently, however, smaller low pressure systems have impacted Haiti on a yearly basis.

*Table A**Error! No text of specified style in document.**.9 History of Floods in Northern Haiti*

Year	Event	Description
1996	Flooding	Very heavy rains have caused floods in several parts of the country, in particular the departments of the North, the Northwest, the Grande Anse and the Gonave island.
2003	Flooding	Following rains between Saturday, 20 and Monday, 22 December, severe flooding occurred in northern Haiti.
2006	Flooding	On the 22 and 23 November, heavy rains caused flooding in Grand'Anse Department and the Nippes and Nord-Ouest departments; Damage to roadways including the collapse of a bridge across Ravine Sable at Trou-Bonbon.
2007	Flooding	On 17 March, 50 people had to be evacuated from areas at risk in Grand Anse. New floods were recorded in Cap-Haitien, in other parts of North and Grand Anse.
2012	Flooding	Tropical Storm Isaac hit Haiti on 25 Aug 2012, killing at least 19 people. 15,000 people had to be evacuated and 335 homes were destroyed.
2012	Flooding	Flooding caused by Hurricane Sandy killed 60 people and significantly damaged critical infrastructure such as roads, schools and hospitals. 1.8 million people have been affected, and more than 18,000 homes have been flooded, damaged or destroyed. (UN News, 2 Nov 2012)
2012	Flooding	Heavy rains during the night of 8-9 Nov 2012 in the Nord, Nord-est, Nord-ouest and Nippes departments of Haiti resulted in flooding, damage to homes and 10 deaths in Cap Haitien. More than 1,500 people were housed in 14 shelters.
2013	Flooding	Heavy rains on 14, 15 and 28 Jun 2013 caused flooding in Haiti's Artibonite, Nord-ouest and Centre departments. Six people were killed and over 6,600 families affected. Extensive damage was reported in the agriculture and livestock sectors.

Source: Relief web, accessed on December 10, 2013,
http://reliefweb.int/disasters?f%5B%5D=field_country%3A113&f%5B%5D=field_disaster_type%3A4611

Haiti's rugged and mountainous terrain coupled with environmental degradation and poor watershed management has created optimal conditions for over bank flooding problems. Haiti's surface waters are concentrated in a restricted number of important rivers that account for about 60 percent of the flow regime (World Bank, 1991). At present it is not unusual for Haiti's rivers to reach or exceed the high water line twice each year (USAID, 2007).

The two principal watersheds in the Study Area are the Trou du Nord and the Grande Rivière du Nord. The principal river of the Trou du Nord Watershed is the Rivière Trou Du Nord. The Trou du Nord watershed measures 110 Km^2 and the average annual flow rate is estimated to be 0.98 m^3/sec (UniQ, 2010). It has a permanent source of water available year round. River flow tests, which were conducted as part of a hydrological assessment of the watershed in 2011, estimated river flows to be 0.45 m^3/s (February, 2011) and 70 m^3/s in (July, 2011). The Rivière Franiche, Rivière Pilette and Rivière Cabaret are the main tributaries to this river and are intermittent streams and are dry part of the year. The Petite Rivière, an intermittent river, is also located in this basin and drains into the Trou du Nord plain. The Grande Rivière du Nord watershed measures 680 Km^2 and the average discharge (mean daily flow) 5.44 is m^3/sec. (USAID, 2007). The Rivière Caracol and

Rivière Cartache are main tributaries to this river. The Rivière Caracol is a permanent river with a constant source of water, while the Rivière Cartache is an intermittent stream and is dry part of the year.

In a 2007 study to compare and rank Haiti's watersheds quantitatively, USAID along with the Haitian Government, established review criteria for prioritizing watershed interventions. The USAID[6] study explored the relative ranking of watersheds based on their vulnerability to loss of human life, productive infrastructure, soil potential, or erosion risk. Out of Haiti's 54 watersheds, the study found that the relative vulnerability ranking of the Trou de Nord and Grand Rivière du Nord watersheds to be significant.

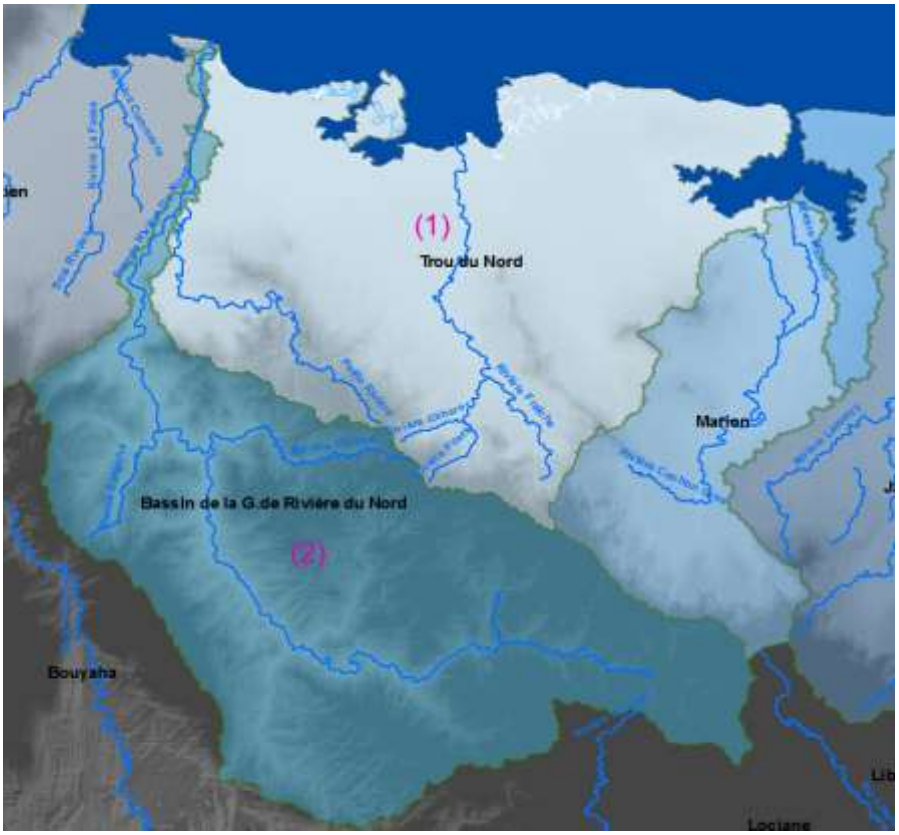

*Figure A**Error! No text of specified style in document.**.13 Key watersheds in the Study area*

Source: ERM, CNGIS

The general susceptibility of these watersheds in the Northern Development Corridor, has not declined in recent years. In fact, the widespread deforestation, clearing of land for agriculture and increased urbanization has served to exacerbate flooding problems in the region. Urban expansion and unplanned urban development, does not allow aquifers to function as storage and floodplain to work as filters during intense rainfall events (USAID, 2007).

The commune of Quarter Morin, which is situated in a moist, low lying alluvial plan and bordered on the east by the Grand Riviere du Nord, is prone to flooding. Several factors have worked to increase the susceptibility of flooding, including more intense climatic events, increased run-off, and the accumulation of debris

[6] USAID 2007, Environmental Vulnerability in Haiti: Findings & Recommendations

downstream. Limonade is bordered by the Grand Riviere du Nord on the west. While the Barrage de Tannerie previously helped to contain flood waters and provide irrigation during the dry season, the dam failed in the 1960s and has not been repaired. Intense rainfall causes flooding and the accumulation of water in low-lying areas which are slow to drain following flooding events due to limited or inadequate storm water drainage infrastructure. Limonade receives an average of 1200-1400 mm rainfall annually.

In Trou du Nord, the terrain, rainfall and soil types, in both the mountains and plains, give rise to a fairly dense network of rivers. The Trou-du-Nord river is the most important river system. In low-lying portions of commune, there are a series of smaller tributaries and torrential gullies. Large areas of the plain are subject to frequent flooding caused by torrential downpours. The heavy clay content of the soil causes erosion and results in frequent sediment build up in streams. Urban areas are adjacent to the main river with development occurring in riparian zones. Historically, the city has been flooded severely.

Flood risks are also present in the northeast portion of the Terrier Rouge commune, sometimes impacting the city on its northern edge. To the south, settlements experience higher annual rainfall amounts, and as a result, experience flash floods. The urban development of the city is constrained by low lying topography, which is prone to flooding. The annual rainfall averages 900 mm on the coast to 1200 mm south of the RN6.

Determination of Flood Hazard

A detailed flood hazard assessment methodology was pursued to include a meteorological analysis that includes a probabilistic simulation of rainfall which has considered climate change. The hydrological modeling has been conducted for the Basin de la Grande Riviere du Nord and Basin Trou de Nord. The Hydrologic Modeling System (HEC-HMS) is designed to simulate the precipitation-runoff processes of dendritic watershed systems so as to take into consideration total drainage to account for geometric profiles of watersheds. We have used high resolution DTM to conduct the hydrological modeling to generate the precipitation-runoff processes (i.e. flows). Finally, hydraulic modeling of the main rivers identified above have been undertaken to develop probabilistic flood forecast maps for six return periods (i.e. 2-, 5-,10-, 25-, 50-, 100-return periods) for the portions of the basin that intersect the study area.

Challenges in Flood Hazard Model

The main challenges presented focused attention on filling in gaps of daily precipitation data and resolving issues associated integrating DTMs at different resolutions of DTMs for the study area.

Precipitation Modeling

The lack of reliable flooding data, as well as the lack of instrumental rainfall and discharge or flow data within the region, has predicated the need to depend on older national level historical rainfall data or regional proxies in order to understand the hydrology of watersheds within the region. National and regional precipitation data from pluviometric stations that was collected revealed that there was extensive data collected at monthly time intervals and very poor or limited data for 24 hr intervals. The paucity of 24 hr data, which is needed for flood modeling, predicated the need to fill gaps by developing a 24 hr precipitation baseline by comparing monthly rainfall data and global models (i.e. Santa Clara University). This was done in order to ensure that an appropriate approximation was developed to understand flows in the hydrological model. The development of a 24 hr intensity baseline was essential for the execution of a hydrological model given the small size of the study area.

It is important to note that various global rainfall data models were compared, evaluated against each other and available monthly rainfall data. The various data compared have been given in

Table A**Error! No text of specified style in document.**.10.

*Table A**Error! No text of specified style in document.**.10 Various Global Data Compared for Deriving Daily Rainfall Distribution*

Sr.No	Data	Temporal Resolution	Availability	Period
1	CPC .25x.25 Daily US Unified Precipitation	Daily	USA	1948 to 2006
2	CPC Hourly Precipitation	Hourly	USA	From 1948
3	CMAP global gridded precipitation means	Monthly	Global	1979 to near present
4	Global Precipitation Climatology Centre (GPCC)	Monthly	Global	1901-present
5	GPCP V2.2 Precipitation	Monthly	Global	1979-present
6	U. of Delaware Precipitation and Air Temperature	Monthly	Global	1901-2010
7	TRMM- Tropical Rainfall Measuring Mission	Radar Based Rainfall Sub daily	near global	2000 onwards
8	Santa Clara University - Gridded Observed Rainfall	Daily	Global	1950-1999

For probabilistic return period analysis of rainfall, at 30 years of continuous records are desirable so were data at a daily time interval. Therefore, the Santa Clara University data was utilized for the time period of 1950-1999, which matches with the longest and consistent data recorded in Haiti.

Figure AError**! No text of specified style in document.**.14 provides a depiction of a comparison of the monthly precipitation data from Santa Clara University and that of the Cap Haitien pluviometric station. The 24 hour rainfall data from nearest grid point of Santa Clara University has been processed and a time distribution has been applied over the monthly rainfall data that has been collected for pluviometric stations in and around the study area. Snapshot of estimated daily time step data is given below (Figure AError**! No text of specified style in document.**.15).

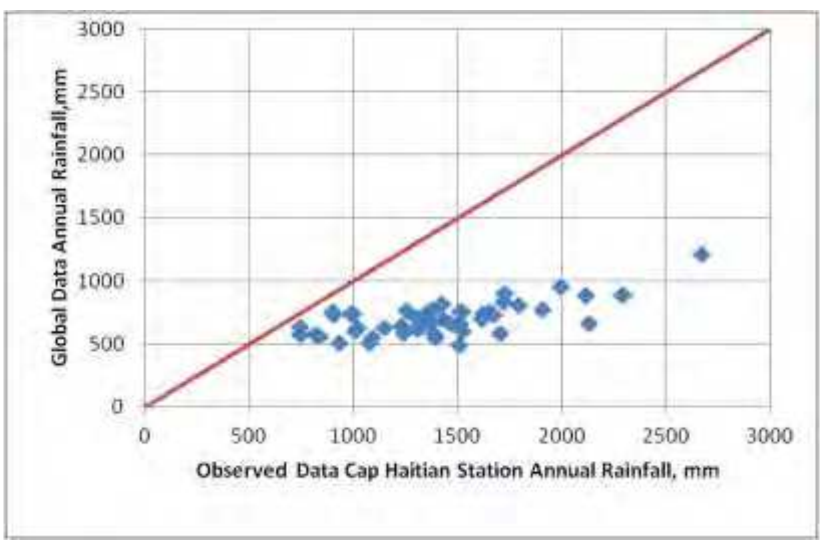

*Figure A**Error! No text of specified style in document.**.14 Comparison of Santa Clara Data with observed monthly precipitation data*

Year	Month	Day	SC Daily Rainfall	UID	Santa Clara Monthly	Distribution %	Observed Monthly	Estimated Daily
1950	1	1	3.23	1950_1	51.58	6.26%	62.1	3.89
1950	1	2	0	1950_1	51.58	0.00%	62.1	0.00
1950	1	3	1.43	1950_1	51.58	2.77%	62.1	1.72
1950	1	4	0	1950_1	51.58	0.00%	62.1	0.00
1950	1	5	1.33	1950_1	51.58	2.58%	62.1	1.60
1950	1	6	0	1950_1	51.58	0.00%	62.1	0.00
1950	1	7	0	1950_1	51.58	0.00%	62.1	0.00
1950	1	8	4.56	1950_1	51.58	8.84%	62.1	5.49
1950	1	9	0	1950_1	51.58	0.00%	62.1	0.00
1950	1	10	0	1950_1	51.58	0.00%	62.1	0.00
1950	1	11	0	1950_1	51.58	0.00%	62.1	0.00
1950	1	12	5.43	1950_1	51.58	10.53%	62.1	6.54
1950	1	13	0	1950_1	51.58	0.00%	62.1	0.00
1999	12	16	0.15	1999_12	66.79	0.22%	53.1	0.11
1999	12	17	0	1999_12	66.79	0.00%	53.1	0.00
1999	12	18	0	1999_12	66.79	0.00%	53.1	0.00
1999	12	19	0.11	1999_12	66.79	0.16%	53.1	0.09
1999	12	20	0.25	1999_12	66.79	0.37%	53.1	0.20
1999	12	21	1.23	1999_12	66.79	1.84%	53.1	0.98
1999	12	22	0.22	1999_12	66.79	0.33%	53.1	0.17
1999	12	23	2.15	1999_12	66.79	3.22%	53.1	1.71
1999	12	24	0.45	1999_12	66.79	0.67%	53.1	0.36
1999	12	25	1.37	1999_12	66.79	2.05%	53.1	1.09
1999	12	26	3.47	1999_12	66.79	5.20%	53.1	2.76
1999	12	27	2.85	1999_12	66.79	4.27%	53.1	2.27
1999	12	28	0	1999_12	66.79	0.00%	53.1	0.00
1999	12	29	0	1999_12	66.79	0.00%	53.1	0.00
1999	12	30	5.42	1999_12	66.79	8.11%	53.1	4.31
1999	12	31	4.02	1999_12	66.79	6.02%	53.1	3.20

*Figure A**Error! No text of specified style in document.**.15 Snapshot of estimated daily rainfall using observed monthly rainfall and Santa Clara data*

The simulated daily rainfall data for the pluvimetric stations have been used to estimate probabilities or return period rainfall. Using simulated data series, annual maximum 24hr was derived for 49 years to fit the probability distribution. Using Log Pearson Type III distribution return period rainfall for 2, 5, 10, 25, 50, and 100 years has been estimated (Figure AError**! No text of specified style in document.**.16).

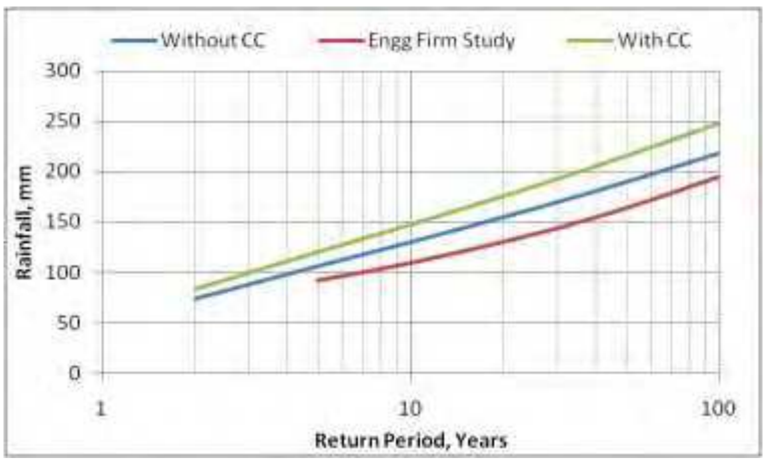

*Figure A**Error! No text of specified style in document.**.16 Estimated Return Period Rainfalls*

The estimated return period rainfall has been given as input to HEC-HMS model for simulation of flows to corresponding return periods.

Digital Elevation Model Development

Initially only a 10 m DTM was available for the study area. The hydrological modeling was initiated to determine if this resolution was sufficient for modeling purposes. It was found that the 10 m DTM was quite flat in coastal areas, with very negligible variation (i.e. the coastal areas showed mostly 0 m elevation). Instead, a 2 m DTM was made available for a more confined study area and required that the 2 m DTM be merged with the 10m DTM in order to create an elevation model with sufficient resolution for flood modeling. The merging of the two elevation models presented challenges as there was a high variation in the elevation in overlapping areas particularly at the southern edges (Figure AError**! No text of specified style in document.**.17).

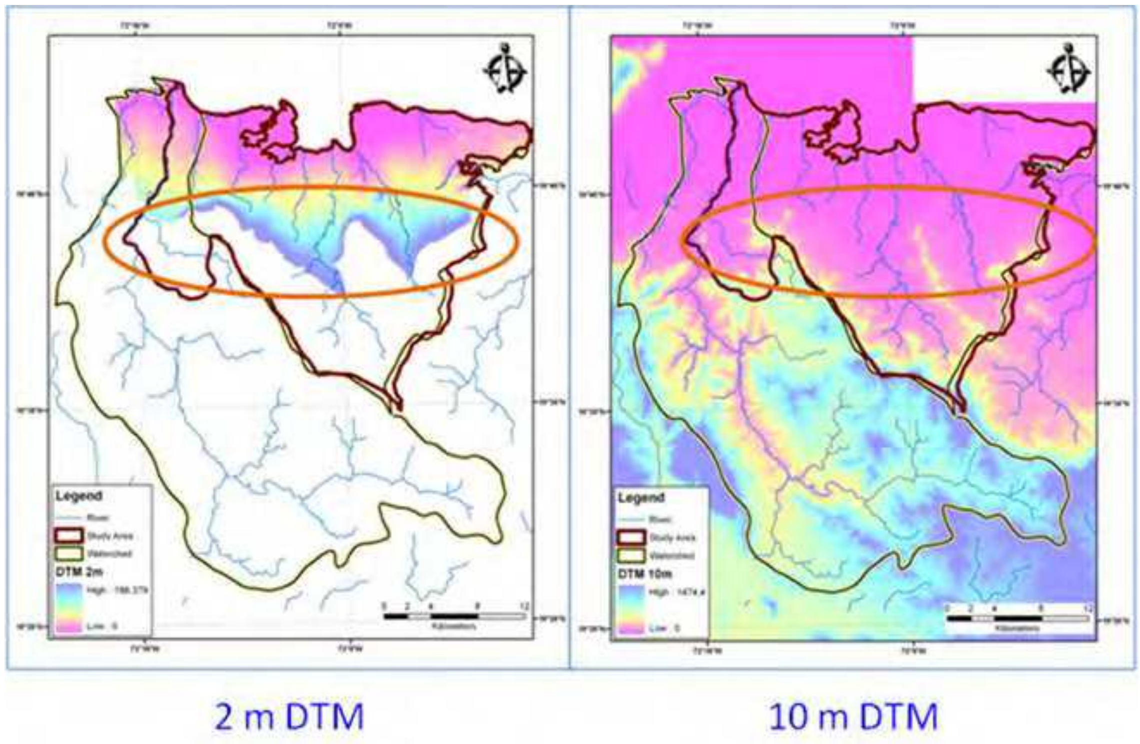

*Figure A**Error! No text of specified style in document.**.17 Two different DTMs available for study area and beyond*

As discussed above, two DTMs (of 2m and 10m resolutions) were evaluated separately. It was found that overlapping areas of two DTMs showed elevation difference of + 10 m at the edge of 2 m DTM predicating a more complex merger procedure that involved the overlaying of contours to understand elevation differences and the use of generalized and point specific data to refine data to desired the 2 m resolution. This merged 2 m DTM was cross checked with 9 Geodetic Control Points made available by IDB and the comparison revealed only a 0.12m average differential in elevation (Table AError**! No text of specified style in document.**.11).

*Table A**Error! No text of specified style in document.**.11 Various Global Data Compared for Deriving Daily Rainfall Distribution*

GCP Point	GCP Elevation	Merged DTM Elevation, m	Difference, m
2	11.55	11.21	0.34
3	14.80	14.53	0.26
4	3.06	2.15	0.91
5	23.67	23.80	-0.13
6	14.25	14.07	0.18
7	35.73	36.21	-0.48
8	24.20	24.11	0.09
9	5.24	5.06	0.18
10	1.71	2.00	-0.29
		Average	0.12

Hydrological Model

A Hydrological model for key watersheds/drainage basins of the study area have been developed using HEC–HMS model. The hydrologic model was established in a GIS framework using Environmental Systems Research Institute (ESRI) ArcGIS and HEC-GeoHMS 4.2 software. HEC-GeoHMS 4.2 is an extension application that supports identification of the river network and division of the catchment (basin area) into a number of sub areas. This procedure requires a digital elevation model (DEM). As mentioned earlier, the 2 m merged DTM was used to delineate basin and river networks. Using HEC Geo-HMS, the river network and sub basins have been delineated using a systematic approach. The approach creates raster grids for catchment delineation. Activities to complete the model include filling sinks, creating flow direction and flow accumulation grids, processing catchment grid, and processing drainage line.

The physical representation of the basin incorporates various hydrologic elements (sub basins, river reaches, and junctions), which are connected in a dendritic network to simulate the rainfall-run-off process. Based on the DTM, soil and land use information, various parameters such as abstractions, infiltration, routing have been estimated for each sub basin and are given as input to the model.

Grand Rivere du Nord: The hydrological basin area of Grand Rivere du Nord is estimated to be approximately 611 square kilometers. Through basin delineation and hydrological model development process, fifty-one (51) sub basins were developed for this basin, which also included 25 stream reaches. The HMS model schematic for this basin is shown in Figure AError**! No text of specified style in document.**.18.

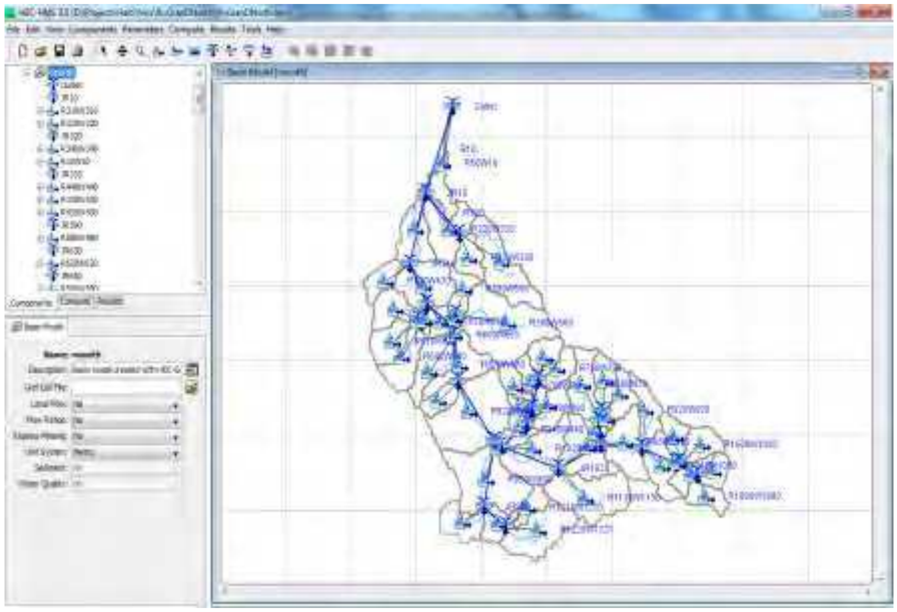

*Figure A***Error! No text of specified style in document.***.18 HMS set up for River Grand du Nord*

Trou du Nord: The basin area of main stream of Trou du Nord is estimated to be approximately 106 square kilometers. Through basin delineation and hydrological model development process in all 11 sub basins were developed for this basin, which also included 5 stream reaches. HMS model schematic for this basin is shown in Figure AError**! No text of specified style in document.**.19. The HMS model schematic for another stream in Trou du Nord basin is shown in Figure AError**! No text of specified style in document.**.19 HMS set up for River Trou du Nord

.

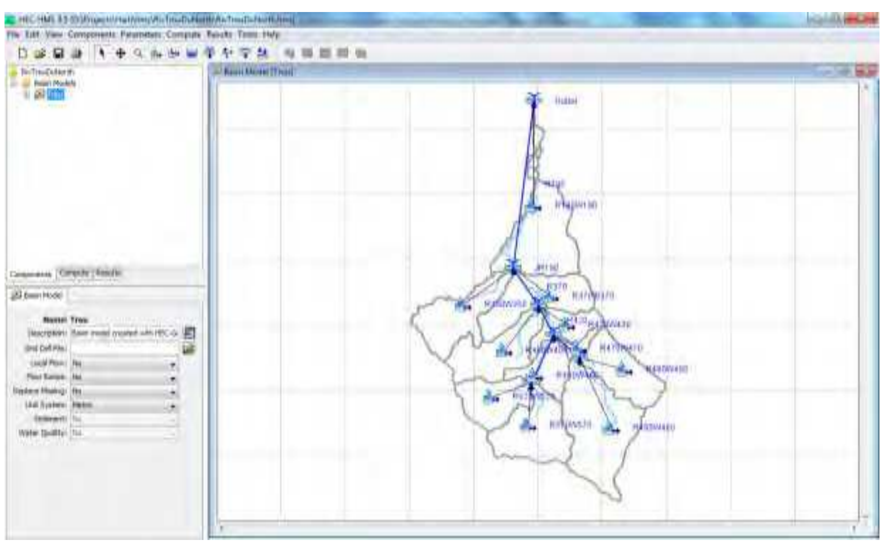

*Figure A***Error! No text of specified style in document.***.19 HMS set up for River Trou du Nord*

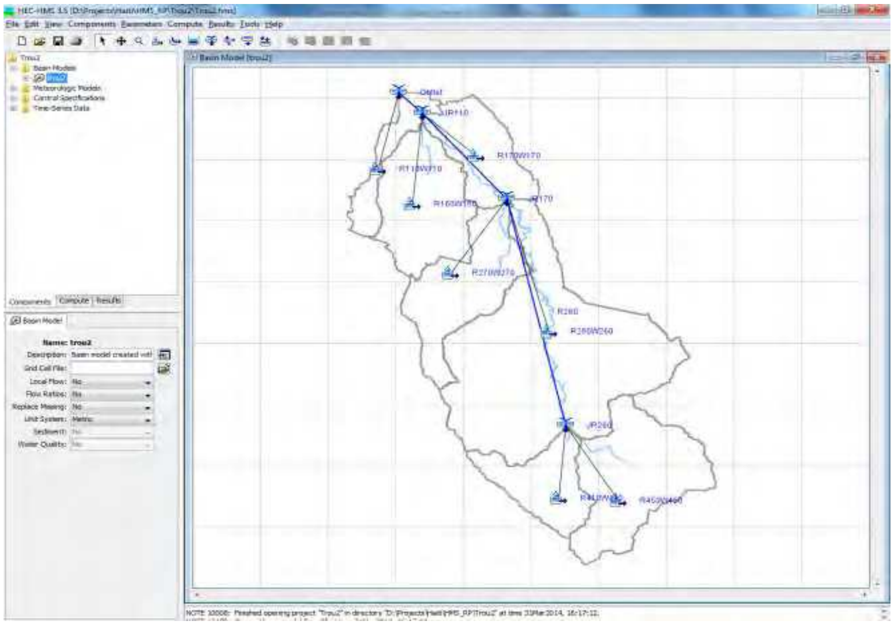

*Figure A**Error! No text of specified style in document.**.20 HMS set up for River Trou du Nord (Stream 2)*

The key selected parameters three watersheds are given in Table AError**! No text of specified style in document.**.12.

*Table A**Error! No text of specified style in document.**.12 Various Global Data Compared for Deriving Daily Rainfall Distribution*[7]

River Basin	Area, Km^2	length of principal river, m	Elevation, m	Slope, m/m	Concentration time (min)
Grand River Du Nord	611	107,949	471	0.0044	1,186
Trou Du Nord-Stream1	106	25,325	69.9	0.0028	463
Trou Du Nord –Stream2	87	20,221	48.3	0.0024	412

In absence of the observed historical flow or discharge information, detailed hydrological model calibration and validation was not possible. In order achieve the reasonable confidence in developed models, runoff coefficients (ratio of runoff to rainfall) from reported studies (MARNDR, MPCE, MICT, MDE, 2000) were compared with simulated runoff coefficient from the model developed in this study. The study MARNDR, MPCE, MICT, MDE, 2000 reported runoff coefficient for River Grand Du Nord as 20.5%. Various simulations of the model used for this study gave an average runoff coefficient of 18.1%. The difference between observed and simulated runoff coefficient is 2.4 % and was determined to be within acceptable range, and as a result, the average run-off coefficient (i.e. 18.1%) was used to simulate the return period flows for various streams.

[7] In absence of recorded daily rainfall, analysis is based on mix of observed monthly and modeled rainfall records and only with very extensive and reliable flow information would we be able to accurately model hydrological regime.

Hydraulic Model

In many applications of river flood modeling, a one-dimensional full hydrodynamic modeling system is used. The one-dimensional hydrodynamic model HEC-RAS, developed by the United States Army Corps of Engineer's Hydrologic Engineering Centre, was used for performing hydraulic calculations for the river stretches.

HEC-RAS is an integrated system of software. It can calculate water surface profiles for both steady and unsteady, gradually varied flows for a full network of natural and constructed channels. Steady flow simulation was adopted for this study. The model comprises channel and floodplain geometry, which is defined by a series of cross-sections or transects together with hydraulic structures such as bridges, weirs, and levees. The basic computational procedure is based on the solution of the one-dimensional energy equation. Energy losses are evaluated by friction, expansion, and contraction losses. The momentum equation is utilized in situations where the water surface profile is varying rapidly. The situations include a mixed flow regime.

Cross Sections

The HEC Geo-RAS software application was used in a Geographic Information Systems (GIS) (ESRI Arc GIS 10) to develop and verify geometry of principal river systems by developing cross section of the channels and floodplains.

HEC- GeoRAS is a set of procedures, tools and utilities that were used to process georeferenced data in a GIS environment to facilitate and complete the job with HEC- RAS . For this study, the cross sections of the channel and the geometry of the terrain in HEC- GeoRAS were digitized and then the file is exported to HEC- RAS to calculate flow rates. Cross-sections have been extracted from DEM at a spacing of about 100 m.

The HEC- RAS tool interpolates channel cross sections, as shown in the figures below. After performing hydraulic modeling with HEC- RAS , HEC- with a post-process generated the final GeoRAS results that are flooding surfaces for each return period was performed. Figure AError**! No text of specified style in document.**.21 and Figure AError**! No text of specified style in document.**.22 show the cross sections for river Grand Du Nord and River Trou Du Nord respectively.

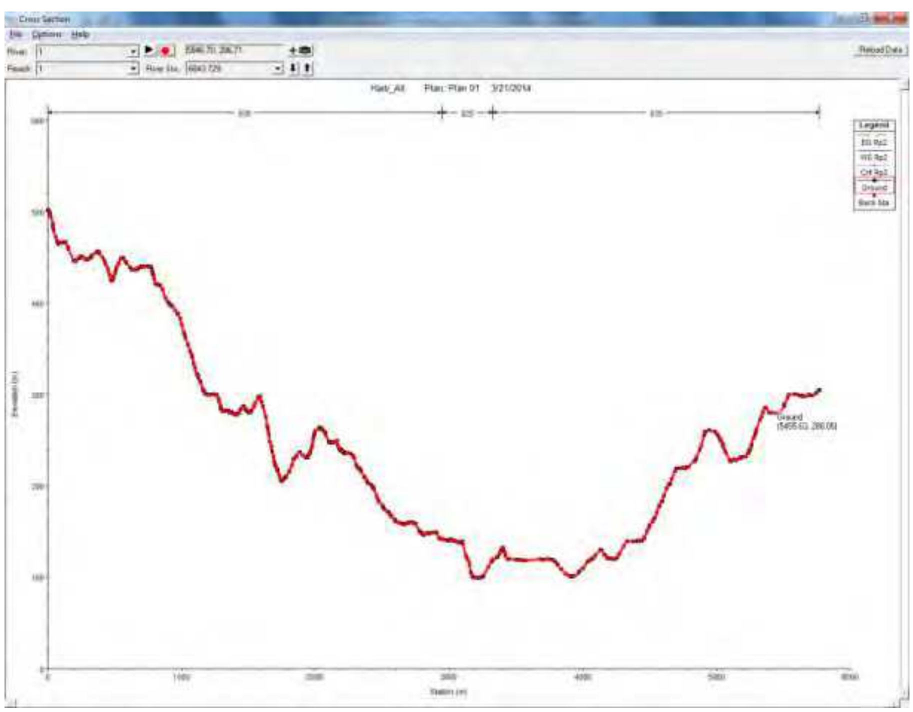

*Figure A**Error! No text of specified style in document.**.21 Cross section for River Grand du Nord*

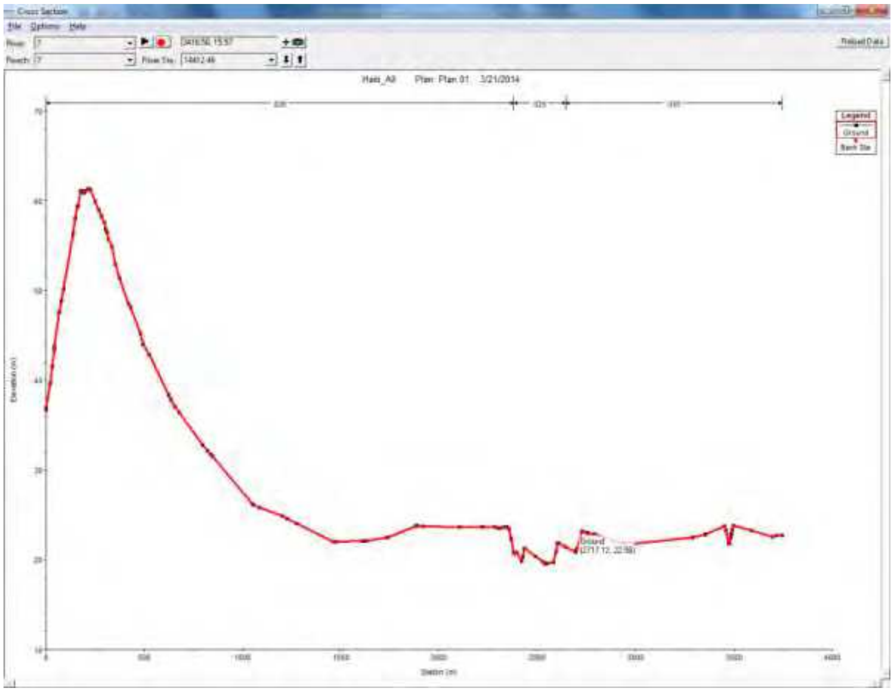

*Figure A**Error! No text of specified style in document.**.22 Cross section for River Trou du Nord*

Roughness Coefficients

The Manning roughness coefficients were determined based on land use information available. Manning coefficients for the main channel and floodplains are shown in Table AError**! No text of specified style in document.**.13 below.

*Table A**Error! No text of specified style in document.**.13 Roughness Coefficients*

River	Flood Plain	Main Channel
River Grand Du Nord	0.035	0.025
River Trou Du Nord	0.035	0.025

Peak flow Rates

Table AError**! No text of specified style in document.**.14 presents the flow rates (cumec) for return periods of 2, 5, 10, 25, 50 and 100 years.

*Table A**Error! No text of specified style in document.**.14 Peak flow rates for major rivers*

Return Period, Years	Grand River Du Nord			Trou Du Nord		
	Stream1	Stream2	Main Stream	Stream1	Stream2	Main Stream
2	113.0	10.0	123.0	4.0	4.3	10.0
5	238.5	25.0	263.5	10.7	14.7	38.0
10	323.0	36.0	359.0	16.9	20.0	50.0
25	384.0	52.0	436.0	23.4	28.4	74.0
50	528.0	65.0	593.0	28.7	35.8	90.0
100	635.0	78.0	713.0	36.0	42.2	108.0

The summary of flow rates represents appropriate scenarios for modeling the flood hazard in the study area. Having said this, the analysis is based on modeled rainfall records and only with very extensive and reliable flow information would we be able to accurately model hydrological regime.

Flood Hazard Maps

The above data was used to understand flood hazard, particularly the overflow channels in the Northern Development Corridor of Haiti by defining associated flood events with different probabilities. For the calculation of these variables the HEC-RAS hydraulic model was used to characterize inland flooding in the study area. Flood hazard maps for 50 and 100 year return periods are shown in Figure AError**! No text of specified style in document.**.23 and Figure AError**! No text of specified style in document.**.23 Flood Hazard Map without Climate Change 50 year return period

.

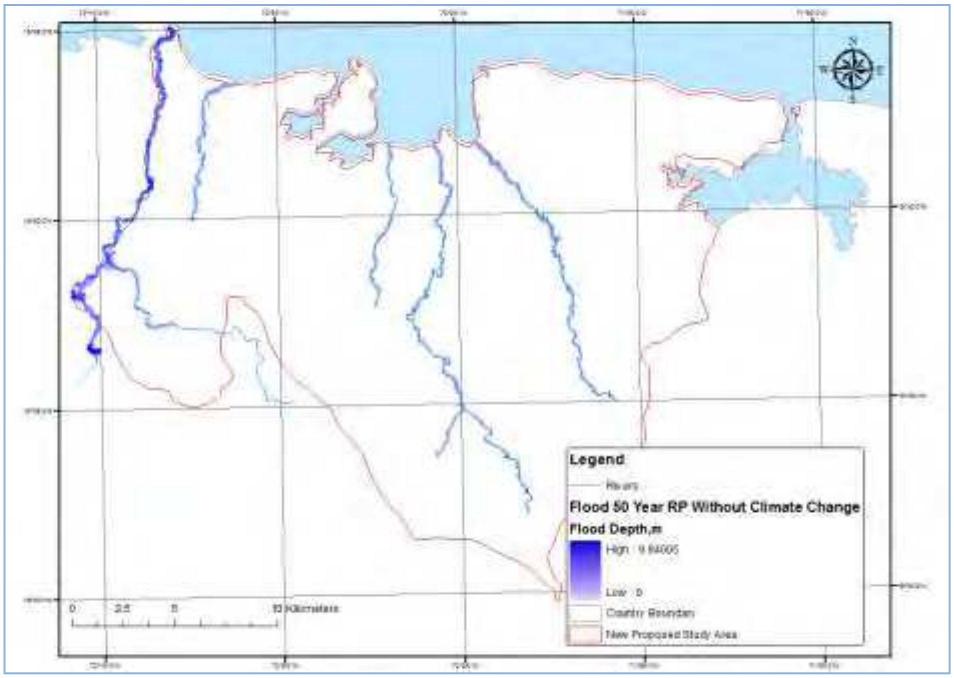

*Figure A**Error! No text of specified style in document.**.23 Flood Hazard Map without Climate Change 50 year return period*

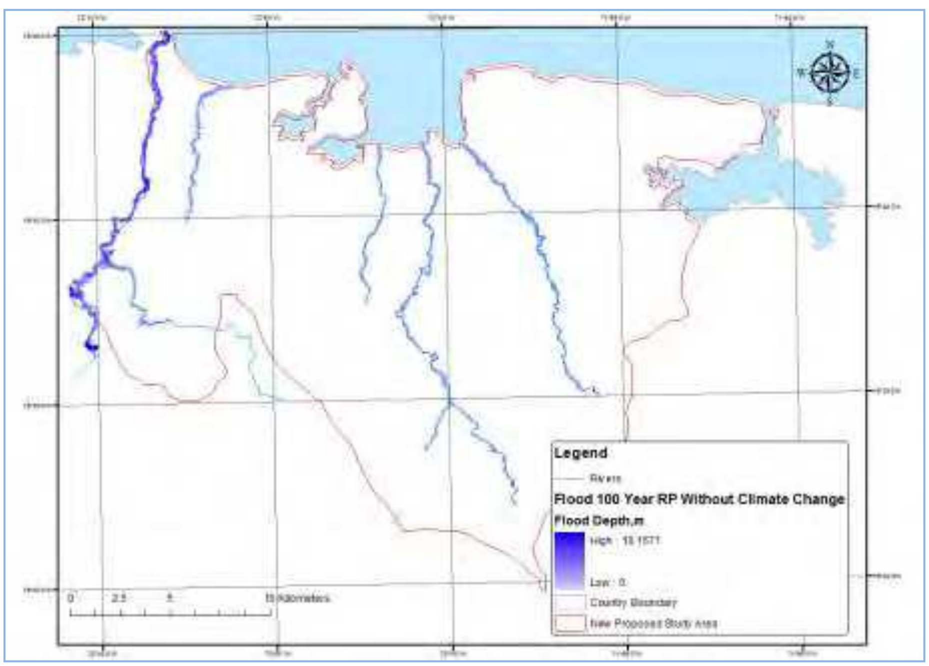

*Figure A**Error! No text of specified style in document.**.24 Flood Hazard Map without Climate Change 100 year return period*

Climate Variability, Hazard Frequency and Magnitude

Climate Change Variability including Climate Change

The main step in delineating the extent of flooding under future climatic conditions involves the use of climate projections (taken from the University of West Indies studies in Appendix 3). Rainfall data, particularly the potential increase in extreme rainfall events, in return flow values at 2, 5, 10, 25, 50, and 100 year return periods to understand changes in susceptibility to flooding due to climate change were applied. The resulting impacts are manifested in changes in the extent of flooding.

The projected impact on climate change is presented in Table AError**! No text of specified style in document.**.15, which shows the variance in maximum flow rates for events of 2, 5, 10, 25, 50, and 100 year return periods, as well as shown in Figure AError**! No text of specified style in document.**.25 for main stream of river Trou Du Nord for all return periods.

*Table A**Error! No text of specified style in document.**.15 Peak flow rates for major rivers with and without climate change*

Basin	Stream	T=50	T^{CC}=50	T=100	T^{CC}=100
Grand River Du Nord	Stream1	528.0	632.0	635.0	737.0
	Stream2	65.0	75.0	78.0	92.0
	Main Stream	593.0	707.0	713.0	829.0
Trou Du Nord	Stream1	28.7	34.9	36.0	42.2
	Stream2	35.8	41.2	42.2	48.5
	Main Stream	90.0	108.0	108.0	128.0

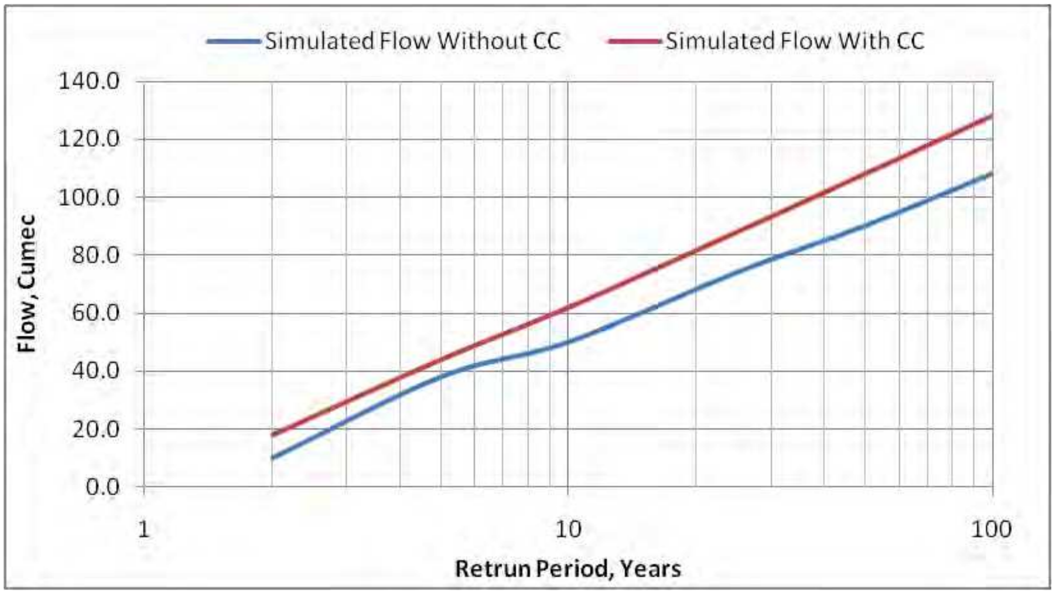

Figure AError! No text of specified style in document..25 Return Period Flows with and without climate change for Trou du Nord river

Frequency and Magnitude

Table AError**! No text of specified style in document.**.16 shows maximum flood depths simulated for the study area with and without climate change. Results shows that with climate change on an average flood depth will increase by about 0.23 m (23 cm) across all return periods. With climate change, the flood depth for a 100 year return period is expected to be 10.17m. Flood hazard maps for 50 and 100 year return periods with climate change are shown in Figure AError**! No text of specified style in document.**.26 and Figure AError**! No text of specified style in document.**.27.

Table AError! No text of specified style in document..16 Various Global Data Compared for Deriving Daily Rainfall Distribution

Return Period, Years	Maximum Flood Depth, m	
	Without CC	**With CC**
2	8.71	8.89
5	9.2	9.36
10	9.46	9.81
25	9.63	9.91
50	9.94	10.16
100	10.17	10.36

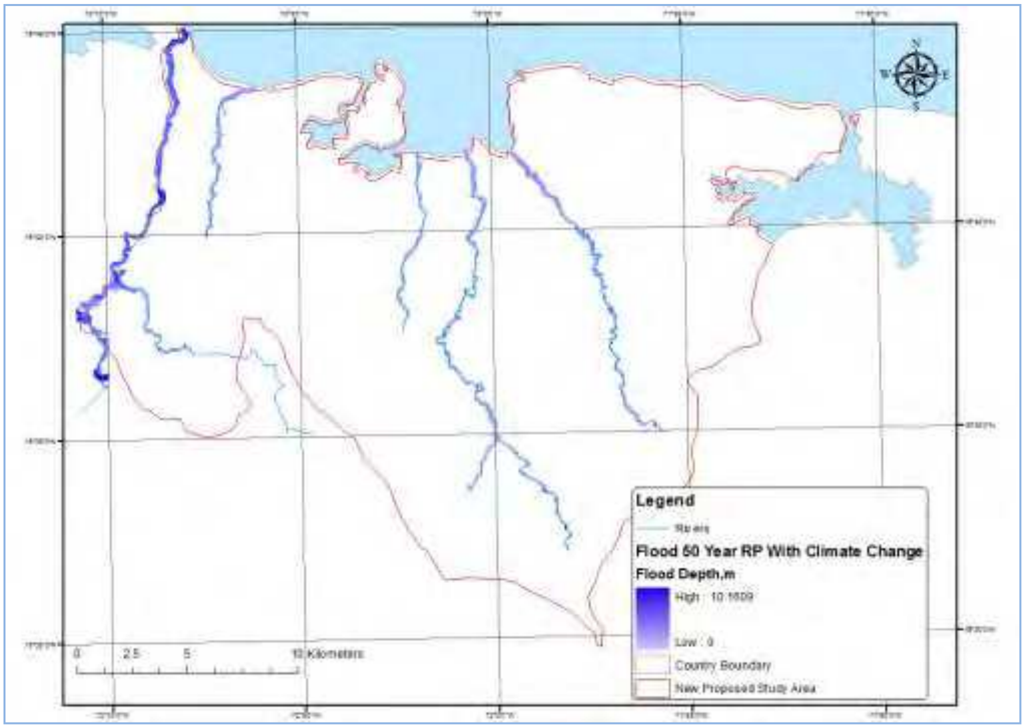

*Figure A**Error! No text of specified style in document.**.26 Flood Hazard Map with Climate Change 50 year return period*

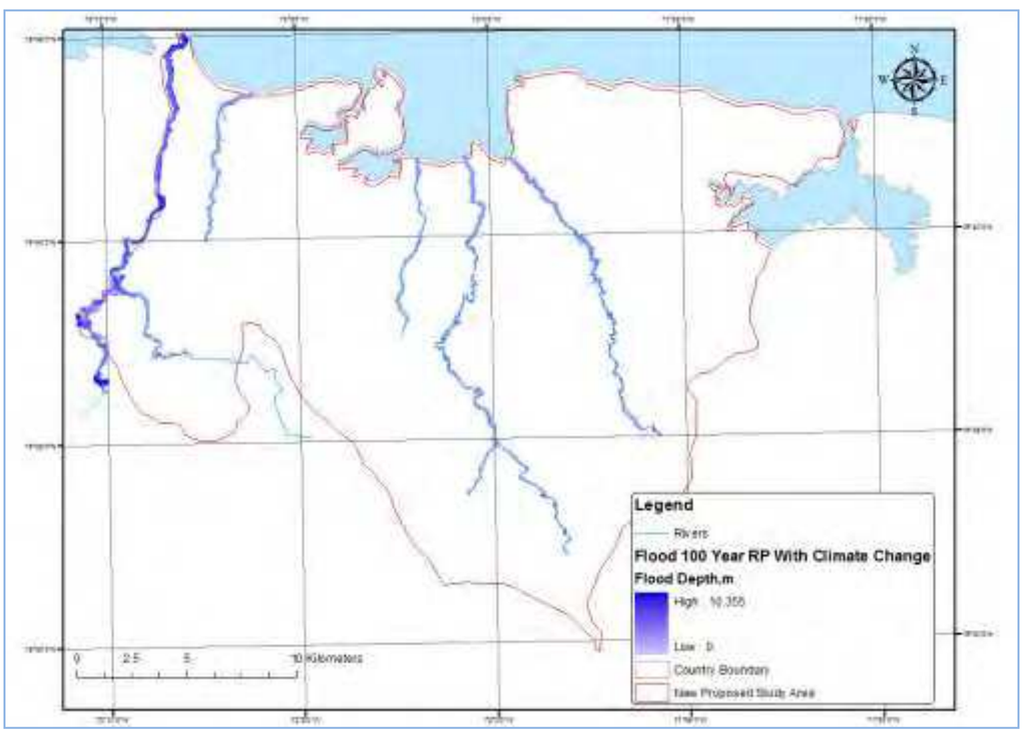

*Figure A**Error! No text of specified style in document.**.27 Flood Hazard Map with Climate Change 100 year return period*

Through climate change impact assessment on floods it is observed that slight increase in frequency and magnitude will have minor impact on vulnerability of the structures in the study area. Overall impact in terms of climate change induced flood risk shall have minor implications in planning stage.

Comparing the areas of the floodplain without climate change reveals that the flood zone for the event 50 years would be 12.21 km^2 and the floodplain for the event 100 years would be 13.09 km^2. In other words, there is only a slight change (7.2 % increases) in the extent of the floodplain for the 100 year event. The comparison between flood zones for events 50 and 100 years with climate change reveals bit smaller difference in the flooded area (about 5.2 % increase as shown in Table AError**! No text of specified style in document.**.17)

*Table A**Error! No text of specified style in document.**.17 Comparison of Inundation area with and without climate change*

Return Period, Years	Inundation Area, sq km	
	Without CC	With CC
2	7.52	8.25
5	9.69	10.3
10	10.59	11.37
25	11.53	12.41
50	12.21	12.97
100	13.09	13.64

A comparison between the return period of 50 years without and with climate change reveals just a 6.2 % increase, while the difference in the floodplain for the event 100 years with and without climate change was 4.2 %.

A4.5 Coastal Flood Hazard

Context

High waves associated with tropical cyclones are potentially very dangerous and damaging to the coastal settlements. The United States National Oceanic and Atmospheric Administration (NOAA)[8] identify this phenomenon as storm surge, which is defined as an abnormal rise of water generated by a storm, over and above the predicted astronomical tides. NOAA furthers that storm surge should not be confused with storm tide, which is defined as the water level rise due to the combination of storm surge and the astronomical tide. This rise in water level can cause extreme flooding in coastal areas particularly when storm surge coincides with normal high tide.

The storm surge is produced by water being pushed toward the shore by the force of the winds moving cyclonically around the storm. The impact on surge of the low pressure associated with intense storms is minimal in comparison to the water being forced toward the shore by the wind. In the Caribbean, hurricane categories can be used to approximate expected storm surges. The resulting potential inundation areas are grouped by categories which refers to the Saffir-Simpson Hurricane Intensity Scale described in

[8] http://www.nhc.noaa.gov/surge/

Table A**Error! No text of specified style in document.**.18.

*Table A**Error! No text of specified style in document.**.18 Saffir-Simpson Hurricane Scale and expected storm surge*

Category	Storm Surge (feet above normal sea level)
1	4–5 ft.
2	6–8 ft.
3	9–12 ft.
4	13–18 ft.
5	> 18 ft.

The intensity of the storm surge is affected by the width and slope of the continental shelf. A shallow slope will potentially produce a greater storm surge than a steep shelf. In the north, continental shelf drops off very quickly, which works to lessen the impact of storm surge.

The interaction of these various processes is illustrated in

. The total design water level can be computed by addition of three components. The wave setup heights are the heights of wave crests above the storm surge level in open water. The coastal provinces of Northern Haiti experience coastal flooding due to the destructive effects of total design water levels.

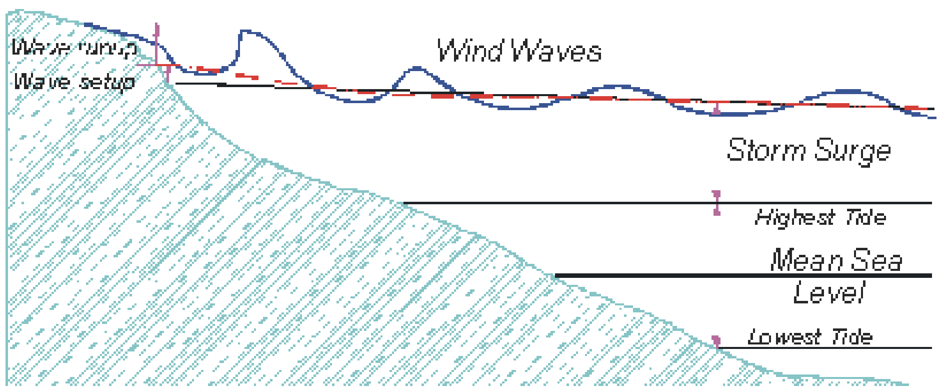

*Figure A**Error! No text of specified style in document.**.28 Systematic diagram illustrating the contributions to coastal sea level from tides, storm surge and wave processes*

Source: http://www.cmar.csiro.au/sealevel/sl_drives_short.html

Zahibo[9] (2012), however, postulates that the position of the island of Hispaniola may give it special protection from extreme waves. The presence of several banks (Figure AError**! No text of specified style in document.**.29), such as the Turks and Caicos, Mouchoir and Silver banks, protect coastal areas against the long swells of generated in the North Atlantic. Zahibo furthers that these extensive shallow areas (50-150 meters in depth) dissipate the energy of longer swells and thus reduce the potential impact from waves.

[9] unpublished paper as part of NATHAT

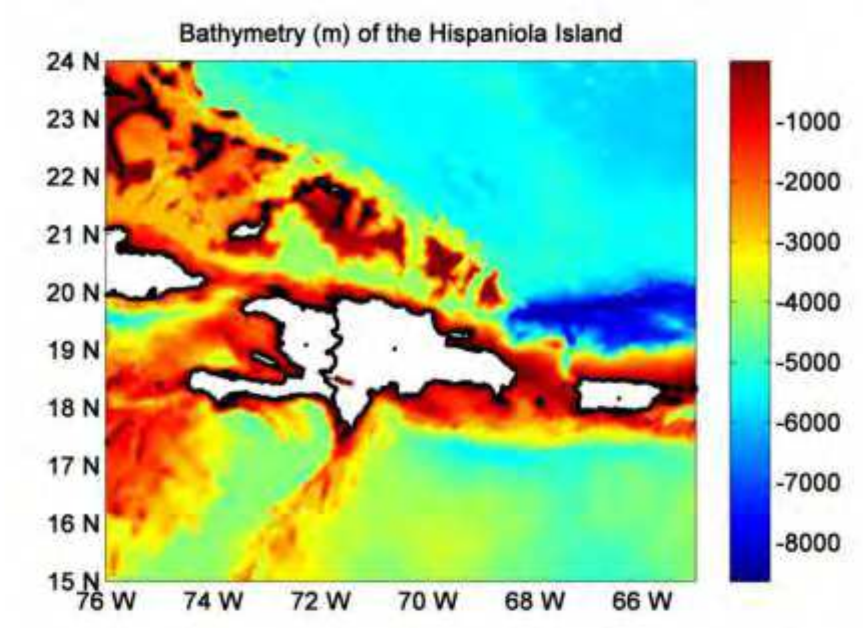

*Figure A**Error! No text of specified style in document.**.29 Bathymetry of the Island of Hispaniola*

Source: Adopted from Zahibo, 2012, General Bathymetric Chart of the Oceans, 2008

In Northern Haiti, towns such as Bor de Mer de Limonade, Caracol and Phaeton are susceptible to coastal flooding caused by storm surge. The American Association of Architects, indicate that these settlements are in a precarious location to shoreline (American Institute of Architects, 2012). Similarly, populated areas that are peripheral to the study area, such as Cap Haitian and Petite Anse to the west and Fort Liberte in the east, are also susceptible to coastal flooding. There is, however, limited documented history concerning storm surges in Haiti, let alone well documented instances of coastal flooding within the Northern Development Corridor.

Hazard Determination

The hurricane induced probable storm surge heights can be derived in a scientific manner based on hydrodynamic modeling. This approach consists of two major components. The first component comprises a hurricane wind field model that provides estimates of the wind speed and direction based on key hurricane parameters at an arbitrary position. The second portion of the model is the surge model uses numerical methods to predict storm surges by solving equations to determine the response of the sea and associated inland extent of flooding that could be generated by a hurricane (cyclonic surface wind field) crossing any coastal stretch.

Such models are data intensive and require extensive modeling of a number of parameters such as oceanographic and meteorological parameters, hydrological input, basin characteristics, coastal geometry, wind stress and seabed friction, and information about astronomical tides. In addition, the accuracy of the surge height and associated flood depth and extent of horizontal inundation depends heavily on the accuracy and resolution of the bathymetry data and elevation data that is available for coastal areas.

Coastal Hazard Flood Model

Since the data requirements for the development of a detailed determination of the coastal flooding hazard were unavailable for this study effort, a regional model was utilized and adopted to understand wave and surge heights in the study area. The information utilized for this study effort was derived from the *Atlas of Probable Storm Effects in the Caribbean Sea*, which was developed under the Caribbean Disaster Mitigation Project

(CDMP), a joint effort of the Organization of American States (OAS) and the US Agency for International Development (USAID).

The Arbiter of Storms (TAOS) hazard modeling system was used to create the storm hazard data sets that were used for this study. Technical details of the TAOS model system are documented in various published papers noted in the bibliography, in particular Watson and Johnson (1999).

The TAOS combined three wind, hydrodynamic and wave models using the ensemble assimilation methodology used to analyze the results of multiple models may be found in (Watson, 1995; Watson and Johnson, 1999)

TOAS wind modeling

Winds represent sustained 1-minute winds at 10 m above the surface, and include both surface friction and topographic effects at a resolution of 30 arc-seconds. Friction factors were used for land-cover classification, with water, forest and open land predominating.

TAOS Wave Modeling

The wave model configuration used for the Caribbean simulation consisted of the NOAA Wavewatch III model, modified within the TAOS storm centered grid system. Modeling was carried on regional basis on a 30 meter grid cell, allowing for an adequate treatment of the near-shore wave environments. Waves are the heights of wave crests above the storm surge level in open water.

TAOS Storm Hazard modeling

The TAOS storm hazard modeling system contains three primary storm surge modeling modules that include the effects of astronomical tides, which take into consideration relative to mean sea level. Wave setup (but not wave run-up) is included in the storm surge values. Surges over land are shown as elevation above sea level, not water depth.

Hazard Maps

Based on the results, TAOS provided wave and storm surge heights for four return periods (10, 20, 50, and 100 years), which were reported for specific points along the Haitian coast. For this study, wave height and surge heights that were reported for Cap Haitian were adopted for the entire study area.

The total surface water levels were computed as a linear addition of storm surge amplitudes, tidal amplitudes, and wave setup. These water levels were then projected onto the coastal land using GIS techniques and intersected with a 2M Digital Terrain Model (DTM) to demarcate the horizontal extent of inundation.

As the surges considered tidal information and are assumed to reflect flooding at mean sea level, the flood depths are deduced by subtracting local topography from the total water levels.

Based on this information given in the Table AError**! No text of specified style in document.**.19, probabilistic coastal inundation maps of the following the 10-, 25-, 50- and 100-year return periods were developed for the entire study area and are depicted in Figure AError**! No text of specified style in document.**.30, Figure AError**! No text of specified style in document.**.31, Figure AError**! No text of specified style in document.**.32 and Figure AError**! No text of specified style in document.**.32 50 Year Return Period

.

*Table A**Error! No text of specified style in document.**.19 Newly Available high resolution DTM for study area (DTM source used)*

Return Period	Wave Height (m)	Surge Height (m)	Total Surface Water Levels (m)
10 Year	2.9	0.3	3.2
25 Year	3.7	0.6	4.3
50 Year	4.2	0.8	5.0
100 Year	4.7	1.1	5.8

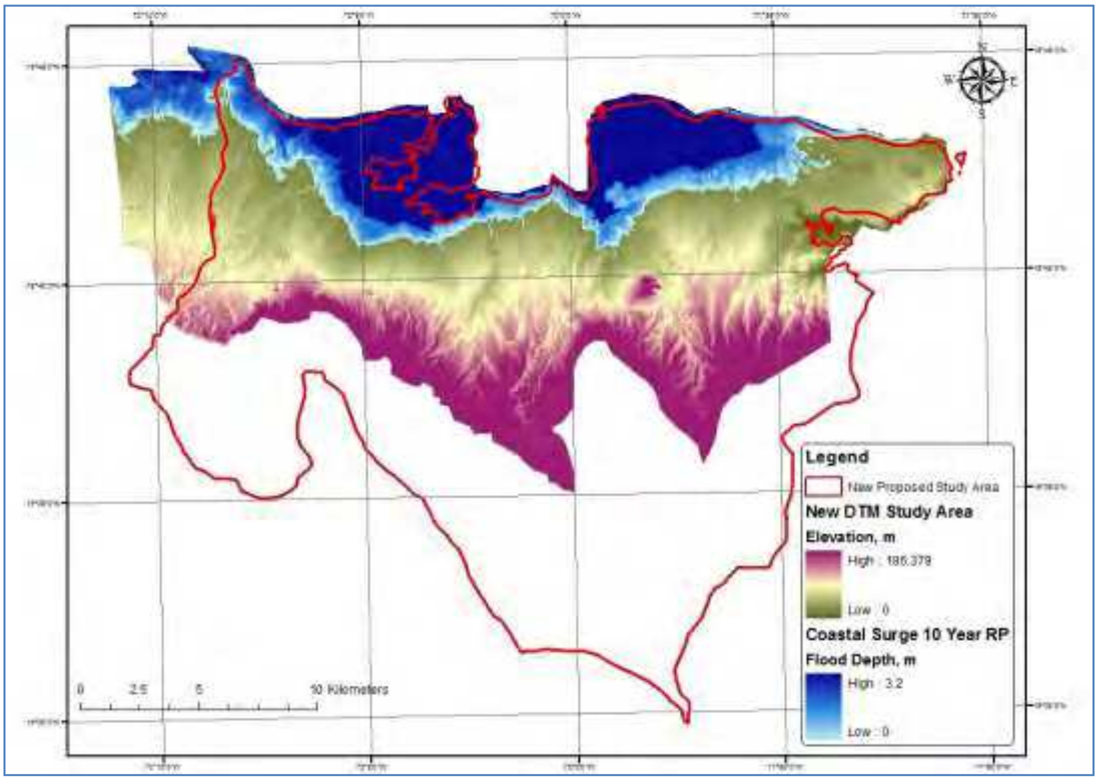

*Figure A**Error! No text of specified style in document.**.30 10 Year Return Period*

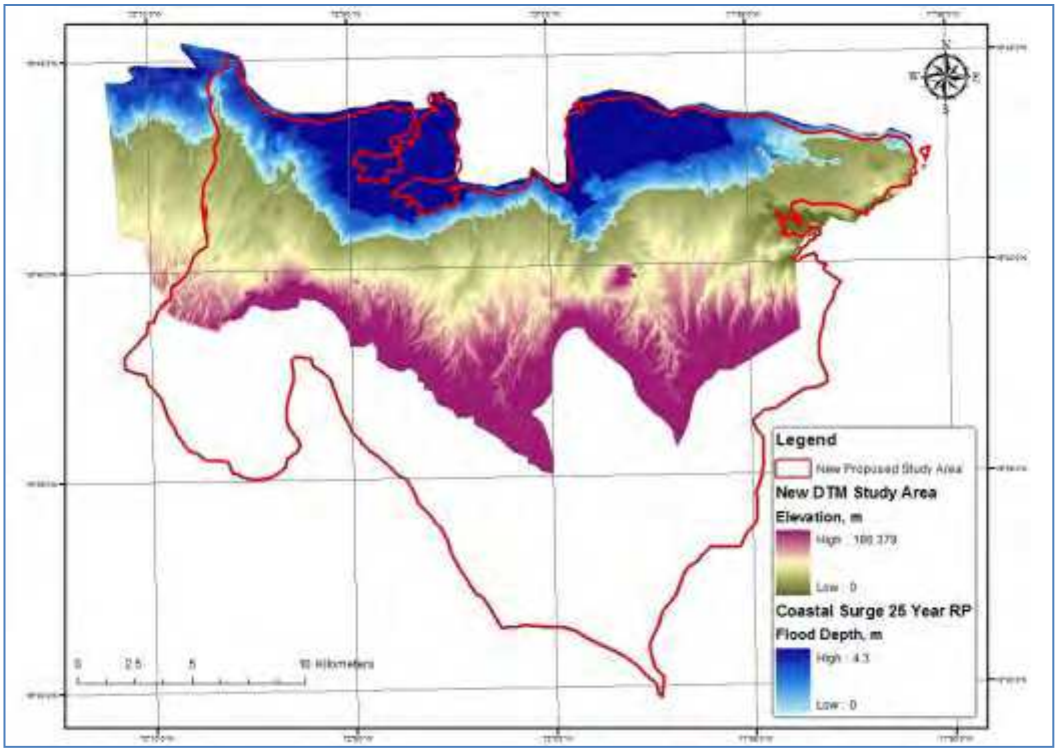

*Figure A***Error! No text of specified style in document.***.31 25 Year Return Period*

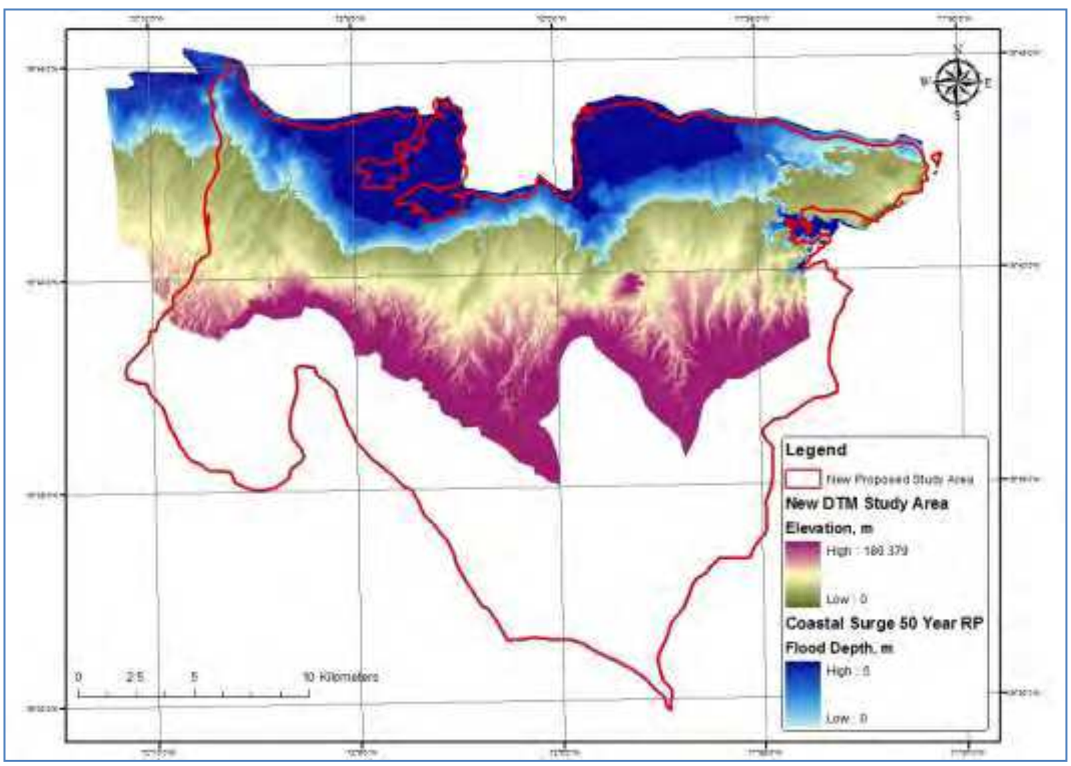

*Figure A***Error! No text of specified style in document.***.32 50 Year Return Period*

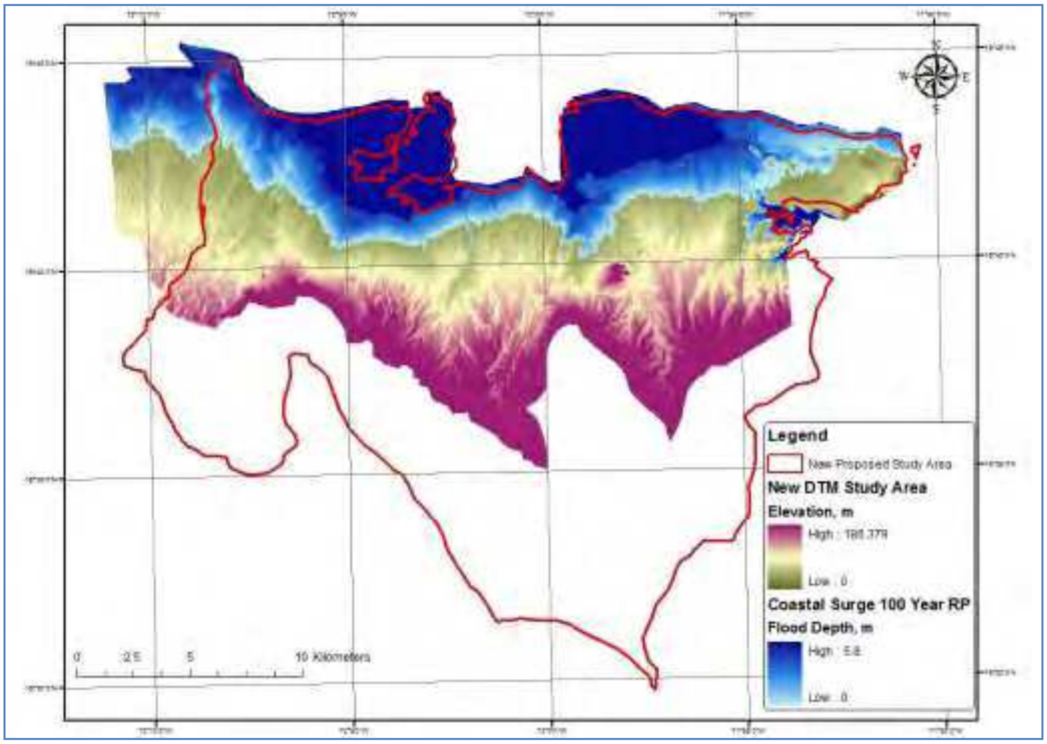

*Figure A**Error! No text of specified style in document.**.33 100 Year Return Period*

Climate Variability, Hazard Frequency and Magnitude

Climate Change Variability

The Caribbean region has been characterized as among the most vulnerable to climate change and climate extremes. One of the major challenges facing island states is that posed by tropical cyclone events and sea level rise. Sea-level rise greatly impacts human activity near the coastal zone (IPCC, 2007) since in many cases the majority of human settlements, economic activity, infrastructure and services are located at or near the coast and local economies are often reliant on just a few sectors such as tourism and agriculture (Nicholls, 1998). Sea level rise therefore exacerbates the vulnerability of coastal regions to other physical processes (e.g. storm surges, storm waves).

Evaluations of global sea level change suggest that the current average of rise is approximately 1.5mm per year meanwhile the global mean surface temperature risen around 0.5^0 C has been widely accepted.

Frequency and Magnitude

The IPCC Fifth Assessment Report of the Intergovernmental Panel on Climate Change (IPCC AR5) indicates that the frequency of the most intense storms and associated storm surges or coastal floods is more likely than not to increase by more than +10% (IPCC 2013, AR5), while the annual frequency of tropical cyclones and associated storm surges or coastal floods are projected to decrease or remain relatively unchanged for the North Atlantic.

This suggests no major change in the frequency of hurricanes and associated storm surges or coastal floods in North Atlantic region comprising Haiti. The SRES scenario A1B for study area of Haiti suggests that the sea level rise are projected to increase by small magnitude of 0.35 m over the projected for the 2040s relative to the 1960-1990 baseline. These projected changes have applied to estimated water surface elevations over the return period to develop coastal flood hazard maps for Haiti that reflect projected climate change scenarios.

The `estimated maximum depth of flooding, including the projected climate change scenario, are compared to estimated maximum flood depth without climate change for Haiti and are outlined in Table AError**! No text of specified style in document.**.20.

*Table A**Error! No text of specified style in document.**.20 Coastal Flood Depth with Climate Change*

Return Period	Estimated Maximum Depth of Flooding, m	Estimated Maximum Depth of Flooding with Climate Change, m
10	3.2	3.55
25	4.3	4.65
50	5.0	5.35
100	5.8	6.15

Results

Minor changes in sea level rise are represented on the extent of flooding. The difference between the total area of the surface of the water (inundation) for all normal return period events (from 10 year to 100 year) and the water surface with the projection scenario of climate change (i.e. Projection with Climate Change for all return period events) are presented in Table AError**! No text of specified style in document.**.21 below.

*Table A**Error! No text of specified style in document.**.21 Extent of Coastal Flooding with and without Climate Variability, Km^2*

Return Period	Flooding Area without CC	Flooding Area with CC
10-Year	95.73 km^2	101.00 km^2
25-Year	111.07 km^2	115.46 km^2
50 – Year	123.40 km^2	127.79 km^2
100 – Year	134.21 km^2	140.79 km^2

Comparing the areas of the coastal flood inundation area without climate change reveals that the flood area for the 50-year event would be 123.4 km^2 and the floodplain for the event 100 years would be 134.21 km^2. In other words, there is only a slight change (i.e. an 8.8% increase) in the extent of the floodplain for the 100 year event. The comparison between flood zones for events 50 and 100 years with climate change reveals almost the same difference in the flooded area (about 10.2 % increase). A comparison between the return period of 50 years without and with climate change reveals just a 3.6 % increase in the inundation area, while the difference in the floodplain for the event 100 years with and without climate change was 4.9 %.

A4.6 Drought Hazard

Context

Drought manifests itself in many forms. The drought hazard in Haiti results from a combination of erratic rainfall patterns during the two distinct rainy seasons: April–June and October–November. According to the World Bank, El Niño/ ENSO episodes have tended to delay the arrival of the rainy season(s) and create drought conditions[10] in the country.

NATHAT (2012), in a national level hazard assessment, indicated that farmers are reporting longer dry seasons and wetter and shorter rainy seasons. The NATHAT study has also categorized most of the northern coast as being susceptible to drought hazard. The cumulative effects of longer dry periods are crop losses and that more

[10] http://www.gfdrr.org/sites/gfdrr.org/files/Haiti-2010.pdf

families are becoming reliant on food assistance during the “hunger season”, which is the three-month period between rainy seasons, in which there is little harvesting and employment opportunities.

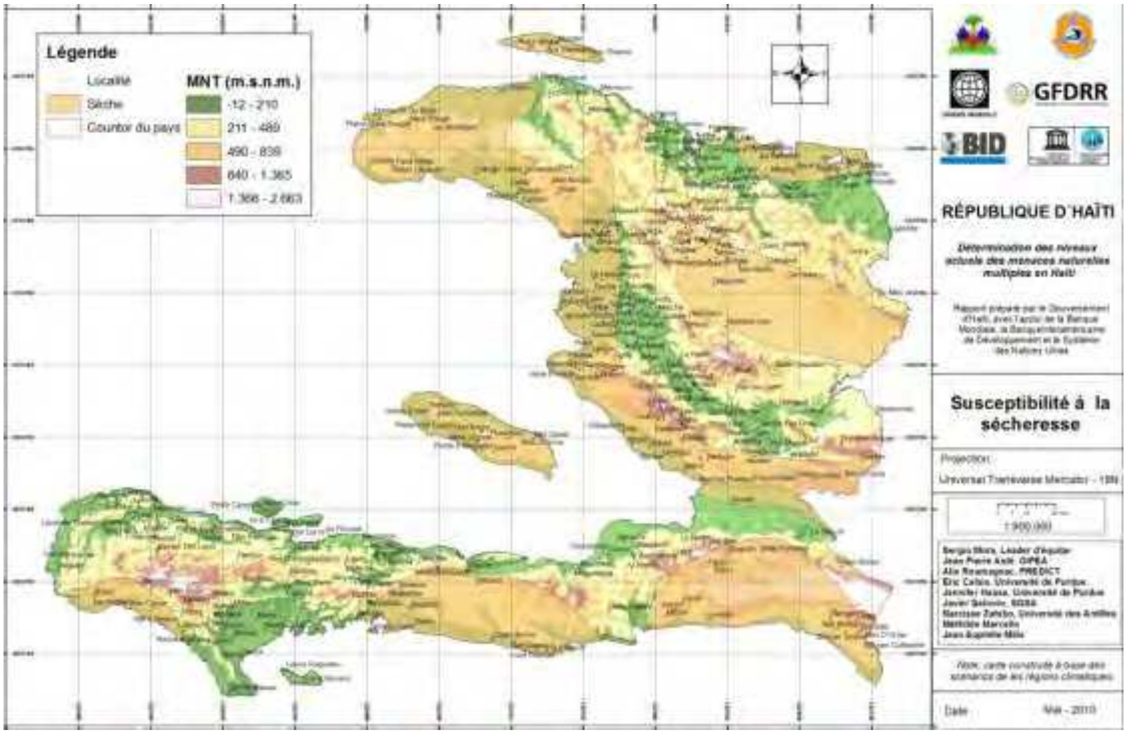

Figure A4.34 Areas Most Likely To Drought And Land Degradation on the island of Haiti

Source: NATHAT, 2012

EM-DAT, the OFDA/CRED International Disaster Database, reported that during a period of 1960 to 2003, there were seven (7) droughts in Haiti and have indicated where they have located and number of persons affected (See Table A4.22 below).

Table A4.22 Droughts in Haiti from 1968-2000

Year	S	SE	GA	O	A	C	NO	N	NE	Persons Affected
1968							X			210,217
1974-1975	X	X	X	X	X	X	X	X	X	507,000
1976-1977	X	X	X	X	X	X	X	X	X	450,000
1981	X		X							103,000
1982-1983	X	X					X		X	100,000
1984							X			45,000
1986-1987	X	X	X	X	X	X	X	X	X	
1990-1991	X	X	X	X	X	X	X	X	X	
1996-1997							X	X	X	
2000	X	X	X	X	X	X	X	X	X	
2003	NA	NA	NA	NA	NA	NA	NA	NA	NA	35,000
Total	7	6	6	5	5	6	9	6	7	

Source: Cartes et etude de risqué, de la vulnerabile et des capacities de response en Haiti; EM-DAT: The OFDA/CRED International Disaster Database – www.emdat.be – Université catholique de Louvain – Brussels – Belgium.

The Famine Early Warning System Network (FEWS NET) reported in August 2011 that the north and northeast were affected by drought and estimated that major crop yields would be diminished by 20 percent. The FEWS Net furthered detailed what is a recurring phenomenon in the northern coastal plains and reported that "rainfall in wet mountain areas [of the Northeast] has helped spur crop growth and development, while crops in Ferrié, Fort Liberté (except on the Maribaroux plains), Terrier Rouge, Caracol, and Trou-du-Nord have failed due to the drought conditions in these areas, prolonging the lean season, which generally "ends in June... [and that]… virtually the entire northern region has been affected by the drought which delayed the start of the spring planting season, which eventually got underway in June with the onset of the rains..." (FEWS, 2012).

Of greater concern to stakeholders is the impact that these short term fluctuations in precipitation will have on the surface and subsurface water supply or the hydrological regime of watersheds that intersect the Northern Development Corridor. It takes longer to recognize the affects of hydrological drought on soil moisture levels, stream flows, as well as in groundwater and reservoir levels. The frequency of hydrological drought is typically measured over the longer term and predicates a need for understanding of both the supply and demand for water. Hydrological drought concerned with the problems associated with deficiencies in precipitation (the supply) and that of competing interests for water access and utilization (the demand).

Water availability and access is exacerbated by limited water management infrastructure[11] , and in an IDB commissioned assessment of environmental resources of the Northern corridor, the American Association of Architects (AIA) maintained that future urban expansion will place increasing pressure on water resources. Future development, the study maintained, will continue to consume agricultural soils. The study furthered that to maintain current levels of food security, promote economic development and improve climate resilience, investments in irrigation and improved drainage would be required (AIA, 2012).

It should be noted that the access to water, represents one of the most significant challenges that Haiti faces. The water access issue is influenced by socio-economic, political, developmental and environmental factors and consequently is an issue that is beyond the scope and intent of this study.

Determination of Hydrological Drought

The assessment of drought in this study will therefore be focused on the influence of precipitation, and how this is coupled with the anticipated impacts of development and climate variability, will impact the current and future water supply. The current and future water balance will be estimated for the two main watersheds that intersect the study region. This study does not attempt to address and factor in the broader environmental, political and socio-economical factors that also play a role in exasperating the problem of water access.

The hydrological drought assessment has been done by estimating components of the classical hydrological cycle. The movement of water through the hydrological cycle varies significantly in both time and space. The hydrological cycle emphasizes the four factors of interest to hydrologists: precipitation, evapotranspiration, surface runoff and groundwater. For this analysis, the hydrological models, that developed as part of this study for the flood hazard assessment, along with other conventional methods of hydrological assessment, have been used to assess potential water availability for the watersheds of Grand River Du Nord and Trou Du Nord.

Grand Rivere du Nord: The hydrological basin area of Grand Rivere du Nord is estimated to be approximately 611 square kilometers. Through basin delineation and hydrological model development process, fifty-one (51) sub basins were developed for this basin, which also included 25 stream reaches.

[11] http:// sdwebx.worldbank.org/climateportalb/doc/GFDRRCountryProfiles/ wb_gfdrr_climate_change_country_profile_for_HTI.pdf

Trou du Nord: The basin area of main stream of Trou du Nord is estimated to be approximately 106 square kilometers. Through basin delineation and hydrological model development process in all 11 sub basins were developed for this basin, which also included 5 stream reaches.

A water balance model can be considered as a system of equations designed to represent various aspects of the hydrological cycle. A bucket model has been used in the assessment of water balance that considers a unit area (such as watershed) as a bucket, which is filled by the rainfall and emptied by evapotraspiration. When bucket is full, extra water is assumed as deep drainage (usually some part goes to groundwater). This model requires a recorded rainfall and evapotranspiration. A simplified concept of water balance is shown in Figure A4.35.

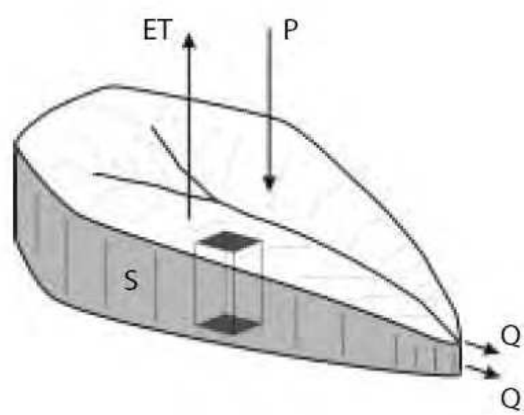

Figure A4.35 Simplified Concept of hydrological water balance

Where, S = water storage (as ground water recharge); ET = evapotranspiration; P = rainfall; Q = Surface runoff and base flow.

In mathematical terms, the bucket model can be represented as follows.

$$P-ET-Losses = Q+S$$

The losses in the above equation include the interception, infiltration and percolation.

The water balance estimates have performed at a daily level. Water availability potentials have been summarized on monthly and annual basis using the outcomes of the daily level calculations. The details of the estimation of various components of the cycle are given below.

- **Rainfall:** The rainfall is often the largest term in the water balance equation, which forms as major source of input to the system. The historically recorded monthly rainfalls have used in the analysis. As described in the flood hazard assessment and methodology, monthly rainfall data has been distributed to the daily time step. Overall the study area has average annual rainfall of about 1400 mm for current conditions and 1600 mm for climate change.

- **Evapotranspiration:** Evapotranspiration combines the two terms evaporation (generally from the ground surface) and transpiration (generally from the plants). This term forms one of the largest sources of losses from the system. Evapotranspiration can be estimated from meteorological and soil moisture data or measured directly. In this analysis available monthly estimates have been used to derive an average annual evapotranspirati**on rate. In the study area, it is estimated to be approximately 1600 mm** for current climate conditions and approximately 2000 mm considering climate change projections.

- **Surface Runoff:** Surface runoff parameters have been estimated by using the hydrological models to assess surface runoff. Using rainfall and evapotranspiration data, effective rainfall values have been estimated. These effective rainfall values have been used in the estimation of surface runoff and other abstraction losses. The losses include the interception, infiltration and percolation. The **annual average surface runoff** for the study area has been estimated at 165 mm for **current conditions** and 141 mm taking in account climate change projections.

- **Ground Water Recharge:** The losses pertaining to infiltration and percolation are often termed as the abstraction losses. These abstraction losses in the soil strata are divided into two parts 1) baseflow and 2) groundwater recharge. Base flow is the lateral sub-soil flow, which usually joins the surface runoff and is generally a small portion in the hydrological cycle. The vertical component of sub-soil flow, which moves down, is known as ground water recharge. The estimated value of annual average ground water recharge for the study area is 195 mm for current climate conditions and 288 mm considering climate change projections.

Figure A4.36 and A4.37 provide a monthly snapshot the parameters of hydrological cycle in study area for current conditions and climate change respectively. The projected climate change estimates also considers the change in land use over years.

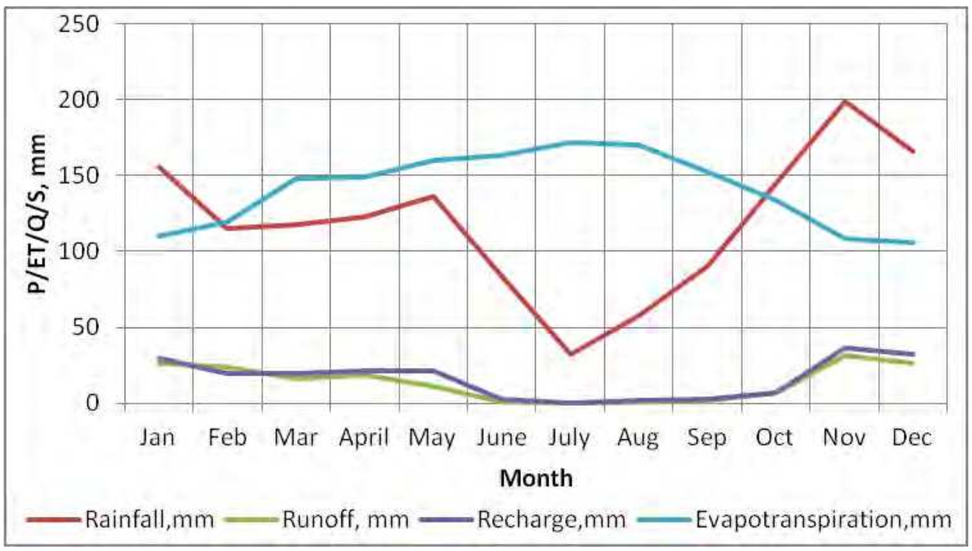

Figure A4.36 Monthly parameters of hydrological cycle for current conditions

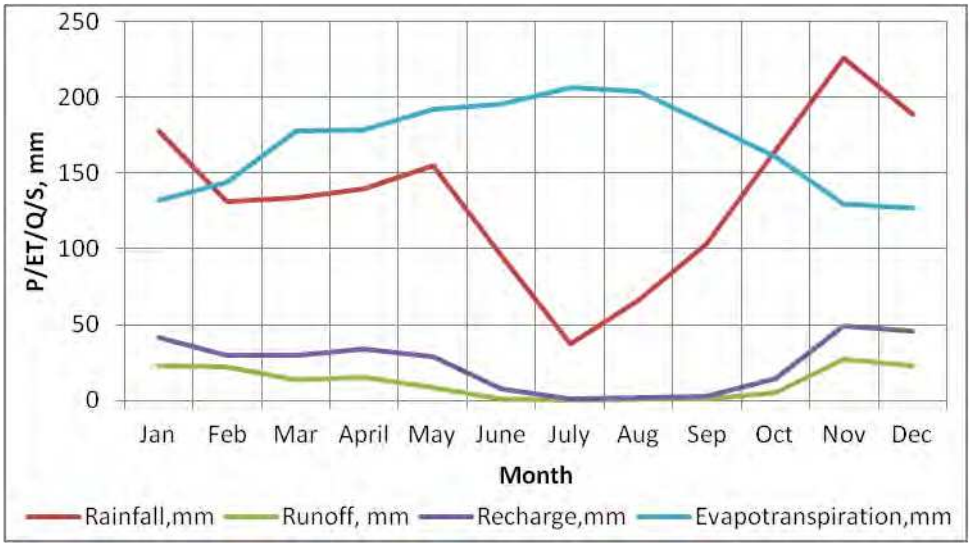

Figure A4.37 Monthly parameters of hydrological cycle for climate change projections

Water Availability

Based on the hydrological estimates as summarized above, the water availability potential has been estimated on volumetric terms (million cubic meters). These numbers have been estimated over the entire study area for current climate conditions and projected to consider climate change. The climate projections suggest the increase in the rainfall by 13% and temperature increase by 2^0C. The scenario of climate change also consider changes in land use based on parameters derived from CE3, which introduced sustainable land use planning recommendations as a risk reduction measure. Due to combined impact of climate change and changes in land use, the surface runoff will decrease, ground water recharge will increase. Monthly values of water availability potential are summarized in Table A4.23. In both the cases the ground potential is more than the surface water potential. These numbers are estimates of potential, which needs to be harnessed by developing them.

Table A4.23 Monthly variations in water availability potential

Month	Current Conditions			Climate Change and CE3 Land Use Projections, 2040		
	Surface Water Potential, Mm^3	Groundwater Potential, Mm^3	Total Potential, Mm^3	Surface Water Potential, Mm^3	Groundwater Potential, Mm^3	Total Potential, Mm^3
Jan	13.9	15.7	29.6	12.2	22.2	34.4
Feb	12.6	10.3	22.9	11.6	16.0	27.6
Mar	8.5	10.6	19.0	7.2	15.7	22.9
Apr	9.8	11.4	21.2	8.3	17.9	26.2
May	6.0	11.4	17.4	4.7	15.4	20.2
Jun	0.8	1.6	2.4	0.5	4.3	4.8
Jul	0.1	0.3	0.4	0.1	0.5	0.6
Aug	0.6	0.8	1.4	0.5	0.8	1.3
Sep	0.8	1.4	2.2	0.6	1.6	2.2
Oct	3.5	3.5	7.1	2.7	7.8	10.5
Nov	16.7	19.5	36.2	14.4	26.3	40.7
Dec	14.2	17.3	31.5	12.2	24.4	36.6
Annual	87.6	103.7	191.3	75.0	152.9	228.0

Water Demands

Considering the developmental scenarios, two projections have been used to assess water demand in the study area (Table A4.24).

Table A4.24 Developmental scenarios for water demands

Data Element	Current (2013)	Climate Change and CE3 Land Use Projections, 2040
Population	167,729	292,597
Housing	15,902	64,235
Urban Demand (spatial), ha	594	746
Agriculture Land Use (spatial) , ha	12630	17,000
Industrial Demand, sq m	67,000	229,000

The water demands include domestic demands from rural and urban areas for domestic uses, industrial demands and agricultural or irrigation requirements. The domestic use includes all of the expected per-capita use by person for activities such as drinking, showers, faucets, and toilets. A demand of 170 liters per day per head and demand of 80 liters per day per head have been estimated for urban and rural areas respectively. Individual demand estimates are based on earlier water assessments conducted for the Haiti (USACE, 1999), and for the industrial park (IDB, 2011). These studies are consistent with projections cited in global studies.

Industrial demand is estimated on per square meter basis based on current utilization and future projections for the PIC and other targeted development projects for the study area. This estimates industrial utilization to approximately 100 liters per square meter of the industrial area. Other water use and demands have considered as 250 liter per day per head. The agricultural or irrigation requirements have also been estimated using the crop area, crop coefficients (kc) and evapotranspiration.

For the future development projections, climate change projections have been incorporated. All the demands have estimated on the annual time step on volumetric basis. Table A2.25 shows the water demands for the current and future development scenario as contemplated by CE3.

Table A4.25- Summary of Water Demands

Water Demand, Mm3	Current	Climate Change and CE3 Land Use Projections, 2040
Urban Population,Mm3	5.2	5.4
Rural Population,Mm3	2.4	6.0
Industrial Demand,Mm3	2.4	8.4
Water Use and Demand ,Mm3	1.5	5.9
Agricultural Demand,Mm3	101.0	163.2
Total Demend,Mm3	112.6	188.8

Water Balance

Based on the estimates of water availability potential and demands, overall summary of water balance is shown in Table A4.26. As represented in the table, the current water availability potential is considerably more than the demands. But in future projections, the water availability potential is merely sufficient to meet the projected demands.

Table A4.26 Summary of water balance of study area

	Current	Climate Change and CE3 Land Use Projections, 2040
Water Demand, Mm^3		
Urban Population, Mm^3	5.2	5.4
Rural Population, Mm^3	2.4	6.0
Industrial Demand, Mm^3	2.4	8.4
Water Use and Demand , Mm^3	1.5	5.9
Agricultural Demand, Mm^3	101.0	163.2
Total Demand, Mm^3	112.6	188.8
Water Availability Potential, Mm^3		
Surface Water Potential (Runoff), Mm^3	87.6	75.0
Ground Water Potential (Recharge), Mm^3	103.7	152.9
Total Water Potential, Mm^3	191.3	228.0
Surplus/Deficit, Mm^3		
Water Surplus, Mm^3	78.7	39.1

The monthly variations in the availability and demand potentials are shown in Figure A4.38 for present day, while Figure A4.39 shows the monthly variation for future growth scenario that takes into consideration climate change. Monthly variation shows that during the dry season of the year, the gap between demand and availability increases as compared to the wet season.

Figure A4.38 Monthly variation in demand and availability for current conditions

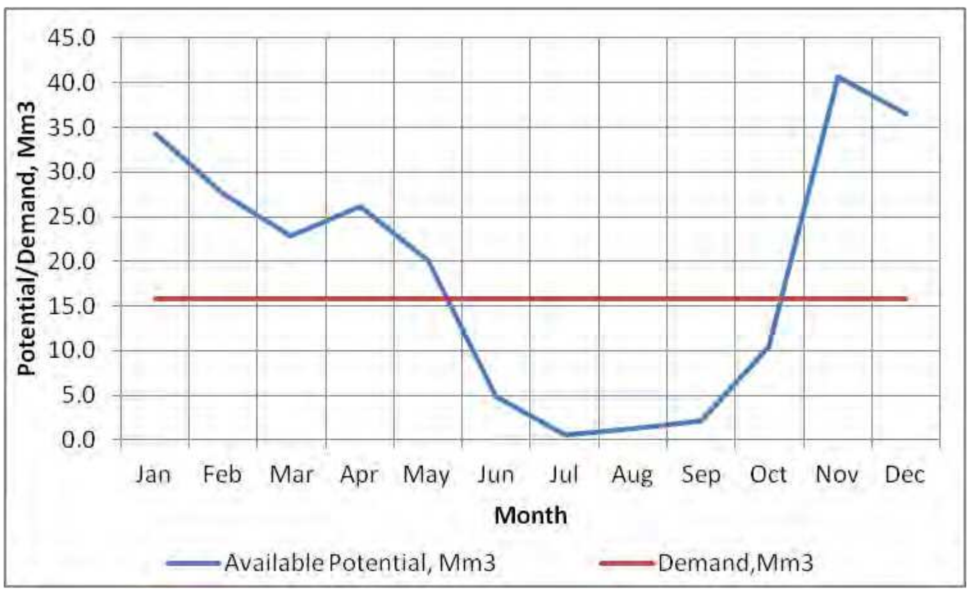

Figure A4.39 Monthly variation in demand and availability with climate change projection

From the hydrological drought assessment conducted for study area, it can be concluded that on annual basis, water availability potential is sufficient to meet the current as well as future demands. However, as shown in the Figures A4.38 and A4.39 above, on monthly basis, there is a significant gap between the demand and availability potential particularly during the dry season (June to October) as compared to the wet season. As seen from the figures, during the current and future scenarios, there is a considerable water deficit during the dry period indicating prolonged period of hydrological drought. Climate change and projected growth will reduce the available water stock and make the impacts of prolonged periods of water deficit which is likely to impact agricultural production, further exacerbate food storages, reduce water quality, and increase land degradation. Such impacts will become more pronounced during years with below average rainfall.

A4.7 References

American Institute of Architects, Inter-American Development Bank, USAID / OTI, 2012, Cumulative Impact Assessment For Regional Development In The Cap-Haïtien To Ouanaminthe Urban Corridor accessed at http://www.ute.gouv.ht/caracol/images/stories/docs/AI_CIA_Final_26-08-12.pdf)

Bender, M.A., Knutson, T.R., Tuleya, R.E., Sirutis, J.J., Vecchi, G.A., Garner, S.T., Held, I.M. (2010). Modeled Impact of Anthropogenic Warming on the Frequency of Intense Atlantic Hurricanes, Science 327, 454-458, doi:10.1126/science.1180568.

Bengtsson, L., Hodges, K. I., Esch, M., Keenlyside, N., Kornblueh, L., LUO, J. J., & Yamagata, T. (2007). How may tropical cyclones change in a warmer climate?. Tellus A, 59(4), 539-561.

Boore et al. (1997)

Boore D. M., Thompson E. M., and cadet H., (2011), Regional Correlations of VS30 and Velocities Averaged Over Depths Less Than and Greater Than 30 Meters, Bulletin of the Seismological Society of America, Vol. 101, No. 6, pp. 3046–3059, December 2011, doi: 10.1785/0120110071

BSSC 2001

Calais, E. 2001. Vers un projet "Aléa sismique en Haïti". CNRS ; Géosciences Azur. Sophia Antipolis, France. Unpublished report; 11pp.

Campbell K., Abrahamson N., Power M., Chiou B., Bozorgnia Y., Shantz T., and Roblee C. (2009), Next Generation Attenuation (Nga) Project: Empirical Ground Motion Prediction Equations For Active Tectonic Regions, Sixth International Conference on Urban Earthquake Engineering, March 3-4, 2009, Tokyo Institute of Technology, Tokyo, Japan

Atlas of Probable Storm Effects in the Caribbean Sea

Choi, Y., and J. P. Stewart (2005), "Nonlinear site amplification as function of 30 m shear wave velocity", Earthquake Spectra, vol.21, no. 1, pp.1–30

Coppersmith 1994

Elsner, J. B., Kossin, J. P., & Jagger, T. H. (2008). The increasing intensity of the strongest tropical cyclones. Nature, 455(7209), 92-95.

Emanuel, K. A., S. Ravela, E. Vivant and C. Risi (2006), A Statistical determinstic approach to hurricane risk assessment,Bull Amer Meteor Soc., 19, 299-314.

Emanuel 2007

Engdahl and Villasensor Catalog (2002)

Famine Early Warning Systems Network, HAITI Food Security Outlook Update, June 2012

Food and Agriculture Organization of the United Nations, 2004. Technical Cooperation Programme. Project Title: Assistance to improve Local Agricultural Emergency Preparedness in Caribbean countries highly prone to hurricane related disasters.

Frankel A., Harmsen S., Mueller C., Calais E. and Haase J., 2011, Seismic Hazard Maps for Haiti, Earthquake Spectra, Volume 27, No. S1, pages S23–S41

Frankel, A., Mueller, C., Barnhard, T., Leyendecker, E., Wesson, R., Harmsen, S., Klein, F.,Perkins, D., Dickman, N., Hanson,S., and Hopper, M., 2000, USGS national seismic hazard maps: Earthquake Spectra, v. 16, p. 1 – 19.

Frankel, Arthur, Harmsen, Stephen, Mueller, Charles, Calais, Eric, and Haase, Jennifer, 2010, Documentation for initial seismic hazard maps for Haiti: U.S. Geological Survey Open-File Report 2010-1067, 12 p.

Frankel 1995

Gualdi, S., Scoccimarro, E., & Navarra, A. (2008). Changes in tropical cyclone activity due to global warming: Results from a high-resolution coupled general circulation model. Journal of climate, 21(20), 5204-5228.

IDB, 2011, Preliminary Hydrological Assessment for the Development of an Industrial Park in Haiti, Prepared for: Inter-American Development Bank Washington, D.C. Prepared by: ENVIRON International Corporation, Washington, D.C.

IPCC AR4, 2007, The IPCC Fourth Assessment Report of the Intergovernmental Panel on Climate Change

IPCC AR5, 2014, IPCC Fifth Assessment Report of the Intergovernmental Panel on Climate Change

Knutson, T. R., Sirutis, J. J., Garner, S. T., Vecchi, G. A., & Held, I. M. (2008). Simulated reduction in Atlantic hurricane frequency under twenty-first-century warming conditions. Nature Geoscience, 1(6), 359-364.

Kossin, J. P., Knapp, K. R., Vimont, D. J., Murnane, R. J., & Harper, B. A. (2007). A globally consistent reanalysis of hurricane variability and trends.Geophysical Research Letters, 34(4).

Landsea, C. W., Feuer, S., Hagen, A., Glenn, D. A., Sims, J., Perez, R., ... & Anderson, N. (2012). A Reanalysis of the 1921-30 Atlantic Hurricane Database*. Journal of Climate, 25(3), 865-885.

MARNDR, MPCE, MICT, MDE. 2000. Actes de l'atelier de concertation interministérielle pour la gestion des bassins versants. 120 pp.

McCann, W.R., 2006, Estimating the threat of tsunamagenic earthquakes and earthquake induced landslide tsunamis in the Caribbean, in Aurelio, M., and Philip, L., eds., Caribbean tsunami hazard: Singapore, World Scientific Publishing, p. 43 – 65.

McCann 2001

NATHAT 2012

Nicholls, R. J. (1998). Assessing erosion of sandy beaches due to sea-level rise. Geological Society, London, Engineering Geology Special Publications,15(1), 71-76.

Oouchi, K., Yoshimura, J., Yoshimura, H., Mizuta, R., Kusunoki, S., & Noda, A. (2006). Tropical cyclone climatology in a global-warming climate as simulated in a 20 km-mesh global atmospheric model: Frequency and wind intensity analyses. J.Meteorol.Soc.Jpn, 84(2), 259-276.

OFDA/USAID

RMS FAQ: 2010 Haiti Earthquake and Caribbean Earthquake Risk, Accessed at https://support.rms.com/publications/Haiti_Earthquake_FAQ.pdf

Sandıkkaya M.A., Akkar S., and Bard P-Y., (2013), A Nonlinear Site-Amplification Model for the Next Pan-European Ground-Motion Prediction Equations, Bulletin of the Seismological Society of America, Vol. 103, No. 1, pp. 19–32, February 2013, doi: 10.1785/0120120008

Schott C., and Schwarz J., (2004), Reliability Of Eurocode 8 Spectra And The Problems Of Their Application To Central European Earthquake Regions, 13th World Conference on Earthquake Engineering, Vancouver, B.C., Canada, August 1-6, 2004, Paper No. 3403

Sugi, M., Murakami, H., & Yoshimura, J. (2009). A reduction in global tropical cyclone frequency due to global warming. Sola, 5(0), 164-167.

The World Bank, 1991, Haiti Agricultural Sector Review Report No. 9357-HA

UniQ 2010

UN Global study

United Nations Strategy for Disaster Reduction (UNISDR) and Global Assessment Report on Disaster Risk Reduction (GAR) report

USACE, 1999, Water Resources Assessment of Haiti, US Army Corps of Engineers, Mobile District and Topographic Engineering Center

USGS 2010

USAID, 2007, Environmental Vulnerability In Haiti Findings & Recommendations, http://pdf.usaid.gov/pdf_docs/PNADN816.pdf

Vickery, P. J. P.F., Skerij, A.C. Stekley and L.A. Twisdale Jr. 2000, Hurricane wind field model for use in Hurricane Simulations. J Struct Eng 126. 1303-1221.

Vickery, P. (2008), Development of Design Wind Speed Maps for the Caribbean for Application with Wind Load Provisions of ASCE 7 ARA Rep. No. 18108-1, Pan American Health Organization, Regional Office for the Americas World Health Organization, Disaster management Programme, 525 23rd Street, NW Washington, DC.

Vickery, P. (2012) Design Wind Speeds in the Caribbean. Advances in Hurricane Engineering: pp. 1136-1147. doi: 10.1061/9780784412626.099

Vickery, P.J., 2005. Simple empirical models for estimating the increase in the central pressure of tropical cyclones after landfall along the coastline of the United States. J. Appl. Meteorol. 44, 1807–1826.

Wald, D. J., and T. I. Allen (2007). Topographic slope as a proxy for seismic site conditions and amplification, Bull. Seismol. Soc. Am. 97,1379–1395.

Wald, D. J., B. Worden, V. Quitoriano, and K. Pankow, (2004). Shake Map Manual: Technical Manual, Users Guide, And Software Guide, U.S. Geological Survey Open-File Report, in preparation

Walling, M, Walter Silva, and Norman Abrahamson (2008). Nonlinear site amplification factors for constraining the NGA Models, Earthquake Spectra 24:1, 243-256

Watson, C. C. and M. E. Johnson. (1999). "Design, Implementation, andOperation of a Modular Integrated Tropical Cyclone Hazard Model," AMS 23rd Conference on Hurricanes and Tropical Meteorology, Dallas, TX.

Watson, C. C., Jr. (1995), "The Arbiter of Storms: A High Resolution, GIS-based System for Integrated Storm Hazard Modeling," National Weather Digest, 20, 2-9.

Wills et al 2000

APPENDIX 5: Characteristics of Assets Exposed

A5 CHARACTERISTICS OF ASSETS EXPOSED

A5.1 Context

The inventory of exposed assets involves understanding the distribution of people, buildings and infrastructure that may be affected by natural phenomena. In the Northern Development Corridor of Haiti, there was not enough detailed information available to carry out a site specific assessment of all buildings, and it was therefore necessary to carry out a rapid field assessment method to estimate the number and distribution of assets in the study area.

A review of various reports and geospatial databases was conducted in order to ascertain useful information for understanding land uses and building practices in Haiti, and in the study region. Initially it was perceived that reports and databases would provide information that would be useful for ascertain the distribution buildings and infrastructure and their characteristics. However, much of the information focused on damages that occurred as a result of the 2010 Earthquake and was confined to dense urban areas of the capital. Damage assessment reports, nevertheless, provided useful information to understand building practices. The review of geospatial data helped us to understand land uses, population distribution and density, and the location of critical facilities and infrastructure.

Remote sensing data as well as information gathered from a rapid field assessment were utilized to capture priority building information. Within the study area, satellite images are interpreted to understand building density and types for each land use category and administrative boundary. Administrative boundaries (i.e. section communal) were then subdivided based on density of building footprints so as to allow for the definition of an appropriate scale from which to capture inventory elements.

This mapping process provided the basis for classifying buildings and for using a suitable classification hierarchy for the capture of a wide range of structures and densities. A rapid field assessment that was conducted in August, 2013 informed the interpretation of remote sensing data and facilitated the classification of buildings into general occupancy classes. Photographic survey was utilized to inform the development of an exposure model so as to incorporate a number of statistical assumptions to calculate the building type (house or apartment), age, structure (wall and roof type, number of stories), construction and to estimate replacement costs.

Such an approach is consistent with standard methodologies used to develop exposure models and supports the required inputs for undertaking a probabilistic risk assessment by providing an approximate spatial location of exposed elements for each block subdivision within the section communal.

A5.2 Building Base Map for Inventory Assessment

Haiti is divided into ten (10) departments. The departments are subdivided into arrondissements, which are further subdivided into communes, which in turn are divided into sections communales.

Because the section communales represent too crude of an administrative boundary from which to categorize the built environment to facilitate a mapping of exposed elements and risk, the section communales have been further subdivided into blocks to facilitate analysis at finer level. The block boundaries have been created by overlaying commune boundaries on the remote sensing data in a GIS so as to facilitate an understanding of the density buildings and distribution of different building types throughout the study area.

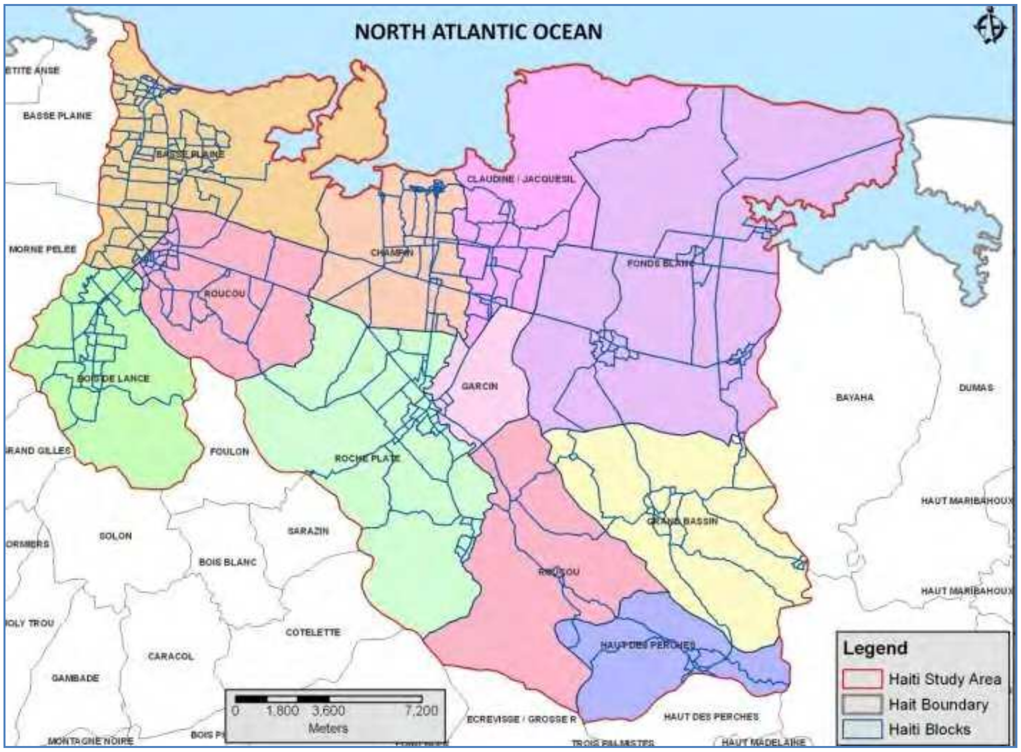

*Figure A**Error! No text of specified style in document.**.1 Distribution of block boundaries in the study area*

Each section communale was divided into multiple blocks by taking into consideration building density and road network. Smaller blocks have been created in the cities where there are higher building densities, while in less dense rural areas larger blocks have been delineated. In most of the cases road lines have been followed for creating blocks boundaries to facilitate a consistent mapping across the study area. The total number of blocks in each section communale.

*Table A**Error! No text of specified style in document.**.1 Number of blocks for each section communale*

Section Communales	No of Blocks
Basse Plaine	79
Bois De Lance	32
Champin	52
Claudine / Jacquesil	22
Fonds Blanc	41
Garcin	5
Grand Bassin	23
Haut Des Perches	13
Roche Plate	39
Roucou	42
Grand Total	**348**

A5.3 Building Occupancy Mapping and Distribution

The field survey conducted in August 2013 facilitated an understanding of general building distribution in the study area. A building distribution schema was developed to facilitate an understanding of the distribution of buildings and uses. Using remote sensing data, attention was given to densities and texture information to each sub-divided administrative unit (i.e. Block) to identify homogenous land uses where the distribution of buildings would be similar. By using remote sensing data, each block was visually checked to determine the distribution of building types and to identify any anomalies so as to aggregate building information to each block.

The development of a building mapping schema, which was informed by field work, allows for a more precise definition of the expected distribution of different types of buildings and infrastructure in the study area. It also informed the distribution of building uses or occupancy. The schema, coupled with building footprints data, facilitated a general understanding of the square area of buildings, which is important for determining the generalized replacement value of each structure. This will facilitate that application of standard construction costs per building type and allow for exposure values to be aggregated by administrative unit.

Statistical tools were used to help determine that the final results are in line with the sample data. In addition, the building distribution schema was reviewed graphically in a mapping interface to assure that the results were reasonable. This was an involved process, where generalized distribution was checked against homogenous zones that were investigated in the field, to make sure that the number and distribution of buildings was appropriate.

Structure Classification

Structural information is an important factor in determining the vulnerability or how likely structures are to fail when they are subjected to hazards, such as wind pressure that exceeds their design. In order to conduct basic analyses and gather information useful to determine general loss estimates, structural engineers and planners categorized buildings into the eight (8) different structure types, which are similar to those identified by *Institut Haïtien de Statistique et d'Informatique (IHSI)* of the *Ministère de l'Economie et des Finances*. This was done to capture the general features of the structures of the buildings according to local current construction practices.

The models of the different types of infrastructure were determined based on experience with the typical construction of Haiti. The basic structural systems were grouped according to the following general construction: reinforced concrete, masonry structure, unreinforced masonry, and earthen. The field analysis, however, indicated that there was a need to slightly modify building classifications outlined by the IHSI. A new structure distribution schema (shown in Table A**Error! No text of specified style in document.**.2 below) was developed for the Northern Development Corridor, which were reviewed and verified by architects and civil engineers familiar with the study area.

*Table A**Error! No text of specified style in document.**.2 Structure Classification Matrix in Northern Development Corridor of Haiti*

Structure Type	Code	Quality	Age	Floors	Walls	Roof	Foundation
Low Rise Reinforced Concrete	ST-1	Poor	5-10 yrs	1	Reinforced Columns, block in-fill	Wood Frame, Corrugated Metal	Mass Masonry/ Rubble
Low Rise Reinforced Concrete	ST-2	Moderate	5-10 yrs	1	Reinforced Columns, block in-fill	Concrete Slab	Concrete Slab
Mid Rise Reinforced Concrete	ST-3	Poor	5-10 yrs	2	Reinforced Columns, block in-fill	Concrete Slab	Mass Masonry/ Rubble
Mid Rise Reinforced Concrete	ST-4	Moderate	5-10 yrs	2/3	Reinforced Columns, block in-fill	Concrete Slab	Concrete Slab
Low Rise Steel Frame	ST-5	Good	1-5 yrs	1	Slab on Grade	Concrete Slab	Concrete Slab
Mid Rise Steel Frame	ST-6	Good	1-5 yrs	2/3	Slab on Grade	Concrete Slab	Concrete Slab
Low Rise Masonry	ST-7	Moderate	20 Yrs +	1	Mass Masonry	Wood Frame, Corrugated Metal	Mass Masonry/ Rubble
Mid Rise Masonry	ST-8	Moderate	20 Yrs +	2/3	Mass Masonry/ Concrete	Wood Frame, Corrugated Metal	Mass Masonry/ Rubble
Wattle and Daub/Adobe	ST-9	Poor	20 Yrs +	1	Earth, covered with light concrete plaster	Wood Frame, Corrugated Metal	Earth/Rock

Each building type has a unique and distinct behavior, due to a number of factors including the behavior of the material, height, pre and post disaster incorporation of new building requirements, and quality of prevalent construction practices.

Building Replacement Values

To relate the number of building and occupancy classes to specific building types, a two-dimensional matrix was developed. It allowed project team members to understand the distribution of identified building types for a specific occupancy class for each block. To estimate replacement values for buildings in each block, local construction parameters were developed by a review of local construction practitioners (i.e. architects, engineers) to understand the construction cost (USD/m2) for the following occupancy classes and are provided in

Table A**Error! No text of specified style in document.**.3.

*Table A**Error! No text of specified style in document.**.3 Construction Costs, Occupancy Type*

Occupancy Class	***Average Construction Cost Estimates (USD/M^2)***	***Notes***
Residential (formal)	\$800 to \$1100	Housing that goes through the formalities of architecture plans, permits, etc.
Residential (informal 1)	\$600 to \$800	Housing that would be self-built or with the help of skilled personal
Residential (informal 2)	\$450 to \$500	Housing that would be self-built without help of skilled personal
Residential (international donor)	\$800 to \$1,200	Housing that has been built or USAID or other international donors
Commercial	\$1000	This may include construction for commercial enterprises which follows formal construction process of developing architectural plans and permits and is constructed by professional contractors. Only construction costs required.
Industrial (outside park)	\$1000	This may include construction for industrial enterprises (i.e. agricultural processing facilities), which will follows formal construction process of developing architectural plans and permits and is constructed by professional contractors. Only construction costs required
Industrial (PIC)	\$1200	Construction costs for the development of industrial production facilities inside the park.

The identification and understanding of construction parameters as well as field work assisted in the determination of values for urbanized or built-up areas by occupancy class. Image analysis informed a determination of building counts for certain building type clusters found in rural areas.

Inventory Aggregation and Valuation

This methodology facilitates the development of occupancy-building type mapping schemes which help determine the distribution and aggregate exposure for general building stock. Specific values estimates and site specific geospatial data were collected to understand specific exposure values for infrastructure and critical facilities.

General Building Stock

The composition of the general building stock (i.e. residential, commercial and industrial building stock) was therefore aggregated to the given block boundary. As previously described, its distribution was determined by field work and careful review of imagery so as to provide the most accurate distribution of building types for block boundary.

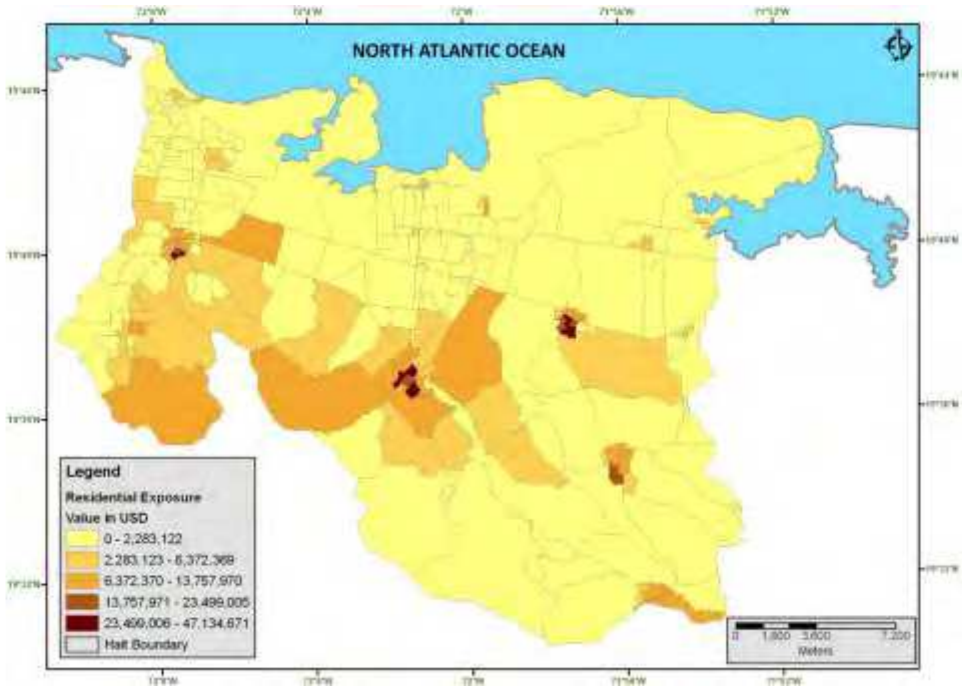

*Figure A**Error! No text of specified style in document.**.2 Distribution and Exposure Values of Residential Buildings in the Area of Study*

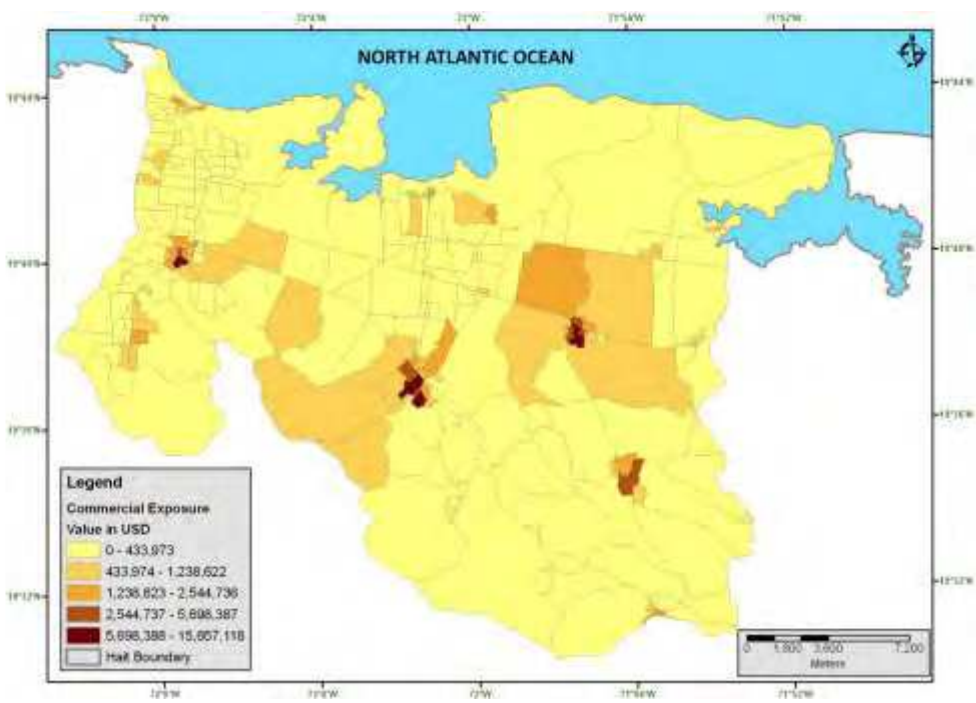

*Figure A**Error! No text of specified style in document.**.3 Distribution and Exposure Values of Commercial Buildings in the Area of Study*

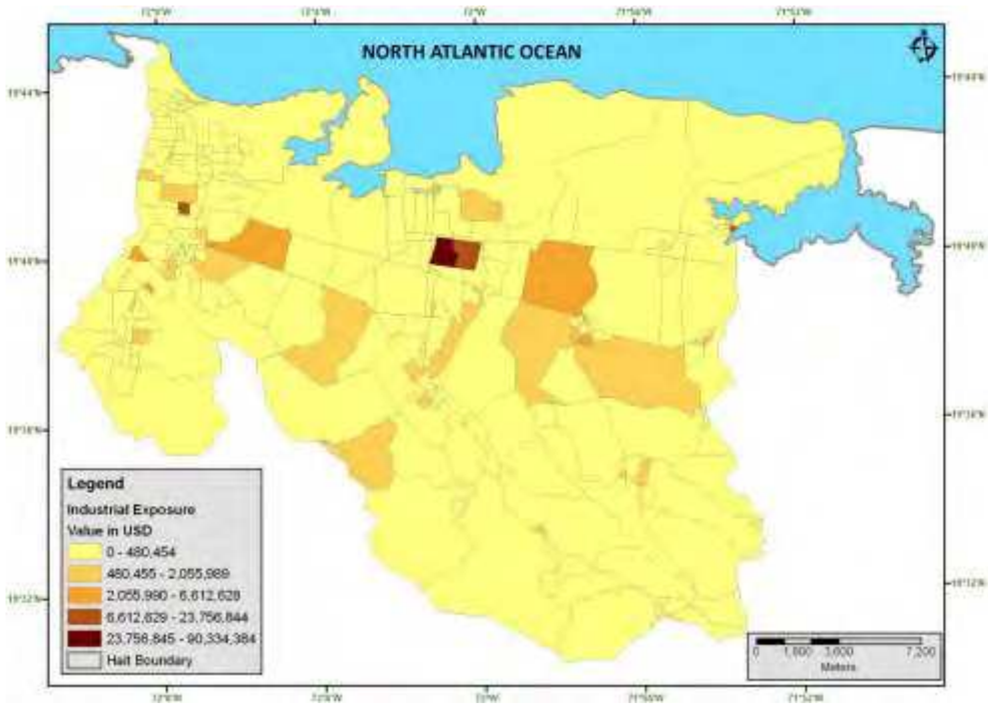

*Figure A**Error! No text of specified style in document.**.4 Distribution and Exposure Values of Industrial Buildings in the Area of Study*

This analysis, which is consistent with HAZUS-MH Level 2 Analysis[1], was conducted using a Geographic Information System, and Table A5.4 presents the results which were aggregated for both the Commune (Administrative Level 3) and Section Commune (Administrative Level 4) administrative boundaries in the Northern Development Corridor.

[1] At this point, some basic background information about methodology utilized to develop the inventory. The methodology undertaken is undertaken is consistent with methodologies used for HAZUS-MH. There can be three levels dependent on the amount of data that is available: *Level 1* analyses use default data that has been assembled for HAZUS-MH from US national databases, which is not applicable outside the United States. This data provides a basic estimate of exposure that is useful for broad scale planning efforts. *Level 2* analyses involve the input of more detailed data about local conditions, building stocks etc. and yields correspondingly more detailed and useful results. Likewise, *Level 3* analyses provide the most accurate estimates of losses but require detailed engineering and physical conditions data to customize results at a level that is not clearly warranted by this type of study.

*Table A**Error! No text of specified style in document.**.4 Economic value (Million USD) for General Building Stock, by Occupancy types*

Commune/Section Commune	Residential (Million USD)	Commercial (Million USD)	Industrial (Million USD)
Basse Plaine	123	21	32
Bois De Lance	62	10	6
Champin	56	12	95
Claudine/ Jacquesil	17	6	23
Fonds Blanc	179	49	39
Garcin	21	3	2
Grand Bassin	96	20	2
Haut des Perches	60	7	0
Roche Plate	328	63	6
Roucou	207	48	6
Grand Total	1,147	236	211

Facilities and Infrastructure

For purposes of this study, the following three part definition of critical facilities and infrastructure has been applied:

Critical Facilities - are those facilities that provide services to the community and should be functional after a hazard event. They include:

- Hospitals
  - Hospitals (Level 1 – Major Medical Facility)
  - Hospitals (Level 2 – Medical Facility/Clinic)
  - Hospital (Level 3 – Rural Clinic)
- Education
  - Kindergarten
  - Primary
  - College
  - University

Transportation Infrastructure - enables the movement of goods, particularly goods and emergency relief supplies. They include:

- Roads, km (Highway)
- Roads, km (Secondary)
- Roads, km (Tertiary)
- Bridges

Utilities and Infrastructure - are facilities that, if damaged, could have far-reaching consequences for the environment. They include:

- Electric Infrastructure

    - Electric Power Plant
    - Electric Lines, km
- Water Infrastructure
    - Water Lines,
    - Water Pumping Stations,
    - Reservoirs/Catchment, and
    - Wells
- Waste Water Infrastructure
    - Culverts,
    - Waste Water Treatment Plants

Facilities and infrastructure have been categorized facilities and infrastructure by their structural characteristics relevant to vulnerability to the prominent hazards identified in the study.

Replacement and content values for facilities were evaluated based on field inspections which allowed for approximation building area and construction cost (i.e. exposure) by facility type or infrastructure class. Facility and infrastructure costs were informed by civil engineers familiar with construction practices in Haiti.

*Table A**Error! No text of specified style in document.**.5 Estimated Value of Critical Facilities and Infrastructure*

Facility/Infrastructure Type	Number of Facilities, Class	Total Exposure (USD)
Critical Facilities		
Hospitals (Level 1 – Major Medical Facility)	4	6,597,869
Hospitals (Level 2 – Medical Facility/Clinic)	14	2,494,585
Hospital (Level 3 – Rural Clinic)	5	423,946
Kindergarten	9	461,546
Primary	120	23,238,825
College	4	2,285,514
University	9	10,043,189
Transportation Infrastructure		
Roads, km (Highway)	29	4,043,638
Roads, km (Secondary)	11	804,225
Roads, km (Tertiary)	464	69,658
Bridges	55 (747 meter)	16,434,000
Public Service Infrastructure		
Electric Infrastructure		
Electric Power Plant	1	400,000,000
Electric Lines, km	29	2,610,000
Water Infrastructure		
Water Lines, km	40	3,856,903
Water Pumping Stations	7	1,225,000
Reservoirs/Catchment	1	1,500,000
Wells	33	330,000
Waste Water Infrastructure		
Culverts	77	646,800
Waste Water Treatment Plants	1	3,600,000

APPENDIX 6: Impacts and Losses

A6 IMPACTS AND LOSSES

A6.1 Methodology

This section presents an estimate of the losses attributable to each hazard. The findings can be used to support local and regional planners understanding of the potential impacts of each hazard and allow a comparison of hazards by quantifying potential impacts.

The application of a risk assessment methodology has resulted in an *approximation* of risk. These estimates should be used to understand relative risk from hazards and potential losses; however it is important to understand that uncertainties are inherent in any loss estimation methodology, arising in part from incomplete scientific knowledge concerning natural hazards and their effects on the built environment. Uncertainties also result from approximations and simplifications that are necessary for a comprehensive analysis (such as abbreviated inventories, and model parameters such as precipitation data or economic parameters).

Risk Metrics

The economic loss results are presented here using three risk indicators:

- *Probable Maximum Loss (PML)*, which provides an estimate of losses that are likely to occur, considering existing mitigation features, due to a single hazard event;

- *Loss Exceedance Curve* which plots the consequences (losses) against the probability for different events with different return periods; and

- *Average Annualized Loss (AAL)*, which is the estimated long-term value of losses to assets in any single year within the study area. By annualizing estimated losses, we understand historic patterns of events so as to provide a balanced assessment of risk. The AAL is the summation of products of event losses and event occurrence probabilities for all stochastic events in a loss model and is expressed as:

$$\text{Average Annual Losses} = \sum_i P_i L_i$$

The use of the annualized losses approach has two primary benefits, including: the ability to assess potential losses from all future disasters; and provides an objective means to evaluate mitigation alternatives.

Risk Mapping

The risk metrics described above, particularly, the AAL, can be used to provide an understanding of the spatial extent of losses and help to identify and prioritize the urban areas or localities that are under risk. The street light indicator methodology, where the colors on the map coincide with the level of risk, has been used to map risk:

Very Low	Low	Moderate	High	Very High

By mapping risk at the block level, stakeholders have a better understanding of where potential losses will be the highest and where monies should be allocated for risk reduction. All the areas and exposure categories that have a high and very high risk are automatic choices for risk reduction measures.

A6.2 Earthquake Hazard

Earthquakes have the potential to cause damages due to waves that are produced by a release of energy through the earth. The way the earth responds to the energy of an earthquake depends on the geology of the area. Shaking may not cause damage to the ground itself, but may cause significant damage to structures including infrastructure and lifelines.

The expected intensity of an earthquake in the area is significant with an expected peak ground acceleration (PGA in g) with site amplification varying from 0.244 to 0.448 for 475 years return period and 0.406 to 0.853 (in g) for 2500 year return period.

The Northern Development Corridor of Haiti is almost entirely comprised of alluvial deposits (i.e. areas of wet sand or silt), which makes it susceptible to liquefaction (i.e. where the ground could be shaken enough that the pressure of the water in the soil builds up to make it liquefy). In addition to physical geography, the potential impacts of the earthquakes in northern Haiti are tied to the construction practices and materials. The pattern of construction that is found throughout the areas is the prevalent factor influencing the physical vulnerability of the area (i.e. structural damages). The majority of the buildings are low rise structures (i.e. one story) constructed out of one of four materials: concrete/blocks, earthen materials, 'clisse' (translated "woven wood mats"), or bricks/rocks. The construction of walls and flooring is with little or no reinforcement, which are the key factors that influenced the collapse of numerous buildings and loss of life during the catastrophic seismic event in 2010.

Estimated Probable Losses

The estimates for the earthquake hazard are provided in Table A**Error! No text of specified style in document.**.1 below, and represent the maximum probable losses for general occupancy classes. Losses are presented for two return periods.

*Table A**Error! No text of specified style in document.**.1 Probable Maximum Losses (PML) for Earthquake Hazard*

Return Period Years	Loss (10^6 USD)		
	Residential	Commercial	Industrial
475	704.5	141.3	106.6
2500	1,071.5	194.7	161.0

Loss Exceedence and Average Annual Losses

Figure A**Error! No text of specified style in document.**.1 depicts the Loss Exceedance Curve and the AAL for the earthquake hazard in the study region, and Figures A6.2-A6.4 show the corresponding AAL maps for Earthquake Hazard.

LEC, Residential

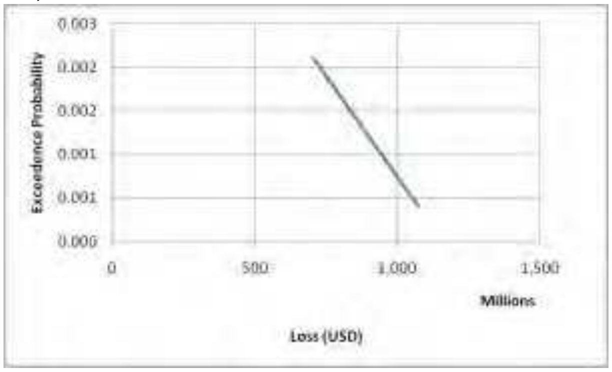

LEC, Commercial

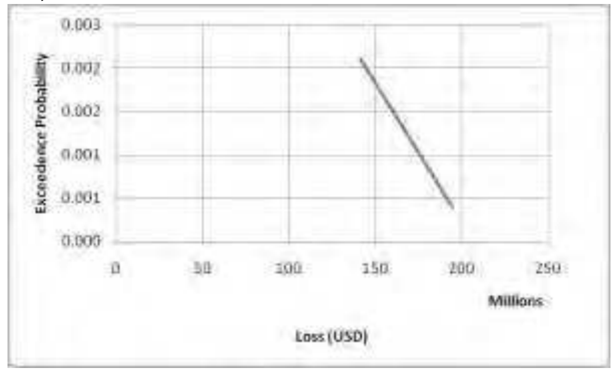

LEC, Industrial

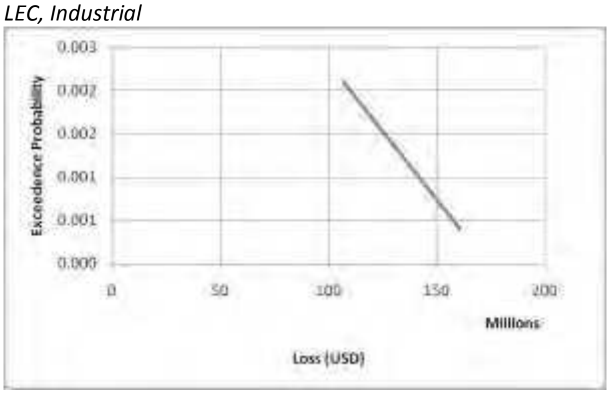

Average Annual Losses (AAL)					
Residential		Commercial		Industrial	
USD$ x 10^6	% de Exposure	USD$ x 10^6	% de Exposure	USD$ x 10^6	
1.6	0.076%	0.3	0.095%	0.2	0.083%

*Figure A**Error! No text of specified style in document.**.1 Loss Exceedance Curve and the AAL for Earthquake Hazard*

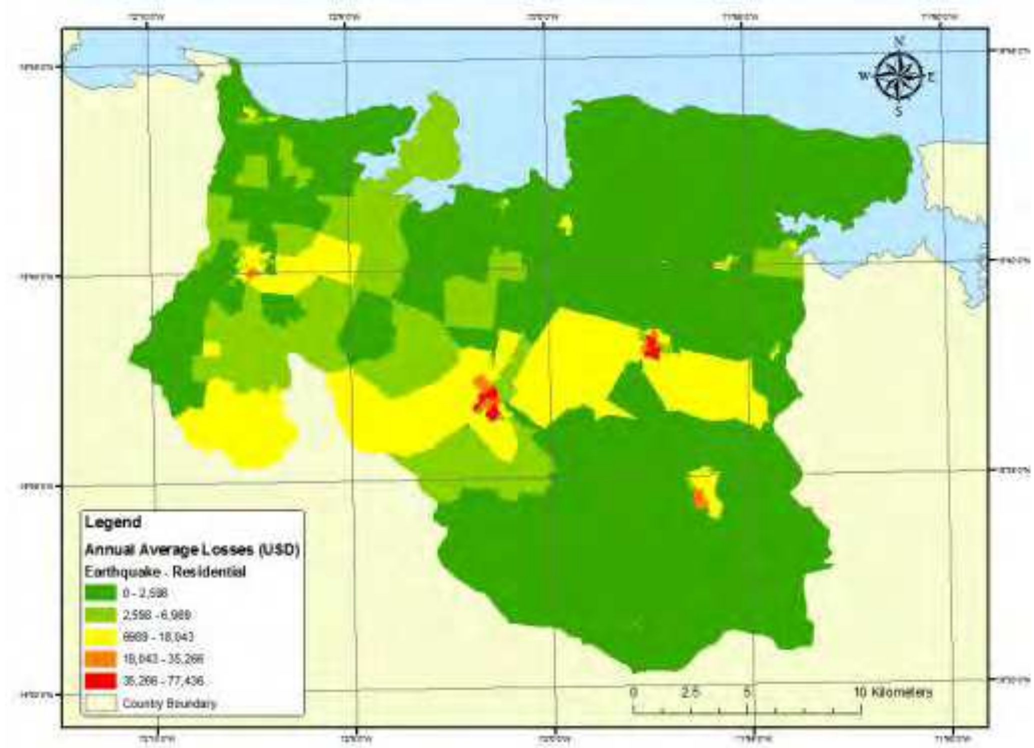

*Figure A**Error! No text of specified style in document.**.2 Risk Map: AAL for Earthquake Hazard, Residential*

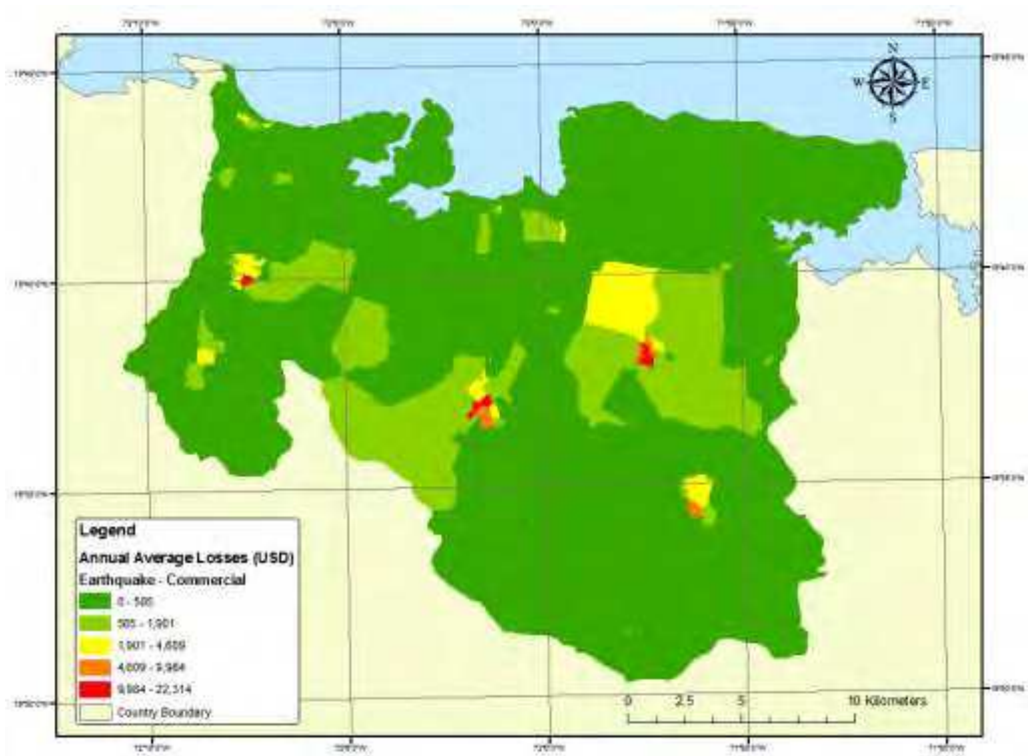

*Figure A**Error! No text of specified style in document.**.3 Risk Map: AAL for Earthquake Hazard, Commercial*

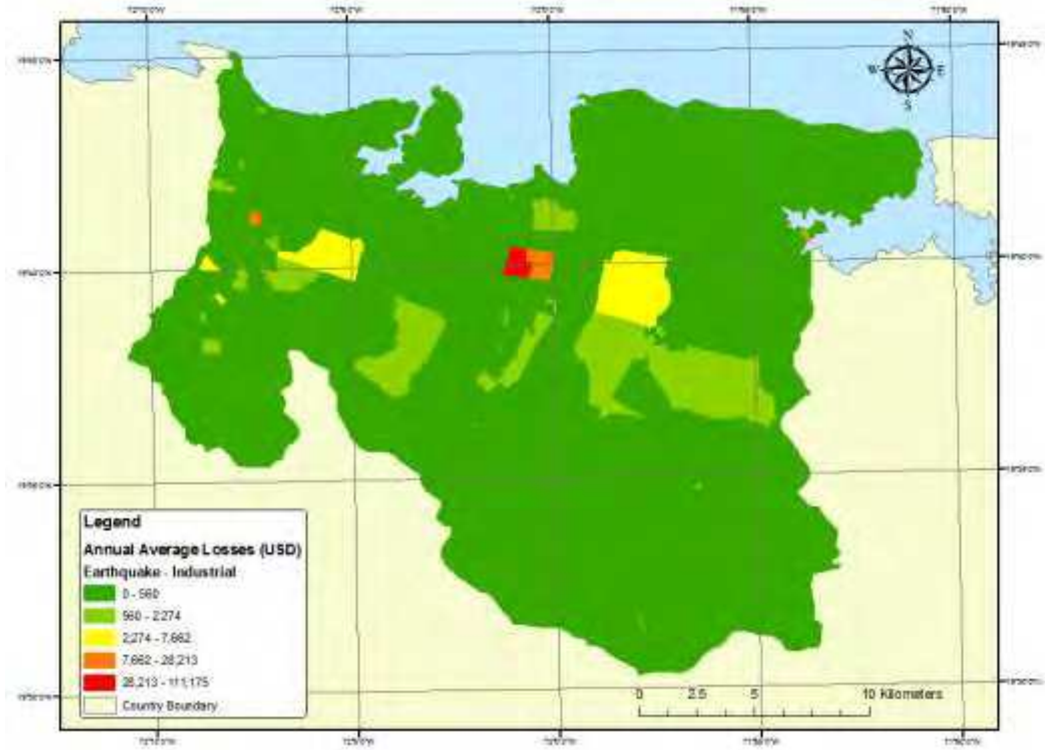

*Figure A**Error! No text of specified style in document.**.4 Risk Map: AAL for Earthquake Hazard, Industrial*

Losses to Critical Facilities and Infrastructure

Table AError**! No text of specified style in document.**.2 depicts critical facilities and infrastructure losses for the earthquake hazard.

*Table A**Error! No text of specified style in document.**.2 Losses to Critical Facilities and Infrastructure for Earthquake Hazard*

Facility/Infrastructure Type	**Number of Facilities, Class**	**475 Year**		**2500 Year**	
Critical Facilities		USD 10^6	%	USD 10^6 USD	%
Hospitals (Level 1 – Major Medical Facility)	4	2,092,581	31.7%	3,390,100	51.4%
Hospitals (Level 2 – Medical Facility/Clinic)	14	879,788	35.3%	1,339,951	53.7%
Hospital (Level 3 – Rural Clinic)	5	69,121	16.3%	112,487	26.5%
Kindergarten	9	176,847	38.3%	260,794	56.5%
Primary	120	9,146,441	39.4%	13,348,272	57.5%
College	4	931,367	40.8%	1,322,628	57.9%
University	9	3,967,362	39.5%	5,782,997	57.6%
Transportation Infrastructure					
Roads, km (Highway)	29	47,339	1.2%	348,493	8.6%
Roads, km (Secondary)	11	8,683	1.1%	65,710	8.2%

Roads, km (Teritary)	464	681	1.0%	5,273	7.6%
Bridges	55 (747 meter)	3,691,453	22.5%	4,619,793	28.1%
Public Service Infrastructure					
Electric Infrastructure					
Electric Power Plant	1	141,774,845	35.4%	234,249,808	58.6%
Electric Lines, km	29	96,399	3.7%	356,803	13.7%
Water Infrastructure					
Water Lines, km	40	35,591	0.9%	286,294	7.4%
Water Pumping Stations	7	85,578	7.0%	175,047	14.3%
Reseviors/Catchment	1	153,617	10.2%	356,672	23.8%
Wells	33	23,299	7.1%	48,754	14.8%
Waste Water Infrastructure					
Culverts	77	144,423	22.3%	179,839	27.8%
Waste Water Treatment Plants	1	591,690	16.4%	1,024,518	28.5%

A6.3 Hurricane Hazard

The interplay of factors such as wind speed, wind direction, storm duration makes it quite difficult to predict the impact of a hurricane, nevertheless, the expected intensity of a hurricane in the area is significant with an expected 124 mph wind speed for three second gusts for a height of 10 meters for a flat terrain for 100 year return period and 156 mph for a 700 year return period. With this level of expected intensity, the expected damages to housing, institutional buildings and infrastructure is expected to extensive.

The key variable for defining the vulnerability to the wind hazard in Northern Development Corridor of Haiti is the quality of construction, of which the majority of construction takes place without proper architectural and engineering oversight. Residential construction, in particular, is especially vulnerable with the roofs being the most susceptible component to damages. Residential housing in both rural and urban areas either had roof constructed of inadequate materials or had poor connections to walls making a majority of residential structures vulnerable to heavy wind gusts associated with hurricanes. Institutional buildings such as local government offices and industrial structures were found to be engineered a bit better and will most probably respond better, but may still experience extensive damages due to heavy wind loads or gusts associated with hurricanes.

Estimated Probable Losses, Hurricane Hazard

The estimates for the hurricane hazard are provided in Table **Error! No text of specified style in document.**.3 below, and represent the maximum probable losses for general occupancy classes. Losses are presented for four return periods.

*Table **Error! No text of specified style in document.**.3 Probable Maximum Losses (PML) for Hurricane Hazard*

Return Period Years	Loss (10^6 USD)		
	Residential	Commercial	Industrial
50	58.7	4.4	1.9
100	92.7	9.4	3.9
700	239.2	34.6	14.0
1700	386.0	60.0	24.2

Loss Exceedance Curve and the AAL

Figure A**Error! No text of specified style in document.**.5 depicts the Loss Exceedance Curve and the AAL for the hurricane hazard in the study region, and Figures A6.6-A6.8 show the corresponding AAL maps for Hurricane Hazard.

*Figure A**Error! No text of specified style in document.**.5 Loss Exceedance Curve and the AAL for Hurricane Hazard*

LEC, Residential

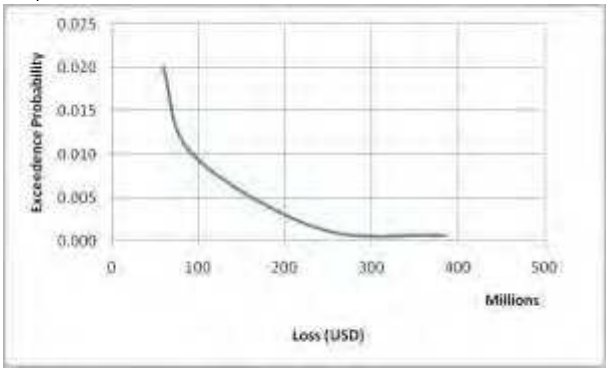

LEC, Commercial

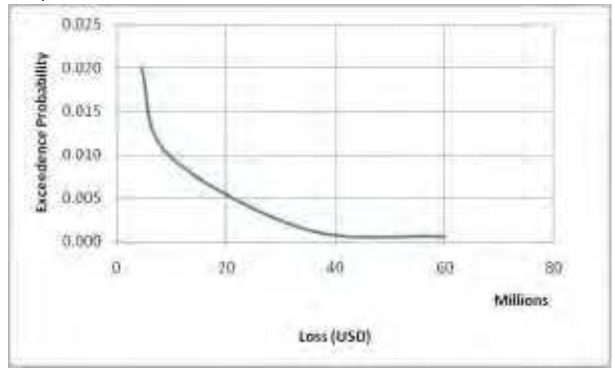

LEC, Industrial

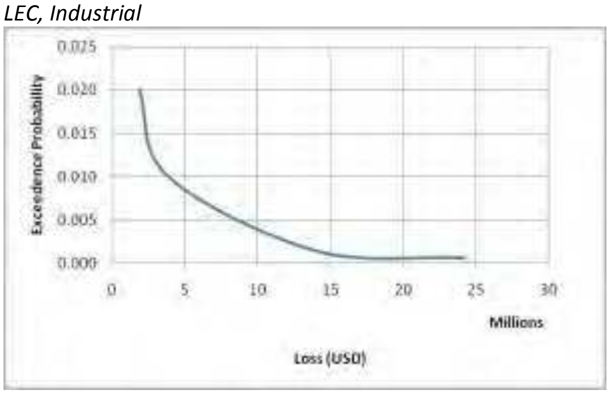

Average Annual Losses (AAL)					
Residential		Commercial		Industrial	
USD$ x 10^6	% de Exposure	USD$ x 10^6	% de Exposure	USD$ x 10^6	% de Exposure
1.8	0.084%	0.2	0.056%	0.1	0.026%

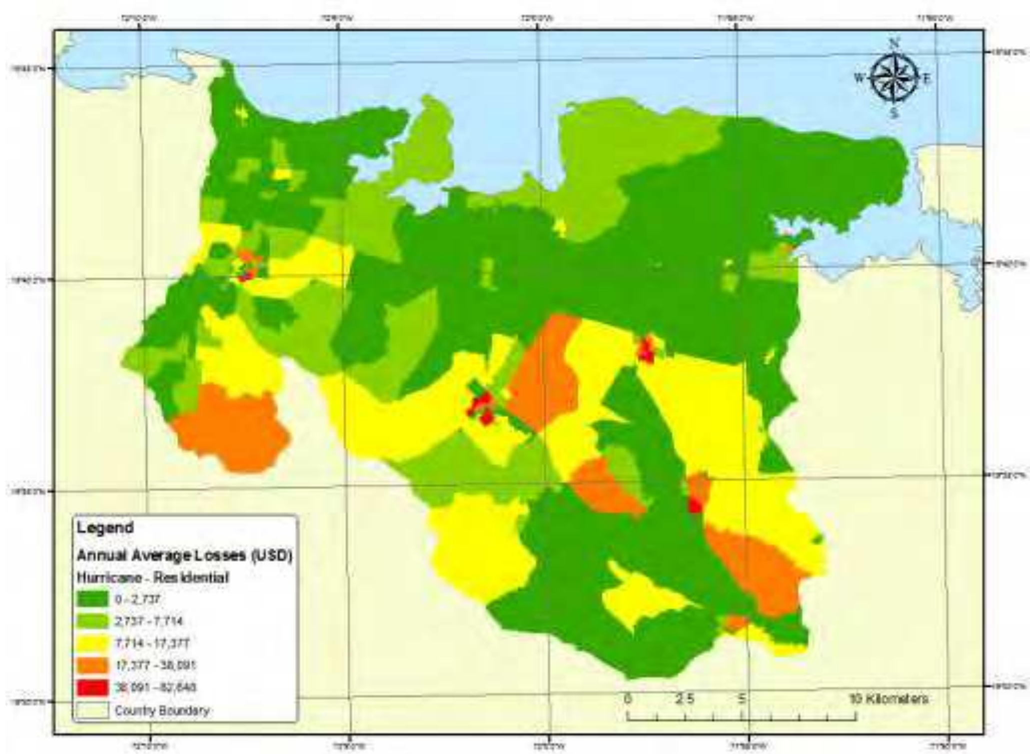

*Figure A**Error! No text of specified style in document.**.6 Risk Map: AAL for Hurricane Hazard, Residential*

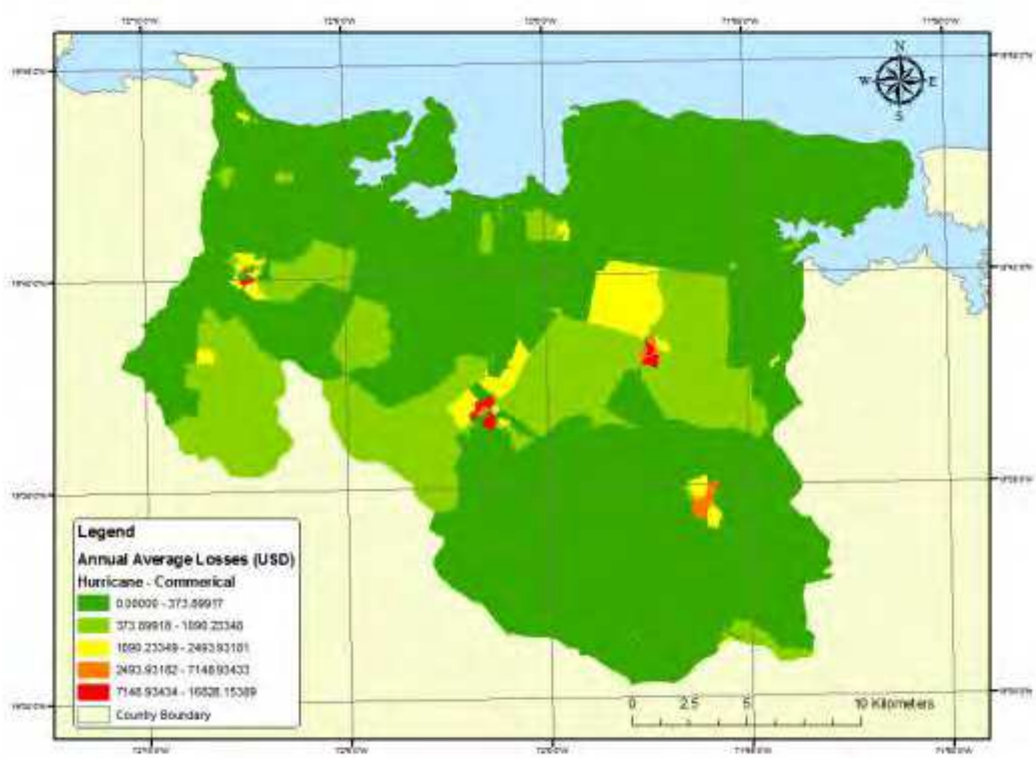

*Figure A**Error! No text of specified style in document.**.7 Risk Map: AAL for Hurricane Hazard, Commercial*

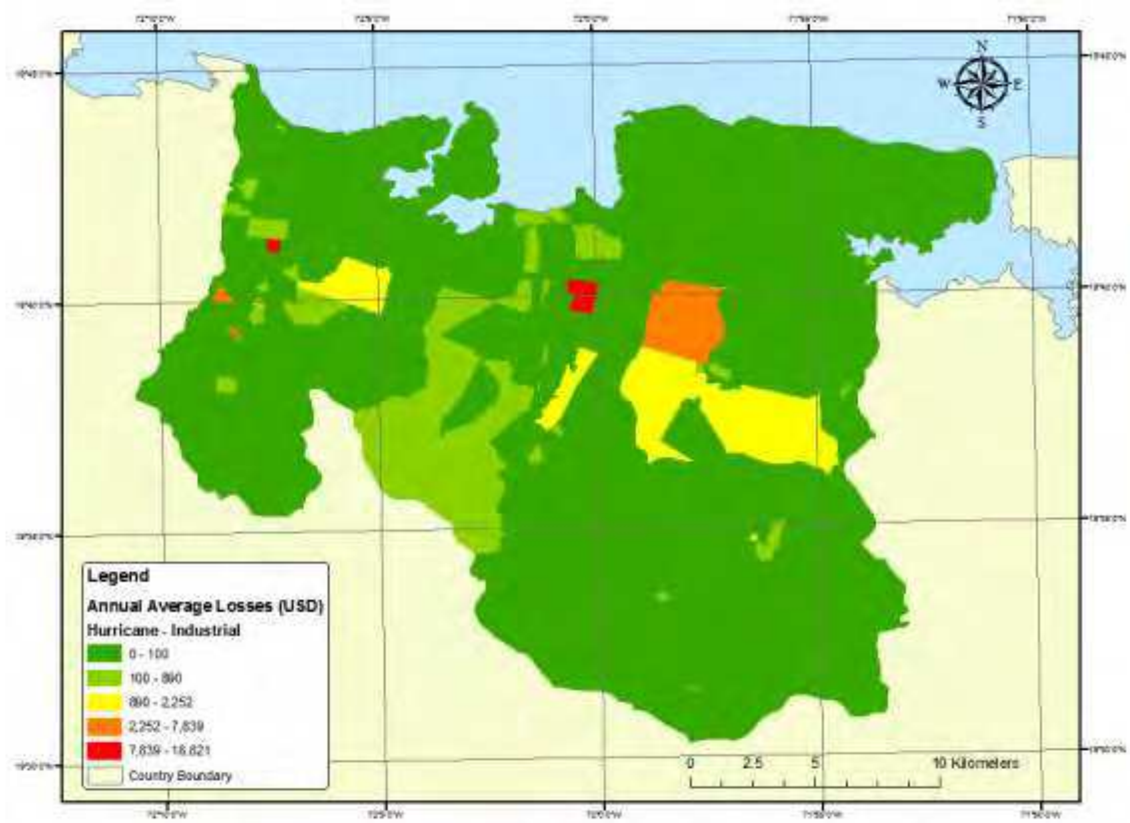

*Figure A**Error! No text of specified style in document.**.8 Risk Map: AAL for Hurricane Hazard, Industrial*

Losses to Critical Facilities and Infrastructure

Table AError**! No text of specified style in document.**.4 depicts critical facilities and infrastructure losses for the hurricane hazard.

*Table A**Error! No text of specified style in document.**.4 Losses to Critical Facilities and Infrastructure for the Hurricane Hazard*

Facility/Infrastructure Type	**Number of Facilities/ Class**	**100 Year**		**700 Year**		**1700 Year**	
Critical Facilities		USD 10^6	%	USD 10^6	%	USD 10^6	%
Hospitals (Level 1 – Major	4	238,272	3.6%	882,309	13.4%	1,533,785	23.2%
Hospitals (Level 2 – Medical	14	89,594	3.6%	333,592	13.4%	579,908	23.2%
Hospital (Level 3 – Rural Clinic)	5	15,495	3.7%	58,414	13.8%	98,553	23.2%
Kindergarten	9	16,698	3.6%	61,721	13.4%	107,294	23.2%
Primary	120	829,994	3.6%	3,107,643	13.4%	5,402,255	23.3%
College	4	82,889	3.6%	305,633	13.4%	531,306	23.2%
University	9	355,736	3.5%	1,343,039	13.4%	2,334,708	23.2%

Transportation Infrastructure							
Roads, km (Highway)	29		0.0%		0.0%		0.0%
Roads, km (Secondary)	11		0.0%		0.0%		0.0%
Roads, km (Teritary)	464		0.0%		0.0%		0.0%
Bridges	55 (747m)	4,862,519	29.6%	10,555,678	64.2%	13,100,210	79.7%
Public Service Infrastructure							
Electric Infrastructure							
Electric Power Plant	1	118,632,228	29.7%	256,769,64	64.2%	318,666,06	79.7%
Electric Lines, km	29	765,519	29.3%	1,502,118	57.6%	1,710,287	65.5%
Water Infrastructure							
Water Lines, km	40		0.0%		0.0%		0.0%
Water Pumping Stations	7	89,294	7.3%	327,630	26.7%	569,544	46.5%
Reseviors/Catchment	1	42,009	2.8%	150,442	10.0%	261,525	17.4%
Wells	33		0.0%		0.0%		
Waste Water Infrastructure							
Culverts	77	60,328	9.3%	98,480	15.2%	119,298	18.4%
Waste Water Treatment Plants	1	89,294	2.5%	327,630	9.1%	569,544	15.8%

A6.4 Flood Hazard

There are several factors that must be emphasized in regards to flooding in the Northern Development Corridor of Haiti. They relate to the precipitation data used to model the flood hazard, the surrounding environmental degradation that increases overland flows and the increasing population which has put pressure on the existing storm water drainage infrastructure.

As outlined in the section above, the lack of reliable 24 hour precipitation data in flood hazard model predicated the need to rely on a limited 24-hour intensity data and monthly rainfall data to global models (i.e. Santa Clara University). This facilitated an approximation to understand flows in the hydrological model, but also introduces a high degree of uncertainty in the analysis of risk. The results show that the flooding hazard is quite significant in the study area and that with climate change the average flood depth will increase by about 0.23 m (23 cm) across all return periods. The expected flood depth for a 100 year flood event is expected to be 10.17m, which is significant given the flat terrain of the majority of the study area.

Flooding must also be viewed in the context of environmental degradation occurring throughout Haiti which has resulted from deforestation. This has resulted in an increase in flood event frequency due to increasing volumes of overland flows. The combination of hillside degradation and urban development has reduced infiltration. The interplay of these factors has placed strains on existing drainage infrastructure, which are inadequate for population densities in urban areas and/or not present in rural areas. Urban drainage infrastructure is susceptible to blockage from an inflow of both earthen and man-made debris (garbage). Such debris inflows have resulted in blockages and/or increased and prolonged flooding in urban areas. In rural areas, the lack of drainage infrastructure or riverine stabilizers has resulted in erosion of river banks during high magnitude rainfall events and furthers siltation, blockage or overflow where infrastructure is in place.

Therefore, it is likely given the interplay of these factors that flooding will become a bigger problem unless storm water drainage infrastructure is improved to increase infiltration and alleviate flash flooding problems.

Estimated Probable Losses, Flood Hazard

The estimates for the flood hazard are provided in Table A**Error! No text of specified style in document.**.5 below, and represent the maximum probable losses for general occupancy classes. Losses are presented for six return periods.

*Table A**Error! No text of specified style in document.**.5 Probable Maximum Losses (PML) for the Flood Hazard*

Return Period Years	**Loss (10^6 USD)**		
	Residential	**Commercial**	**Industrial**
2	3.0	0.5	0.2
5	4.7	0.8	0.4
10	5.5	0.9	0.5
25	6.7	1.1	0.6
50	7.2	1.2	0.9
100	8.0	1.3	1.0

Loss Exceedance Curve and the AAL

Figure A**Error! No text of specified style in document.**.9 depicts the Loss Exceedance Curve and the AAL for the flood hazard in the study region, and Figures A6.10-A6.12 show the corresponding AAL maps for the Flood Hazard.

LEC, Residential

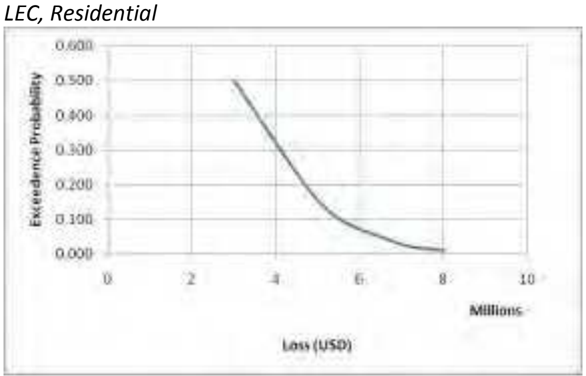

LEC, Commercial

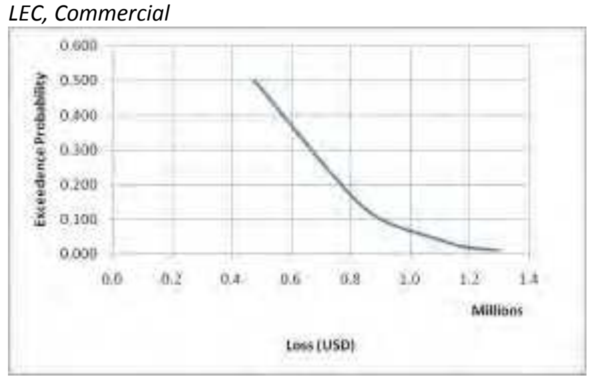

LEC, Industrial

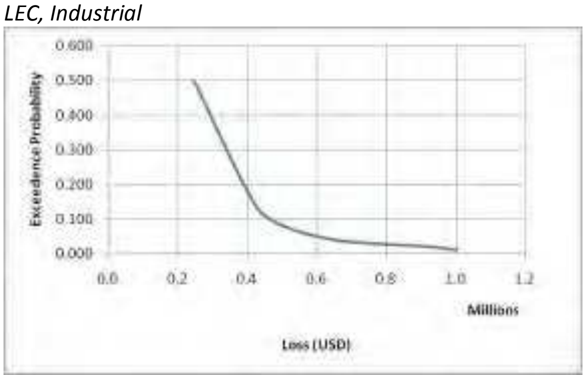

Average Annual Losses (AAL)					
Residential		**Commercial**		**Industrial**	
USD$ x 10^6	**% de Exposure**	**USD$ x 10^6**	**% de Exposure**	**USD$ x 10^6**	**% de Exposure**

2.0	0.092%	0.3	0.095%	0.2	0.058%

*Figure A**Error! No text of specified style in document.**.9 Loss Exceedance Curve and the AAL for the Flood Hazard*

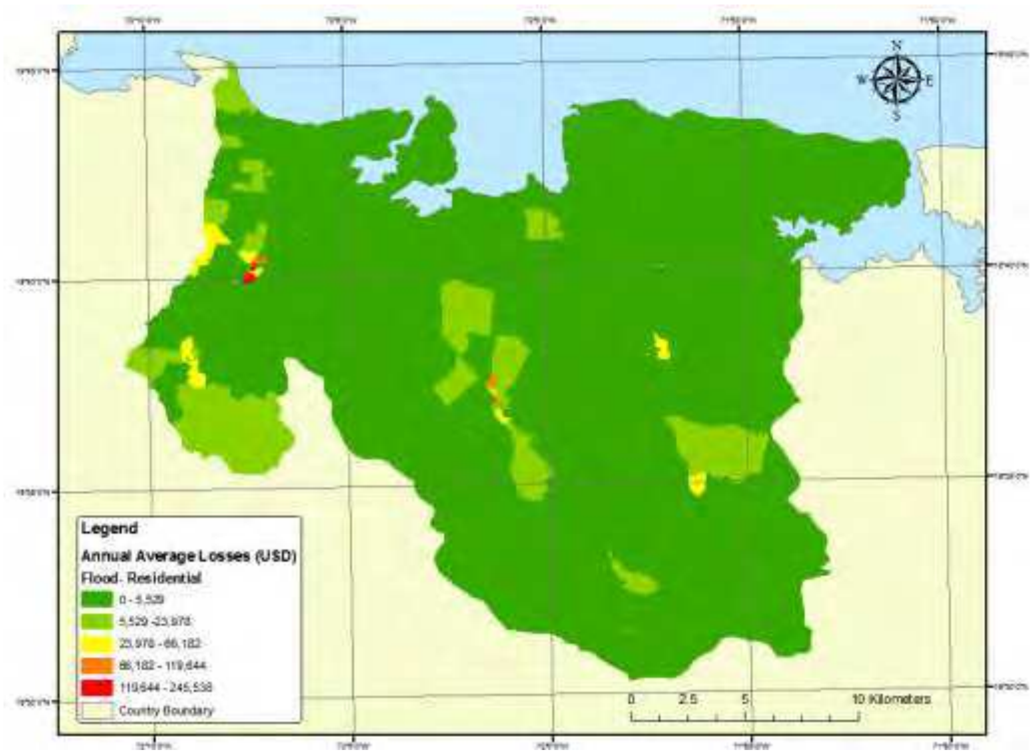

*Figure A**Error! No text of specified style in document.**.10 Risk Map: AAL for Flooding Hazard, Residential*

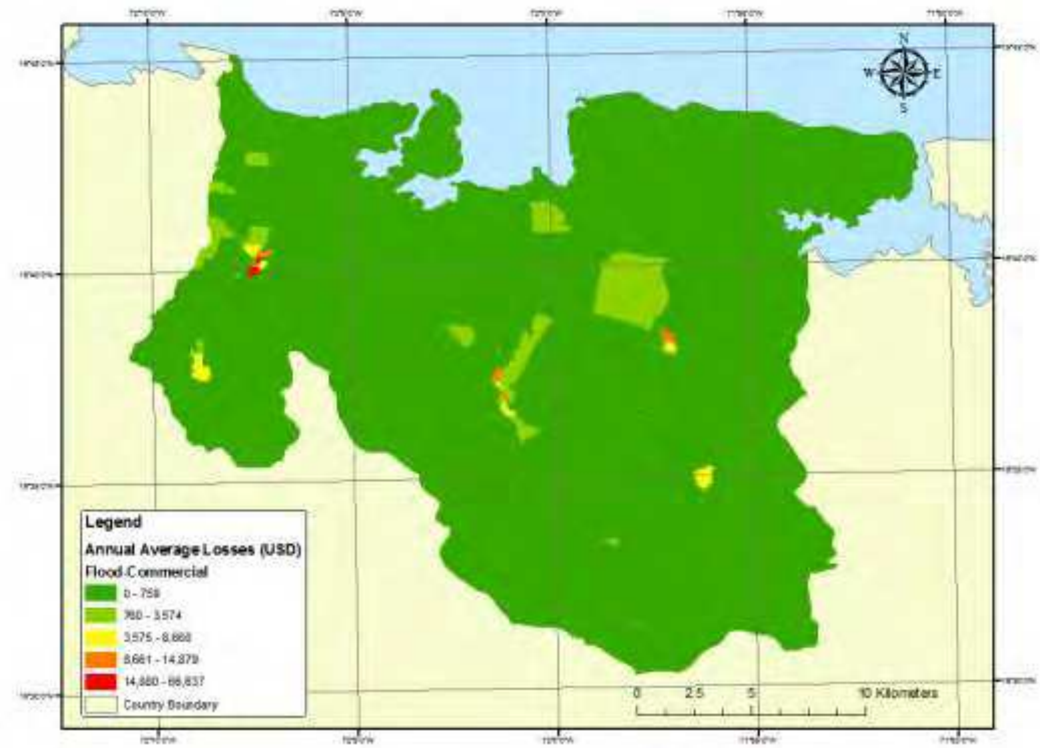

*Figure A**Error! No text of specified style in document.**.11 Risk Map: AAL for Flooding Hazard, Commercial*

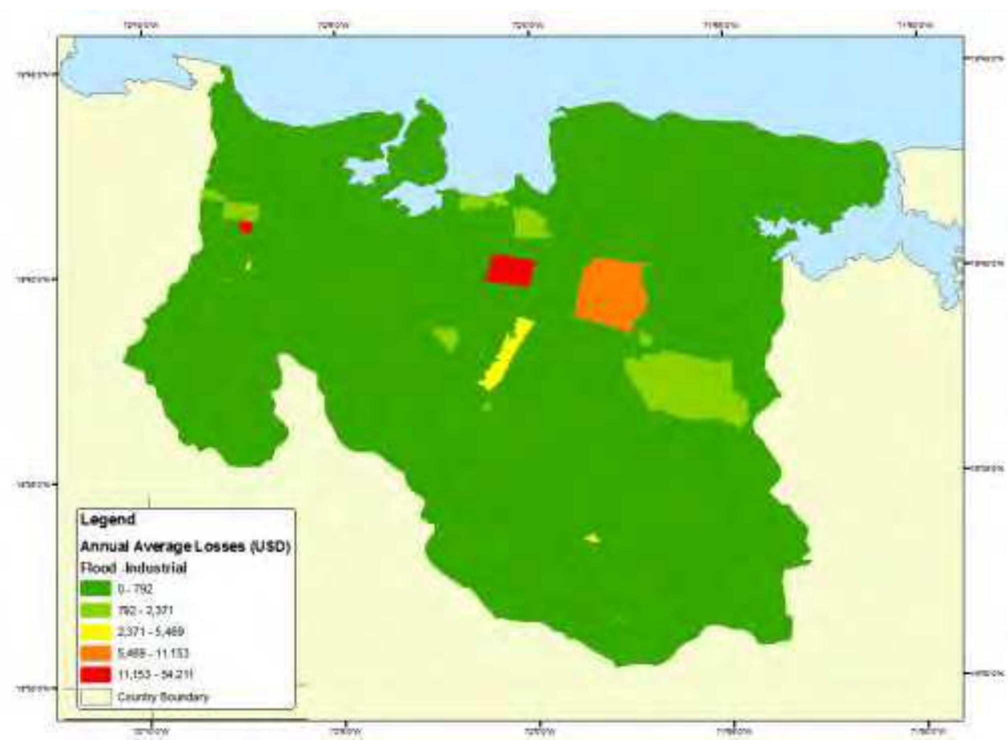

*Figure A**Error! No text of specified style in document.**.12 Risk Map: AAL for Flooding Hazard, Industrial*

Losses to Critical Facilities and Infrastructure

Table AError**! No text of specified style in document.**.6 depicts critical facilities and infrastructure losses for the flood hazard.

*Table A**Error! No text of specified style in document.**.6 Losses to Critical Facilities and Infrastructure for the Flood Hazard*

Facility/Infrastructure Type	**Number of Facilities/ Class**	**25 Year**		**50 Year**		**100 Year**	
Critical Facilities		USD	%	USD 10^6	%	USD 10^6	%
Hospitals (Level 1 – Major Medical	4		0.0%		0.0%		0.0%
Hospitals (Level 2 – Medical	14		0.0%		0.0%		0.0%
Hospital (Level 3 – Rural Clinic)	5		0.0%		0.0%		0.0%
Kindergarten	9		0.0%		0.0%		0.0%
Primary	120	36,795	0.158%	37,513	0.161%	38,542	0.166%
College	4		0.0%		0.0%		0.0%
University	9		0.0%		0.0%		0.0%
Transportation Infrastructure							
Roads, km (Highway)	29	1,153	0.029%	1,224	0.030%	1,307	0.032%
Roads, km (Secondary)	11	857	0.11%	925	0.11%	1,063	0.13%
Roads, km (Tertiary)	464	50	0.07%	54	0.08%	60	0.09%
Bridges	55 (747				0.0%		0.0%
Public Service Infrastructure							
Electric Infrastructure							
Electric Power Plant	1		0.0%		0.0%		0.0%
Electric Lines, km	29	70	0.0027%	78	0.0030%	89	0.0034%
Water Infrastructure							
Water Lines, km	40	1,026	0.0%	1,193	0.0%	1,376	0.0%
Water Pumping Stations	7	53,372	4.4%	54,652	4.5%	57,733	4.7%
Reseviors/Catchment	1				0.0%		0.0%
Wells	33				0.0%		0.0%
Waste Water Infrastructure							
Culverts	77		0.0%		0.0%		0.0%
Waste Water Treatment Plants	1	236,033	6.6%	298,540	8.3%	349,981	9.7%

A6.5 Coastal Flood Hazard

The Northern Development Corridor is most likely to be affected by a combined effect of storm surges and wave action associated with hurricanes and strong winds as indicated by the Total Arbiter of Storms (TAOS) hazard modeling system. The TAOS results combined with climate change suggests that the expected estimated water surface elevations (i.e. maximum depth of flooding) for a 50 year return period is expected to be 5.35 m, while the projected estimated water surface elevations for a 100 year return period is expected to be 6.15 m.

These results clearly show that there will be significant impact to coastal developments and that the flooding could occur up to +1000 m inland impacting - population, agriculture, industry and infrastructure. Coastal flooding will cause disruption of settlements and may inhibit the movement of persons. In coastal settlements such as Limonade du Mer and Caracol the situation will become dire, especially as drainage systems, which are already under stress, are overwhelmed by a combination of water from coastal surges and waves and accumulation of inland flows associated with storms.

Therefore, it is likely that coastal flooding will become a bigger problem if settlements in high hazards areas continue to grow and drainage systems are not improved.

Estimated Probable Losses, Coastal Flood Hazard

The estimates for the flood hazard are provided in Table A6.7 below, and represent the maximum probable losses for general occupancy classes. Losses are presented for four return periods.

*Table A**Error! No text of specified style in document.**.7 Probable Maximum Losses (PML) for the Coastal Flood Hazard*

Return Period Years	Loss (10^6 USD)		
	Residential	Commercial	Industrial
10	34.6	5.1	1.4
25	51.0	7.2	2.0
50	63.9	8.8	4.4
100	75.9	10.3	5.6

Loss Exceedance Curve and the AAL

Figure AError**! No text of specified style in document.**.13 depicts the Loss Exceedance Curve and the AAL for the Coastal Flood Hazard in the study region, and Figures A6.14-A6.16 show the corresponding AAL maps for the Coastal Flood Hazard.

LEC, Residential

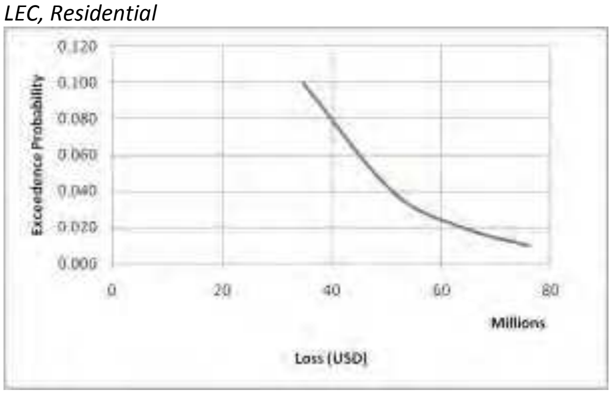

LEC, Commercial

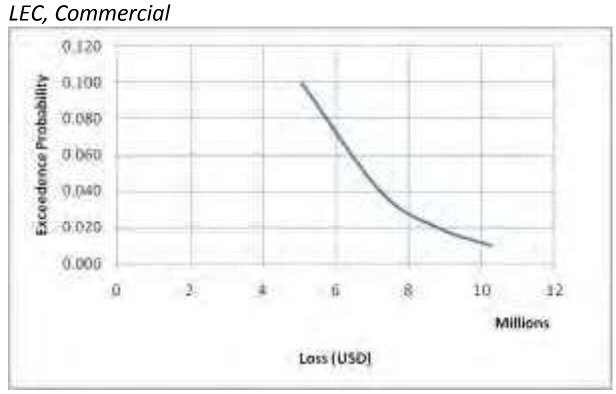

LEC, Industrial

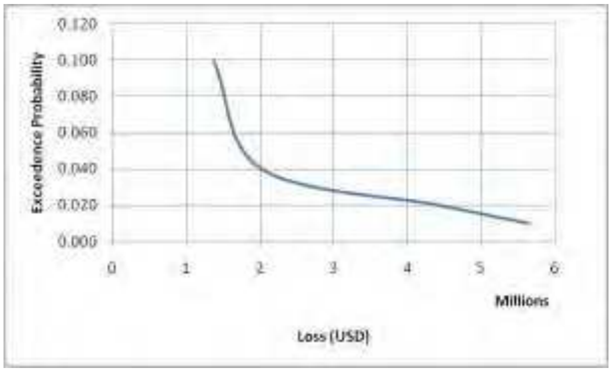

Average Annual Losses (AAL)					
Residential		Commercial		Industrial	
USD$ x 10^6	% de Exposure	USD$ x 10^6	% de Exposure	USD$ x 10^6	
4.5	0.209%	0.6	0.190%	0.2	0.075%

*Figure A**Error! No text of specified style in document.**.13 Loss Exceedance Curve and the AAL for Coastal Flood Hazard*

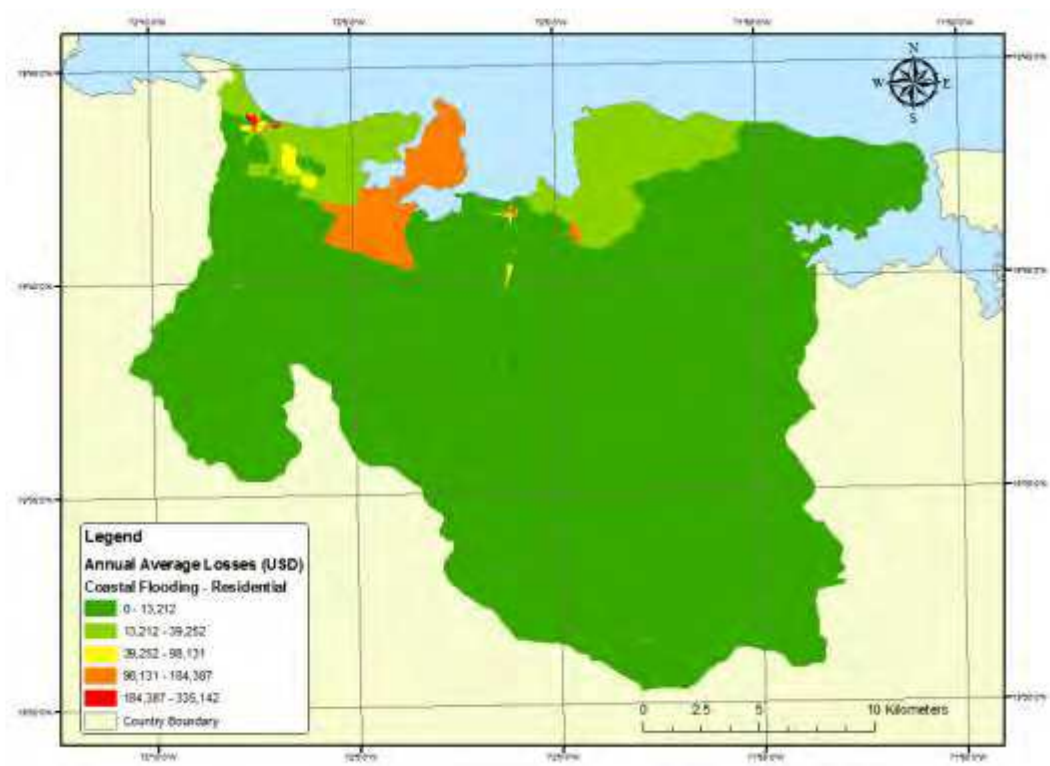

*Figure A**Error! No text of specified style in document.**.14 Risk Map: AAL for Coastal Flooding Hazard, Residential*

*Figure A**Error! No text of specified style in document.**.15 Risk Map: AAL for Coastal Flooding Hazard, Commercial*

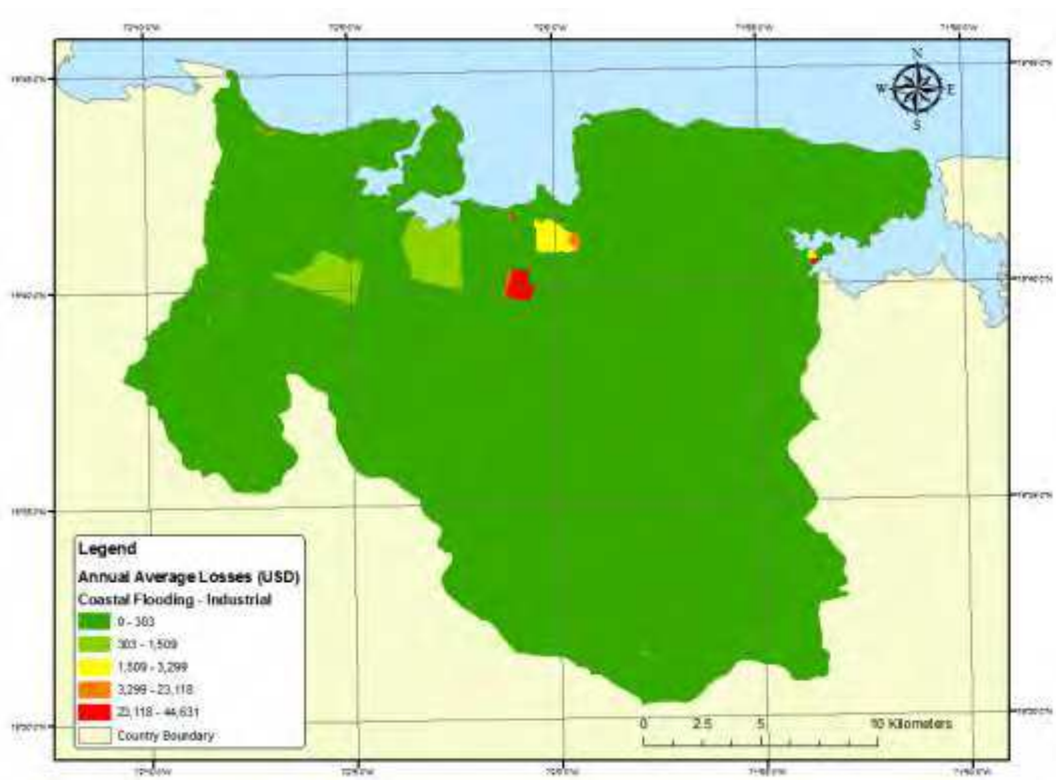

*Figure A**Error! No text of specified style in document.**.16 Risk Map: AAL for Coastal Flooding Hazard, Industrial*

Losses to Critical Facilities and Infrastructure

Table AError**! No text of specified style in document.**.8 depicts critical facilities and infrastructure losses for the Coastal Flood Hazard.

*Table A**Error! No text of specified style in document.**.8 Losses to Critical Facilities and Infrastructure for the Coastal Flood Hazard*

Facility/Infrastructure Type	**Number of Facilities/Class**	**100 Year**	
Critical Facilities		USD 10^6	%
Hospitals (Level 1 – Major Medical Facility)	4		0.0%
Hospitals (Level 2 – Medical Facility/Clinic)	14	116,000	4.6%
Hospital (Level 3 – Rural Clinic)	5	2,931	0.7%
Kindergarten	9	117,243	25.4%
Primary	120	1,370,935	5.9%
College	4		0.0%
University	9		0.0%
Transportation Infrastructure			
Roads, km (Highway)	29		0.0%
Roads, km (Secondary)	11		0.0%
Roads, km (Tertiary)	464	208	0.3%
Bridges	55 (747 meter)		0.0%
Public Service Infrastructure			
Electric Infrastructure			
Electric Power Plant	1		0.0%
Electric Lines, km	29		0.0%
Water Infrastructure			
Water Lines, km	40	4,286	0.1%
Water Pumping Stations	7		0.0%
Reseviors/Catchment	1		0.0%
Wells	33	14,040	4.3%
Waste Water Infrastructure			
Culverts	77		0.0%
Waste Water Treatment Plants	1		0.0%

A6.6 Drought Hazard

Drought has been estimated using a hydrological model to obtain water balance of two major watersheds, and has sought to delineate the watershed and obtain the drainage and precipitation characteristics, including evaporation and outflows so as to determine water balance in the study area, which is primarily focused on understanding current and future water utilization demands.

An impact assessment of the drought hazard was not pursued as part of the study. The assessment of drought is concerned rather with the capacity of the current water system to store, accumulate and release ample water for current and future demands, incorporating the impact of climate change. All things considered, water shortage by hydrological droughts combined with growing water demand could lead to increasing water stock reduction and negatively impact agriculture, including cultivation of land and grazing. Food production will be one strain on water as will growth of urban settlements. Climate change plays into the equation as land use changes due to urbanization will increase evaporation and surface and subsurface water discharge, thus further decreasing water supply.

It is also necessary to note that changes in water availability, both increases as well as decreases, can affect water quality. Increased water availability, especially through heavy rainfall, can lead to increased suspended matter in water bodies, as well as a washing out of contaminants (e.g. fertilizer, toxins) into water and groundwater.

APPENDIX 7: Restrictions Maps

Figure A7.1 – Weighted Impact of Natural Hazards Risk: Flooding and Seismic

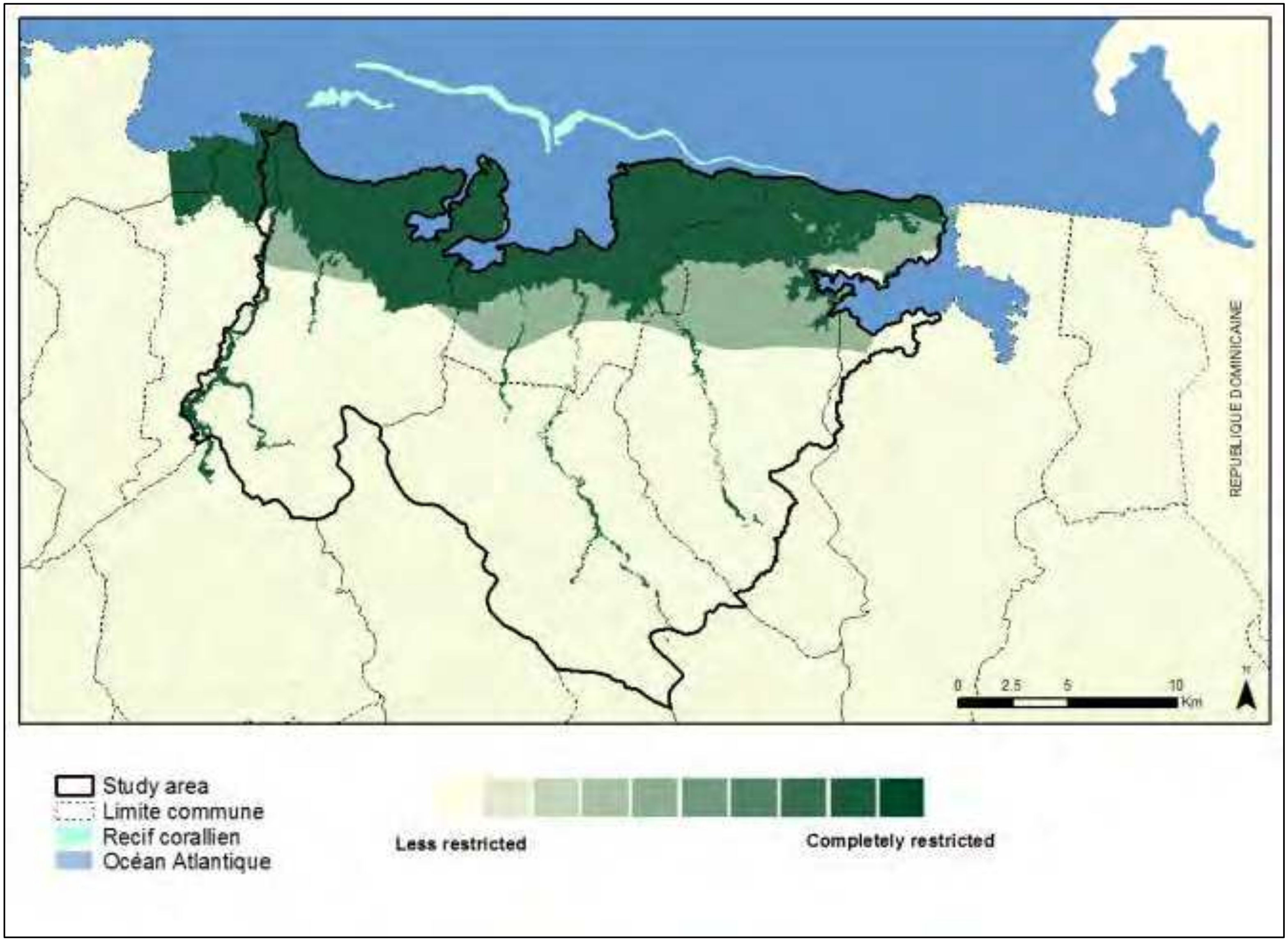

Map source: From geographic information layers by AIA (2012), CIAT (2012), CNGIS (c.2012), IADB (c.2013), NATHAT (2010), USAID-OFDA (c.2012), OSM (2013), OCHA (c.2010), PDNA (2010) and DTM (2013). Georeferencing, digitizing and remote sensing analysis from satellite imagery 1986, 2010 and 2013.

Figure A7.2 Restriction factors: Topography and slopes

Figure A7.3 Restriction factors: Hydric System – Superficial Water

Figure A7.4 *Restriction factors: Strategic Ecosystems and Protected Areas*

Figure 1 Restriction factors: Strategic Ecosystems and Protected Areas

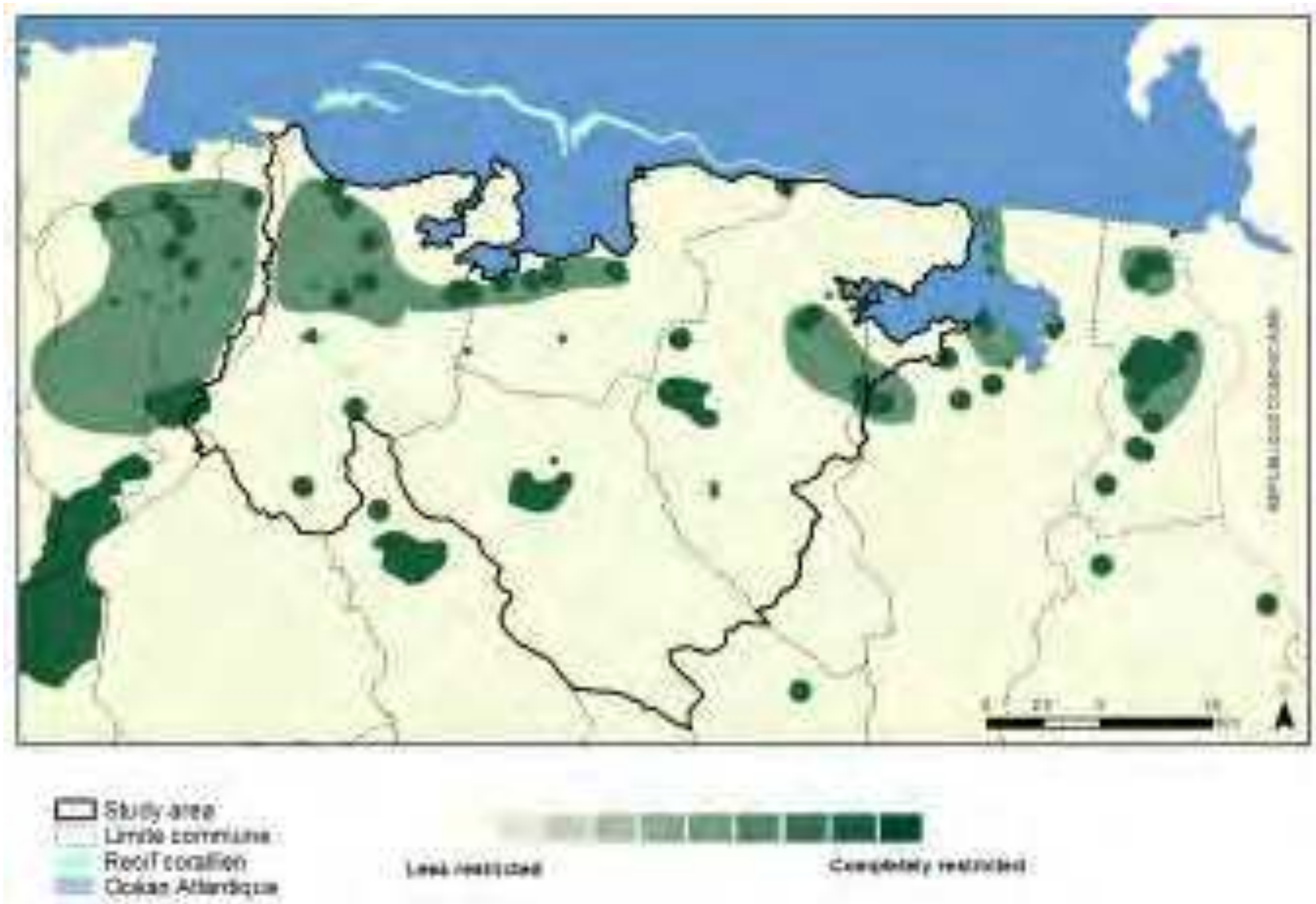

Figure A7.6 Restriction factors: Adequate Land Use

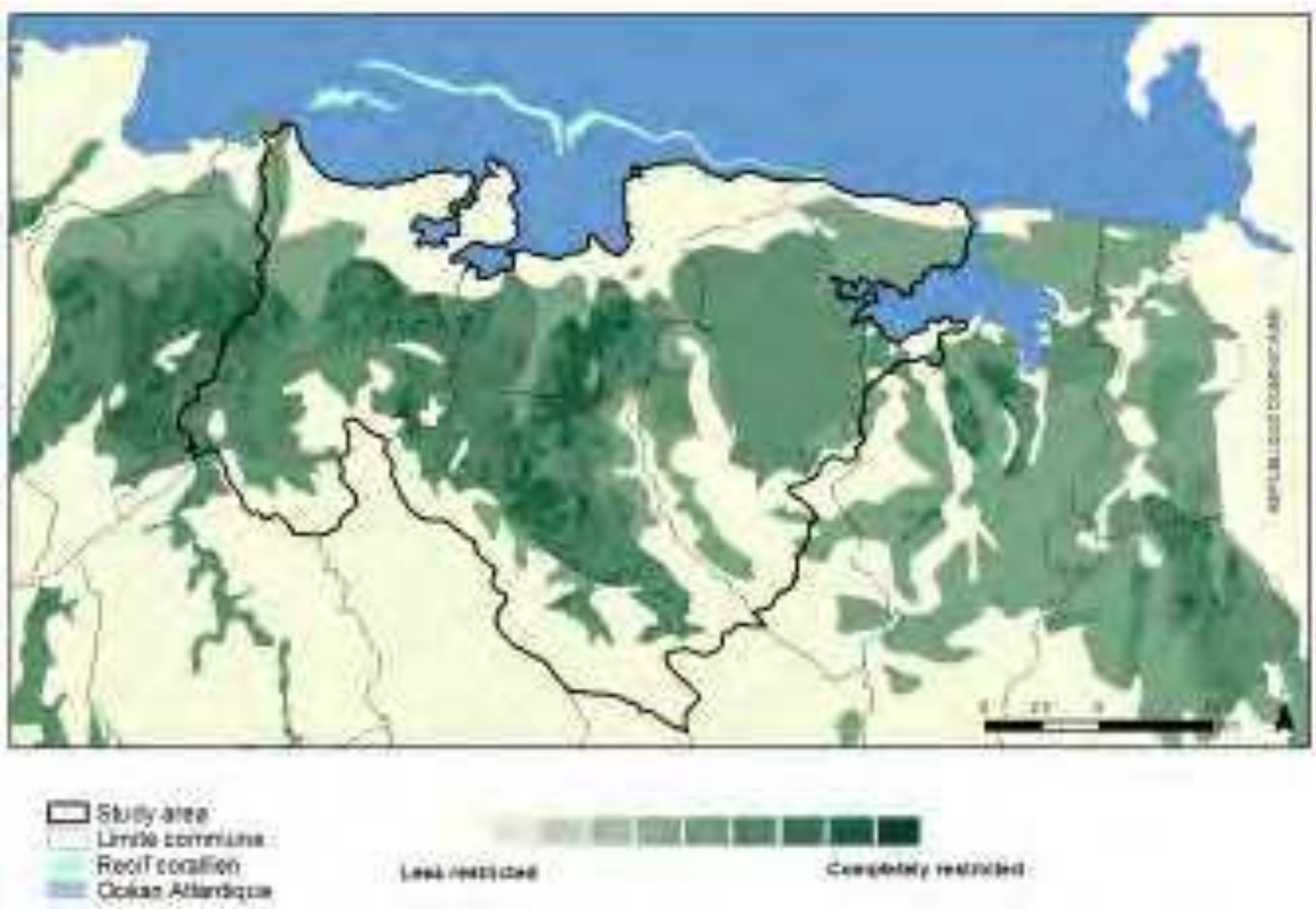

Figure A7.7 Restriction factors: Mining

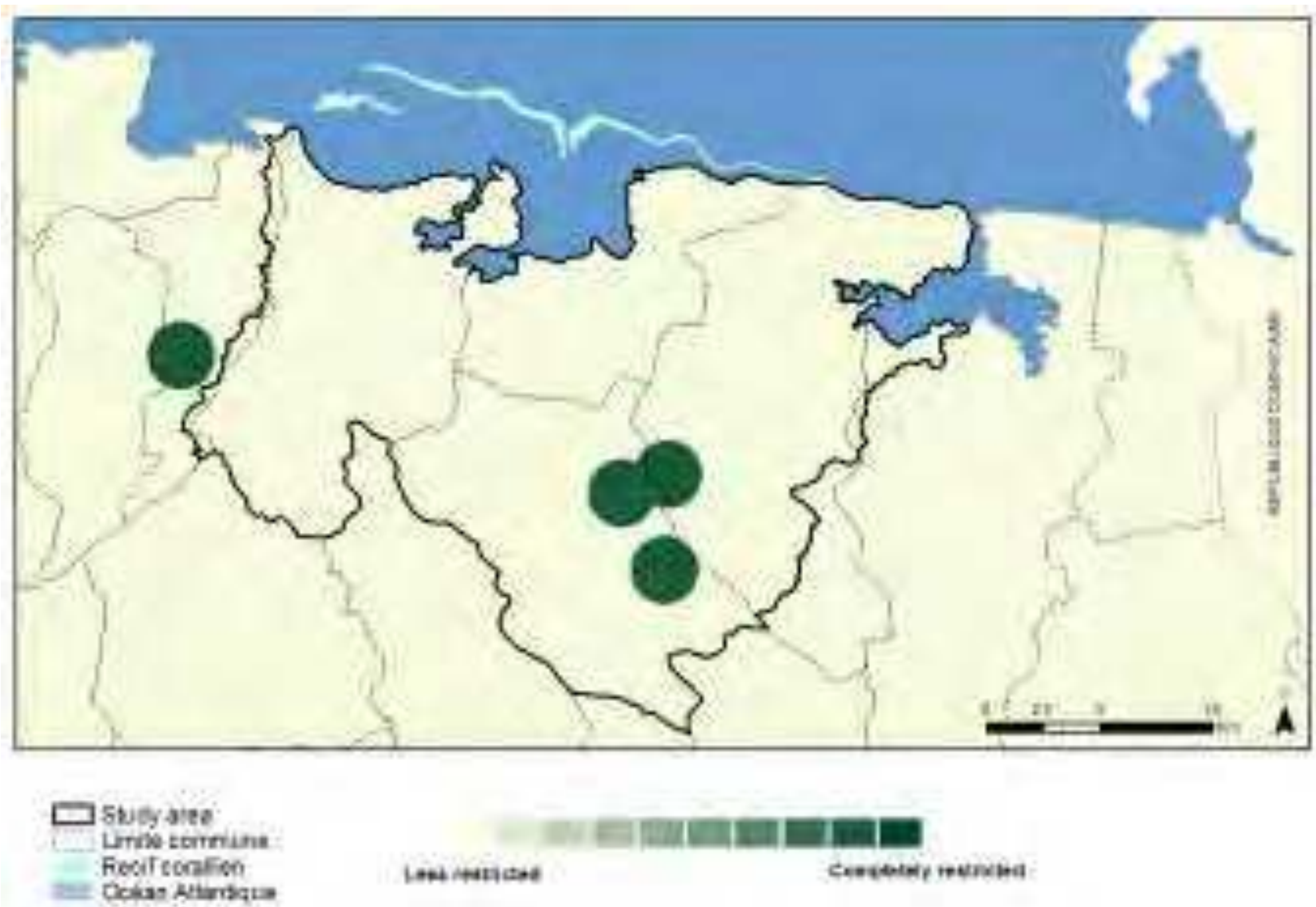

APPENDIX 8: Attractions Maps

Figure A8.1 Attraction factors: Agglomeration

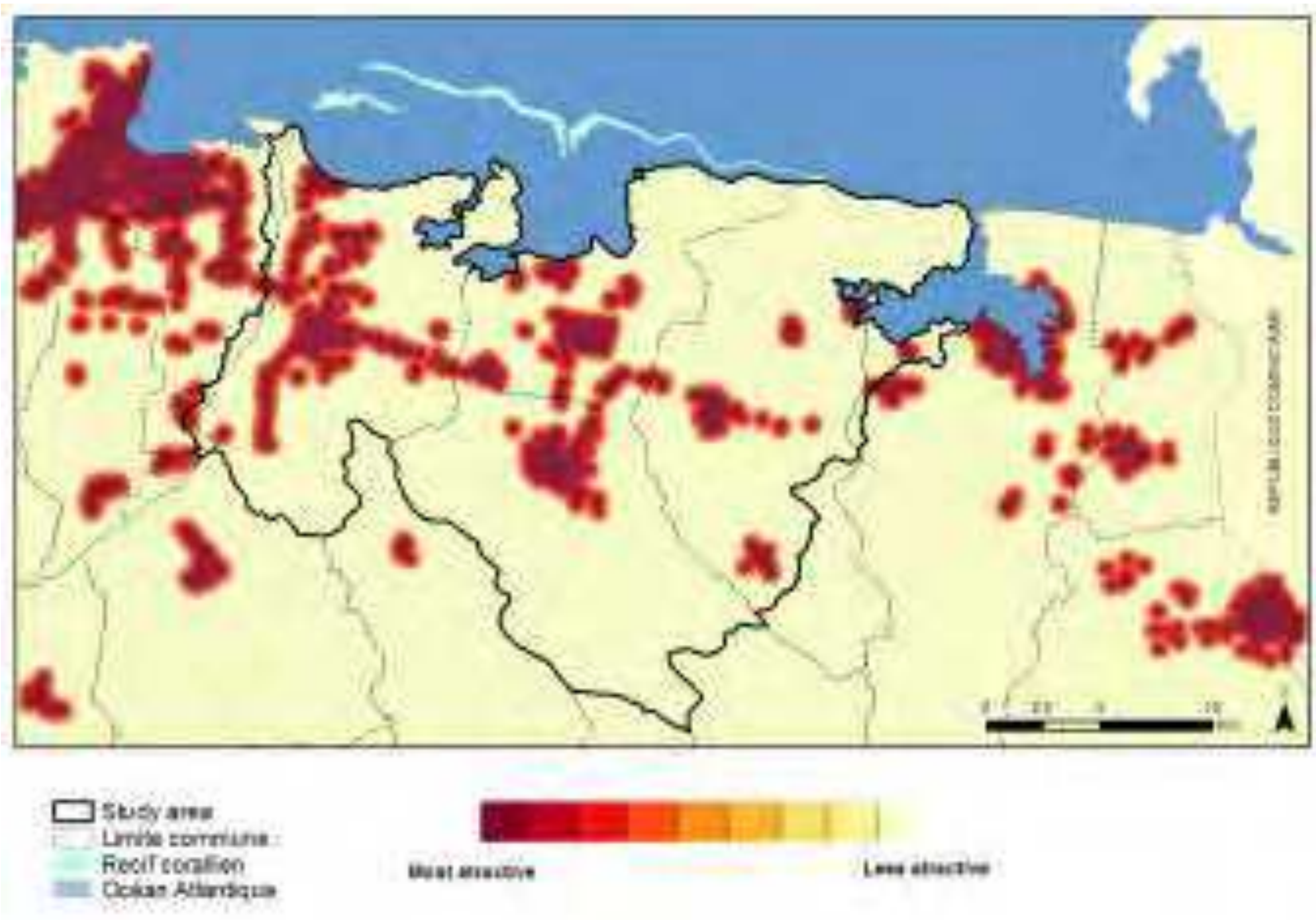

Figure A8.2 Attraction factors: Road System

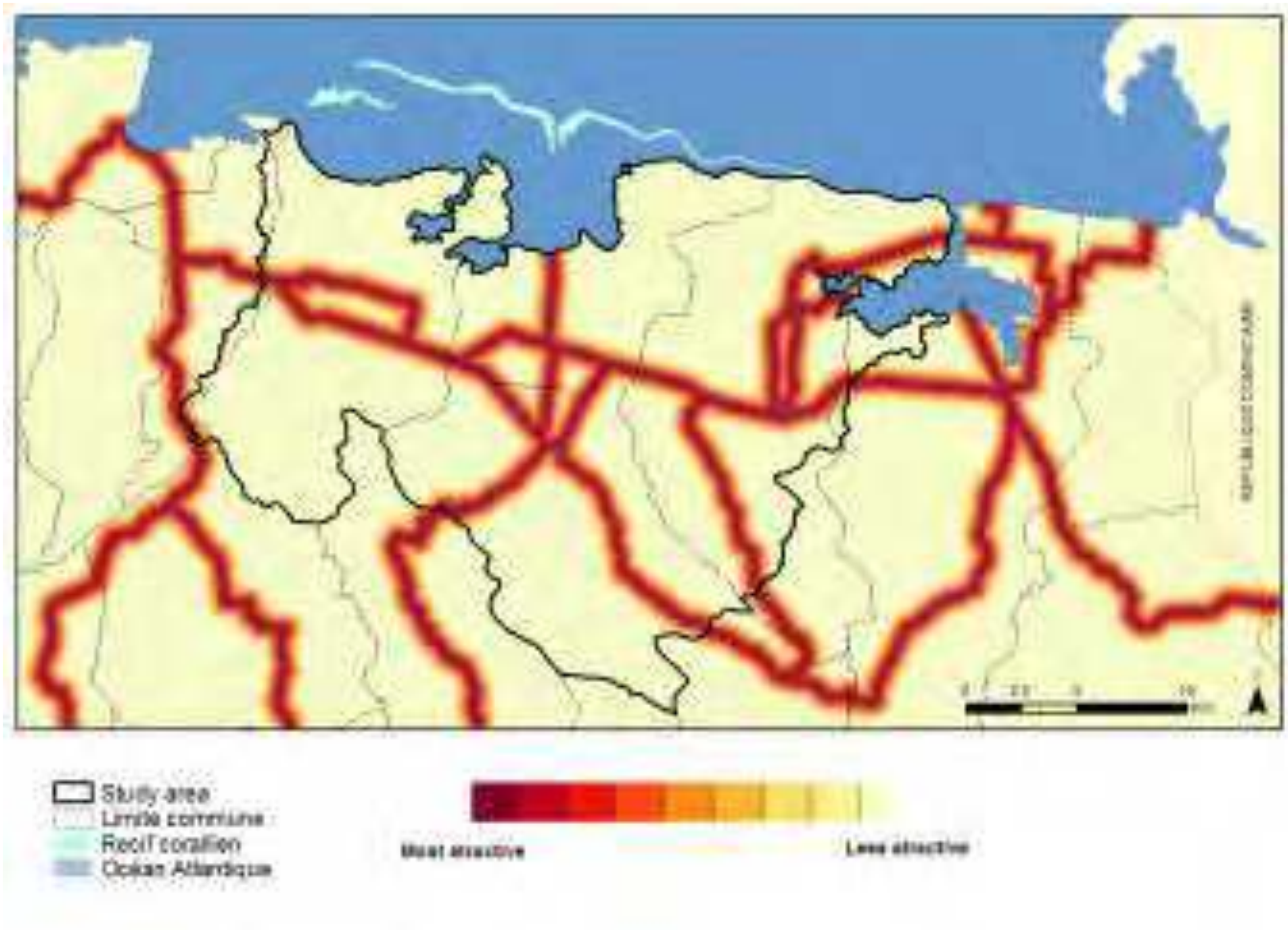

Figure A8.3 Attraction factors: Public Utilities – Water supply

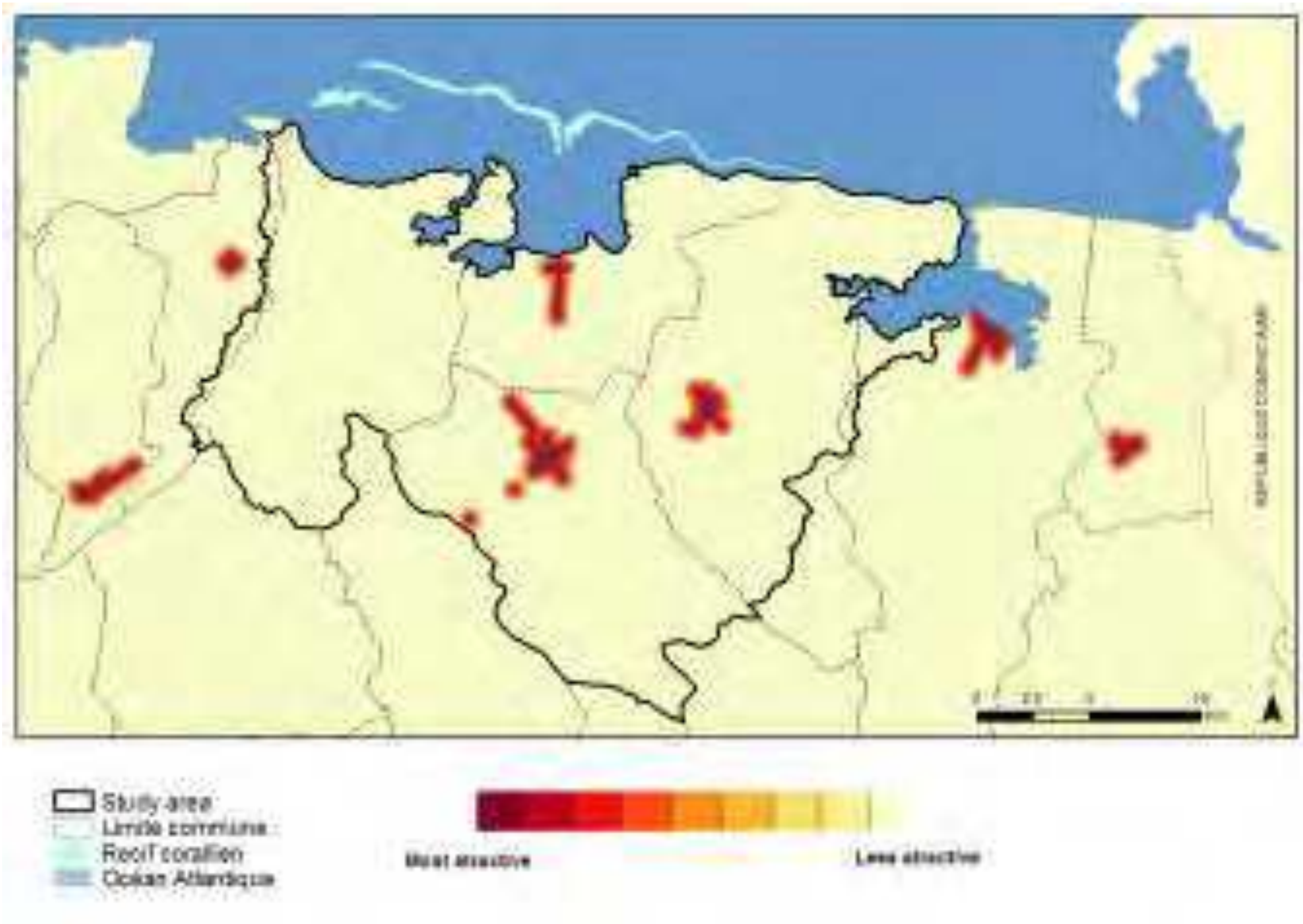

Figure A8.4 Attraction factors: Public Utilities – Electric System

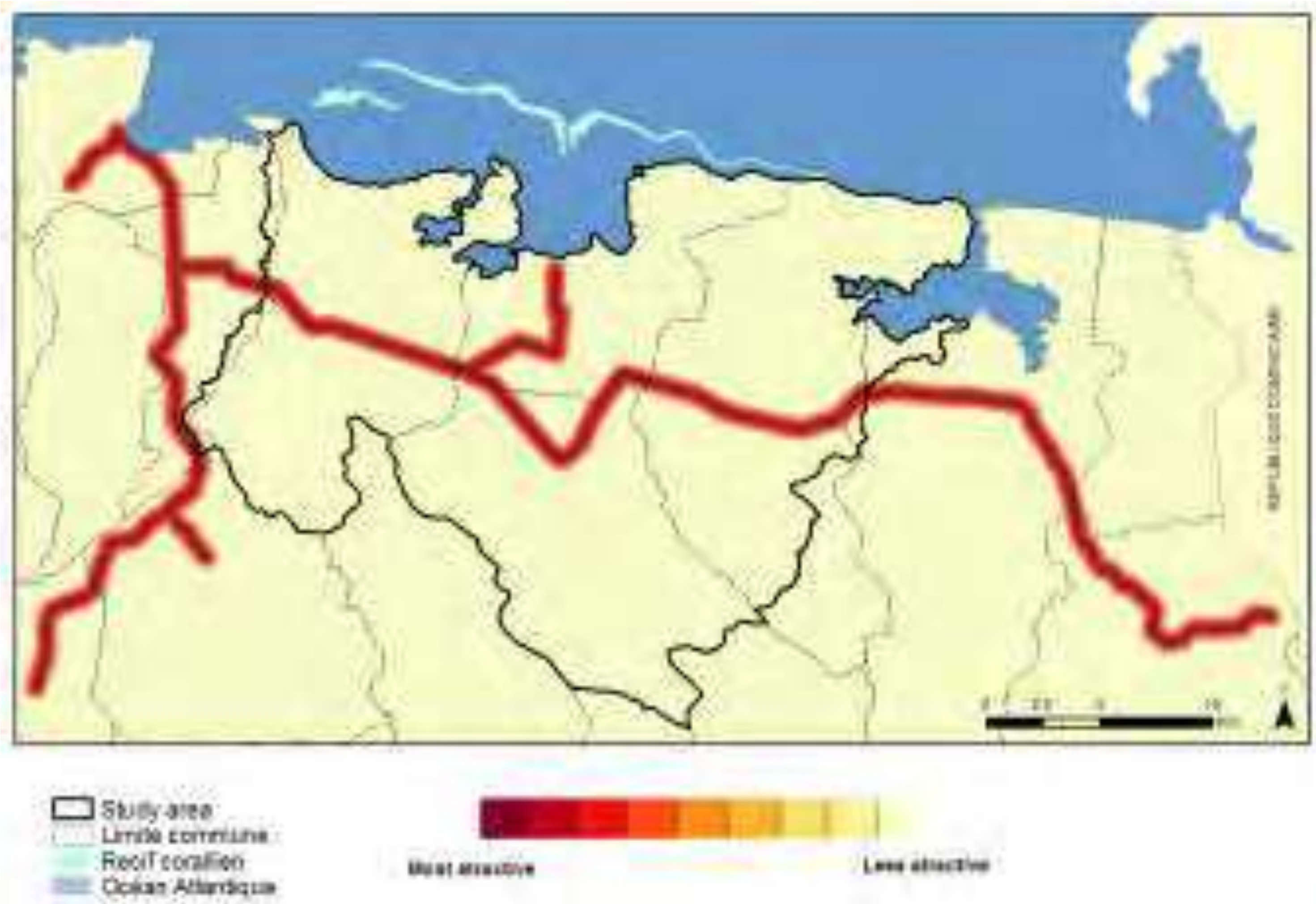

Figure A8.5 *Attraction factors: Social Services*

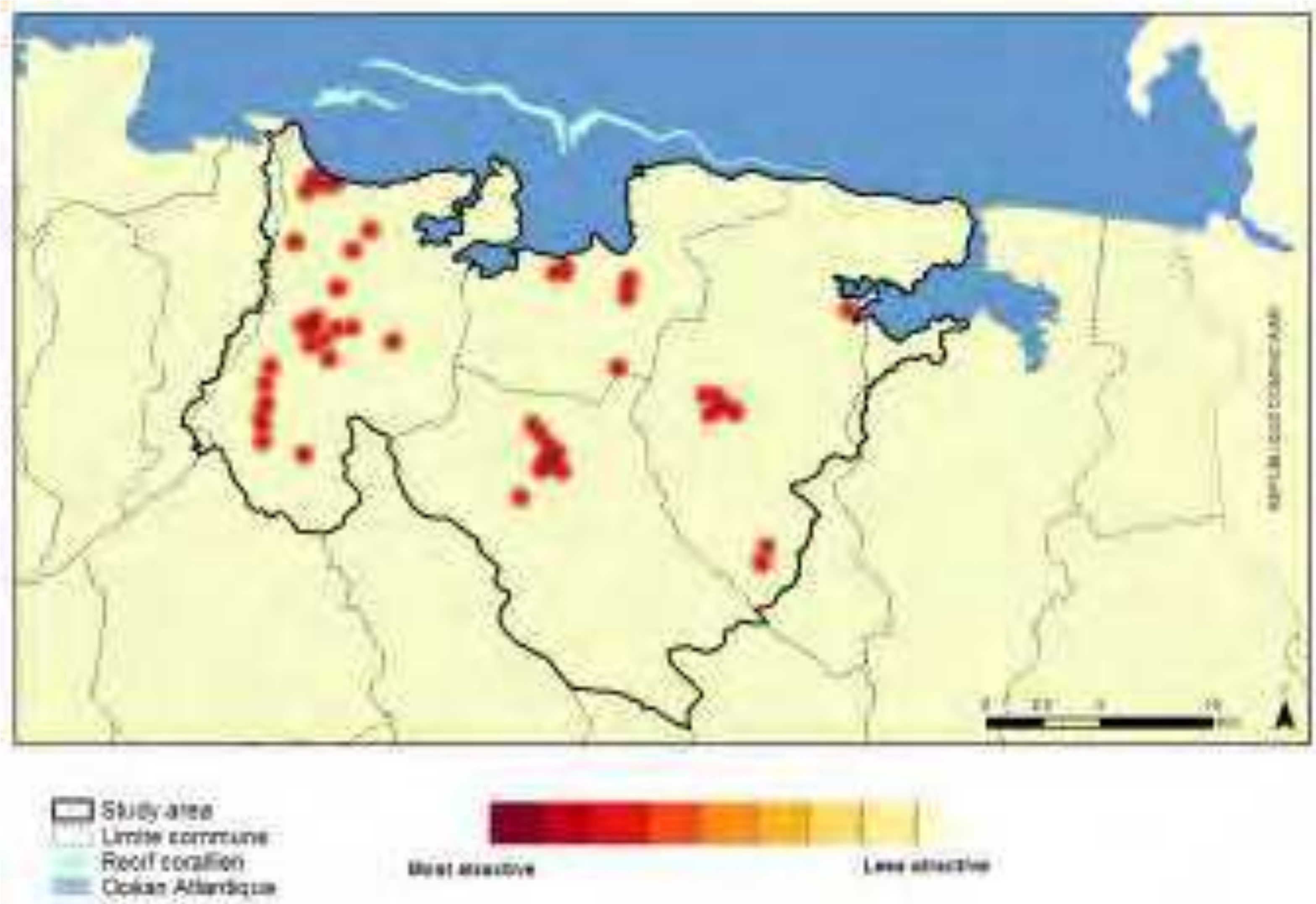

APPENDIX 9: Development Project Maps

Figure A9.1 *Attraction factors: Urban Agglomeration*

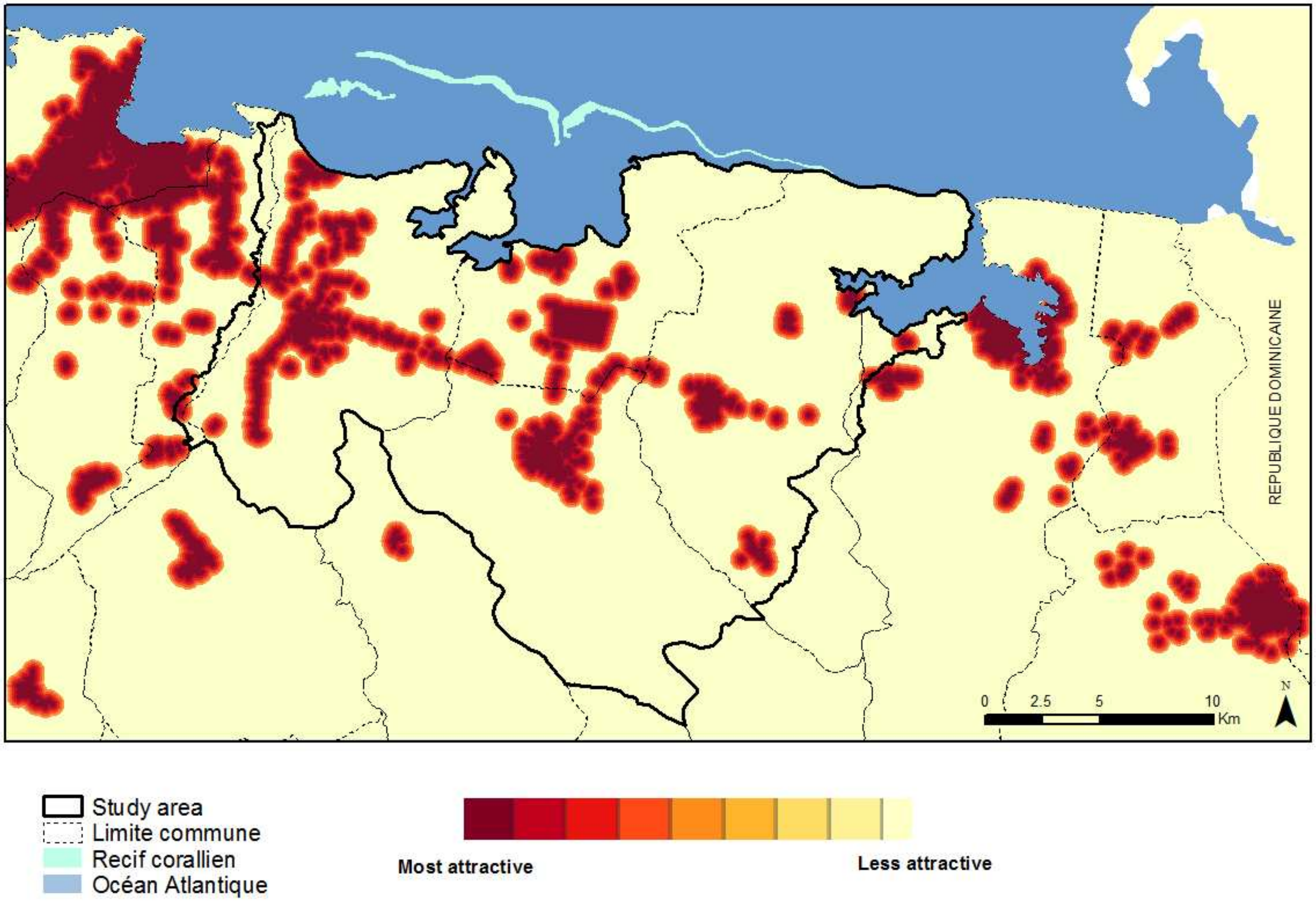

Figure A9.2 Attraction factors: Sea Port Expansion

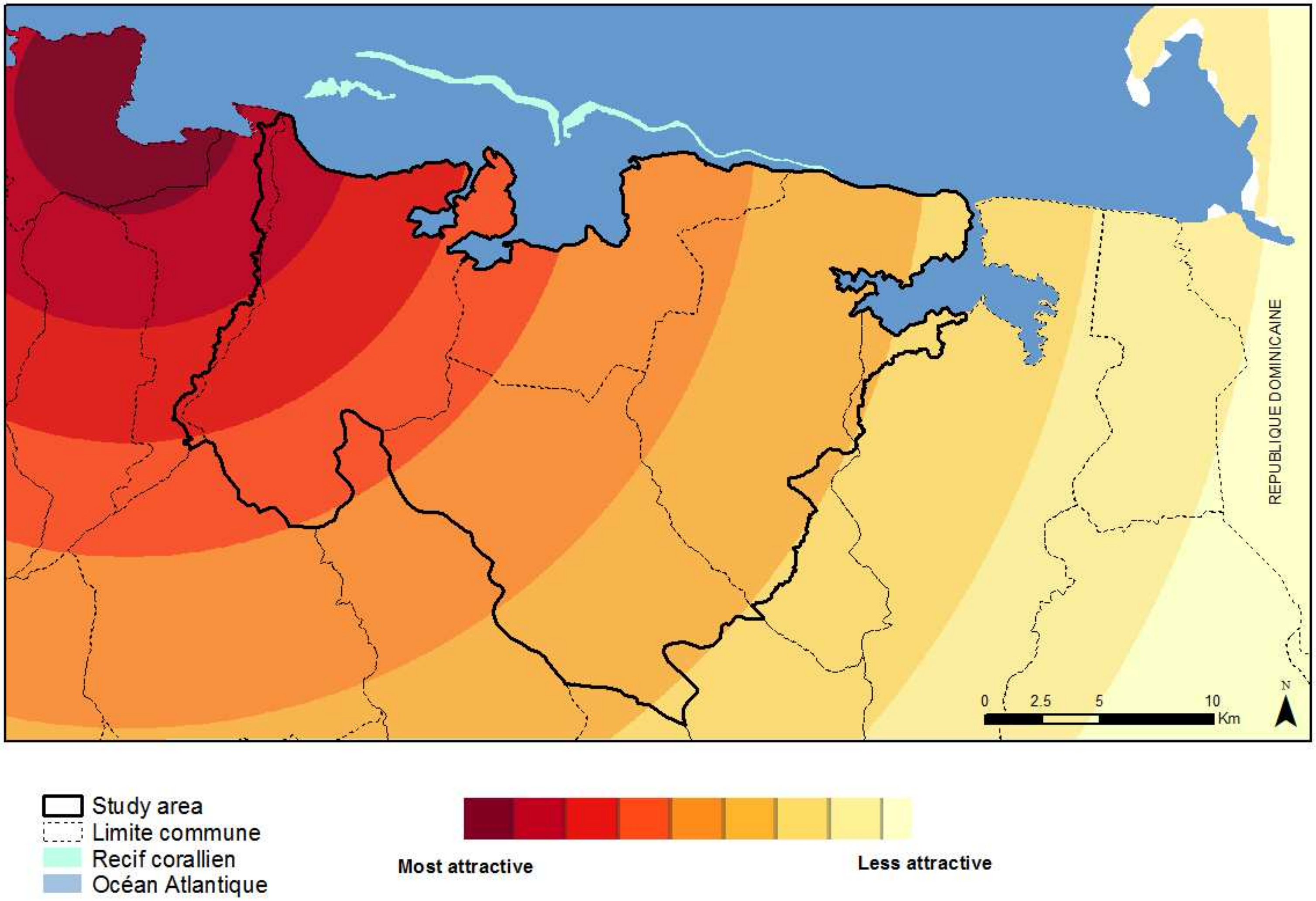

Figure A9.3		*Attraction factors: Infrastructure*

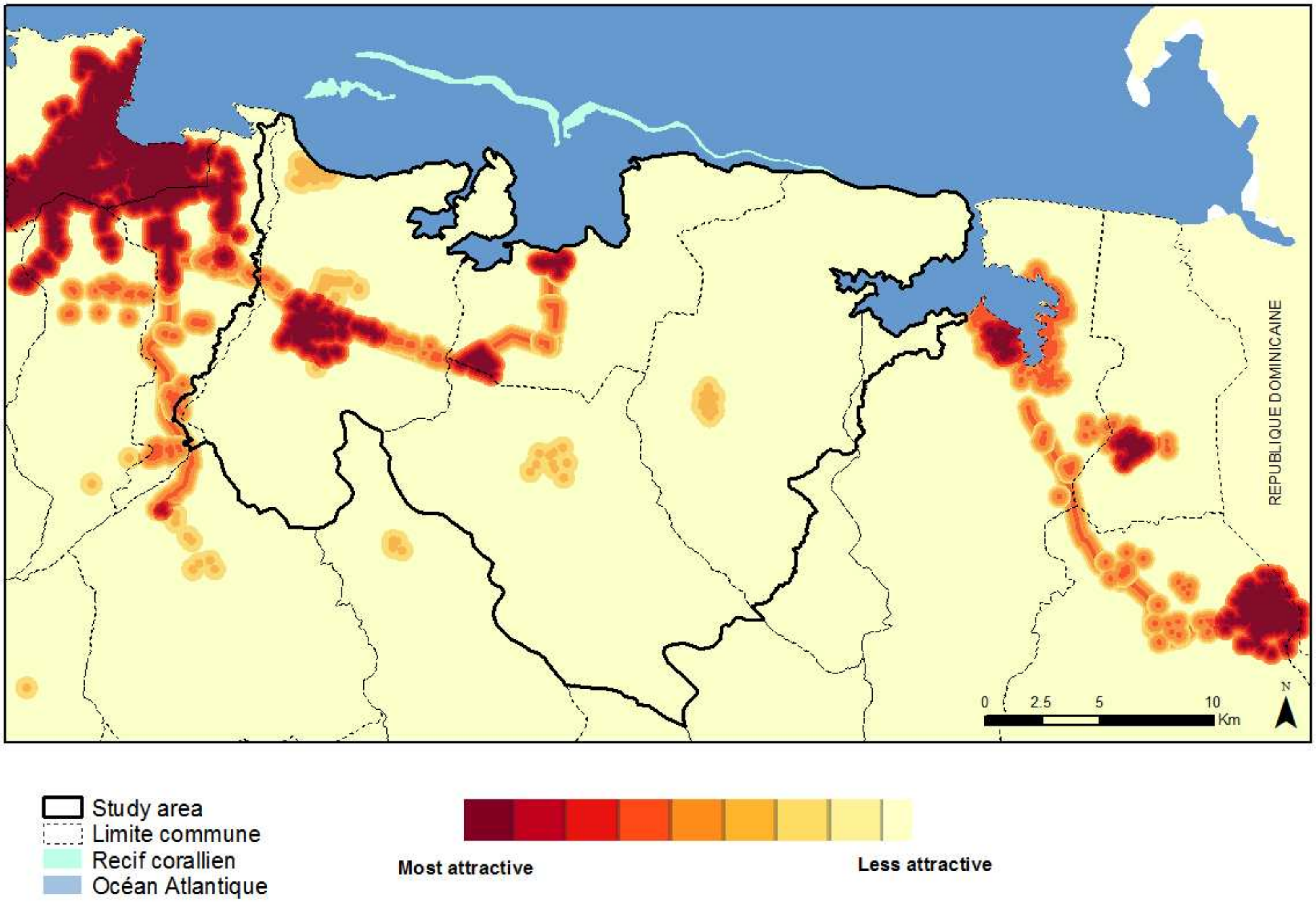

Figure A9.4 Attraction factors: Employment

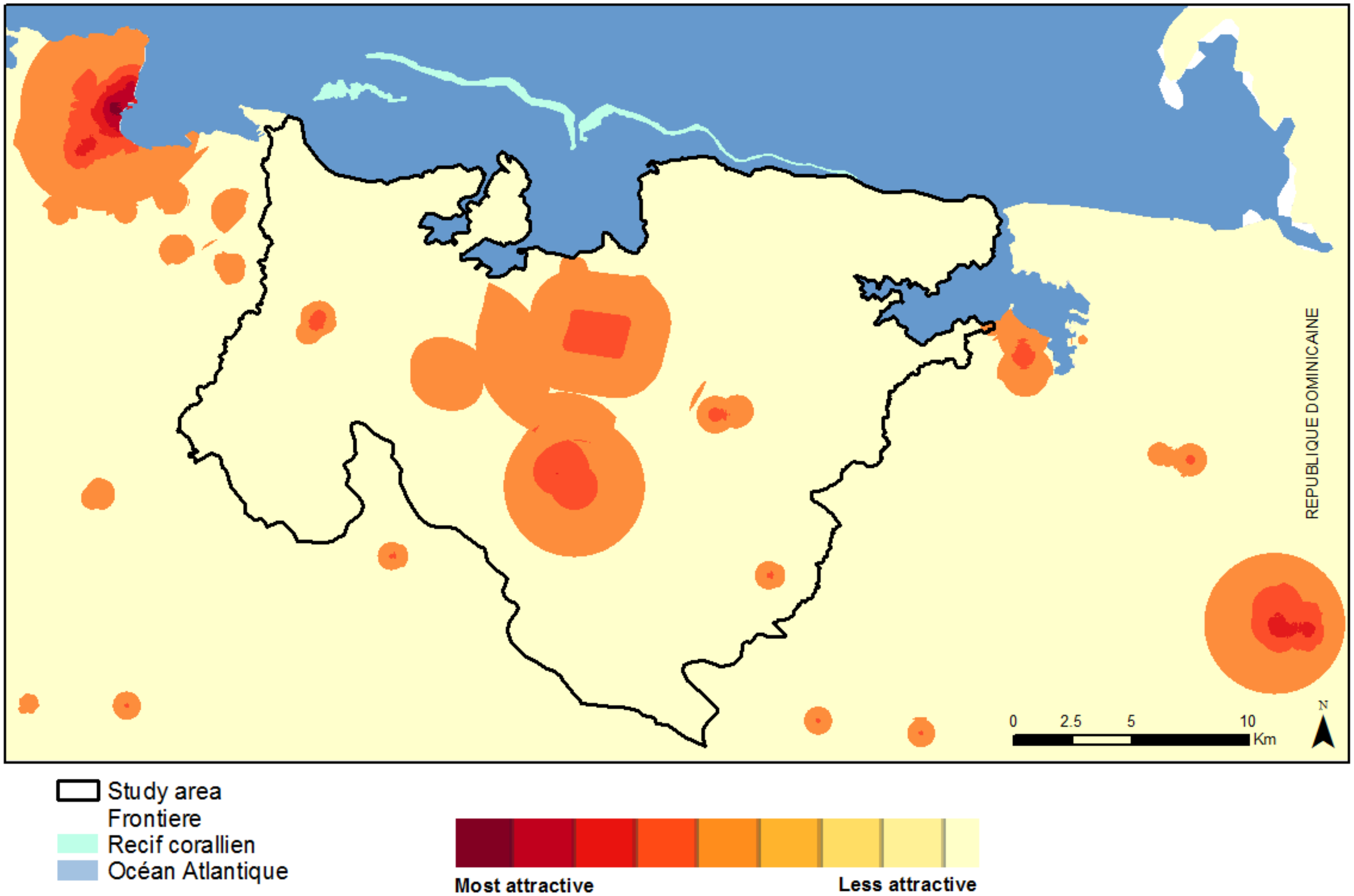

APPENDIX 10: Risk Reduction Assessment

A10 RISK REDUCTION ASSESSMENT

A10.1 Approach

Specific recommendations and projects that are assessed in this section have been scrutinized using a Cost Benefit Analysis (CBA) model to assess the likely costs and benefits of identified mitigation measures. It is not surprising, given the intensity and frequency of flooding (both inland and coastal) that these hazards have been given priority for risk reduction assessment.

This section of the report highlights the methodology followed for a risk reduction assessment and introduces and conducts a scenario analysis for various mitigation strategies in high risk areas so as provide an estimate of the costs and benefits. The risk reduction assessment comprises of all activities, including structural and non-structural measures, to avoid (prevent) or to limit (mitigate) adverse effects of hazards (ISDR 2004).

Outlining the benefits of risk reduction in terms of reduced damages and other associated benefits can help in decision making for allocation of limited resources for investments in risk reduction. A CBA is used to assess the likely costs and benefits of risk reduction measures.

The terms "mitigation alternatives" and "what if analysis" have been used interchangeably to indicate options that can be to be taken forward for more detailed engineering analysis and specific implementation. *Table A10.1* provides a listing of the scenarios, identified by the project team, and analyzed in this study.

Table A10.1 List of Mitigation Scenarios

Project	Mitigation Scenario
1	Upgrade Urban Drainage Infrastructure
2	Rural Drainage Infrastructure Implementation
3	Revitalize Historical Canal System To Alleviate Flooding
4	Upland Reforestation
5	Mangrove Protection In The 3Bay Park

The risk assessment that has been carried out for the area, provides the basis to assess the benefits and costs of possible mitigation measures. The risk assessment considers hazard, exposure, and vulnerability for buildings, infrastructure, and society. The overall approach followed for the CBA is shown in Figure A10.1 and considers the various benefits expected from strategies and the corresponding costs involved.

The risk models developed for this study have been used to analyze the risk (losses) if a particular mitigation option is implemented. Next, the risk metrics [average annual loss (AAL), loss exceedence curve and loss cost] are used to identify and prioritize areas or localities that are under risk. The benefits of mitigation are then estimated by taking the difference between direct and indirect losses with and without mitigation. The benefits have been estimated as present value of future (recurring) benefits considering the life of the building/infrastructure that is being proposed. The costs of mitigation have also been estimated. These include the cost of structural interventions, setting up systems, recurring costs such as maintenance, etc.

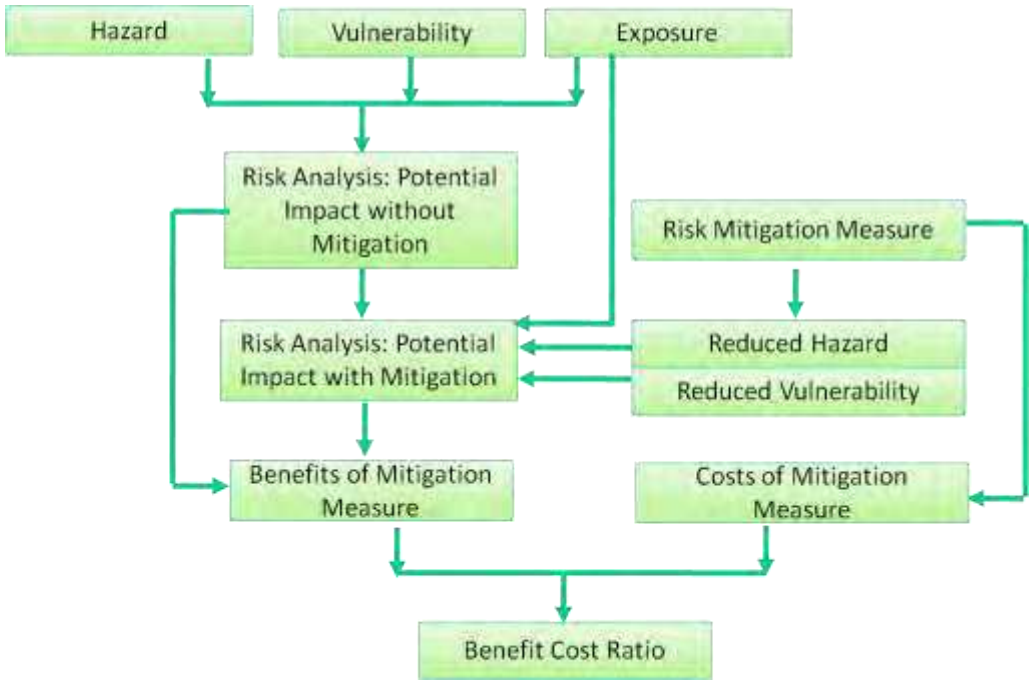

Figure A10.1 Cost Benefit Analysis

A10.2 Mitigation Option No. 1.: Upgrade Urban Drainage Infrastructure in Limonade

Limonade has been selected to demonstrate how improvement to urban infrastructure can be used to effectively mitigate damages and reduce losses. The example has been identified to address the problem of overland flow when the amount of rainfall exceeds the capacity of existing infrastructure. The increasing urbanization and inadequate infrastructure results in urban flooding Often rainfall water exceeds the capacity of storm water drainage infrastructure or the system becomes blocked due to debris. An increase in artificial drainage infrastructure (open catchpit drainage and culverts) is proposed to address alleviate the flooding so as to discharge water into the receiving watercourses and eventually the ocean. The proposed project shall benefit seven blocks in the Limonade (Figure A10.2). The estimated length of open drains is about 18 km, of which 9 km is assumed to be in place (existing), and an additional 9 km is proposed as new construction. Along with the 9 km of new proposed construction drains, it is anticipated that approximately 75 culverts may be needed at the various road crossings to facilitate drainage.

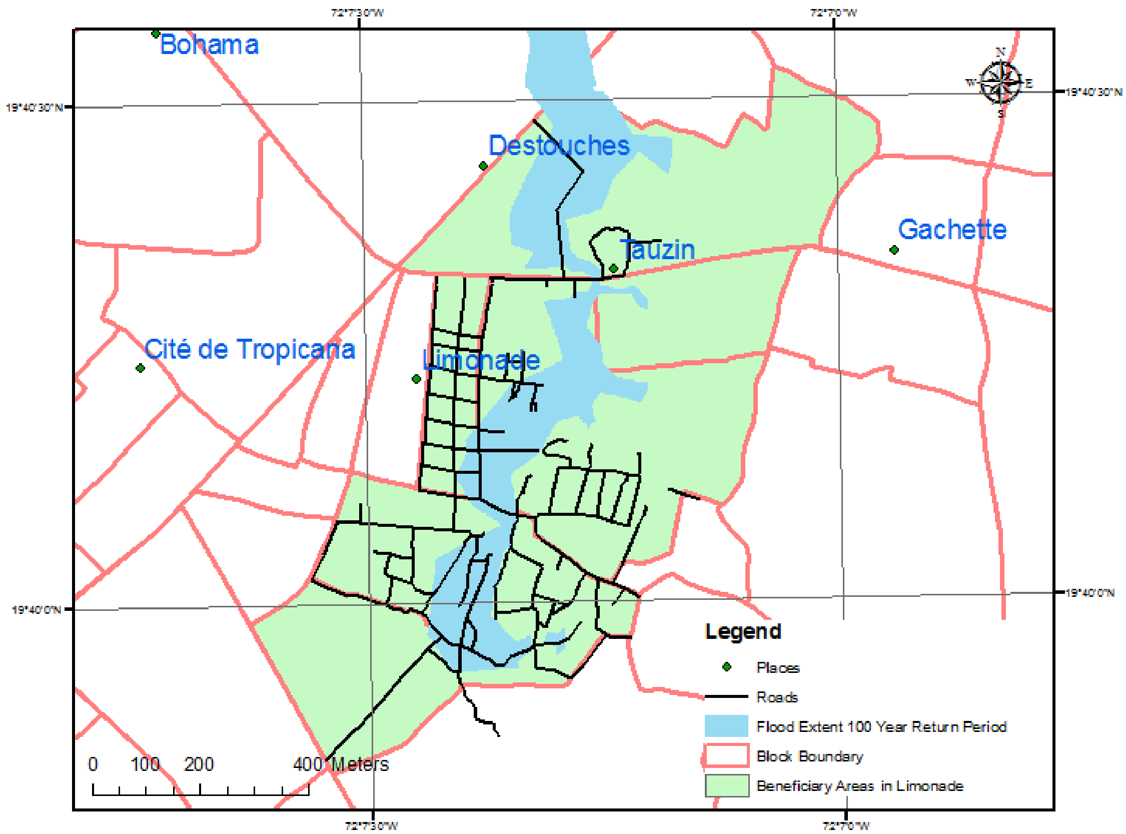

Figure A10.2 Potential Beneficiary Area in Limonade

Approach

The urban drainage system comprising of open ditches and culverts is proposed as mitigation scenario for inland flood protection. This system will be helpful in reducing the flood inundation by providing a passage to the flood waters. With reduced flood inundation, it is expected the risk of flooding in the area of interest (Limonade) will also be reduced.

Probabilistic risk assessment results derived earlier in this study have used to estimate the reduction in risk and overall benefits (losses avoided). The base case risk metrics (AAL, LEC and Loss Cost) have been used to identify blocks within the Limonade which are likely to be benefited from the drainage infrastructure improvements. As shown in the above map, much of the urban area in Limonade benefits from this mitigation action. Since the town is vulnerable to both inland and urban floods, it is assumed that this system will bring down the overall risk in this area by 50%.

Finally, the benefits to the area of interest are calculated by comparing the base case (AAL) and the AAL with the mitigation options in place. Cost benefit ratio measures the costs incurred and the benefits accrued from a policy or action - in this case the construction of urban drainage system.

Costs: The costs of drainage system construction and upgrades are considered. The system comprises of construction of new open ditches or catch-pits, upgrading of existing ditches and construction of new culverts. Costing of construction includes all the components such as costs of materials, equipment, labor forces, support, benefits, and other miscellaneous costs. The project costs include:

- New Open catch-pit of 0.5x0.5 m is estimated at about USD $180,000 per km.

- Upgrade of the existing drainage system is assumed to be 70% of new construction, which amounts to USD $126, 000.
- Cost of construction of the culvert is estimated to be USD 3,600 for 6 m length of the culvert.

As mentioned above, in the seven beneficiary urban blocks of Limonade, the estimated length of open drains is about 18 km. About 9 km are assumed as existing ones and rest 9 km is proposed for new construction. Along the 9 km of new proposed construction drains, an about 75 culverts are estimated.

Thus the total cost of proposed drainage system is estimated to be USD 3,024,000. The costs are assumed one-time investments with expected benefits spread over the life of the system. The life of the system has been taken as 20 years.

Benefits: Different benefits due to mitigation are considered for the cost benefit analysis that include indirect and direct benefits (both tangible and intangible). Benefits of mitigation are estimated by taking the difference between losses with and without mitigation (Kunreuther, 2001). A portion of the direct tangible benefits of a flood damage reduction project is due to a reduction in the inundation area which will reduce damage due to flooding of structures and other properties. Mathematically, we compute this inundation-reduction benefit B_{IR} as:

$$\mathrm{B_{IR} = X_{Without} - X_{with}}$$

in which:
Xwithout – expected damages or economic impact without project; and
Xwith - expected damage or economic impact if the project is implemented.

The benefits include reduced losses to residential and commercial buildings due to the improvement of the drainage system. The benefits due to reduction in losses for various sectors (as shown in above equation) are estimated as the difference between present values of future flood AAL with the project in place and AAL without improvements to the drainage system. Since these benefits accrue over the life of the project (buildings/infrastructure/systems), it is important to discount them to a present value so that benefits accruing at different times can be made comparable.

The benefits are estimated as present value of future (recurring) benefits considering the life of the system. The life of system is usually considered as the minimum time period in which system will be functional. In case of drainage systems (catch-pits, culverts, etc), it is taken to be 20 years. The present values of future benefits are estimated as:

$$\mathrm{PV = C_o x \frac{(1+d)^t - 1}{d\,x\,(1+d)^t}}$$

Where,
PV = Present value
C_0 = Cost (In this case average annual loss)
d = discount rates (assumed 3%)
t = time, years (assumed ≈ life of the system 20 years)

The outcome of the above equation is the present value of future benefits over the time (considered as the life of the system). The total present values of benefits with the proposed mitigation action is USD $ 7,694,826.

Cost Benefit Analysis

As described above, various benefits and costs are considered in the cost benefit analysis to estimate the cost benefit ratio. The proposed urban drainage system is expected to benefit most of the urban area in Limonade and reduce flood losses to various exposure sectors.

TableA10.2 evaluates the mitigation option of introducing urban drainage system in comparison to base case. The base case is status quo condition generally assumed to be the losses without a mitigation action.

Table A10.2: Cost benefit analysis of urban drainage system in Limonade

Particular	Details	Base Case	Option
Other Information	Life of the Drainage System, Years	20	20
	Growth Factor	14.9	14.9
Flood AAL	Residential Building AAL, USD	838,692	419,346
	Commercial Building AAL, USD	194,171	97,086
	Industrial Building AAL, USD	-	-
Present value of future Flood losses	Residential Building AAL, USD	12,496,504	6,248,252
	Commercial Building AAL, USD	2,893,148	1,446,574
	Industrial Building AAL, USD	-	-
Costs	Cost of Drainage System Construction, USD		3,024,000
	Total cost, USD		**3,024,000**
Present Value of Benefits	Residential Building, USD		6,248,252
	Commercial Building , USD		1,446,574
	Industrial Building , USD		-
	Total Benefits, USD		**7,694,826**
Cost benefit Ratio	Cost benefit Ratio		2.54

Base Case: The results from base case analysis of the probabilistic risk assessment have been used to establish this scenario. The results from the defined beneficiary urban area suggest that AAL for buildings due to floods is USD $1,032,863. The present values of future flood AAL to the buildings in the base case condition are estimated over a 20 year period to be USD $15,389,652.

Cost benefit Ratio of Mitigation Option: Since the total cost of construction of drainage system is estimated to USD $3,024,000. The total present values of benefits with the proposed drainage options are estimated to be USD $7,694,826.

The cost benefit ratio (BCR) is computed by taking a ratio of present value of all benefits due to mitigation and total costs of mitigation.

$$\text{BCR} = \frac{\sum \text{Present Value of Benefits}}{\sum \text{Costs of Mitigation}}$$

Considering the total benefits of USD $7,694,826 against the total costs of the mitigation action (USD 3,024,000), the BCR for this mitigation scenario is **2.54**. A BCR, greater than one, suggests that benefits are higher than the cost of the project, indicating that the project is a good investment (i.e. the benefits outweigh the costs).

Considering the satisfactory cost benefit ratio, this option may be taken forward for possible planning, pre-feasibility studies, etc.

A10.3 Mitigation Option No 2. Rural Drainage Infrastructure Implementation

A proto-typical rural infrastructure solution has been identified to address the problem of overland flows in rural areas. Where in urban areas problems arise due to the fact that drainage infrastructure is overloaded or outdated, in rural areas infrastructure to divert water flows is largely unavailable. To address flooding, especially along transportation corridors and settlement areas, a system of linear concrete drainage outlets such as culvert pipes and rolling cross drains (catchpits) are proposed to divert water away from settlements. Drain canals are to be reinforced with rock and masonry to prevent erosion. It is important that consideration to the impact the flow of water will have on settlement areas in the lower reaches of the watershed so as not to exacerbate flooding in other areas. As shown in Figure A10.3, the diversion drain (1.0 X 1.5 m) starting from area south of industrial park and draining in to the sea (west of Caracol town) may comprise a length of about 7.1 km and 5 culverts. It is assumed that at present there is no infrastructure available and proposed infrastructure will be newly constructed.

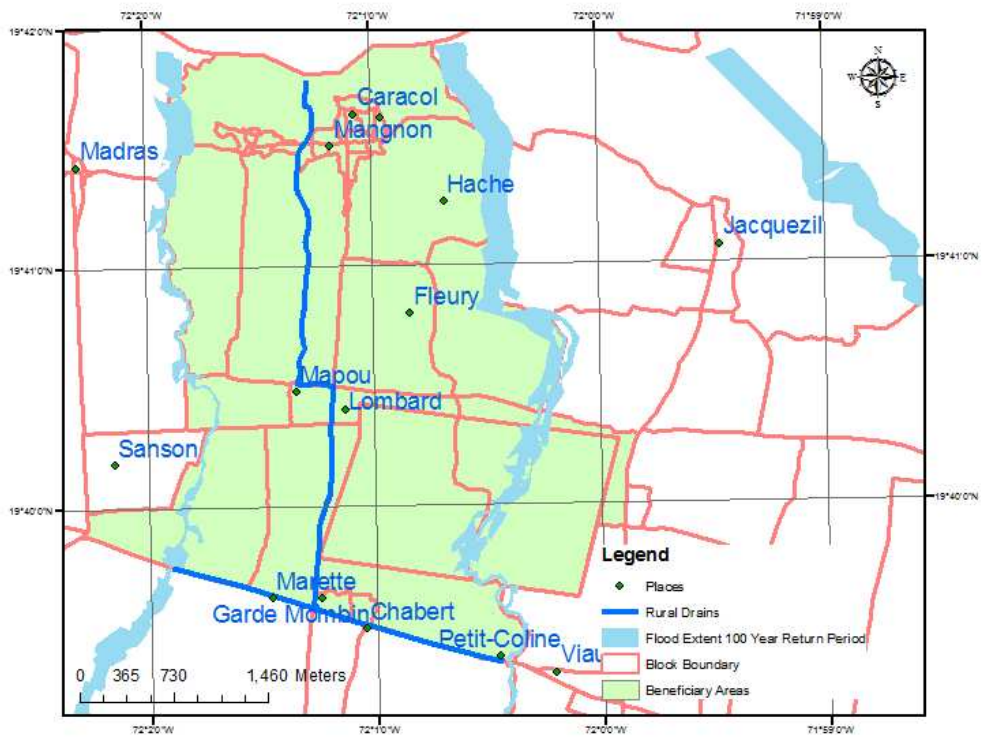

Figure A10.3 Potential Beneficiary Area for Rural Infrastructure

Approach

To alleviate flooding, especially along transportation corridors and settlement areas, a system of linear concrete drainage outlets such as culvert pipes and rolling cross drains (catch pits) are proposed to divert water away from settlements. Drains canals are to be reinforced with rock and masonry to prevent erosion. This system will be helpful in reducing the flood inundation by providing a diversion to the flood waters. With reduced flooding, it is expected the risk of flooding in the area of interest (linear settlements occurring near and around the industrial park) will also be reduced. Probabilistic risk assessment results derived earlier in this study have used to estimate the reduction in risk and overall benefits (losses avoided). The base case risk metrics (AAL, LEC and Loss Cost) have been used to identify and blocks within the area of interest which are likely to be benefited. As shown in the above map, approximately 39 blocks will benefit from this mitigation action. Since the area is vulnerable to inland floods and proposed system dimensions shall carry more floodwaters, it is assumed that this system will bring down the overall risk in this area by 70%. Finally, the benefits to the area of interest are calculated by comparing the base case (AAL) and the AAL with the mitigation options in place. Cost benefit ratio measures the costs incurred and the benefits accrued from a policy or action - in this case the construction of rural drainage system.

Costs: The costs primarily include the costs of drainage system construction. The system comprises of construction of new open ditches or catch-pits and new culverts. Generally, the costs of drainage system construction and upgrades include all the components such as the costs of materials, equipment, labor forces, support, benefits, and other miscellaneous costs. The project costs include:

- New open catch-pit of 1.0X1.5 m is estimated at about USD $135,000 per km.
- Cost of construction of the culvert is taken USD 3,600 for 6 m length of the culvert.

As mentioned above, there are 39 beneficiary blocks and the estimated length of the proposed drains is about 7.1 km. Along the 7.1 km of new proposed construction drains, a about 5 culverts are estimated. Thus the total cost of proposed drainage system works out at about USD 980,550. The costs are assumed one-time investments with expected benefits spread over the life of the system. The life of the system has been taken as 20 years.

Benefits: Different benefits due to mitigation are considered for the cost benefit analyses that include indirect and direct benefits (both tangible and intangible). These studies are generally taken up later in the implementation and engineering design stage of the project. Benefits of mitigation are estimated by taking the difference between losses with and without mitigation (Kunreuther, 2001). A portion of the direct tangible benefits of a flood damage reduction project is due to a reduction in the inundation area which will reduce damage due to flooding of structures and other properties. Mathematically, we compute this inundation-reduction benefit B_{IR} as:

$$B_{IR} = X_{Without} - X_{with}$$

in which
Xwithout – expected damages or economic impact without project; and
Xwith - expected damage or economic impact if the project is implemented.

The benefits include reduced losses to residential and commercial buildings due to the improvement of the drainage system. The benefits due to reduction in losses for various sectors (as shown in above equation) are estimated as the difference between present values of future flood AAL with the project in place and AAL without improvements to the drainage system. Since these benefits accrue over the life of the project (buildings/infrastructure/systems), it is important to discount them to a present value so that benefits accruing at different times can be made comparable.

The benefits are estimated as present value of future (recurring) benefits considering the life of the system. The life of system is usually considered as the minimum time period in which system will be functional. In case of drainage systems (catch-pits, culverts, etc), it is taken as 20 years. The present values of future benefits are estimated as:

$$PV = C_o x \frac{(1 + d)^t - 1}{d\ x\ (1 + d)^t}$$

Where,
PV = Present value
C_0 = Cost (In this case average annual loss)
d = discount rates (assumed 3%)
t = time, years (assumed ≈ life of the system 20 years)

The outcome of the above equation is the present value of future benefits over the time (considered as the life of the system).

The outcome of the above equation is the present value of future benefits over the time (considered as the life of the system). The total present values of benefits with the proposed mitigation action is USD $1,049,532.

Cost benefit Analysis

As described above, various benefits and costs are considered in the cost benefit analysis to estimate the cost benefit ratio. The proposed rural drainage system is expected to benefit most of the area near industrial park and reduce flood losses to various exposure sectors.

TableA10.3 evaluates the mitigation option of introducing rural drainage system in comparison to base case. The base case is status quo condition generally assumed to be the losses without a mitigation action.

Table A10.3: Cost benefit analysis of rural drainage system

Particular	Details	Base Case	Option
Other Information	Life of the Drainage System, Years	20	20
	Growth Factor	14.9	14.9
Flood AAL	Residential Building AAL, USD	7,238	2,171
	Commercial Building AAL, USD	1,402	421
	Industrial Building AAL, USD	91,986	27,596
Present value of future Flood losses	Residential Building AAL, USD	107,848	32,355
	Commercial Building AAL, USD	20,885	6,265
	Industrial Building AAL, USD	1,370,599	411,180
Costs	Cost of Drainage System Construction, USD		980,550
	Total cost, USD		**980,550**
Present Value of Benefits	Residential Building, USD		75,494
	Commercial Building , USD		14,619
	Industrial Building , USD		959,419
	Total Benefits, USD		**1,049,532**
Cost benefit Ratio	Cost benefit Ratio		1.07

Base Case: The results from base case analysis of the probabilistic risk assessment have been used to establish this scenario. The results from the defined beneficiary urban area suggest that AAL for buildings due to floods is USD $ 100,626. The present values of future flood AAL to the buildings in the base case condition are estimated over a 20 year period to be USD $1,499,332.

Cost benefit Ratio of Mitigation Option: Since the total cost of construction of drainage system is estimated to USD $ 980,550 and the total present values of benefits with the proposed drainage options are estimated to be USD $ 1,049,532. The cost benefit ratio (BCR) is computed by taking a ratio of present value of all benefits due to mitigation and total costs of mitigation.

$$\mathrm{BCR} = \frac{\sum \text{Present Value of Benefits}}{\sum \text{Costs of Mitigation}}$$

The comparison of the total benefits of USD $1,049,532 against the total costs of mitigation action of USD $980,550, the BCR is 1.07. The cost benefit ratio, greater than one, suggests that benefits are higher than the cost of the project, indicating that the project is a conservative investment (i.e. the benefits slightly outweigh the costs). Considering the satisfactory cost benefit ratio, this option may be taken forward for possible planning, pre feasibility studies, etc.

A10.4 Mitigation Option No. 3: Revitalize Historical Canal System to Alleviate Flooding

The revitalization of the canals in northern Haiti is focused on a revitalizing existing drainage and irrigation systems that were put in place during the plantation era. In historical times, these canals helped serve as a regulatory mechanism for the conservation of fresh runoff water during times when there was a significant lag time between significant rainfalls. Today, the canal system lies in decay (silted) on defunct plantations, and this mitigation scenario, explores whether revitalizing certain areas can help play a role in mitigating flood problems by providing critical drainage in the lower reaches of the watersheds. Specifically, the revitalization of canals will include dredging to remove silt and increasing the cross-sectional area of the canals so as to divert flooding and overland flows to natural watercourses and/or ocean. Key considerations for this project will include providing an adequate site for discarded material and ensuring that natural barriers are in place to manage sediment and nutrients loads in coastal environs. Another key consideration is to ensure that there are mechanisms in place to ensure that there is maintenance or upkeep. As shown in Figure A10.4, the possibility of dredging a series of canals that total a length of 3.8 km is evaluated. Considering the dimensions 4m X 6m for a typical canal system, the dredging volume is estimated at 40,800 m^3.

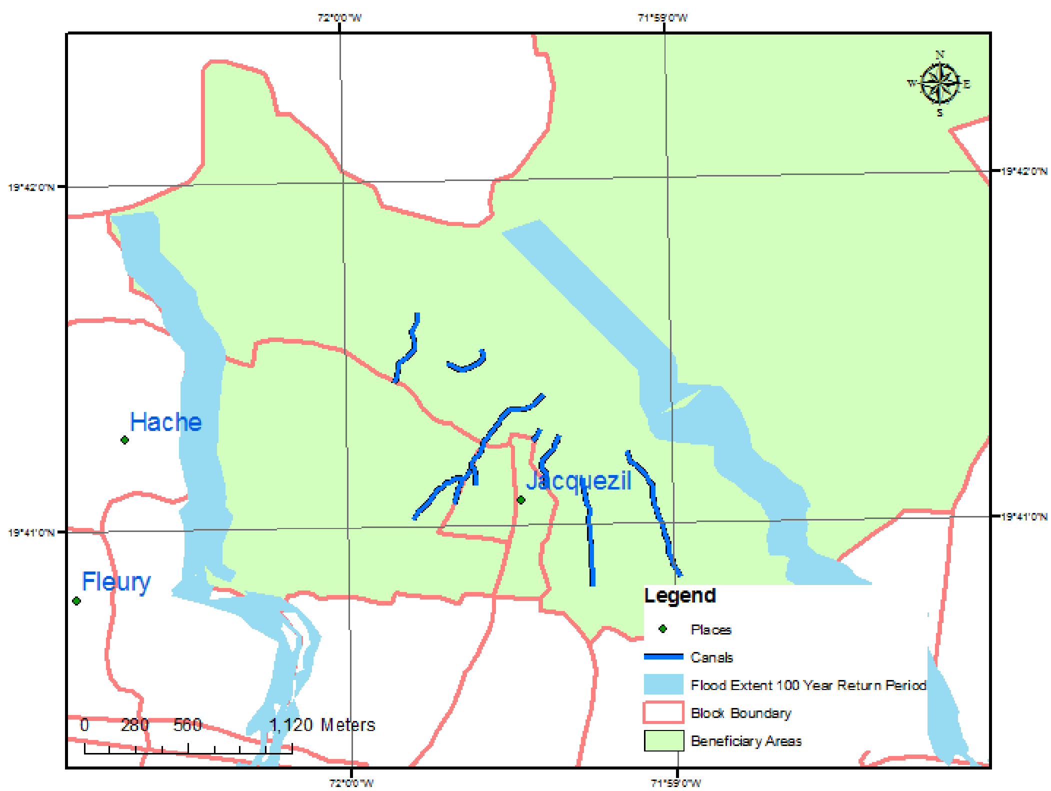

Figure A10.4 Potential Beneficiary Area for Canal System

Approach

Dredging provides a mitigating effect for flooding by increasing the cross-sectional area of the canals so as to divert flows to natural watercourse and/or ocean. A possibility of rehabilitation of canal system in the area of interest has been evaluated in this section. With reduced flooding, it is expected the risk of flooding in the area of interest (near Jacquezil) will also be reduced. Probabilistic risk assessment results derived earlier in this study have used to estimate the reduction in risk and overall benefits (losses avoided). The base case risk metrics (AAL, LEC and Loss Cost) have been used to identify and blocks within the area of interest which are likely to benefit. As shown in the above map, about four blocks in the area of interest will benefit from this mitigation action. Since the area is vulnerable to inland floods and proposed system dimensions shall carry more floodwaters, it is assumed that this system will bring down the overall risk in this area by 70%.

Finally, the benefits to the area of interest are calculated by comparing the base case (AAL) and the AAL with the mitigation options in place. Cost benefit ratio measures the costs incurred and the benefits accrued from a policy or action - in this case the construction of rural drainage system.

Costs: The costs include the costs of dredging. The project cost of dredging of canals of 4 X 6 m for the length of 3.8 km (40, 800 m^3) is estimated at about USD $ 183,600 considering a unit cost of USD 4.5/m^3. The costs are assumed one-time investments with expected benefits spread over the life of the system. The life of the system has been taken as 20 years.

Benefits: Different benefits due to mitigation are considered for the cost benefit analysis. For this project, a portion of the direct tangible benefits of a flood damage reduction is expected as inundation decreases. Mathematically, we compute this inundation-reduction benefit B_{IR} as:

$$\mathrm{B_{IR}} = \mathrm{X_{Without}} - \mathrm{X_{with}}$$

in which
Xwithout – expected damages or economic impact without project; and
Xwith - expected damage or economic impact if the project is implemented.

The benefits include reduced losses to residential and commercial buildings due to the improvement of the canal drainage system. The benefits due to reduction in losses for various sectors (as shown in above equation) are estimated as the difference between present values of future flood AAL with the project in place and AAL without improvements to the drainage system. Since these benefits accrue over the life of the project (buildings/infrastructure/systems), it is important to discount them to a present value so that benefits accruing at different times can be made comparable.

The benefits are estimated as present value of future (recurring) benefits considering the life of the system. The life of system is usually considered as the minimum time period in which system will be functional. In case of drainage systems (canals, catch-pits, culverts, etc), it is taken as 20 years. The present values of future benefits are estimated as:

$$\mathrm{PV} = \mathrm{C_o x} \frac{(1+\mathrm{d})^{\mathrm{t}} - 1}{\mathrm{d\,x\,}(1+\mathrm{d})^{\mathrm{t}}}$$

Where,
PV = Present value
C_0 = Cost (In this case average annual loss)
d = discount rates (assumed 3%)
t = time, years (assumed ≈ life of the system 20 years)

The outcome of the above equation is the present value of future benefits over the time (considered as the life of the system). The total present values of benefits with the proposed mitigation action is USD $ 127,505.

Cost benefit Analysis

As described above, various benefits and costs are considered in the cost benefit analysis to estimate the cost benefit ratio. The proposed rehabilitation of canal system is expected to benefit most of the area near Jacquezil and reduce flood losses to various exposure sectors.

Table A10.4 evaluates this mitigation option in comparison to base case. The base case is status quo condition generally assumed without mitigation.

Table A10.4: Cost benefit analysis of Canal Rehabilitation

Particular	Details	Base Case	Option
Other Information	Life of the Canal System, Years	20	20
	Growth Factor	14.9	14.9
Flood AAL	Residential Building AAL, USD	7,137	2,141
	Commercial Building AAL, USD	5,088	1,526
	Industrial Building AAL, USD	-	-
Present value of future Flood losses	Residential Building AAL, USD	106,339	31,902
	Commercial Building AAL, USD	75,810	22,743
	Industrial Building AAL, USD	-	-
Costs	Cost of Dredging, USD		183,600
	Total cost, USD		**183,600**
Present Value of Benefits	Residential Building, USD		74,438
	Commercial Building , USD		53,067
	Industrial Building , USD		-
	Total Benefits, USD		**127,505**
Cost benefit Ratio	Cost benefit Ratio		0.69

Base Case: The results from base case analysis of the probabilistic risk assessment have been used to establish this scenario. The results from the defined beneficiary area suggest that AAL for buildings due to floods is USD $ 12,225. The present values of future flood AAL to the buildings in the base case condition are estimated over a 20 year period to be USD $182,149.

Cost benefit Ratio of Mitigation Option: Since the total cost of construction of dredging is estimated to USD $ 183,600. The decreased AAL and the present values of future flood losses with the proposed drainage improvements in place are given in Table A10.4.

The cost benefit ratio (BCR) is computed by taking a ratio of present value of all benefits due to mitigation and total costs of mitigation.

$$\mathrm{BCR} = \frac{\sum \text{Present Value of Benefits}}{\sum \text{Costs of Mitigation}}$$

The total present values of benefits with the proposed drainage options are estimated to be USD $ 127,505 against the total costs of mitigation of USD $183,600, the BCR is 0.69. The cost benefit ratio, less than one, suggests that benefits are lower than the cost of the project, indicating that the project is a not a good investment (i.e. the benefits under weigh the costs).

Considering the non-satisfactory cost benefit ratio, this option should not be taken forward for possible planning, pre-feasibility studies, etc.

A10.5 Mitigation Option No. 4.: Upland Reforestation of the Trou Du Nord Watershed

Deforestation and environmental degradation in Haiti has been caused by growing populations and a reliance on wood as source of energy, which places great strains on forests. The changed vegetation cover affects the hydrological behavior of catchments and has resulted in recent times to an increase number of intense flood disasters throughout the country. The reforestation of Trou du Nord watershed is being proposed as an example of a sustainable mitigation measure to increase the interception of water in the upper reaches of watershed so as to decrease the peak and total storm flow during intense rainfall events. This mitigation measure will also work to prevent soil erosion and contribute to forest conservation which in turn enhancing carbon dioxide removal. Key considerations for the implementation of this measure are to understand that the potential benefits will be tied to a longer time horizon (i.e. storm flows depend on the maturity of the forest) and to ensure that the replanted areas remain undisturbed (i.e. enforcement). It is proposed that the barren hillsides (which are results of degradation) be planted with commercial crops like coffee. In Trou Du Nord watershed, lands that are barren are estimated to be about 487 ha. The areas are mostly in the upstream of the watershed (Figure A10.5), and contribute significant amount of flows to main stream of Trou Du Nord.

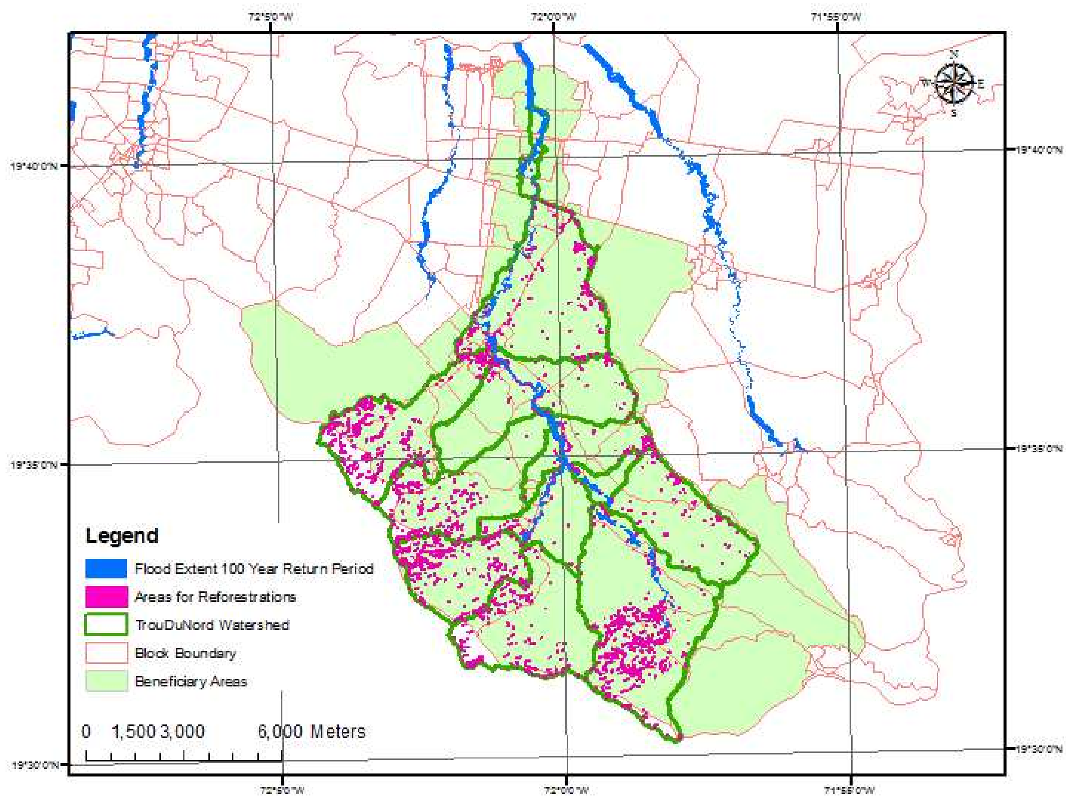

Figure A10.5 Trou du Nord Watershed and Re-Forestration Areas

Approach

The reforestation of Trou du Nord watershed is being proposed as an example of a sustainable mitigation measure to increase the interception of water in the upper reaches of watershed so as to decrease the peak and total storm flow in intense rainfall events. It proposed that the barren lands (which are results of degradation) may be planted with coffee. The planting of commercial crops will improve the water holding capacity of the soil and reduce the peak flows. The hydrological and hydraulic models developed in this study have been used to estimate the impact of the planting of upland crops on the reduction of flows. The abstraction parameters (initial losses, infiltration losses, etc.) have been estimated with improved land use and model simulations which suggest that there would be a reduction of flooding by 27%. The reduction is estimated higher in lower return periods (low magnitude events) as compared to higher return periods. With reduced flood inundation, it is expected the risk of flooding in the area of interest (Trou Du Nord Watershed) will also be reduced. Probabilistic risk assessment results derived earlier in this study have used to estimate the reduction in risk and overall benefits (losses avoided). The base case risk metrics (AAL, LEC and Loss Cost) have been used to identify and blocks within the area of interest which are likely to be benefited. As shown in the above map, about 67 blocks in the area of interest benefits from this mitigation action.

Finally, the benefits to the area of interest are calculated by comparing the base case (AAL) and the AAL with the mitigation options in place. Cost benefit ratio measures the costs incurred and the benefits accrued from a policy or action - in this case the watershed re-forestation.

Costs: The costs primarily include the costs of planting of coffee in upland areas. The project cost for crop planting in 487 ha area is estimated at about USD $ 1,217,500 considering a unit cost of USD 2,500/ha. The costs are assumed one-time investments with expected benefits spread over the life of the crop. The life of the crop has been taken as 20 years.

Benefits: Different benefits due to mitigation are considered for the cost benefit analysis. For this project, a portion of the direct tangible benefits of a flood damage reduction is expected as inundation decreases. Mathematically, we compute this inundation-reduction benefit B_{IR} as:

$$\mathrm{B_{IR}} = \mathrm{X_{Without}} - \mathrm{X_{with}}$$

in which
Xwithout – expected damages or economic impact without project; and
Xwith - expected damage or economic impact if the project is implemented.

The benefits include reduced losses to residential and commercial buildings due to reduction in flood flows. The benefits due to reduction in losses for various sectors (as shown in above equation) are estimated as the difference between present values of future flood AAL with the project in place and AAL without improvements to the drainage system. Since these benefits accrue over the life of the project (buildings/infrastructure/systems), it is important to discount them to a present value so that benefits accruing at different times can be made comparable.

The benefits are estimated as present value of future (recurring) benefits considering the life of the system. The life of system is usually considered as the minimum time period in which system will be functional. Though, the average life of the crop is 40 years, but the benefits starts with the complete maturity of the crop and established of renewed hydrological cycle in the watershed. Hence, in this case life of the crop is taken as 20 years. The present values of future benefits are estimated as:

$$\mathrm{PV} = \mathrm{C_o x}\, \frac{(1+\mathrm{d})^{\mathrm{t}} - 1}{\mathrm{d\,x}\,(1+\mathrm{d})^{\mathrm{t}}}$$

Where,
PV = Present value
C_0 = Cost (In this case average annual loss)
d = discount rates (assumed 3%)
t = time, years (assumed ≈ life of the crop 20 years)

The outcome of the above equation is the present value of future benefits over the time (considered as the life of the system). The total present values of benefits with the proposed mitigation action is USD$2,772,785.

Cost benefit Analysis

As described above, various benefits and costs are considered in the cost benefit analysis to estimate the cost benefit ratio. The proposed watershed reforestation is expected to benefit most of the area in Trou Du Nord watershed and reduce flood losses to various exposure sectors.

Table A10.5 evaluates this mitigation option in comparison to base case. The base case is status quo condition generally assumed without mitigation.

Table A10.5 Cost benefit analysis of Watershed Reforestation

Particular	Details	Base Case	Option
Other Information	Life of the Plantation, Years	20	20
	Growth Factor	14.9	14.9
Flood AAL	Residential Building AAL, USD	520,112	379,682
	Commercial Building AAL, USD	169,121	123,459
	Industrial Building AAL, USD	-	-
Present value of future Flood losses	Residential Building AAL, USD	7,749,665	5,657,255
	Commercial Building AAL, USD	2,519,908	1,839,533
	Industrial Building AAL, USD	-	-
Costs	Cost of Plantation, USD		1,217,500
	Total cost, USD		**1,217,500**
Present Value of Benefits	Residential Building, USD		2,092,410
	Commercial Building , USD		680,375
	Industrial Building , USD		-
	Total Benefits, USD		**2,772,785**
Cost benefit Ratio	Cost benefit Ratio		2.28

Base Case: The results from base case analysis of the probabilistic risk assessment have been used to establish this scenario. The results from the defined beneficiary area suggest that AAL for buildings (RES and COM) due to floods is USD $ 689,233. The present values of future flood AAL to the buildings in the base case condition are estimated at USD $ 10,269,572.

Cost benefit Ratio of Mitigation Option: Since the total cost of planting is estimated to USD 1,217,500. The total present values of benefits with the proposed drainage options are estimated to be USD $ 2,772,785.

The cost benefit ratio (BCR) is computed by taking a ratio of present value of all benefits due to mitigation and total costs of mitigation.

$$\mathrm{BCR} = \frac{\sum \text{Present Value of Benefits}}{\sum \text{Costs of Mitigation}}$$

The comparison of the total benefits of USD $ 2,772,785 against the total costs of mitigation of USD $ 1,217,500, the BCR is 2.28. The cost benefit ratio, greater than one, suggests that benefits are higher than the cost of the project, indicating that the project is a good investment (i.e. the benefits outweigh the costs).

Considering the satisfactory cost benefit ratio, this option may be taken forward for possible planning, pre feasibility studies, etc.

A10.6 Mitigation Option No. 5.: Mangrove Reforestation in the Parc National Trois Baies

Forested wetlands that are linked to the coastal environs serve as a natural buffer against storm surges, sea-level rise and wave action in particular. Natural features help to absorb large volumes of advancing water, and as a result, have a dissipating effect on wave energy. In this regard the wetlands, particularly the mangrove forests, that are part of the Parc National Trois Baies, are vital for mitigating the effects of coastal flooding in

Northern Haiti. Mangrove forests in particular play an important ecological role while providing a variety of services that include protection from erosion, flooding cyclones and tidal waves. An increase in the spatial extent of mangrove forests in the Parc National Trois Baies will not only serve as a mitigation measure against coastal hazards and climate change, but also contributes to conservation Haiti ecological systems, natural environment and biodiversity that are becoming increasing important to everyone around the world. Along the coastal line of about 60 km of Parc National Trois Baies, it proposed that a 5km strip of mangrove be reforested. This would mean about 300 sq.km of area would be planted. The targeted area would benefit about 138 blocks from coastal flooding (Figure A10.6).

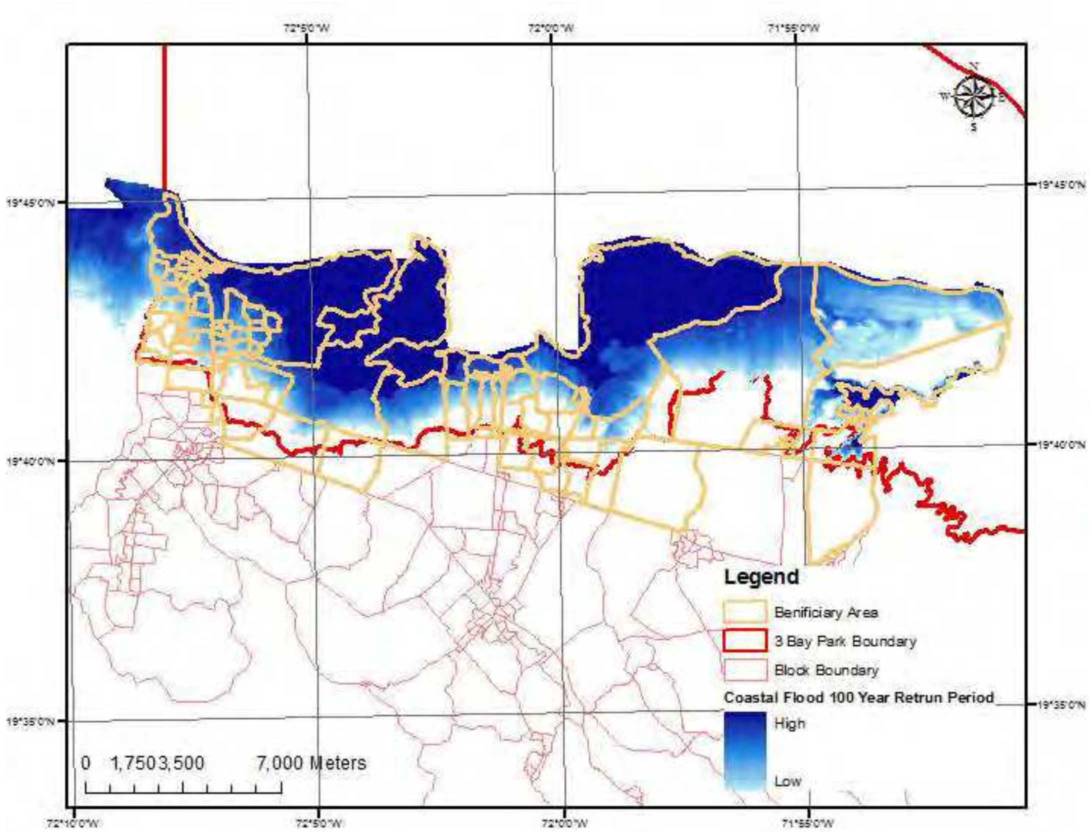

Figure A10.6 Beneficiary Areas from Mangroves

Approach

Natural features like Mangroves help to absorb large volumes of advancing water, and as a result, have a dissipating effect on wave energy. In this regard the wetlands, particularly the mangrove forests, that are part of the Parc National Trois Baies are vital for mitigating the effects of coastal flooding in Northern Haiti. It is proposed to reforest a 5km of strip of Mangroves along the coastal line of about 60 km of PN3B comprising 300 sq.km of area. With reduced flood inundation, it is expected the risk of flooding in the area of interest (in 138 blocks on northern coast of Haiti) will also be reduced. Probabilistic risk assessment results derived earlier in this study have used to estimate the reduction in risk and overall benefits (losses avoided). The base case risk metrics (AAL, LEC and Loss Cost) have been used to identify and blocks within the area of interest which are likely to be benefited (approximately 138 blocks).

Finally, the benefits to the area of interest are calculated by comparing the base case (AAL) and the AAL with the mitigation options in place. Cost benefit ratio measures the costs incurred and the benefits accrued from a policy or action - in this case the Mangrove protection.

Costs: The costs of this measure include the costs of planting mangrove trees. The project cost for crop planting in 300 sq.km area is estimated at about USD $ 6,750,000 considering a unit cost of USD 22,500/sq.km. The costs are assumed one-time investments with expected benefits spread over the life of the system. The life of the system has been taken as 50 years.

Benefits: Different benefits due to mitigation are considered for the cost benefit analysis. For this project, a portion of the direct tangible benefits of a flood damage reduction is expected as inundation decreases. Mathematically, we compute this inundation-reduction benefit B_{IR} as:

$$B_{IR} = X_{Without} - X_{with}$$

in which
Xwithout – expected damages or economic impact without project; and
Xwith - expected damage or economic impact if the project is implemented.

The benefits include reduced losses to residential, commercial and industrial buildings due to the mangrove protection. The benefits due to reduction in losses for various sectors (as shown in above equation) are estimated as the difference between present values of future flood AAL with the project in place and AAL without improvements to the drainage system. Since these benefits accrue over the life of the project (buildings/infrastructure/systems), it is important to discount them to a present value so that benefits accruing at different times can be made comparable.

The benefits are estimated as present value of future (recurring) benefits considering the life of the system. The life of system is usually considered as the minimum time period in which system will be functional. Though, the average life of the mangrove is generally more than 50 years, but the benefits starts with the complete maturity of the plats and established of renewed ecosystem cycle in the area. Hence, in this case life of the system is taken as 50 years. The present values of future benefits are estimated as:

$$PV = C_o x \frac{(1+d)^t - 1}{d \, x \, (1+d)^t}$$

Where,
PV = Present value
C_0 = Cost (In this case average annual loss)
d = discount rates (assumed 3%)
t = time, years (assumed ≈ life of the system 50 years)

The outcome of the above equation is the present value of future benefits over the time (considered as the life of the system). The total present values of benefits with the proposed mitigation action is UD USD $ 60,472,298.

Cost benefit Analysis

As described above, various benefits and costs are considered in the cost benefit analysis to estimate the cost benefit ratio. The proposed mangrove protection is expected to benefit most of the area in north coast and reduce flood losses to various exposure sectors.

Table A10.6 evaluates this mitigation option in comparison to base case. The base case is status quo condition generally assumed without mitigation.

Table A10.6 Cost benefit analysis of mangrove protection

Particular	Details	Base Case	Option
Other Information	Life of the Plantation, Years	50	50
	Growth Factor	25.7	25.7
Coastal Flood AAL	Residential Building AAL, USD	4,403,444	2,421,894
	Commercial Building AAL, USD	825,462	454,004
	Industrial Building AAL, USD	-	-
Present value of future Flood losses	Residential Building AAL, USD	113,168,505	62,242,678
	Commercial Building AAL, USD	21,214,379	11,667,909
	Industrial Building AAL, USD	-	-
Costs	Cost of Plantation, USD		6,750,000
	Total cost, USD		**6,750,000**
Present Value of Benefits	Residential Building, USD		50,925,827
	Commercial Building , USD		9,546,471
	Industrial Building , USD		-
	Total Benefits, USD		**60,472,298**
Cost benefit Ratio	Cost benefit Ratio		8.96

Base Case: The results from base case analysis of the probabilistic risk assessment have been used to establish this scenario. The results from the defined beneficiary area suggest that AAL for buildings due to floods is USD $ 5,228,906. The present values of future flood AAL to the buildings in the base case condition are estimated at USD $ 134,382,884.

Cost benefit Ratio of Mitigation Option: Since the total cost of planting is estimated to USD 6,750,000. The decreased AAL and the present values of future flood losses with the proposed mitigation in place are given in Table A10.6. The total present values of benefits with the proposed drainage options are estimated to be USD $ 60,472,298.

The cost benefit ratio (BCR) is computed by taking a ratio of present value of all benefits due to mitigation and total costs of mitigation.

$$\mathrm{BCR} = \frac{\sum \text{Present Value of Benefits}}{\sum \text{Costs of Mitigation}}$$

The comparison of the total benefits of USD $ 60,472,298 against the total costs of mitigation of USD $ 6,750,000, the BCR is 8.96. The cost benefit ratio, greater than one, suggests that benefits are higher than the cost of the project, indicating that the project is a good investment (i.e. the benefits outweigh the costs). Considering the satisfactory cost benefit ratio, this option may be taken forward for possible planning, pre feasibility studies, etc.

A10.7 References

ISDR 2004

Kunreuther, H., Cyr, C., Grossi, P., Tao, W., Using Cost-benefit Analysis to Evaluate Mitigation for Lifeline Systems, Wharton Risk Management and Decision Processes Center, The Wharton School, University of Pennsylvania, 2001.